1993

Mathematical model for the mass transfer of ozone into water systems

Phillip Craig Wright
University of Wollongong

"MATHEMATICAL MODEL FOR THE MASS TRANSFER OF OZONE INTO WATER SYSTEMS."

A THESIS SUBMITTED IN FULFILMENT OF THE

REQUIREMENTS FOR THE DEGREE

HONOURS MASTER OF ENGINEERING

from

UNIVERSITY OF WOLLONGONG

by

PHILLIP CRAIG WRIGHT BE (Chem.) Hons

DEPARTMENT OF MECHANICAL ENGINEERING

(1993)

TABLE OF CONTENTS

ABSTRACT

In this work a mathematical model initially developed for a counter-current bubble column gas-liquid contactor was examined. The model was developed by a lumped parameter approach to mass transfer with chemical reaction occurring completely within the liquid phase.

An extensive literature review was carried out on gas-liquid mass transfer and in particular ozone-water mass transfer in co-current down flow. There are large gaps in the literature on this phenomenon, which indicated the need for this kind of study.

The mathematical model was applied to study the behaviour of a jet pump contactor. Limited experimentation was carried out to examine some of the important characteristics of the reactor. The co-current downflow reactor was found to operate completely in annular flow with very high gas to liquid volumetric flow ratios (9 to 19).

Experimental and model of determination of volumetric mass transfer coefficient revealed an extremely high value ($k_L a$=230 sec^{-1}), which was nearly independent of flows or flow ratios.

Limited reactor flow pattern modelling, and mass transfer modelling have provided a large scope for future research. The flow pattern modelling of annular flow shows that velocities of the phases in the reactor are very high, and this leads to vastly decreased residence times. The velocities are 10 times those expected from superficial velocity calculations.

Modelling has shown that for the jet pump to become successful in microbiol disinfection in cooling tower water, that the residual liquid ozone concentration and/or the reactor residence time needs to be significantly increased to provide adequate CT disinfection criteria.

This study has provided useful information on the jet pump, and shown that high mass transfer coefficients, high gas hold-ups and high gas to liquid flow ratios occur. The models provide a framework for further work with all hydrodynamic and chemical properties easily adjusted.

ACKNOWLEDGEMENTS

I would like to thank the following people who gave help or advice in the preparation of this thesis:

- Dr Wee King Soh.

- Mr Keith Maywald.

- David Wright for computer technical advice and help.

- My parents for continued support.

1.0 INTRODUCTION

In recent years there has been an explosion of interest in the community on environmental issues. This is particularly important in the case of public health, where society now realises that their environment is not as clean as they imagined.

Various practices are being changed in response to public and government pressures. It is no longer acceptable to use the cheapest method available. There is now pressure to examine the effect of all human practices on the environment.

These pressures are becoming particularly evident in the area of water treatment.

The areas of water treatment range from industrial and municipal water, to those of drinking water and cooling tower water.

In the past much of the treatment of these waters was done using chlorine (Cl_2) compounds. However, chlorine is a very toxic substance with many storage and handling problems. It has been the usual choice as a microbiocide because it is relatively effective and has a reasonable cost. There are also several other types of microbiocide in use.

Many of these treatments have large problems in that the biocide concentration is heavily regulated due to their toxicity. There is also the problem that some bacteria are immune to current treatments, or that the allowable concentration of biocide is ineffective.

In Nice, France, there has been another way of treating drinking water. This technique has been in use for over 90 years. Ozone has been used to treat the drinking water, and currently in the world in 1989, some 15 million cubic mètres of water was treated with ozone daily.[1].

Ozone (O_3) is made up from three atoms of oxygen in an angular configuration. Ozone is a very strong oxidant; many times stronger than oxygen (O_2) and chlorine.

Ozone, then, appears to be an effective replacement for the chlorinated methods. It does not have many of the disadvantages of the chlorine systems, yet it is still not as widely used as it could be. Part of this reason is that the efficiency of its generation and transfer into the

water environment is not very high. This leads to higher installation and running costs than the chlorine-type systems.

The aim of this study is to investigate via mathematical computer modelling, the mass transfer of ozone into water systems. This model examines the importance of various mass transfer parameters. The model will also determine the effect of mass transfer of ozone with chemical reaction as well as the type of ozone-water contactor. An examination of a two phase downflow is also included, as this is essential to evaluate the hydrodynamic properties of the contactor.

This study has practical emphasis on a new type of ozone-water contactor, the jet pump (or venturi scrubber system) reactor.

2.0 BACKGROUND INFORMATION ON OZONE

2.1 WATER TREATMENT

There are various methods for treating the many types of industrial and municipal waters. The water from various industrial plants may contain an exotic cocktail of compounds covering the spectrum of chemicals, and may range from base and heavy metals through to multi-chained organic compounds, algae and bacteria.

Municipal waste waters may also have an exotic mix, ranging from sewage through pesticides, and small industrial run-off such as oils and solvents.

All of these waters end up in rivers, oceans and water collection areas. It is important that these waters be cleaned to a reasonable level. It is vitally important that water collected for drinking (potable water) be clear of contaminants and bacteria.

It is important that water not used for human consumption be also clean, although the level of cleanliness is not as strict. An example of this type of water is the water used in cooling towers for industrial cooling and air conditioning.

2.1.1 DRINKING WATER DISINFECTION

Water for human consumption obviously has the most stringent guidelines placed on its quality.

It has been found by Coin and Gomella [3] that the water must be ozonated to a concentration of 0.4 mg/l (4 ppm) for a minimum contact time of 4 minutes in order to be fully disinfected. According to Bourbigot [1], this level of ozonation is maintained at current drinking water treatment plants.

It has been found that ozone is very useful in treating drinking water because [5]:

- Ozone inactivates viruses.

- Ozone disinfects bacteria.

- Ozone oxidises inorganic material such as soluble iron and manganese.

- Ozone oxidises the compounds which give water its various tastes, odours and colours.

- Ozone oxidises organic complexes of manganese, thereby removing manganese from the complex.

- Ozone acts as a biocide in the removal of algae.

- Ozone oxidises various 'nasty' organics such as pesticides, phenols and detergents.

- Ozone oxidises such inorganics as cyanides, nitrites and sulfites. This renders them more safe and biodegradable.

- Ozone acts as a flocculent for many small dissolved organics.

- Ozone can aid in the reduction of turbidity by flocculation and precipitation.

- Ozone is extremely useful as a pre treatment for other water treatment procedures.

Many of these benefits are of use in the treatment of other water systems, such as cooling towers and air conditioning and ventilation systems.

2.1.2 COOLING TOWER SYSTEMS

Cooling tower systems are collections of units that provide a mechanical type of ventilation such as air conditioning or water cooling. In some of these situations the conditions are very favourable for the growth of various micro-organisms. Some of these

micro-bacteria can cause various human respiratory complaints such as Hypersensitivity Pneumonitis, Humidifier Fever and Legionnaires' Disease [4].

Legionnaires' Disease has the most public face of the above disorders. In fact it is the most dangerous illness, and death from pneumonia can result within several days of exposure [4].

There are several simple methods that can be employed to prevent bacteria growth in the aforementioned systems. These methods are as follows [4]:

- Regular maintenance and cleaning

- Correct operation and maintenance procedures

- Correct water treatment

- Good ventilation system design

It is not usually necessary to treat the system specifically for the removal of Legionnaires' Disease, unless there has been a severe outbreak.

Systems that use water from tepid (41-44^{o}C) supplies are now unacceptable. Hot (60^{o}C) and cold water must now be mixed with a thermostatic mixer instead.

2.2 PROPERTIES OF OZONE

Ozone is a compound constructed of three oxygen (O) atoms arranged in an angular pattern. The chemical designation for ozone is O_3. The ozone molecule is a very unstable molecule, formed from an exothermic reaction between oxygen atoms and molecules. The heat of formation of ozone is 142.85 J/mol [6].

Because of the volatility of ozone, evidenced by its highly endothermic nature, it is important that ozone be correctly handled. This is especially true in the case of pressure and

temperature variance. It is very important that the handling be suitable, as ozone can auto react in a highly explosive manner.

Ozone is the third strongest oxidant, as is evidenced by Table 2.2.1 [23].:

TABLE 2.1 REDOX POTENTIAL OF COMMON OXIDANTS [23].

$F_2 + 2e^- \quad <--> \quad 2F^-$	2.65 V
$OH + e^- + H^+ <--> \quad H_2O$	2.80 V
$O_3 + 2H^+ + 3e- \quad <--> \quad O_2 + H_2O$	2.07 V
$MnO_4- + 4H^+ + 3e^- \quad <--> \quad MnO_2 + 2H_2O$	1.69 V
$Cl_2 + 2e^- \quad <--> \quad 2Cl^-$	1.36 V

As can be seen from the table ozone is a much stronger oxidant than chlorine, its redox potential being some 50% greater than chlorine.

The important chemical properties of ozone are summarised in the following table:

TABLE 2.2 SUMMARY OF OZONE PROPERTIES [7].

Molecular Weight	48 kg/kgmol
Boiling Point (760mmHG)	-111.9°C
Melting Point (760mmHG)	-192.7°C
Critical Temperature	-12.1°C
Critical Pressure	5354 kPa
Critical Density	0.437 g/ml
Critical Volume	0.1471 l/mol
Gas Density (0°C)	2.144 g/l
Liquid Density (-183°C)	1.151 g/ml
(-195.4°C)	1.614 g/ml
Surface Tension (-183°C)	48.4 dyne /cm
Heat Capacity (100°C)	43.4kJ/mol. °C
(-173°C)	33.2kJ/mol. °C
Viscosity (liquid -183°C)	1.55 cP

Heat of Evaporation (-112°C)	316 kJ/g
Heat of Formation (25°C)	144 kJ/mol
Heat of Solution (H_2O 18°C)	15.3 kJ/mol
Free Energy (25°C)	135.1 kJ/mol
Van der Waals Constants	
a	3.545 $kg_f/cm^2.l^2.mol^{-2}$
b	0.04903 l/mol
Magnetic Susceptibility ($*10^{-6}$)	
gas	0.002 cgs units
liquid	0.15 cgs units
Thermal Exp'n Coefficient($*10^{-3}$)	
(-183°C)	2.0
(-112.4°C)	2.5
Entropy $S_T + R$	234.5 kJ/mol. °C
S_V	1.59 kJ/mol. °C
Ionisation Potential	12.8 eV
Electron Affinity	1.9 eV
Dipole Moment	0.53 D
Dielectric Constant	
gas (0°C)	1.0019
liquid (-183°C)	4.75

Ozone typically follows a Henry's Law equilibrium relationship with water (see Section 3.2), and in fact is several times more soluble than oxygen [8]. The solubility of the ozone is also related in an approximately linear manner to the partial pressure of the ozone in the gas. It is usually difficult to predict the exact solubility of ozone in the solvent in question due to the problem of predicting the Henry's Law constant [7]. The graph produced in Figure 2.1 was generated from data in Rice [144]. It is useful as a guide only.

FIGURE 2.1 OZONE SOLUBILITY DATA (Data from Rice [144].)

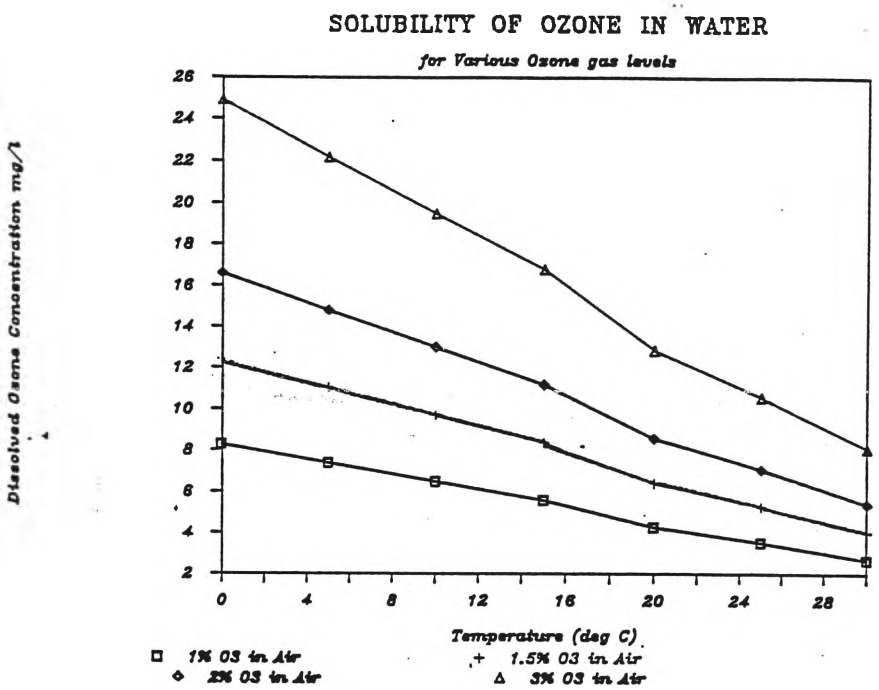

There have been a number of studies done on the solubility behaviour of ozone in the water environment, and Table 2.3 is reproduced from Sotelo et.al [9], and contains their own study.

TABLE 2.3 WORKS ON OZONE ABSORPTION IN WATER FROM LITERATURE [9].

Investigator	Year	pH	Temperature (°C)	Ref.
Kawamura	1932	-	0-60	10
Briner et.al	1939	-	3.5-19.8	11
Rawson	1953	-	9.6-39	12
Stumm	1958	-	5-25	13
Mailfert	1970	-	0-60	14
Li	1977	2.2-7.1	25	16
Roth and Sullivan	1981	0.65-10.2	3.5-60	17

Caprio et.al	1982	-	0.5-41	18
Morris	1988	7	0-60	19
Sotelo et.al	1989	2.5-9	10-50	9

The Sotelo et.al [9] investigation is an extensive investigation with the following variables considered: temperature, ionic strength, gas flow, pH, agitation and O_3 partial pressure.

2.2.1 DECOMPOSITION OF OZONE IN AQUEOUS ACID SOLUTIONS

Much research has gone into the decomposition reactions of ozone in various aqueous solutions. There are quite a number of different steps which are proposed as being the initial step. There is not as much trouble predicting the initiation reaction in high pH solutions, because the rate at these pH ranges (pH 8 to 9) is proportional to the concentrations of O_3 and OH^-, in the presence of radical scavengers. A possible initiation reaction for the decomposition of ozone is:

$$O_3 + OH^- \rightarrow HO_2^- + O_2 \qquad (2.1)$$

where

k = rate constant = 40-70 $dm^3/(mol.sec)$ [83].

It has also been shown that there are likely to be many intermediates with radical species such as OH, OH_2^- and O_3^- being involved.

This model, however, does not account for the rates of ozone decomposition at low pH (i.e. below 4). This is because the very low concentration of OH^-, at these pH's, does not explain the observed rate of ozone decomposition.

It has been postulated in a number of works [84,85] that the ozone reacts directly with the water molecules:

$$O_3 + H_2O \rightarrow 2OH + O_2 \quad (2.2)$$

However, it has been shown that the ozone does not interact with the water molecule in this manner [83,86]. Upon dissociation, there is interaction between the water and ozone, and the active intermediate appears to be OH [83,86].

From work by Sehested et al [83] it has been shown that the oxygen molecule has a retarding effect on the decomposition of ozone. From their [83] experiments they suggest that the following thermal decomposition reaction is also responsible for the decomposition in the aqueous acid phase. This reaction is also a common reaction in the gas phase [83,87]:

$$O_3 \leftrightarrow O + O_2 \quad (2.3)$$

It is also suggested that the next intermediate step in competition with the reverse equilibrium reaction is the following [83,87]:

$$O + H_2O \rightarrow 2OH \quad (2.4)$$

This reaction is not well established in the gas phase, but has been suggested in the vapour phase [88]. After this reaction has occurred, a chain set of reactions can then occur. These are as follows [83]:

$$OH + O_3 \rightarrow HO_2 + O_2 \quad (2.5)$$

[$k=1.1*10^8$ $dm^3/(mol.sec)$ [89]]

$$HO_2 + O_3 \rightarrow OH + 2O_2 \quad (2.6)$$

[$k<10^4$ $dm^3/(mol.sec)$ [89]]

$$HO_2 \leftrightarrow O_2^- + H^+ \quad (2.7)$$

[$pK = 4.8$ [90]]

$$O_2^- + O_3 \rightarrow O_3^- + O_2 \quad (2.8)$$

[$k=1.5*10^9$ $dm^3/(mol.sec)$ [91.]]

$$O_3^- + H^+ \rightarrow OH + O_2 \quad (2.9)$$

[$k=9*10^{10}$ $dm^3/(mol.sec)$ [92.]]

$$OH + HO_2 \rightarrow H_2O + O_2 \quad (2.10)$$

[$k=0.7*10^{10}$ $dm^3/(mol.sec)$ [93.]]

As can be seen from the chain reaction processes (equations 2.3 to 2.10), it is possible to reduce the extent of the decomposition reactions by the increased concentration of oxygen(O_2), and by the lowering of the pH. An increase in the level of dissolved oxygen acts as a stabiliser for ozone decomposition.

2.2.2 OZONE CONSUMPTION

In aqueous solutions there will be an ozone demand, and this demand will be regulated by many factors including the concentration of both inorganic and organic solutes. The rate at which ozone needs to be supplied to the waste system to be treated depends on the kinetics of oxidation of these substances. This will determine the contact time required. The combinations of these substances will be quite individual for a system, and can change with time. Some sort of measure of these substances will need to be implemented to see if the treatment is occurring efficiently. This makes design work for the ozone-waste contactor difficult.

As has been described previously (Section 2.2.1) ozone self-decomposes in water, as well as in air and oxygen. Therefore a "clean" water circuit such as distilled water would provide the minimum design requirement for the ozone contactor. To maintain a certain ozone residual (say 4ppm) in the water then, places a constraint on the contactor size and throughput.

An example of continuous treatment service is a cooling tower. In this case the ozone acts as more of a prevention rather than a cure for the effluent problems. The ozone can oxidise the organic material as it forms. However, as each system is individual, this makes the situation difficult to model accurately. There are many complex and complicated reactions and reaction orders. It is much easier to create a lumped parameter model which describes the total system. Such an ozone consumption rate can be described by a first-order rate expression [42,43,104].:

$$r = w * [O_3] \qquad (2.11)$$

where r = rate of utilisation of ozone (mol/[l.sec])

w = rate constant for ozone utilisation (sec^{-1})

$[O_3]$ = ozone concentration in the solution bulk at any point in time (mol/l)

The estimation of w is the calculation which is the most difficult to achieve. If the system is a 'simple' system such as pure water and one organic constituent, then published or kinetic data is either available, or easily determined. If, however, the system contains a variable number of complex constituents then this makes the determination of w much more difficult. The variation from one system to another can be quite large, even in relatively clean waters [42,104].

As has been shown (Section 2.2.1) there is a large pH dependency, with the ozone half life considerably reduced in high pH (alkaline) solutions.

A good study on some of the kinetic aspects of ozone decomposition has been carried out by Gurol and Singer [45]. In this paper an extensive reference list is provided.

It can be shown that the decomposition rate of ozone is not very significant below pH 6, however, even at pH 9.5 the rate of decomposition is not sufficiently fast to make systems mass transfer limited [45].

There are several factors which can affect the mass transfer coefficient, and some of these from a physical sense can be put down to the surface tension of the liquid which may affect the interfacial area (a) which will in turn affect $k_L a$ (see chapter 3 on mass transfer) [45].

From studies by Yuteri and Gurol [104] it has been shown that for waters not heavily contaminated with man-made pollutants an estimate of this "w" value can be made within +/- 25% accuracy.

This estimate is made using the following relationship:

$$\log_{10} w = -3.98 + 0.66pH + 0.61\log_{10}(TOC) - 0.42\log_{10}(alk/10) \qquad (2.12)$$

where w = "specific ozone utilisation rate" [104] ($hour^{-1}$)

TOC = total organic carbon (mg/L)

alk = alkalinity expressed as mg/l Ca_2O_3

From this information it can be seen that for an accurate reactor to be designed and modelled, it is imperative that laboratory modelling of the waste to be treated is essential. From this data the scaled-up model can then be created. However, great care is still required in the scale-up of the model. In scaling up the data and the reactor it is important that non-ideal behaviour is studied. It is therefore recommended that techniques such as residence time distribution studies(RTD) are made.(see Section 7.1)

3.0 MASS TRANSFER

There have been many studies done into ozone mass transfer phenomena. These studies include investigations by Boddeus [37], Gurol [43], Wright [21], Yurteri and Gurol [104,75,44,42], Mehta et al [46] and Munter et.al [76]. Because of the complexity of the mass transfer models and studies, it is difficult to decide on the appropriateness of the model.

There are three main stages which usually characterise the water treatment behaviour of ozone, and these are discussed briefly in the following paragraphs.

The first stage is the movement of the ozone in the gas stream to the gas/liquid interface. This involves diffusion of the ozone molecule through the gas. There are a number of factors which influence this diffusion such as the temperature and the size of the molecules. These are described more fully in Section 3.3.1.

The second stage involves the ozone transfer across the liquid-gas boundary. This can be complicated by various resistances on either the liquid or the gas side of the boundary (See Section 3.3).

The third stage involves movement of the ozone from the liquid side of the gas/liquid boundary into the bulk of the water to be treated (see Sections 3.1.1 and 3.3).

This simple description of the path of the ozone molecule from the gas stream to the pollutant particle is greatly simplified. The mass transfer behaviour is also complicated by the myriad of complex chemical reactions that can occur.

3.1 INTRODUCTION TO MASS TRANSFER PHENOMENA

Mass transfer is a very complex area of study. It is of vital importance in understanding the mechanisms involved in the use of ozone for wastewater treatment. The information obtained from complete mass transfer studies will allow correct ozone dose rates to be designed as well as the optimum contacting equipment.

It is of importance to understand mass transfer, transport phenomena and reaction kinetics to understand the complexities involved in successfully treating cooling tower (or any other) water with ozone.

3.1.1 DIFFUSION

The most basic concept that must be understood in a mass transfer study is that of diffusion. Diffusion is a molecular transport of matter. The are many analogies to mass diffusion, these include conduction of heat along a metal rod.

In diffusion there is a tendency for matter to move from a high concentration to a low concentration. This is described by Fick's Equation [20].:

$$j_i = -(\rho)D \frac{dW_i}{dZ} \qquad (3.1)$$

where j_i = mass flux of i ($kg/m^2.sec$)

ρ = density or mass concentration (kg/m^3)

D = diffusion coefficient (m^2/sec)

Z = direction of mass flux (m)

W_i = mass fraction of i

The crux of this equation is that the mass flux per unit area (j_i) is proportional to the concentration gradient [20].

The constant of proportionality (D) is described above as the diffusion coefficient. It is important to note that there is a concentration gradient term in Fick's Law. This does not mean that the flux is zero if the concentration gradient term (dW_i/dZ) is zero. It simply means that there is no nett mass transfer without a concentration gradient. There is such a thing as self diffusion and random movements. An example of this is the random movement of a single molecule in a gas [20].

The diffusion coefficients for gases are the easiest to calculate. The reason for this is the large open nature of a gas. The particles are far apart with large intervening spaces. In a gas stream the particles are assumed to travel in a straight line until they collide with another particle. This behaviour has been fairly successfully modelled in kinetic theory. This has been possible due to the low intermolecular forces. These forces are really only dominant when collisions are occurring (in a large number of situations).

It is much more difficult to determine with the same level of certainty, the diffusion coefficient of liquids. This is because the molecules are much closer together and so there are many more intermolecular forces. There has been relatively good success with some binary liquid systems through continuum models [20].

Solid diffusion coefficients are much more difficult to predict, due to the extremely high intermolecular forces. The mass transfer behaviour of solids is of little importance in this work.

3.1.1.2 DIFFUSION COEFFICIENTS FOR GASES

From work by Sherwood et al. [23], the diffusion coefficient for gases can be determined from kinetic theory. From this theory it can be shown that the diffusion coefficient is directly proportional to the mean free path (λ) of the molecule and the mean molecular velocity (U).

$$D \propto U\lambda \tag{3.2}$$

This situation holds for an ideal gas, that is for a gas which obeys the ideal gas law :

$$PV = nRT \tag{3.3}$$

where P = pressure (Pa)

V = volume (m^3)

n = number of moles

R = universal gas constant = 8.314 $Pa.m^3/(mol.K)$

T = absolute temperature (Kelvin)

From Sherwood et al.[23] and Hines and Maddox[20], it can be shown by derivation of the above relationship (eqn 3.2) that,

$$D_{AB} = \frac{k'T^{3/2}}{PA_{ave}} \left(\frac{1}{M_A} + \frac{1}{M_B}\right)^{1/2} \quad (3.4)$$

where D_{AB} = diffusivity of gas A into gas B (m^2/sec)

A_{ave} = average cross sectional area of both molecules(m^2)

T = absolute temperature, K

M_A, M_B = molecular weights of A and B

P = pressure (N/m^2), (Pa)

k' = constant of proportionality

There have been several other studies carried out in a semi-empirical manner. These studies include:

Gilliland [24]:

$$D_{AB} = \frac{4.3*10^{-9}\,T^{3/2}}{P(V_A^{1/3} + V_B^{1/3})^2} \left(\frac{1}{M_A} + \frac{1}{M_B}\right)^{1/2} \quad (3.5)$$

where V = molar volume at normal boiling point (m^3/kgmol)

P = pressure in atmospheres (1 atm = 101.3 kPa)

Another more accurate equation based on an experimental curve fit is proposed by Fuller et al. [25]:

$$D_{AB} = \frac{1.0*10^{-9}\, T^{3/2}}{P((S_v)_A^{1/3} + (S_v)_B^{1/3})^2} \frac{(1 + 1)^{1/2}}{(M_A \; M_B)} \qquad (3.6)$$

where P = pressure in atmospheres (1 atm = 101.3 kPa)

S_V = sum of the atomic volumes of the constituent elements that make up the molecule in question (also known as atomic diffusion volumes, m^3/kgatom)

These diffusion volumes are available in Fuller et.al [25], and in Hines and Maddox[20]. The most important values for this study are included in Table 3.1.

TABLE 3.1 ATOMIC AND MOLECULAR DIFFUSION VOLUMES [25].
(Reproduced from Fuller et al.[25])

Atomic and Structural Diffusion Volume Increments

	$v*10^3$ (m^3/kgatom)
Oxygen(O)	5.48
Nitrogen(N)	5.69

Diffusion Volumes for Simple Molecules[25].

	$v*10^3$ (m^3/kgatom)
N_2	17.9
O_2	16.6
Air	20.1

There are several other types of models which can be used to predict the diffusivity of a gas within a gas. For further information the reader is directed to sources such as Hines and Maddox [20].

It is of interest to note than none of the models above, or those contained in Hines and Maddox[20], specifically cover the ozone/oxygen or ozone/air situation.

A good review of a large number of sources is presented by Marrero and Mason [26].

Using data from Fuller et al. [25]. (Table 3.1), equation 3.6 yields the following values:

$Sv_{O3} = 3 * 5.48 = 16.44$

$Sv_{air} = 20.1$

$Sv_{O2} = 16.6$

$M_{O3} = 48$ kg/kgmol

$M_{O2} = 32$ kg/kgmol

$M_{air} = 29$ kg/kgmol

$P = 1$ atm

$T = 298$ K (25°C)

therefore,

$D_{O3,O2} = 4.52*10^{-8}$ m^2/sec

$D_{O3,air} = 4.37*10^{-8}$ m^2/sec

3.1.1.3 DIFFUSION COEFFICIENTS FOR LIQUIDS

As discussed above, the determination of the diffusion coefficient for a liquid system has more uncertainty regarding its accuracy. This is due to the fact that the molecules are much closer together than in a gaseous system. Although the point must be made that the gaseous system discussed above assumes an ideal gas. A non-ideal gas' diffusivity, such as one under high pressure, will not be as easy to predict. In both these cases the relative proximity of the molecules means that the intermolecular forces become more important. These forces are in addition to the random forces present in an ideal gas. The prediction of the transport

properties of the liquid are intermediate between those of the compressed gas and those of the solid phase.

Because of these problems there are several different approaches to the problem. These are quasi-crystalline, fluctuation and hydrodynamical theories [20].

There are several equations based on the hydrodynamical approach [20]. The Stokes-Einstein equation is often used as a basic model for these equations. This equation is derived from two equations. These are the Stokes equation which describes a relationship between the force (F) acting on the particle and its viscosity (μ), velocity (U) and its size (radius,r). The particles are assumed to be hard spheres (for further information see Hines and Maddox[20] and Frenkel[27]).

The Einstein equation relates the diffusivity(D) as a function of mobility (M,velocity per unit force)[20].

The two equations are as follows[20]:

Stokes:

$$F = 6(\pi)(\mu)rU \tag{3.7}$$

Einstein:

$$D = kTM \tag{3.8}$$

Stokes-Einstein:

$$D = \frac{kT}{6(\pi)(\mu)r} \tag{3.9}$$

where D = self diffusion coefficient (m^2/sec)

k = Boltzmann's constant ($kg.m^2.sec^{-2} K^{-1}$)

T = absolute temperature (K)

r = radius of particle (m)

μ = viscosity of liquid (kg/m.sec)

M = velocity per unit force (m/N.sec)

This model has quite a few problems associated with it [20]. (no information given in the primary source), however it provides a useful basis to determine an order of magnitude calculation.

There are several other improvements to this model [20]., however these models mainly deal with self-diffusion and are of little importance to this work.

There are three major categories for diffusion coefficients. These are for dilute non-electrolytes, concentrated electrolytes and dilute electrolytes. These models are all empirical models.

For two dilute non-electrolytes there are two useful models. The first non-electrolyte model is the Wilke-Chang[28]., and the second, which is more useful when water is the solute, is the Sitaraman et al.[29]. equation.

Wilke-Chang[28]. equation:

$$D^{o}_{AB} = \frac{1.17*10^{-13}(E_B M_B)^{1/2} T}{V_A^{0.6}(\mu)} \qquad (3.10)$$

where D^{o}_{AB} = dilute solution interdiffusion coefficient (m^2/s)

μ = viscosity of solution (mPa.sec)

V_A = solute molar volume at the normal boiling point (m^3/kgmol)

M_B = the solvent molecular weight (kg/kgmol)

T = absolute temperature in degrees K

E_B = the solvent association factor

Now for water,

$E_{water} = 2.6$ [28,20].

Now for the Ozone-Water system:

$V_{Oxygen} = 7.4 * 10^{-3}$ m^3/kgatom [20].

therefore,

$V_{O3} = 3*0.0074 = 0.0222$ m^3/kgmol

for T = 293 K (20 °C)

$D_{O3,H2O} = 2.194*10^{-9}$ m^2/sec

(CF for $D_{O2,H2O} = 2.5*10^{-9}$ [34].)

Sitaraman et al. equation [29].:

$$D^{o}_{AB} = \frac{16.79*10^{-14}\ (M_B^{1/2} dH_B^{1/3} T)^{0.93}}{(\mu_B V_A^{1/2} dH_A^{0.3})} \qquad (3.11)$$

where dH_A, dH_B = the latent heats of vaporisation of the solute and solvent respectively at their normal boiling points (J/kg)

Again it must be stressed that the Wilke-Chang equation be used when only if water isn't the solute otherwise 200% errors are not uncommon. It is usual to obtain errors within 11% if water is the solvent [20].

For solutions of concentrated electrolytes, there is a tendency for the liquid to be extremely non-ideal in many cases. For this reason the activity of the solution must be taken into account. This was done with an empirical equation formulated by Vignes [30]. However a

further improvement of Vignes' equation to account for viscosity was done by Leffler and Cullinan [31]:

$$D_{AB}\mu_m = (D^o_{AB}\cdot\mu_B)^{x_B}(D^o_{BA}\cdot\mu_A)^{x_A}\left(1 + \frac{d\ln\{\gamma_A\}}{d\ln x_A}\right) \qquad (3.12)$$

where γ_A = activity coefficient of A

x_A = mole fraction A

μ = viscosity (kg/m.sec)

m = subscript representing mixture

ln = log base e ($\log_e$)

For electrolyte solutes there is dissociation into cation and anion species occurring. For example, when caustic soda (NaOH) is added to water:

$$NaOH \text{ ---> } Na^+_{(aq)} + OH^-_{(aq)} \qquad (3.13)$$

This means that there will be a difference in mobility of the ionic species than if the molecule of NaOH (say) hadn't dissociated. This is due mainly to the difference in size between the dissociated and the original species. However, this does not mean that there is a different migration rate for the positive and negative species. If this occurred then there would be a charge imbalance. This means that the diffusion rates of both ions are the same.

Many studies have been done into this area, and the first and most popular was done by Nernst[32]. The equation for diffusivity at infinite dilution follows[20,32]:

$$D^o_{AB} = 8.931*10^{-14}T\,\frac{\{\lambda_+^o\}\{\lambda^o_-\}}{\{\lambda^o_+\}+\{\lambda^o_-\}}\,\frac{|Z_-|+|Z^+|}{|Z_+Z_-|} \qquad (3.14)$$

where λ^o_+ = cationic conductance at infinite dilution $(A/cm^2)(cm/V)(cm^3/g\text{-equiv})$

λ^o_- = anionic conductance at infinite dilution $(A/cm^2)(cm/V)(cm^3/g\text{-equiv})$

$\{\lambda^o_+\}+\{\lambda l^o_-\}$ = electrolyte conductance at infinite dilution $(A/cm^2)(cm/V)(cm^3/g\text{-equiv})$

Z_+ = cation valence

Z_- = anion valence

Values for the ionic conductance of various anions are available in Robinson and Stokes 33.

All of the previous discussion has been for binary systems. It must be pointed out, however, that binary systems are relatively rare, and the above results should be used with caution in multi-component systems unless the concentrations of other constituents are very low. However, for a mixture of gases the following relationship can be used[20]. It is useful only for diffusion of A through stagnant gases B... .

$$D_{Am} = \frac{1 - x_A}{x_B/D_{AB} + x_C/D_{AC} + ...} \qquad (3.15)$$

3.2 HENRY'S LAW

It is necessary that before Henry's Law is discussed, that fugacity be defined. Fugacity is defined by two separate equations. These equations are as follows[34]:

$$dG = RT\ d\ln(f) \quad \text{;at constant temperature and molar composition} \qquad (3.16)$$

$$\lim_{P \to 0} \frac{f}{P} = 1 \qquad (3.17)$$

where f = fugacity (kPa)

G = gibbs free energy (J/mol)

P = pressure (kPa)

The Gibbs Free(G) energy function is defined as follows[34]:

$$\Delta G^{o}_{f} = \Delta H^{o}_{f} - T\Delta S^{o}_{f} \qquad (3.18)$$

where

ΔH^{o}_{f} = standard heat of formation (J/mol)

T = absolute temperature (K)

ΔS^{o}_{f} = standard entropy of formation (J/mol)

The standard heat of formation is the energy required or given out when a compound is formed from its constituent elements. The standard heat of formation of an element is zero [35]. For example:

Oxygen (O_2) $\Delta H^{o}_{f} = 0$ J/mol (by definition)

Carbon Dioxide(CO_2) $\Delta H^{o}_{f} = -393{,}509$ J/mol [35]

This CO_2 figure is defined as follows:

$$C_{(s)} + O_{2(g)} \rightarrow CO_{2(g)} \qquad (3.19)$$

It is important that the phase is shown in these reactions as this will affect the value of ΔH^{o}_{f}. Hence the subscripts for solid, liquid and gaseous states; s, l and g respectively.

The negative sign for ΔH^{o}_{f} is a thermodynamic representation of an exothermic reaction. This means that in the formation of CO_2, 3.93 kJ of heat is given out per mole. It must also be noted that the usual reference state for which this measurement is made is 298K. This is

represented by ΔH^{o}_{f298}. Heat of formation data is contained in a number of sources, such as Perry et al.[34] and Smith and Van Ness[35]. If the compound is formed from other compounds, then these compounds need to be broken up into their separate heats of formation. These constituents are then added up:

$$\Delta H^{o}_{f} = \Sigma(\Delta H^{o}_{f})_{products} - \Sigma(\Delta H^{o}_{f})_{reactants} \qquad (3.20)$$

Note that reactant and product formations are at the same reference temperature.

Entropy (S) is defined by the following relationship[36]:

$$\Delta S = dQ/T \qquad (3.21)$$

In words this means that the change in entropy is defined by the addition of a small amount of heat at absolute temperature T under reversible conditions. It then follows that:

$$\int dQ/T = 0 \qquad (3.22)$$

for any truly reversible condition. The entropy is a property of the given system.

For a species i in solution with mole fraction x, the definition of fugacity (f) becomes:

$$dG'_i = RT\, d\ln(f'_i) \quad \text{;at constant temperature} \qquad (3.23)$$

$$\lim_{P \to 0} \frac{f'_i}{x_i P} = 1 \qquad (3.24)$$

It can be shown by definition of partial molar properties [34,35]. that:

$$\ln(f) = \Sigma\{x_i \ln(f'_i/x_i)\} \tag{3.25}$$

It then follows that the fugacity of a component in solution (f'_i) is related to the mole fraction of that component. This means that the fugacity in solution is equal to the fugacity ($f'_i = f$) when the mole faction is 1 ($x_i = 1$). It would also, then, follow that when $x_i = 0$ then $f'_i = 0$. The simple relationship that follows on from this is named the Lewis-Randall(LR) rule[34].:

$$f'_i = x_i f_i \tag{3.26}$$

It must be noted that this is only true for certain ideal solutions. In Figure 3.1 it can be seen that there are three lines plotted. These are the solution fugacities based on experiment; the Lewis-Randall (LR) rule and Henry's Law (HL). Henry's Law is thus defined by the below graph. It can be seen that the tangent to the experimental data at low concentration of species i yields a straight line with slope k_i. This slope is known as the Henry's Law Constant.

FIGURE 3.1 FUGACITY VS COMPOSITION FOR A BINARY MIXTURE [34].

(Henry's Law, Experimental, Lewis Randall Rule)

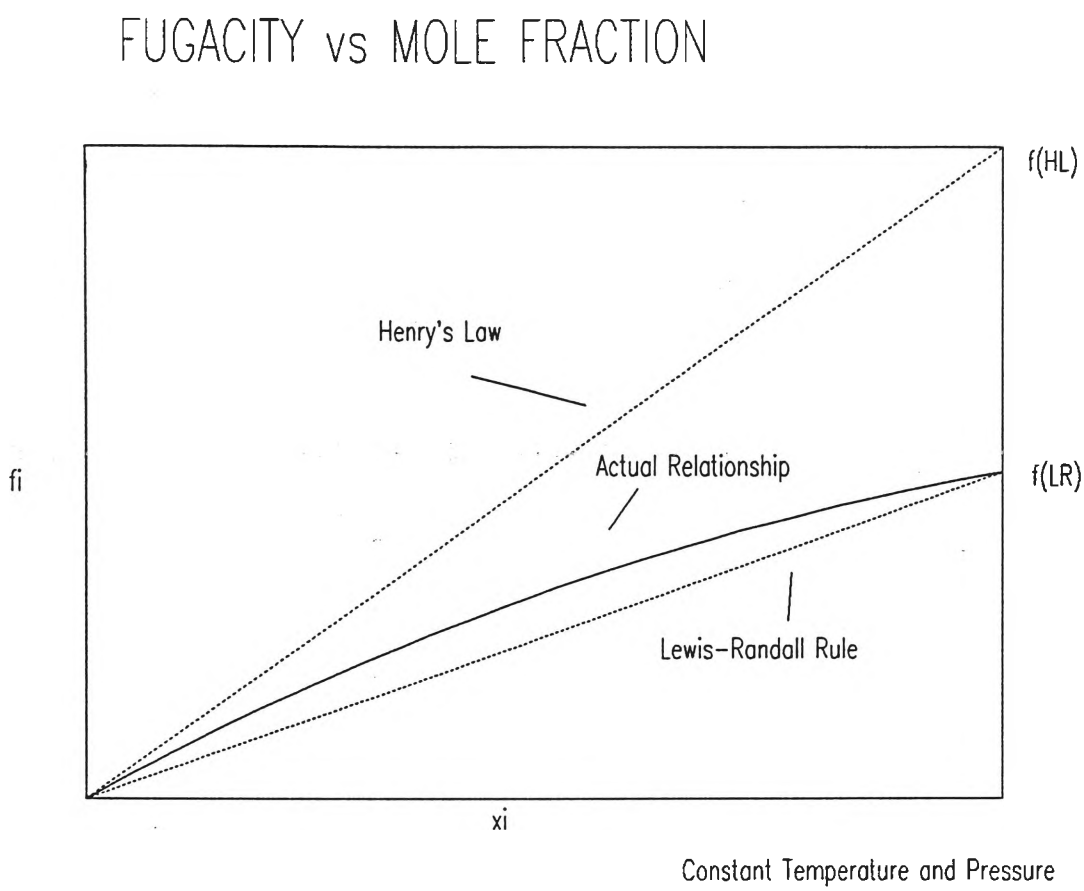

The two important pieces of information that can be gained from the Figure 3.1 are that Henry's Law is valid only at the limiting condition of very low composition, and the Lewis-Randall rule is valid at the limiting condition of very high concentration. Figure 3.1 is only intended as a representation, and is not implied as an actual picture of typical deviations from either law.

In this thesis, Henry's Law is used as a solution model, due to the usually low concentrations of both the pollutant species and the ozone oxidant.

The Henry's Law constant, then, can be used to determine the solubility behaviour of a gas, by relating the partial pressure and the solution concentration. It follows that:

$$p_i = H_i^*[C_i] \qquad (3.27)$$

where p_i = partial pressure of species i (kPa)

H_i = Henry's Law Constant for i (kPa.l/mol)

$[C_i]$ = solution concentration (mol/l)

However, it is often preferable to convert this Henry's Law constant to an easier to use form. This form relates the concentrations in the liquid and gas phase together.

i.e.

$$p_i = y_i * P_T \tag{3.28}$$

and

$$H_i = \frac{p_i}{[C_i]} = \frac{y_i * P_T}{[C_i]} \tag{3.29}$$

Assuming an ideal gas behaviour:

$$P_T = \frac{n_T * R * T}{V_T} \tag{3.30}$$

and

$$y_i = \frac{n_i}{n_T} \tag{3.31}$$

and

$$(C_i) = \frac{n_i}{V_T} \tag{3.32}$$

substituting and solving,

$$H_{i,d} = \frac{H_i}{R*T} = \frac{(C_i)}{[C_i]} \tag{3.33}$$

where

(C_i) = gas phase concentration of i (mol/l)

$H_{i,d}$ = dimensionless Henry's Law Constant

R = 8.314 = Universal Gas Constant (l.kPa/mol.K)

P_T = Total System Pressure (kPa)

y_i = gas phase mole fraction

V_T = total system volume (l)

n_i = number of moles of species i

n_T = total number of moles of all species present

T = equilibrium temperature (K)

$[C_i]$ = liquid phase concentration of i (mol/l)

The dimensionless Henry's Law equation form is the relationship used in mass transfer model development in this study (see Chapter 8).

The Henry's Law equations (3.29 and 3.33) are equilibrium equations. There are two relationships proposed by Danckwerts[125.] which relate the behaviour of Henry's Law constant as a function of temperature [9,125.]:

$$\frac{d\ln H}{d(1/T)} = \frac{-H_i}{R} \qquad (3.34)$$

and in electrolytes [9,125.]:

$$\log(H/H_o) = h.I \qquad (3.35)$$

where R = universal gas constant = 8.314 $Pa.m^3/(mol.K)$

H_i = positive heat of absorption at T(K) (J/mol)

H_o = Henry's Law constant in water

H = Henry's Law constant of the species

I = ionic strength (M)

h = 'the sum of contributions referring to the species of positive and negative ions present and to the species of gas'[9].

The effects of the liquid composition and the equilibrium temperature can also be expressed by [35,65].:

$$H_i = (\gamma)_i . p_i^o \frac{(v_s)}{(R.T_e)} \qquad (3.36)$$

where

$(\gamma)_i$ = liquid phase activity coefficient for species i

p_i^o = vapour pressure of pure i at equilibrium temperature (atm)

v_s = molar volume of the solution (m^3/mol)

= $18*10^{-6}$ for H_2O

3.2.1 PREDICTION OF HENRY'S LAW CONSTANT FOR WATER SYSTEMS

As a general rule in aqueous systems at moderate to low temperatures and pressures (such as atmospheric), the Henry's Law relationship is obeyed [65].. However as the system becomes more complex this may not always be so.

As in most other physical systems it is important to know as accurately as possible the chemical and physical properties of the water. In the case of the Henry's Law constant there are a number of sources for obtaining the constant in clean or distilled water. It has been shown that the temperature dependence of Henry Law follows a similar trend to that of the Arrhenius' Law relationship (equation 3.37), for reaction kinetics [65]. under non-severe conditions.

Arrhenius Law [74]:

$$k = k_o\text{-}E/RT \qquad (3.37)$$

where

k = reaction rate constant$(sec)^{-1}(mol/l)^{1-n}$

n = reaction order (dimensionless)

k_o = frequency factor (units as per rate constant)

E = activation energy (J/mol)

R = universal gas constant = 8.314 J/(K.mol)

T = absolute temperature (K)

Yurteri et.al [65] suggest that for many different complex mixtures the Henry's Law constant may vary quite considerably (by as much as 35%) from predicted values.

It is possible to predict the Henry's Law constant for many chemical species in water by using methods such as the vapour pressure to solubility ratios. However care should be taken in using these methods due to the fact that the chemical composition matrices are not always easy to predict or account for [65].

In a study by Yurteri et.al [65] it was found that species such as humics, surfactants and salts all effect the H values in large and unpredictable ways. This is due to the many competing processes of solvation, salting-out and association that may be occurring [65]. Therefore, it is suggested that at least the parameters of ionic strength(I), temperature and pH are known.

For example, using equations from Sotelo et al [9], it can be shown that for a given pH changing the type of salt, even for a given ionic strength, has the following result (Further information appears in Table 3.2):

pH=6, T=20°C, I=0.45M (Sodium Chloride)

$H = 6.044 * 10^5$ kPa/(mol.fract)

pH=6, T=20°C, I=0.45M (Sodium Sulfate)

$H = 6.58 * 10^5$ kPa/(mol.fract)

In the example above it can be seen that changing the salt type only can still lead to a 13% difference in Henry's Law constant.

It is suggested that good reliable Henry's Law constant measurement methods such as EPICS (Equilibrium Partitioning in Closed Systems)[65,66] are used.

Given the conditional factors described above, the following table reproduced from Sotelo et.al [9] shows the Henry's Law constant for a number of experimental conditions of salt, pH and temperature:

TABLE 3.2 HENRY'S LAW CONSTANT FOR OZONE [9].

SALT TYPE						
Sodium Phosphate		0<T<20	2<pH<8.5	0.001<I<.5M		
*		H=1.03*10^9exp(-2118/T)exp(0.961I)(OH)^0.012				
		r^2=.901	SD=0.108			
Sodium Phosphate &		0<T<20 C		pH=7	0.01<I<.1 M	
Sodium Carbonate			H=4.67*10^7exp(-1364.5/T)exp(2.98I)			
**		r^2=0.98	SD=4.25*10^-3			
Sodium Sulfate		T=20 C	2<pH<7	4.9*10^-2<I<.49M		
*		H=1.76*10^6exp(0.033I)[OH]^0.062				
		r^2=.94	SD=.095			
Sodium Chloride		T=20 C	pH=6	.04<I<.49 M		
**			H=4.87*10^5exp(.48I)			
		r^2=.979	SD=5.64*10^-4			
Sodium Chloride &		T=20 C	pH=7	0.05<I<.5 M		
Sodium Phosphate			H=5.82*10^5exp(0.42I)			
**		r^2=.976	SD=3.36*10^-3			
* indicates: Buffered solutions						
** indicates: Unbuffered solutions. pH initial value.						

where

SD = standard deviation

r^2 = multiple correlation coefficient

H = Henry's Law constant (kPa/molfract)

I = Ionic Strength (M)

T = temperature (^oC)

Other useful correlations for the determination of the Henry's Law Constant for Ozone (O_3) are given by Ouederni et al. [112].:

$$\log(H) = 20.7 - 3547/T \text{ (@pH=7)} \quad (3.38)$$

$$\log(H) = 18.1 - 2876/T \text{ (@pH=2)} \quad (3.39)$$

where

H = Henry's Law Constant (atm)

T = Temperature (K)

The Uoederni et al [112] correlation for neutral pH (pH=7) is also comparable to a number of other studies at various pH's and ionic strengths such as those of Sotelo et al [9].

3.3 MASS TRANSFER THEORY

The phenomenon of absorption from a gas into a liquid is a complicated modelling process and there have been many theories which have attempted to describe this behaviour. The mass transfer process from one phase into another is very important in industry. It forms the basis of many unit operations such as distillation, liquid-liquid extraction and gas absorption. When transfer occurs between one phase and another there is a boundary which must be crossed. There have been a variety of models proposed to described this boundary and its corresponding effect on the mass transfer of the system. These models are described briefly in the following sections (3.3.1 to 3.3.6). General results have been given, with brief derivations where necessary. For a more detailed explanation and review, Coulson et al.[36], Hines and Maddox [20] or Boddeus[37] are recommended. It must be noted that in the following models that there are problems of obtaining accurate data. For this reason overall mass transfer coefficients provide a more practical behavioural model. The use of overall mass transfer coefficients lends itself much more easily to equipment design than do the various phase boundary models.

3.3.1 TWO FILM THEORY

This theory was first examined by Whitman[47], and is useful in describing the conditions of transfer of material from one place to another. It, however, is limited by the fact that the conditions that it describes are not that easily transferred to practical mass transfer equipment.

The main basis of this theory is that the layers at the phase boundary are in a state of laminar flow, rather than in a turbulent state. Outside this layer, in the bulk of that particular phase, the natural random motion of the particles is enhanced or supplemented by turbulent eddy-like motion. This eddy-like motion decreases the resistance to mass transfer. Figure 3.2 shows the basis of the two-film theory. As can be seen the model comprises two thin layers either side of the phase interface, from which the mass transfer occurs. The figure shows that the concentration gradient is near-linear at the phase interface, gradually decreasing until the bulk phase concentration is reached. This is the prediction of what occurs under equimolar counterdiffusion. This is represented in Figure 3.2 as lines ABC and DEF.

The basis of the two-film model, then, is the linear relationship of equimolar counterdiffusion. This model shows that there would be no mass transfer outside the phase boundary layer. This is represented in Figure 3.2 as concentration gradients CG and DH. Figure 3.2 also shows the thickness of the two laminar films (L_1 and L_2). The model also assumes that an equilibrium relationship exists between phase 1 and phase 2. This is shown by the two points C and D. (see Section 3.2 Henry's Law).

FIGURE 3.2 THE TWO FILM THEORY [36].

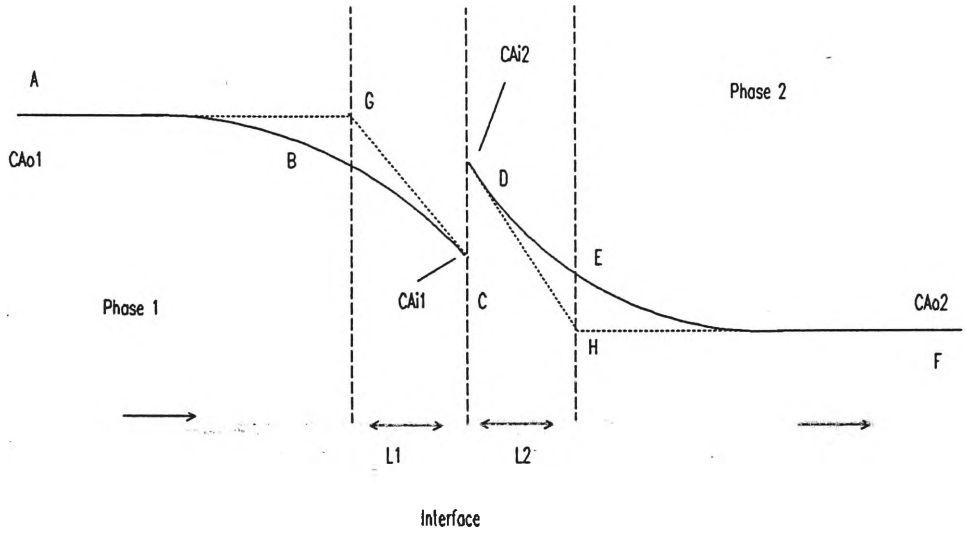

The results that can be obtained from the film theory are:

$$N_A = \frac{D_1}{L_1}(C_{Ao1} - C_{Ai1}) = k_1'(C_{Ao1} - C_{Ai1}) \qquad (3.40)$$

$$N_A = \frac{D_2}{L_2}(C_{Ai2} - C_{Ao2}) = k_2'(C_{Ai2} - C_{Ao2}) \qquad (3.41)$$

As was described above, the diffusion that is occurring is equimolar counter-diffusion, so that the rate of transfer from one-side of the boundary to the other side must be equal unless there is a degree of hold-up in the interface itself. This equimolar counter diffusion is assumed to be the case.

The mass transfer is assumed, then, to be a steady-state phenomenon. These criteria lead to the following result:

$$\frac{k_1'}{k_2'} = \frac{(C_{Ai2} - C_{Ao2})}{(C_{Ao1} - C_{Ai1})} \qquad (3.42)$$

where

k_1' = mass transfer coefficient, phase 1 (m/sec)

k_2' = mass transfer coefficient, phase 2 (m/sec)

C_{Ai1} = interfacial molar concentration in phase 1 (mol/m^3)

C_{Ai2} = interfacial molar concentration in phase 2 (mol/m^3)

C_{Ao1} = bulk molar concentration in phase 1 (mol/m^3)

C_{Ao2} = bulk molar concentration in phase 2 (mol/m^3)

It is not an easy matter to determine the thickness of the film layers (L_1 and L_2). However is it important to note that these two film layers will decrease in thickness as the turbulence of the system increases.

This is a useful model to be used in the gas absorption process where the transfer of the carrier gas is negligible. The mass transfer rate in this situation is greater, and non-linear. See Coulson et al [36.], Boddeus [37.] or Hines and Maddox [20.] for further information.

3.3.2 PENETRATION THEORY

This theory was first expounded by Higbie[48.], where experiments were first carried out in 1935 with carbon dioxide (CO_2) absorption into water in a water-filled vertical column. Slug-like bubbles of CO_2 were used.

This model produces a concentration gradient vs solvent depth such as that shown in figure 3.3.

FIGURE 3.3 PENETRATION MODEL OF SOLUTE INTO SOLVENT [36.]

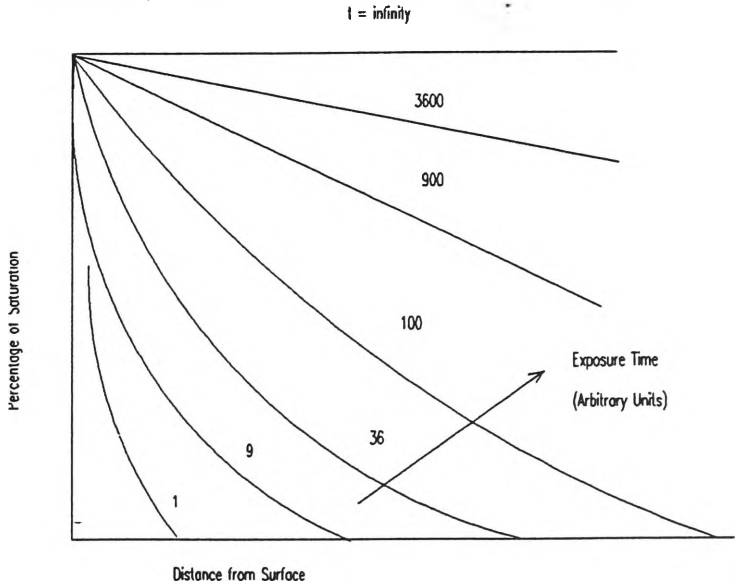

The model works by describing how the concentration gradient of the solute in the solvent builds up over a period of time. The solvent, which initially has no solute concentration, comes into contact with the solute. At zero time only the surface layer of the solvent has any solute in it. In this model, eddies from within the bulk of the solvent bring fresh solvent to the interface. These in turn receive exposure to the solute. The eddies then carry these elements back into the bulk of the solvent. This process then repeats after a fixed interval of time.

The process that occurs between the surface of the solvent and the solute is unsteady-state molecular diffusion. When a surface element of the solvent comes into contact with the solute an equilibrium is reached (See 3.2 Henry's Law). If the contact time is sufficient then near 100% saturation will be achieved.

This model, however, assumes infinite solution depth. This situation can occur only if the exposure time is short enough for a depth of less than the actual solvent depth to be affected. That is, the shorter the exposure time, the more accurate is the model. It is also assumed that there are now velocity gradients within either phase, and that all fluids of all depths are moving at the same velocity as the interface.

In the case of equimolar counter diffusion the unimolar result is:

$$\frac{\delta C_A}{\delta t} = D\frac{\delta^2 C_A}{\delta y^2} \quad \text{(1-dimensional)} \qquad (3.43)$$

where

y = phase depth (m)

t = time (seconds)

The following boundary conditions are:

t = 0	0<y<infinity	then	$C_A = C_{Ao}$
t>0	y = 0	then	$C_A = C_{Ai}$

t>0 y = infinity then $C_A = C_{Ao}$

where C_{Ao} = the concentration of A in the bulk of the particular phase.(mol/l)

C_{Ai} = the equilibrium concentration of A at the phase interface.(mol/l)

Solving,

$$(N_A)_{y=0} = (C_{Ai} - C_{Ao})\sqrt{\frac{D}{\pi t}} \tag{3.44}$$

This equation gives the instantaneous rate of mass transfer for a surface element which has been in contact for a time of t. That is the surface element is of age t. This equation can be integrated with respect to t for any interval. For example 0 to t or t_1 to t_2.

The difference between the effects of diffusivity in this and the two film model is that the diffusivity has a half-power influence in this model.

3.3.3 PENETRATION THEORY WITH RANDOM SURFACE RENEWAL

This is a similar model to the Penetration Model discussed in section 3.3.2, however there are a few differences which are discussed in the following paragraphs.

From work by Danckwerks [49]. it was suggested that it was unreasonable to imagine that all surface elements had the same time of exposure to the second phase. Rather it was more realistic to assume that these surface elements had a distribution of ages. This distribution of ages was also likely to be random. He assumed that it was unlikely that the rate of surface renewal was a function of the amount of time that the element had been at the surface.

This theory forms its basis around the definition of the rate of fresh production of surface per unit total area of surface[36,49]. This is defined by the variable s.

Now from Coulson et al.[36] and Danckwerts[49],

Area of surface age between t and t+dt = f(t)dt (3.45)

So that f(t)dt now equals the area which passes through the given age ranges of:

t-dt ---> t

and, t ---> t+dt

It also follows that f(t)dt will be equal to the area in a particular range minus that included due to replacement of fresh surface in that time of dt.

So,

$$f(t)dt = f(t-dt)dt-[f(t-dt)dt]s\ dt \tag{3.46}$$

and so rearranging yields the following,

$$\frac{f(t) - f(t-dt)}{dt} + sf(t-dt) = 0 \tag{3.47}$$

$$sf(t) + f'(t) = 0 \tag{3.48}$$

and so by taking Laplace Transforms,

$$e^{st}f(t) = (\text{constant}) \tag{3.49}$$

Now if the total area of surface is unity then the integral from zero to infinity of f(t) dt will be unity.

So that the following results,

$f(t) = se^{-st}$ (3.50)

This equation can be substituted into the following relationship:

$$N_A = (C_{Ai} - C_{Ao})\sqrt{\frac{D}{\pi t}}s.e^{-st} \quad (3.51)$$

This can then be integrated over time from 0 to infinity to yield,

$$N_A = (C_{Ai} - C_{Ao})(Ds)^{0.5} \quad (3.52)$$

Based on this derivation it can be seen that there will be tendency to actually underestimate the rate of mass transfer because in a practical situation there will be a finite age for any given surface element rather than an infinite distribution, as is the case in this situation. It can be assumed, however, that the number of these extremely old surface elements is very small and is likely to be extremely small, especially if the fluid tends toward turbulence. That is, the value of s will increase in a turbulent fluid.

It is also useful to note that the value of s will tend toward the same order of magnitude as the velocity in the case of a packed column. Otherwise the value of s is very difficult to estimate.

3.3.3.1 DEFICIENCIES OF THE SURFACE RENEWAL MODEL

In gas-liquid exchange processes, the use of the Higbie [83] surface renewal models should be used with extreme caution. From work by Asher and Pankow [94] it has been shown that the Higbie surface renewal model only really accurately describes transport velocities for a cleaned gas-liquid interface with high levels of turbulence. They [94] also showed that the predictive ability of these models was severely limited if the interfaces were film covered.

3.3.4 PENETRATION THEORY WITH VARYING INTERFACE COMPOSITION
36.

The drawbacks with the penetration model previously discussed are that the model assumes that the solute A is a pure solute, or the solute phase has no significant resistance to mass transfer; and therefore at the phase interface the concentration is constant. This means that the equilibrium relationship that A holds with the second phase will also be constant. However, if the solute phase is not pure A, but rather a mixture, or when the solute phase has a significant resistance to mass transfer, then the concentration of A at the phase interface will likely change with time. In this case, there will be a concentration gradient developed in the solute phase.

Suppose the situation can be modelled as a hybrid of the two-film model and the penetration model. In this case on one side of the phase boundary (phase 1) there can exist for modelling purposes a laminar film layer (see section 3.3.1), whilst in the second phase, the penetration model still applies(see section 3.3.2). In this hybrid model the resistance to mass transfer occurs across the film layer because in the penetration layer the driving force will increase every time the surface element is renewed. As the time of exposure begins to increase so too will the bulk concentration of the solute in phase 2 (penetration phase). This will mean that the resistance to mass transfer contributed by phase 2 will begin to increase due to the decreased concentration driving force from phase 1 to phase 2. From this it can be seen that the bulk concentration of solute in phase 2 (penetration phase) will affect the interface concentration. As time increases towards infinity then the bulk concentration in phase 2 will approach the equilibrium concentration with the first phase.

Now the mathematical result of this model is as follows:

$$N_A = -\frac{D_f}{L_f}(C_{Ai}' - C_{Ao}') \qquad (3.53)$$

where

N_A = mass transfer per unit area of A (kgmol/m^2.sec)

D_f = diffusivity through the film(m^2/sec)

L_f = film thickness(m)

C_{Ai}' = the concentration of A at the interface (kgmol/m^3)

C_{Ao}' = the concentration of A in the bulk (kgmol/m^3)

A similar assumption is made with this model as was made for the two-film model (Section 3.3.1), in that the capacity, or hold-up, of the film for the solute A is assumed to be negligible.

It can also be assumed that if the concentrations are low enough then Henry's Law can be used (Section 3.2). Then,

$$C_{Ai} = \frac{1}{H} C_{Ai}' \tag{3.54}$$

and from Fick's Law (See Section 3.1.1)

$$N_A = -D\left(\frac{dC_A}{dy}\right)_{y=0} \tag{3.55}$$

and so substituting yields,

$$C_{Ai} = \frac{DL_f}{D_f H}\left(\frac{dC_A}{dy}\right)_{y=0} + \frac{C_{Ao}'}{H} \tag{3.56}$$

This can then be substituted and solved to yield the instantaneous mass transfer rate of A from phase 1 into phase 2. That is:

$$N_A = \left(C_{Ao}' - HC_{Ao}\right) D_f \left(e^{\frac{D_f^2 H^2}{DL_f^2}}\right) \times erfc\left(\sqrt{\frac{D_f^2 H^2 t}{DL_f^2}}\right) \quad 5 \tag{3.57}$$

Now, as was done for the two previous models, the average rate of mass transfer can be found by integration over a time period. Thus the result will be based on the penetration models by Higbie[48]. or Danckwerts[49].

3.3.5 PENETRATION THEORY WITH LAMINAR FILM INTERFACE

In work by Harriott [50]., it was suggested that even on the penetration side of the interface there would be a very thin laminar layer caused by the tension between the two different phases in contact. The result of this very thin laminar layer is that it would provide a constant resistance to mass transfer. This is because it would be relatively unaffected by turbulent mixing from within the bulk of the phase. Thus the model is similar to that in the preceding section with the following modifications:

$H = 1$

$D_f = D$

$C_{Ao}' - HC_{Ao}' = C_{Ai} - C_{Ao}$ = Driving force

$L_f = L$

Therefore,

$$N_A = (C_{Ai} - C_{Ao})\frac{D}{L}e^{Dt/L^2}erfc\left(\sqrt{\frac{Dt}{L^2}}\right) \tag{3.58}$$

The following results for average mass transfer determined by the Higbie [48]. or Danckwerts[49]. models are:

Higbie Model [48].:

$$(N_A)_{ave} = (C_{Ai} - C_{Ao})\left[\frac{L}{t}\left(e^{Dt_e/L^2}erfc\sqrt{Dt_e/L^2} - 1\right) + 2\sqrt{\frac{D}{\pi t_e}}\right] \tag{3.59}$$

Danckwerts Model [49]:

$$\left(N_A\right)_{ave} = \left(C_{Ai} - C_{Ao}\right)\frac{D}{L}\left(1+\sqrt{\frac{D}{L^2 s}}\right)^{-1} \tag{3.60}$$

3.3.6 FILM-PENETRATION THEORY

The film-penetration model is a model proposed by Toor and Marchello [51]. The model describes a process whereby the resistance to mass transfer is a single laminar film at the interface of the two phases. This phase is of a finite thickness and behaves similarly to that in the two-film theory (Section 3.3.1). The mass transfer through the aforementioned film, however, is of an unsteady-state nature. As in the penetration theory, fresh surface is brought to the interface via eddy currents within that phase. The difference with the penetration theory is that all of the mass transfer resistance of the penetration phase occurs within the laminar film. Once the material leaves this film it is then mixed completely into the bulk of the phase.

The film-penetration theory has two major cases. For the case where none of the exposed material has left the laminar film, in this case the theory resembles the penetration theory. In the second case where a long period of time has elapsed, then a steady-state gradient has developed, then the theory resembles the two-film theory.

The formulation of the film-penetration model requires a modification to the boundary conditions. The new boundary conditions are as follows:

t=0	0<y<∞	$C_A = C_{Ao}$
t>0	y=0	$C_A = C_{Ai}$
t>0	y=L	$C_A = C_{Ao}$

Now the following results for instantaneous mass transfer are:

$$\pi \leq \frac{L^2}{Dt} \leq \infty \qquad N_A = (C_{Ai} - C_{Ao})\sqrt{\frac{D}{\pi t}}\left(1 + 2e^{-L^2/Dt}\right) \tag{3.61}$$

$$0 < \frac{L^2}{Dt} \leq \pi \qquad N_A = (C_{Ai} - C_{Ao})\frac{D}{L}\left(1 + 2e^{-(\pi^2 Dt)/L^2}\right) \tag{3.62}$$

However, if the exponential terms are neglected then the error will be within 8.64% [36].

$$\pi \leq \frac{L^2}{Dt} \leq \infty \qquad N_A = (C_{Ai} - C_{Ao})\sqrt{\frac{D}{\pi t}} \tag{3.63}$$

$$0 < \frac{L^2}{Dt} \leq \pi \qquad N_A = (C_{Ai} - C_{Ao})\frac{D}{L} \tag{3.64}$$

For full derivation see Toor and Marchello [51], Coulson et al. [36] or Boddeus [37].

Coulson et al.[36] suggests that for practical applications, the first of the two equations (3.61 or 3.63) be used in packed towers with small packings, spray towers and in other applications where there is likely to be dispersal of one of the phases into small drops. The second equation (3.62 or 3.64) is more suited to packed columns with larger packings and for wetted-wall columns [36]. These recommendations are only to be used as a rule of thumb, as there will be exceptions.

It is of interest to note that if this theory were to be applied to the jet pump contactor then the decision on the flow regime would be a difficult one. This is because the flow regime lies between the two aforementioned cases, depending on the water flowrate and the nozzle and mixing tube selection.

Although from data obtained on the jet pump, the two phase flow appears to be annular, so this may suggest that the second equation may be applicable(see Chapter 9).

3.3.7 MASS TRANSFER COEFFICIENTS

As can be seen from the above models (Sections 3.3.1 to 3.3.6) the rate of transfer is always proportional to the concentration driving force. It is the modelling of this constant of proportionality that varies. Therefore:

$$N_A = k'(C_{Ai} - C_{Ao}) \tag{3.65}$$

It must be noted that this equation only holds in the absence of bulk flow. It is also often the case where there is a combination of models occurring. For example the film theory on one side of the phase boundary and the penetration theory on the other side.

If the process is under steady state conditions and the concentrations at the interface are unchanged, then this means that the two-film model is holding. This also means that the mass transfer rate on either side of the boundary will be the same. That is[36]:

$$N_A = k'_1(C_{Ao1} - C_{Ai1}) = k'_2(C_{Ai2} - C_{Ao2}) \tag{3.66}$$

The values of C_{Ai1} and C_{Ai2} will be governed by various phase-equilibria if there is no phase resistance at the boundary. However, the concentrations at the phase boundaries are not usually known and for this reason an overall transfer coefficient is used as follows:

$$N_A = K_1(C_{Ao1} - C_{Ae1}) = K_2(C_{Ae2} - C_{Ao2}) \tag{3.67}$$

where

C_{Ae1} = the concentration of the constituent in phase 1 which is in equilibrium with that in C_{Ao2} in phase 2.(kgmol/m^3)

C_{Ae2} = the concentration of the constituent in phase 2 which is in equilibrium with that in C_{Ao1} in phase 1.(kgmol/m^3)

If the equilibrium relationship between the 2 phases is linear (See Henry's Law Section 3.2) then there will exist a constant, *H*, which will relate the concentrations.

Therefore ;

$$H = \frac{C_{Ao1}}{C_{Ae2}} = \frac{C_{Ae1}}{C_{Ao2}} = \frac{C_{Ai1}}{C_{Ai2}} \qquad (3.68)$$

Now, using the results from the previous three equations (3.66 to 3.68) the following equations can be developed:

$$\frac{1}{K_1} = \frac{1}{k_1'} + \frac{H}{k_2'} \qquad (3.69)$$

$$\frac{1}{K_2} = \frac{1}{Hk_1'} + \frac{1}{k_2'} \qquad (3.70)$$

$$\frac{1}{K_1} = \frac{H}{K_2} \qquad (3.71)$$

It is important to note several relationships which arise when various factors are larger than the others:

$K_2 = k_2'$ if $k_1' >> k_2'$

and,

$K_1 = k_1'$ if $k_2' >> k_1'$

All of the above relationships are only valid if the linear dependence between transfer, driving force and equilibrium hold. Coulson et al.[36] suggest that the following models are appropriate with the following mass transfer coefficient relationships:

- Two film theory

- Penetration theory - only applicable when used for any given instant of time.

- Film-penetration theory - only applicable when used for any given instant of time.

The reason that the film-penetration and penetration theory should only be used with instantaneous rather than with time-averaged coefficients is that the concentrations at the various interfaces change with time. The only time when this does not happen is if there is a situation where one of the phases has a much higher resistance than the other phase.

3.4 MASS TRANSFER WITH CHEMICAL REACTION

The types of reactions that occur in a two phase systems will have a large bearing on the mass transfer of the system. Levenspiel [74] suggests that there are 8 major cases of mass transfer with reaction. These cases vary according to reaction rate, reaction order and mass transfer rate. These cases are shown in Figure 3.4 [74]:

FIGURE 3.4 INTERFACE BEHAVIOUR FOR THE LIQUID PHASE REACTION [74].

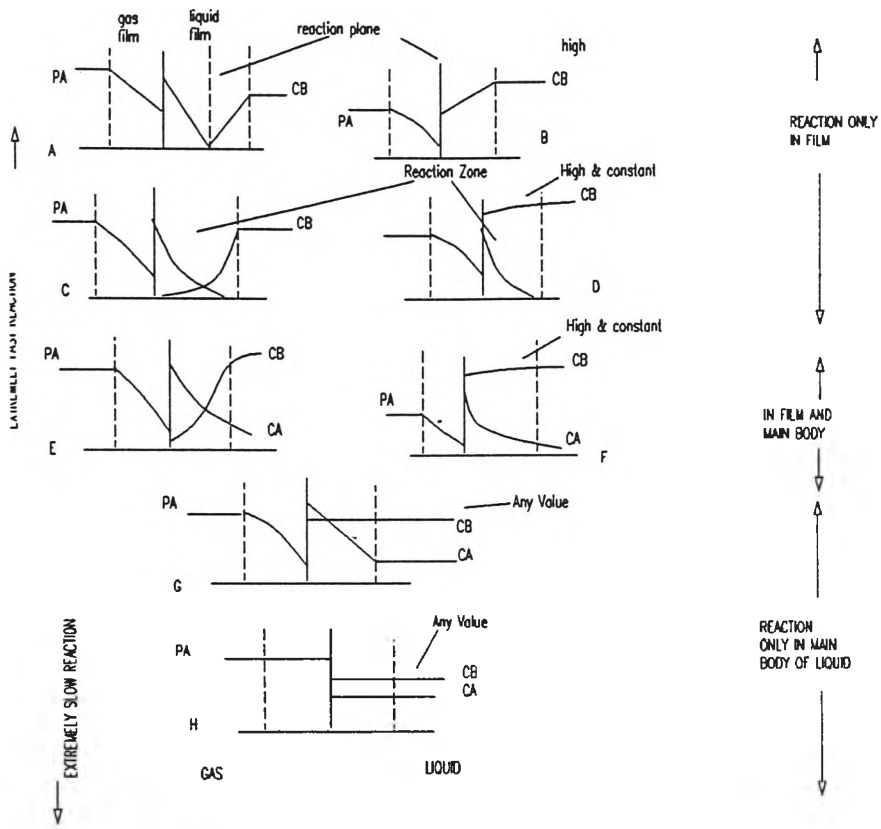

Where

$$A_{(gas)} + bB_{(liquid)} \rightarrow products_{(liquid)}$$

These following definitions are based on those presented by Levenspiel [74]. All reaction rates are classified as fast to extremely slow relative to the mass transfer rate.

Case A: In this case the mass transfer is enhanced because the reaction is taking place at the plane or film between the two phases. Therefore the rate of mass transfer will be controlled by the diffusion rates of A and B in their respective phases. The rate of reaction is very fast.

Case B: If the concentration of the reactant B in the liquid phase is very high, then the rate of mass transfer will be controlled by the rate of diffusion of A in the gas only. The rate of reaction is very fast.

Case C: This is the case where both A and B are present in the liquid film. However, the rate is still fast enough that A does not diffuse into the bulk of phase B. The rate of reaction is a fast second order rate.

Case D: This is the case where the concentration of B in the liquid film is similar to that in the bulk, even after reaction. This case is similar to that of Case C except now the rate can be described as pseudo 1st order.

Case E and F: The rate of reaction is intermediate and so depending upon the concentration of B, some of A may diffuse into the bulk of B.

Case G: The rate of reaction in this case is slow and so all reaction takes place in the bulk of phase B.

Case H: There is essentially no mass transfer resistance here and so the concentrations of A and B are uniform thoughout phase B. The reaction rate is extremely slow.

The following sections (3.4.1 to 3.4.3) deal with cases of interest in ozone disinfection/treatment of waste water. These cases are not the only ones that may apply for O_3-waste water system, and some/all others may apply depending upon the matrix of constituents and environment of the system.

All models developed rely on the film model (see section 3.3.1).

3.4.1 INFINITELY FAST REACTIONS

These reactions are defined by Levenspiel [74] as cases A and B.

If the reaction is that suggested in section 3.4:

$A_{(gas)} + bB_{(liquid)} \rightarrow products_{(liquid)}$

then rates of disappearance of A and B are as follows:

$$-r_A = \frac{-r_B}{b} = k_{Ag}(p_A - p_A^*) = k_{Al}(c_A^* - 0)\underset{x}{x_0} = k_{Bl}(c_B - 0)\underset{(x_0 - x)}{x_0} \qquad (3.72)$$

where

k_{ij} = mass transfer coefficient for respective components in respective phases.(m/sec)

p_A^* = interface concentration = $H_A c_A^*$

H_A = Henry's Law constant (kPa.l/mol)

x_0 = film thickness (m)

If the mass transfer control is via diffusion, then:

$$\frac{k_{Al}}{k_{Bl}} = \frac{D_{Al}/x_0}{D_{Bl}/x_0} = \frac{D_{Al}}{D_{Bl}} \qquad (3.73)$$

where

D_{ij} = molecular diffusion coefficient (m^2/sec) for given phase/component

Substituting the above equations together yields:

$$-r_A = \frac{-1}{S}\frac{dN_A}{dt} = \frac{(D_{Bl}/D_{Al})(c_B/b)+(p_A/H_A)}{(1/H_A k_{Ag})+(1/k_{Al})} \qquad (3.74)$$

If it happens that the gas phase resistance is negligible then the k_{Ag} in the above equation becomes infinity (∞).

For the case of very high concentration of B relative to A then all of the reaction will occur at the phase boundary and hence the gas phase resistance is the controlling resistance:

i.e.

$$-r_A = k_{Ag}p_A \qquad (3.75)$$

3.4.2 SLOW REACTIONS

For slower reactions the reaction tends to take place in both the liquid and the film, and for infinitely slow reactions the reactions take place in the liquid film exclusively.

For intermediate rates [74.]:

$$-\frac{1}{S}\frac{dN_A}{dt} = k_{Ag}(p_A - p_{Ai}) = k_{Al}(c_{Ai} - c_A) \qquad (3.76)$$

and so,

$$-\frac{1}{S}\frac{dN_A}{dt} = kc_Ac_B \qquad (3.77)$$

this leads to,

$$-\frac{1}{S}\frac{dN_A}{dt} = \frac{p_A}{(1/k_{Ag} + H_A/k_{Al} + H_A/kc_B)} \qquad (3.78)$$

Note that in this equation the denominator is a sum of the gas film, liquid film and bulk liquid expressions.

For an infinitely slow reaction the film effectively offers no resistance and so the rate expression is then more usefully expressed in terms of volume(V):

$$-r_{A,i} = -\frac{1}{V}\frac{dN_A}{dt} = kc_Ac_B \qquad (3.79)$$

3.4.3 FILM CONVERSION PARAMETER

In contactor selection the most efficient choice is made on the basis of which reaction/mass transfer regime is being undertaken.

Levenspiel [74.] defines a parameter known as the film conversion parameter(M):

$$M = \frac{\text{maximum possible conversion in film}}{\text{maximum diffusion transport in film}}$$

$$= \frac{kD_{Ai}}{k_{Al}^2} \qquad (3.80)$$

The meaning of this term is as follows [74.]:

M	REGIME
>4	Film Reaction (Cases A,B,C,D)
0.0004<M<4	Intermediate (Cases E,F,G)
<0.0004	Infinitely Slow (Case H)

Levenspiel [74.] suggests that where M is large, then a contactor which has a very large interfacial area such as spray columns and plate columns. For the slower reactions bubble columns are recommended [74.].

3.4.4 MASS TRANSFER AND REACTION SELECTIVITY

There are many factors which are involved in mass transfer and treatment operation. The parameters are not just confined to mass transfer. Each of these separate influences affects the system as a whole. It is important to note that there are a large variety of situations that play a role.

A very important concern in water treatment is the selectivity of the ozone attack, and by which reaction pathway this attack takes place. For example, in work by Stich and Bhattacharyya [52.], it was found that during the treatment of phenol and 2-napthol that there was a significant decrease in the pH, thereby indicating that there were acid species present. For the case of the treated phenol there was a significant decrease in the amount of organic carbon present (Total Organic Carbon, TOC). However, there was no significant decrease in the total organic carbon present in the treated 2-napthol sample for the treatment time observed. In this case the sample has become kinetically limited with kinetically much slower

reaction intermediates formed. This is not as satisfactory as faster kinetics with a $CO_{2(g)}$ final product.

There are many reaction pathways, and many possible intermediates that can be formed. From my experience in the treatment of organics in aluminium industry effluents[21.], it was shown that in fact stable intermediates can form. There is a risk that these are more dangerous, or more of a nuisance, than the initial species.

For example, in the treatment of organics in Bayer Liquors in the aluminium industry the oxidation pathway is as follows [21.]:

FIGURE 3.5 AN EXAMPLE OF AN ORGANIC OXIDATION PATHWAY (ORGANICS PRESENT IN BAYER LIQUORS)[21.]

Cellulose, Calcium/Magnesium Pectates
Lignines

Humic Acid Derivatives
(e.g. - Sodium Humate)

Aromatics (e.g. - Benzene)
Carboxylic Acids

Formic and Oxalic Acid Derivatives
(e.g. Sodium Oxalate and Sodium Carbonate)

Carbon Dioxide

In the Bayer Liquor case, some of the organics are oxidised to the harmless CO_2, however it was found that with increasing O_3 contact time the amount of Sodium Oxalate increased dramatically. This sodium oxalate has nearly as many problems as the initial cellulose and lignines [21.].

The lowering of the pH (in the case of Stich and Bhattacharyya [52] above) also has additional problems in that an acid system can be formed from an essentially neutral or alkaline system. This may lead to various problems in the system such as corrosion and additional equipment to balance the pH. In the case of O_3 treatment, it must be remembered that O_3 reaction kinetics are pH effected (see section 2.2.1).

These situations described above again emphasise the importance of understanding the exact system being dealt with.

In the case of cooling tower treatment for legionella reduction and prevention it may be that in treating the system for the conditions of legionella destruction may lead to compounds which create other problems within the system, such as corrosion amongst others. These may require additional treatment practices. Therefore a balance in system requirements needs to be addressed.

4.0 OZONE-WATER CONTACTING EQUIPMENT AND ITS EFFECT ON MASS TRANSFER ENHANCEMENT

For ozone to be of any benefit in wastewater treatment it must be able to come into intimate contact with the waste to be removed. To achieve this there must be as large as possible area of contact between ozone and water. There are various ways of improving the contact surface for O_3 to water transfer, and these are described in the following sections (4.1 to 4.5). These sections contain design criteria, advantages, disadvantages and recommendations.

4.1 BUBBLE COLUMN CONTACTING EQUIPMENT

In the bubble column, the liquid phase (water effluent) passes through the column and the carrier gas (O_2 or air) carrying the ozone is sparged in either at the base or top of the column. There are a wide variety of sparger designs and geometries. The gas phase then passes through the column either under buoyancy effects or forced flow. The liquid phase enters at the top of the column(usually). If the gas and liquid flow in different directions then this is known as counter-current operation, and in the same direction it is known as a co-current operation.

The column can be empty of mechanical obstructions, or it can be packed. The packing can be purely to increase surface area, or it may be a catalyst. The unpacked column is the simplest column, however, it is most likely to have the lowest efficiency. There are a wide variety of packing styles to help give the desired flow and hence contact pattern through the column, and detail of these can be found in many references [34]. Figure 4.1 shows diagramatically a series of different columns. The most common form of bubble column is the

counter-current bubble column (b). The spray column (c) is included as this column works in a similar way, and is often used for gas scrubbing.

There are many studies into bubble columns and, the bibliography included with this thesis includes a selection of these papers. General treatment is included in works by Hines and Maddox [20], Bird et al. [22], Perry et al. [34], Sherwood et al [63] and Coulson et al [127],[36].

FIGURE 4.1 BUBBLE COLUMN STYLE CONTACTORS

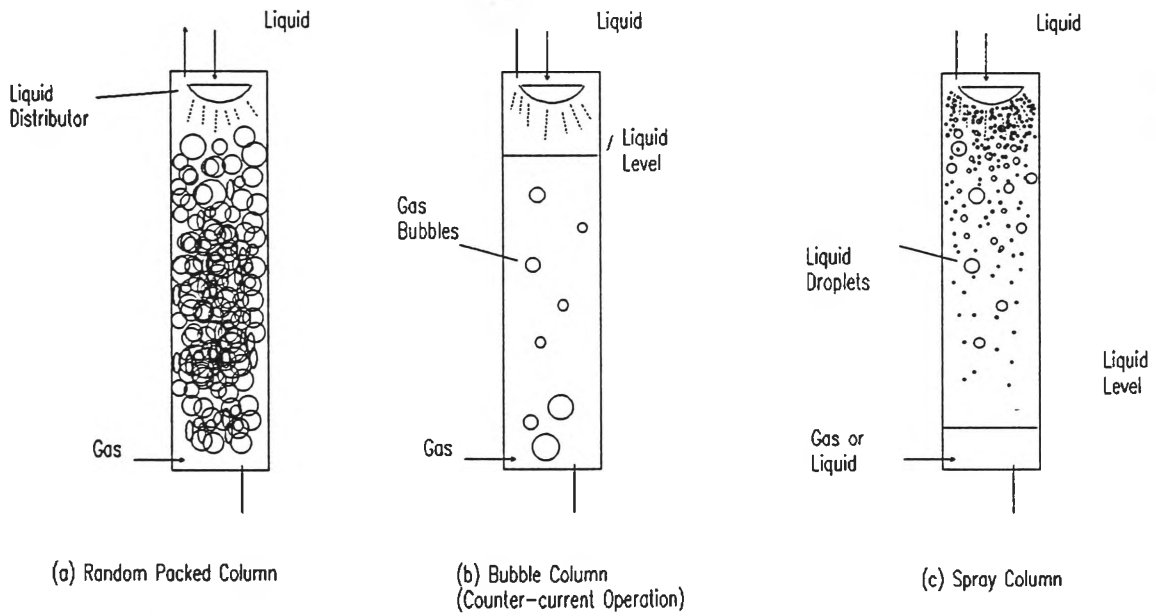

The counter-current bubble column is quite widely used in gas-liquid reactions, and often for fermentors. To design or model a reactor of this kind involves a study of the liquid properties, in particular, as well as the properties of the system.

One of the important characteristics of the bubble column system which will affect the mass transfer rate is the gas hold-up. This is usually defined as fractional gas hold-up (h_G). This variable is determined on the following equation:

$$h_G = \frac{Z_F - Z_L}{Z_F} \qquad (4.1)$$

where

Z_F = height of aerated liquid during column operation (m)

Z_L = height of liquid in column prior to aeration (m)

From work by Akita and Yoshida [38]. it was suggested that elements which can influence the gas hold-up in the column include the diameter of the column(D), the superficial gas velocity(U_{GS}, that velocity which would result if the gas had the whole area of cross-section available for flow), the kinematic viscosity (ν), density(ρ) and surface tension(σ) of the liquid, as well as the orifice diameter of the sparger(d_o) and gravitation(g). It is suggested [38]. that these effects can be analysed in terms of dimensionless groups. Akita and Yoshida [38]. performed a dimensional analysis which yielded the following relationships:

$$h_G = f_1(N_{Bo}, N_{Ga}, N_{Fr}, d_o/D) \tag{4.2}$$

where

$$N_{Bo} = \text{Bond number} = gD^2(\rho)_L/(\sigma) \tag{4.3}$$

$$N_{Fr} = \text{Froude number} = U_{GS}/(gD)^{1/2} \tag{4.4}$$

$$D/d_o = \text{diameter ratio} \tag{4.5}$$

$$N_{Ga} = \text{Galileo number} = gD^3/\nu^2 \tag{4.6}$$

Subscripts

L = liquid

G = gas

S = superficial

It has been shown[38,39] that the effect of the single orifice diameter (d_O) is relatively unimportant. It can also be shown from work by Akita and Yoshida [39] and by Fair et al. [40] that the column diameter effect (D) can be neglected with columns above 0.15m in diameter.

From studies of gases of various densities it can be shown that the effects of gas density on gas hold-up (h_G) can be neglected [38], especially at lower velocities (0.0028 to 0.28 m/sec). Studies[38] also suggest that the liquid rate does not effect the gas hold-up (h_G).

In the case of the jet pump the gas phase velocities range from 0.64 m/sec to 5.08 m/sec after exiting the throat and entering the mixing and draft sections of the column (0.054 and 0.076m in diameter respectively). This is considerably higher than the suggested data from Akita and Yoshida [38] for independence of density. It may be possible then that there will be a density effect.

The end effects of the column due to the entry of the gas from the orifice can be neglected if the column is of sufficient length. It has been found that these end effects are negligible for columns of over 1m in length [38]. In the case of the jet pump, the length of the draft and mixing tube together is over 1.98 m. This should according to Akita and Yoshida [38] negate the end effect.

Akita and Yoshida [38] have found from their experimental work with various gases in various solutions that the following empirical relationship holds:-

$$\frac{h_G}{(1 - h_G)^4} = 0.20(N_{Bo})^{1/8}(N_{Ga})^{1/12}(N_{Fr})^{1.0} \qquad (4.7)$$

$$= 0.2\left(N_{Bo}\right)^{1/8}\left(N_{Ga}\right)^{1/12}\left(u_{GS} / \sqrt{gD}\right) \qquad (4.8)$$

If this correlation is plotted on a log-log scale then a useful graph for determining gas hold-up in bubble columns can be determined. However, if the system is an electrolyte system, then the relationship does not hold as well. This may be due to the changed conditions at the gas-liquid interface due to an electrostatic gradient. It is suggested in this case to use 0.25 as the constant in the equation instead of 0.2, or to increase the values of h_G by 25% [38].

For the determination of the volumetric mass transfer coefficient (k_La) most of the same assumptions for h_G vs U_{GS} correlation can be used [38]. The same dimensional effects also affect mass transfer. There is an additional effect however, that of liquid phase diffusivity (see 3.1.1.3) D_L. The following dimensionless groups need to be defined:

$$N_{Sh} = \text{Sherwood Number} = k_L D/D_L \tag{4.9}$$

$$N_{Sc} = \text{Schmidt Number} = (\mu)_L/D_L \tag{4.10}$$

The dimensional analysis is then [38]:

$$N_{Sh}(aD) = f_2(N_{Sc},N_{Bo},N_{Ga},N_{Fr}) \tag{4.11}$$

or,

$$N_{Sh}(aD) = f_3(N_{Sc},N_{Bo},N_{Ga},h_G) \tag{4.12}$$

Akita and Yoshida [39] showed that for a sodium sulfite(Na_2SO_3)-air solution at 20 °C yielded a straight-line plot of k_La vs $h_G^{1.1}$ on log-log axes. This relationship also held for experiments in a water-O_2 system, except for small columns (0.077m in diameter)[38]. In this thesis the diameter of the column used is 0.076m, therefore according Akita and Yoshida [38] the model for mass transfer will not apply.

From experiment it can be shown that for column sizes 0.152 up to 0.6m, that column diameter and k_La are directly proportional, and produce a straight line on log-log axes. The slope of this line is 0.6 [38]. The correlation for k_La vs h_G is then [38]:

$$k_La = 0.6D_L^{0.5}(\mu)_L^{-0.12}(\sigma/\rho_L)^{-0.62}D^{0.17}g^{0.93}h_G^{1.1} \quad (4.13)$$

In the original work done on this correlation, the data for testing the k_La vs D dependence was only experimentally examined up to a column diameter of 0.6m. There is therefore some doubt on the scale-up ability of this correlation. It is therefore recommended that the k_La value for the 0.6m column be used as a ceiling value [38], although it is possible that it will increase to a certain degree above 0.6m. It is possible that columns modelled on this k_La value may have a k_La value larger than predicted. An experimental evaluation of the k_La vs D dependence of larger columns would be of benefit to allow that validity of the k_La vs h_G correlation to be checked and extended.

In work by Seno et.al [147] similar parameters were studied as in the work of Akita and Yoshida [38], although further development into cocurrent and liquid batch columns were undertaken.

What was found in this work [147] with respect to cocurrent contactors is that the gas hold-up (h_G) decreases with increasing superficial liquid velocity (u_{LS}) in the bubble flow regime. They [147] also developed equations for gas hold-up(h_G):

$$u_{GS}/h_G - u_{LS}/(1-h_G) = 1.24(C_1)^{0.23}(C_2)^{-0.095}(C_3)^{0.5}(1-h_G) \quad (4.14)$$

where

$C_1 = u_{GS}\mu_L/\sigma$

$C_2 = g\mu_L^4/(\rho_L\sigma^3)$

$C_3 = gd$

d = characteristic bubble diameter (m)

this correlation applies for:

$2.55*10^{-5} < C_1 < 6.18*10^{-3}$

$5.33*10^{-12} < C_2 < 3.20*10^{-3}$

$3.00*10^{-3} < C_3 < 4.89*10^{-2}$

A drift flux model of Zuber and Findlay [148] was also examined by Seno et.al [147] for both counter and cocurrent columns for the air-water system. The format of the model is as follows:

$$u_{GS}/h_G = V_b + C_0(u_{LS}+u_{GS}) \qquad (4.15)$$

where

C_0 = distribution parameter which accounts 'for the interaction of velocity and gas void distributions.'[147]

V_b = drift velocity term 'equated to the bubble rise velocity in an infinite medium'[147].

For mass transfer coefficient an increase in u_{LS} yielded a decrease in volumetric mass transfer coefficient (k_La) [147]. This is revealed in the following correlation [147], which is a modification of that by Akita and Yoshida [38]. This modification is for cocurrent flow only.

$$\frac{k_L a D^2}{D_L} = \frac{0.6(u_{GS})}{(u_{LS}+u_{GS})}^{-.39}\left(\frac{N_{Sc}}{\rho_L}\right)^{0.5}\left(\frac{N_{Bo}}{\rho_L}\right)^{.62}\left(\frac{N_{Ga}\rho_L^2}{\mu_L}\right)^{0.31}h_G^{1.1} \qquad (4.16)$$

the correlation applies for the following ranges.

$2.99*10^{-2} < (N_{Sc}) < 3.96*10^{-4}$

$2.84*10^{2} < \frac{(N_{Bo})}{(\rho_L)} < 5.18*10^{2}$

$9.40*10^{4} < \frac{(N_{Ga}\rho_L^2)}{(\mu_L)} < 1.55*10^{9}$

$$2.79*10^{-2} < \frac{(u_{GS})}{(u_{LS}+u_{GS})} < 3.27*10^{-1}$$

4.1.1 EFFECT OF FLOW CHARACTERISTICS THROUGH A BUBBLE COLUMN CONTACTOR ON MASS TRANSFER

Usually when describing, or modelling, a column contacting system the flow through the column is assumed to be plug flow. This means that there is no axial dispersion occurring in the column. The following paragraphs describe the phenomenon for counter-current columns with the liquid phase flowing downwards.

The absence of axial dispersion means that the liquid and gas phases are flowing through the column in an even manner across the whole cross section. If this situation is occurring then there is no back mixing of the phases at any point within the contactor. If there is back mixing in the contactor then this means that the mass transfer coefficient estimated by the design model will be over-estimating the actual mass transfer coefficients.

It should be noted that there are two main zones of operation where this effect is more pronounced. The first case is where the gas is "pumped" through the column from top to bottom. This occurs when the liquid rate is much higher than the gas rate[34]. The second example occurs when the gas rate is much larger than the liquid rate. In this example the liquid phase is likely to be entrained by the rapid gas phase [34].

Further information can be found in Perry et.al [34], Shah et.al [62] and Sherwood et.al [63].

In the downflow co-current jet pump the liquid phase will be "pumped" slightly as well, as the gas velocity is very much greater than the liquid velocity. This causes entrainment in the forwards (or downwards) direction, thereby tending to decrease the liquid residence time (HRT).

4.2 SEMI-BATCH REACTORS

In a semi-batch reaction system the liquid phase is usually contained within the reaction vessel and the ozone-gas is sparged through the reactor. This type of reactor is very good for systems requiring large contact times.

This style of reactor is very common in laboratory scale investigations. It also finds application in a number of industries including polymers, and sewage or waste water treatment.

4.3 JET PUMP CONTACTORS

The jet-pump, or venturi suction, gas liquid contactor is characterised by the liquid stream discharging from a nozzle and dragging gas though a constricting throat. The driving force for the gas phase is formed from the transfer of momentum from the liquid to the gas jet. The water droplets exert a drag on the gas phase and there is a difference in velocity between the two phases (slip velocity) [101]. It is likely that there is a correlation between the hydrodynamic efficiency and the mass transfer efficiencies of the jet pump contactor [101]. It is the purpose of this thesis to examine and model the mass transfer.

From Soh et al. [101] it can be shown that the efficiency of the jet-pump is:

$$n = \frac{\phi(2b-b^2)(1+\phi)(1+K_t+K_d)}{1+K_n-2b+b^2(1+\phi)(1+K_t+K_d)} \qquad (4.17)$$

where

n = efficiency

b = nozzle to mixing tube area ratio

ϕ = Air-Water density ratio

K_t = momentum correction factor

K_d = diffuser loss coefficient

K_n = nozzle loss coefficient

To calculate the loss coefficients and correction factors it is necessary to measure various pressure drops through the jet pump system, as detailed in figure 4.2. A more detailed derivation may be found in Soh et.al [101]. and in Rowley [151].

FIGURE 4.2 JET PUMP SCHEMATIC [101].

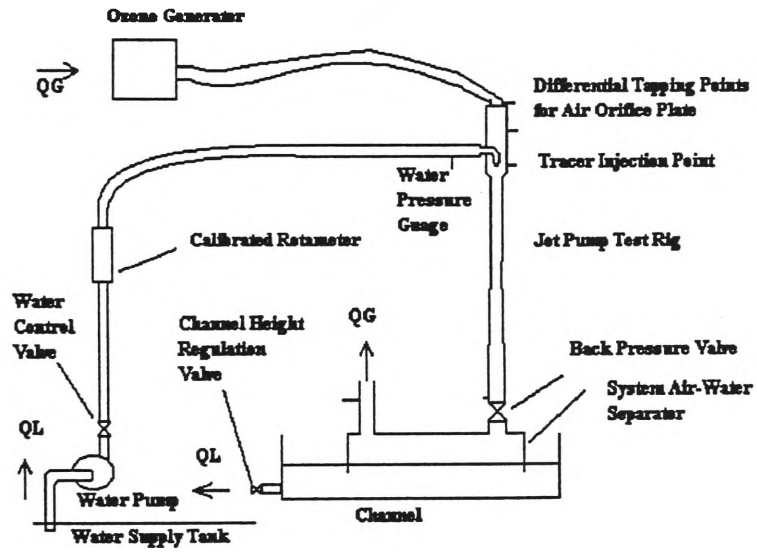

Now,

$$p_3 - p_e = [2b^2 - b^2(1+\phi)(1+K_t+K_d)] \quad (4.18)$$

This allows the value of K_t+K_d to be determined, and similarly the following allows for the determination of K_n.

$$p_0 - p_3 = 0.5\rho_L V_L^2[1+K_n-2b+b^2(1+\phi)(1+K_t+K_d)] \quad (4.19)$$

For the jet-pump used in this study Soh et al. [101] found:

$$O3 = 35 + 28\log(100G) \qquad (4.20)$$

where

O3 = Difference between ozone inlet and outlet flows (g/sec)

G = Index for mass transfer of ozone (s/m^3)

$$= \frac{n}{(Q_L)(\phi)}$$

Q_L = Liquid volumetric flowrate (m^3/sec)

The assumption for this model is that the difference in measured ozone concentration in the gas phase between the inlet and outlet conditions is that ozone which has transferred into the liquid phase. It is also possible that the highly turbulent shock mixing that occurs in the throat of the jet pump, may in fact be leading to dissociation of ozone.

The value of O3 (see equation 4.20), if the above assumption holds, is the absolute mass transfer rate in g/sec. This can be converted to another form more often used, that is to mol/(l.sec).

$$\frac{g}{sec} * \frac{mol}{48\ g} = \frac{mol}{sec}$$

and then dividing this figure by the liquid phase volumetric rate for this same second (Q_L) will yield the consistent units.

Jet pump style of reactors are characterised by high gas to liquid volumetric ratios and high throughputs. It has also been suggested that jet pumps have a very high interfacial area (a) for a given energy dissipation per unit volume [145]. (see Figure 4.3 for various contactor comparisons).

FIGURE 4.3 COMPARISON OF VARIOUS REACTORS [145].

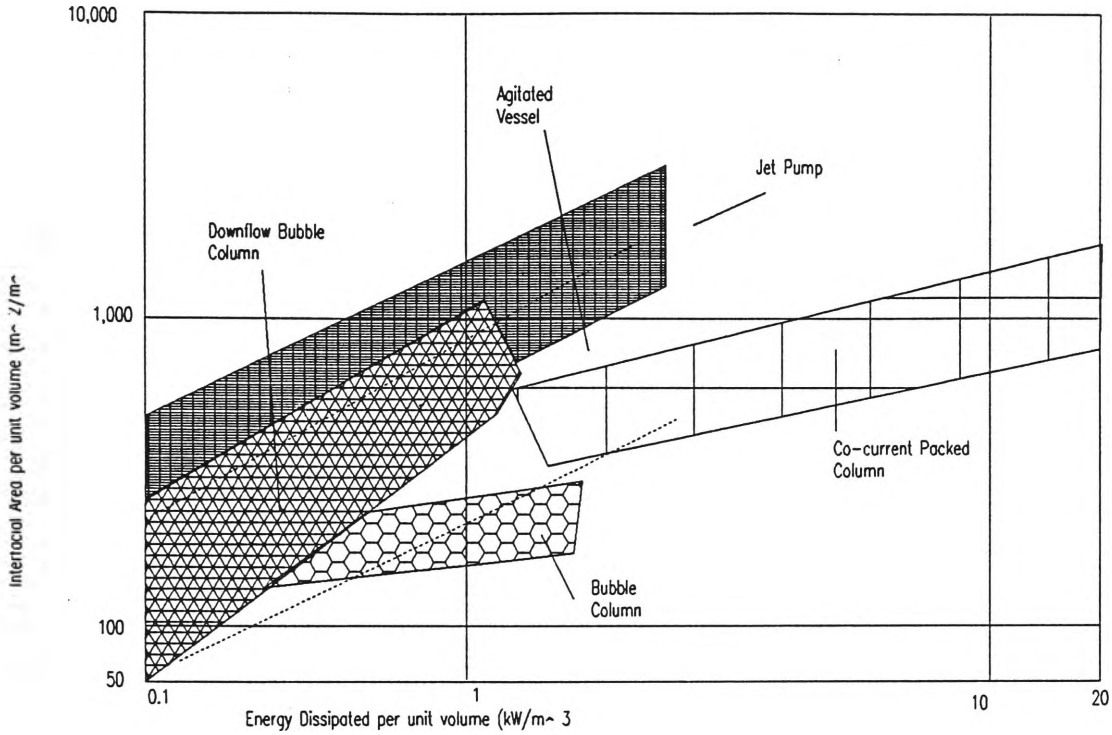

The jet pump also has a very low residence time for the liquid phase, this may mean that CT disinfection requirements are not met (see section 6.1).

4.4 PACKED COLUMNS

In a packed, as opposed to a bubble column, the column is filled with a packing material. The choice of a packed column depends on the type of operation to be performed. This choice is usually made on the basis of empirical observation.

The choice of packing to go into the column is also based on empirical study, although the generic requirement for a packing design is that it should provide very good interfacial contact between the liquid and gas phases. This must be achieved with minimum pressure drop, particularly in the gas phase [127]. The packing may be constructed of a regular mesh type design, or it may be a dumped packing such as raschig rings, pall rings, berl saddles or

intalox saddles [97,127,34]. In the case of chemical reactors, the packing may in fact be a catalyst [34,74].

A packed bed column may operate in either a co-current, or more commonly a counter-current manner. A basic schematic of a counter-current column is presented in figure 4.4.

FIGURE 4.4 PACKED GAS LIQUID CONTACTOR [127].

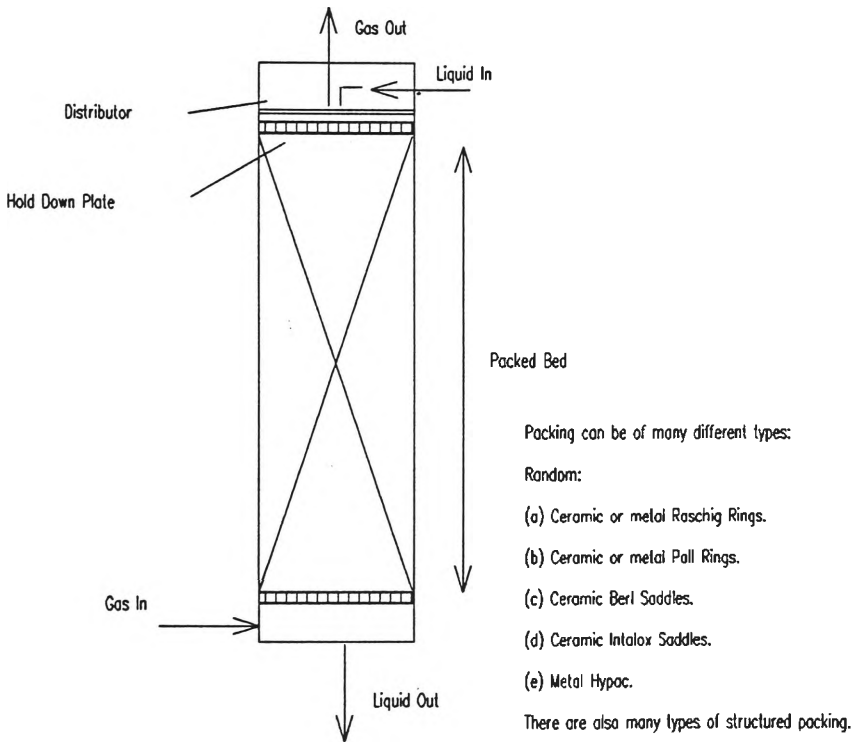

It is obvious that the addition of something such as packing or a fixed catalytic bed will increase the pressure drop through the column. Many correlations are available to estimate how the pressure drop will be affected. One of these is known as the Generalised Pressure Drop Correlation [96]. This correlation will provide information over a large variety of packings for a wide range of hydrodynamic conditions.

4.5 IMPROVEMENT OF MASS TRANSFER EFFICIENCY

If the system is mass transfer limited then an indication of this is to examine the system data to see what effects various parameters are having on the system performance. Typical kinetic improvements to a system include use of catalysts, and heating or cooling the system depending on the exothermic (heat release) nature of the reaction system. For endothermic reactions an increase in the system temperature will tend to improve the speed of reaction. The use of a catalyst, too, will improve the speed of the reaction. It will, however, become obvious that the system is mass transfer controlled if no improvement is noticed under ideal kinetic conditions.

There are several methods which are typically used to improve mass transfer performance. The final improvement, however, is usually on a cost vs efficiency criterion.

The changing of the contacting equipment is often the first choice in this situation. Often the contactor needs to be changed so as to improve the contact between the reactants in the system. A number of these contactors are described in sections 4.1 to 4.4. Many of these contactors work by improving the area of contact and/or by increasing turbulence to keep the system thoroughly mixed. In the case of gas-liquid reaction systems it is imperative that the two phases are in intimate contact for as long as possible. It is very important from a mass transfer point of view that the reactant from one phase be brought into contact with the reactant from the other phase. In ozone water treatment systems it is often the sparingly soluble nature of the ozone that renders the system under mass transfer control. If the solubility of the ozone could be improved then the ozone could come into contact with the reacting species more quickly and easily.

4.5.1 NOVEL MULTIPHASE CONTACTING

Work by various groups [53,54,55,56,57] suggest that it may be possible to conduct the ozone-water reactions in a 2-phase system rather than just in the single (water) phase.

Carrying this further, work by Stich and Bhattacharyya [52.] suggest that it may be possible to perform the O_3-pollutant oxidation reactions in a 2-phase system. Stich and Bhattacharyya [52.] found that on phenol and 2-napthol significant improvements were found in using a fluorocarbon as the solvent for the O_3.

The process works by contacting the O_3 with a fluorocarbon. The O_3-rich fluorocarbon is then contacted with the contaminated water in a reactor. The contents of the reactor are then separated and the fluorocarbon is allowed to recycle. The schematic diagram for this process [52.] is presented in Figure 4.5.

FIGURE 4.5 CONTINUOUS PROCESS FOR A 2-PHASE OZONE WATER TREATMENT SYSTEM [52.].

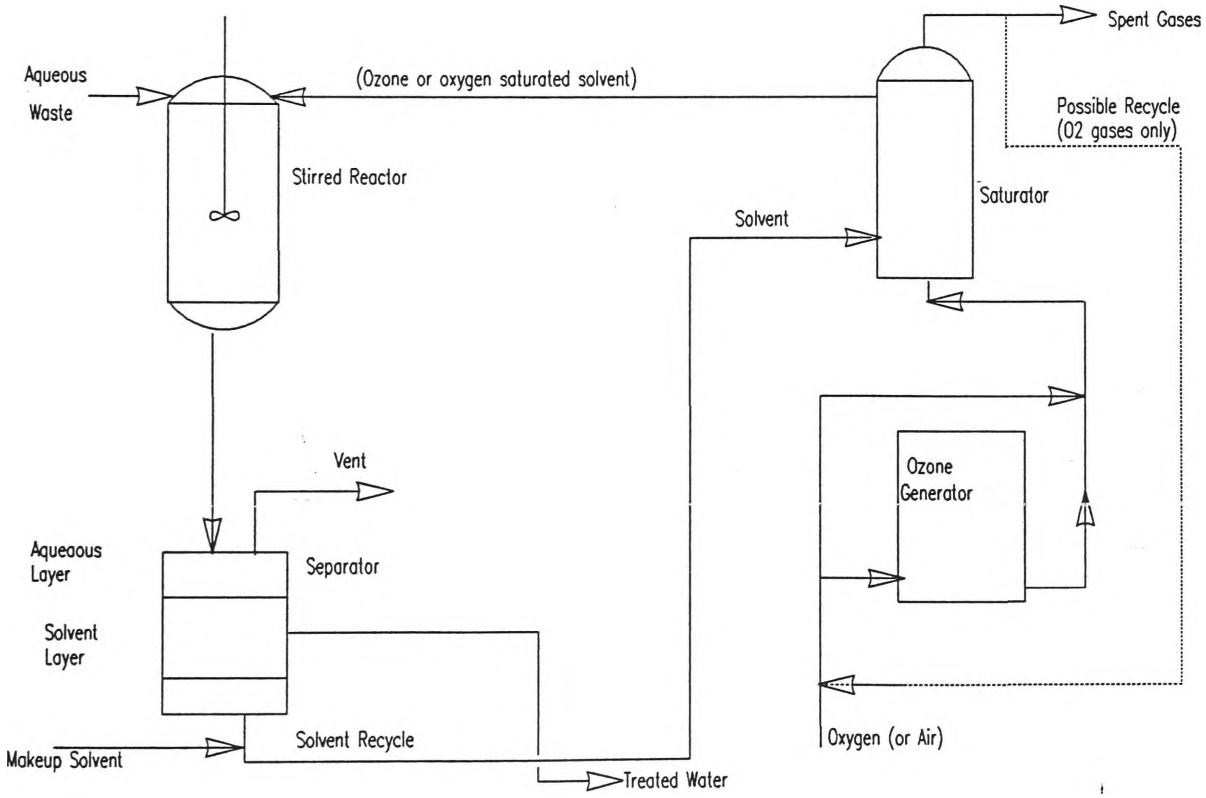

Stich and Bhattacharyya [52.] found that the particular fluorocarbon that they were using, FC77 (Proprietary of the 3M Company), had a 12 to 14 times (3.7ml O_3/100ml) solubility improvement over that of water(0.29ml/100ml)[52.]. However improved solubility performance is not a guarantee of improved treatment performance (see section 3.4.4 on selectivity).

5.0 TWO-PHASE FLOW

In gas-liquid contacting it is important that the phenomenon of two-phase flow is examined. This is the phenomenon that is occurring inside the gas-liquid contactor. The flow regime that exists in the contactor has a bearing not only on the mass transfer, but on the physical design characteristics of the column. This effect is also noted in chapter 4.

The phenomenon of two-phase flow is a much more difficult one to quantify than that for single phase flow. It is generally recognised that the gas velocity is greater that the liquid velocity [36]. It is also useful to note that the phases can be in different flow regimes. That is, they can be in laminar (or streamline) flow and/or in turbulent flow. The usual criterion for whether the flow is laminar or turbulent is usually defined as a function of the Reynolds Number (R_e) when the phase is flowing by itself.

where

$$R_e = \frac{\rho.u.d}{\mu} \qquad (5.1)$$

ρ = fluid density (kg/m^3)

u = fluid velocity (m/sec)

d = diameter of pipe (m)

μ = fluid viscosity (Ns/m^2)

The transition from laminar to turbulent flow usually occurs between Re= 1000 to 2000 [36]. This relationship, however, does breakdown to a certain extent in the case of two-phase flow. This is because the mixing of the two phases may make the flow in one and/or the other phase become turbulent.

The nett result of the two phases flowing together can provide many different flow patterns. The orientation of the pipework also has an effect on the pattern produced. Several examples of two-phase flow patterns are shown in figure 5.1.

FIGURE 5.1 TWO PHASE FLOW PATTERNS [36].

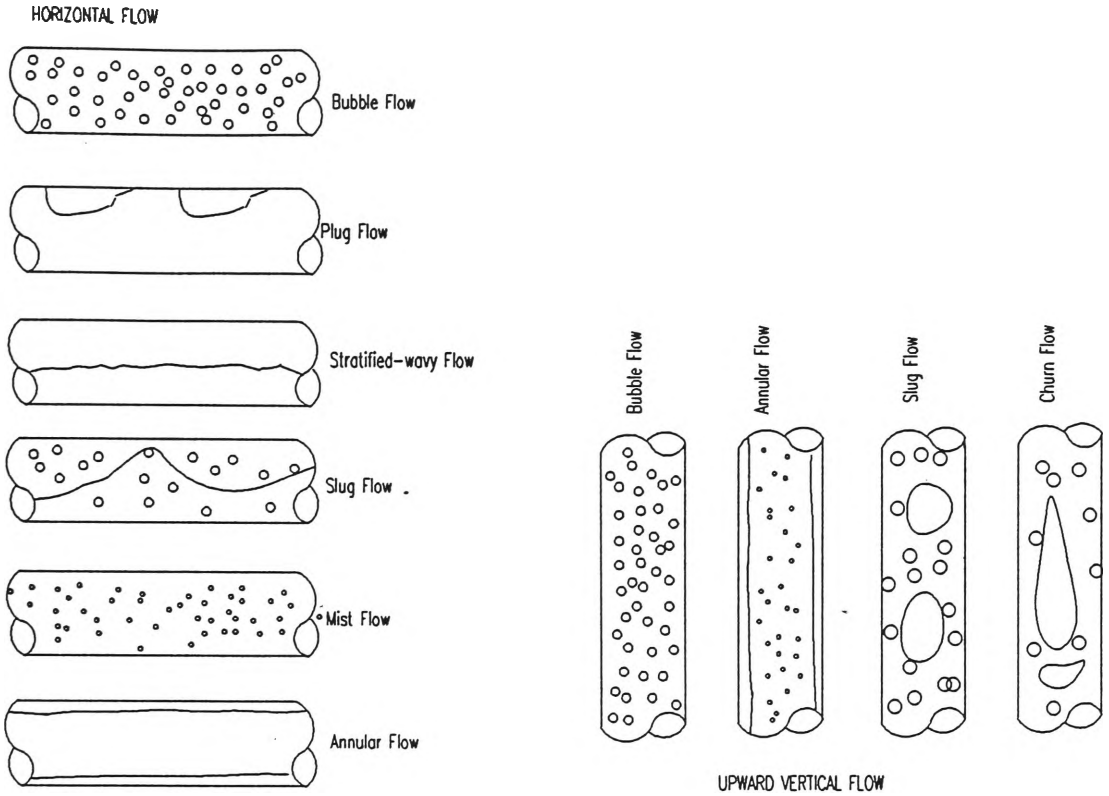

These flow patterns, once developed, may also be slightly unstable. The development of two phase flow patterns also leads to extra complexity in pressure drop and velocity profile studies. The velocity profile in the pipe is very difficult to estimate. A phenomenon of liquid and/or gas hold-up also may develop (see section 4.1). This has mass transfer and reaction implications (see section 3.4), as well as pressure distribution implications.

It is difficult to predict the flow pattern in two phase flow. Table 5.1 has some suggested flow patterns based on superficial velocity (u_{LS} and u_{GS} liquid and gas respectively).

$$u_{LS} = Q_L/A \ (ms^{-1}) \tag{5.2}$$

$$u_{GS} = Q_G/A \ (ms^{-1}) \tag{5.3}$$

where

A = pipe cross-sectional area (m^2)

TABLE 5.1 FLOW REGIMES IN HORIZONAL PIPE [36].

REGIME	DESCRIPTION	u_L	u_G
Bubble[a]	Bubble of gas dispersed in liquid	1.5-5	.3-3
Plug[a]	Plugs of gas in liquid	.6	<1.0
Stratified	Layer of liquid below gas layer	<.15	.6-3
Wavy	Higher velocity version of Strat--ified with wavy interface	<.3	>5
Slug[a]	Slug of gas in liquid	Wide	Wide
Annular[b]	Liquid film on walls around the gas flowing in the centre		>6
Mist[b]	Liquid droplets in gas		>60

[a] Often lumped as Intermittent flow.

[b] Often lumped as annular/mist flow.

5.1 FLOW REGIME TRANSITION

It is important to know the flow regime transition. The flow regime will dramatically effect the mass transfer, and the modelling of the phenomenon ocurring.

There are differences in analysis and behaviour between horizontal and vertical flow, and between co- and counter-current flow. It is also important whether the flow is upwards or downwards. It is beyond the scope of this work to examine all of these cases. Therefore the discussion will be confined to that relevant to the jet pump study, that is, downward co-current flow.

In the case of the jet pump at The University of Wollongong, it is important to understand the transition from annular flow, due to the high gas to liquid ratios and velocities.

5.1.1 TRANSITION FROM ANNULAR FLOW

The flow regime studied in this work was the annular regime, due to the high gas to liquid volumetric flow ratios (Q_G/Q_L) present in the jet pump. This regime is characterised by a gas core. This core contains some of the liquid phase as a series of dispersed droplets. Surrounding the gas core is an annulus of liquid. Thus the liquid forms a film along the wall of the vessel. In downward flow there are always waves and ripples on the surface of the liquid [137]. The phenomenon which occurs as the liquid volumetric flowrate begins to increase relative to the gas volumetric flow rate, is that the liquid film thickness will begin to increase. There comes a point where the film begins to 'bridge the pipe.'[137]. At this point the flow regime may then transfer into slug flow or further into bubble flow. There has not been a large amount of work done in this area. This view is evidenced by a volume of work being undertaken at Imperial College London in vertical annular flow [149].

There is disagreement as to the exact transition points. There are a number of suggested criteria and some of these are presented in Table 5.2.

TABLE 5.2 TRANSITION CRITERIA FOR ANNULAR DOWNFLOW

CRITERIA	REF.
$Q_G/Q_L = 1.3$	134
$Q_G/Q_L = 1.4$ to 0.4 as $Q_L = 2$ to 7 m^3/hr	132
$Q_G/Q_L = 1.2$	131
$Q_G/Q_L = 0.65$	146
$A_L/A >= 0.35$ (for h_L=0.7)	137

The disadvantage of all this data is that they are just empirical observations without any way of reliably comparing one to another. Even the data of Dukler and Taitel [137]., although able to predict regimes for different geometries, inclinations and flowrates, still uses an empirical observation made for horizontal flow .

Figure 5.2 presents a schematic diagram of downward co-current flow. The velocities (u_L and u_G) as well as the wall shear forces(τ_L and τ_i), film thickness (h) and pipe diameter(d) are shown.

FIGURE 5.2 SCHEMATIC OF DOWNWARD ANNULAR FLOW [137].

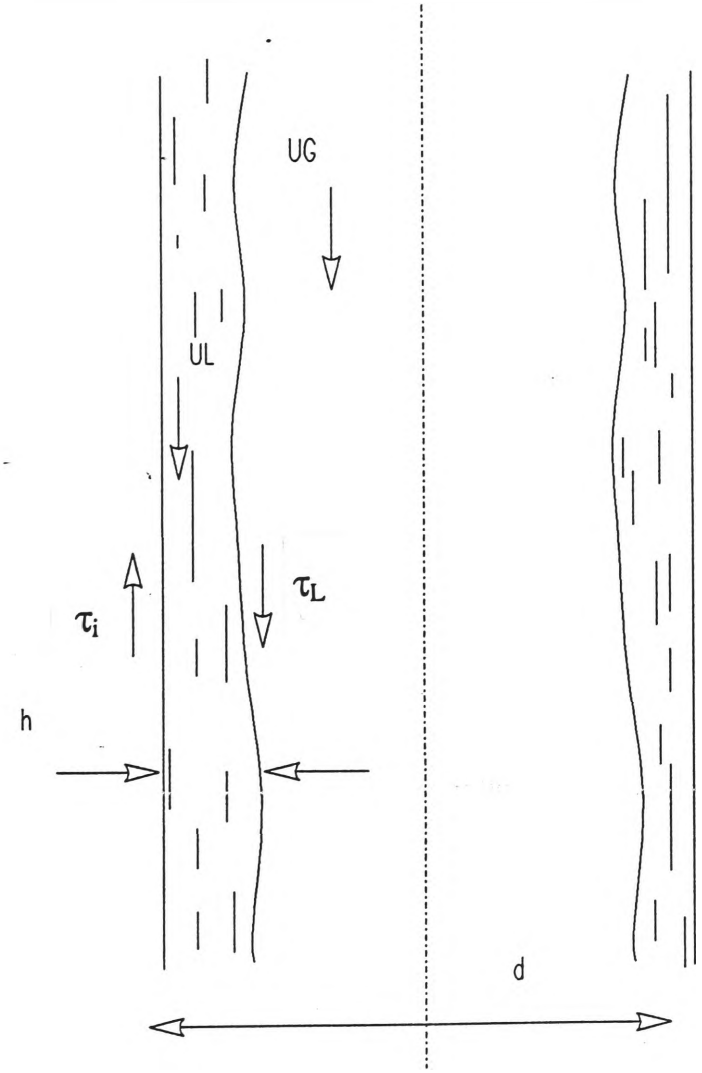

It has been suggested that for horizontal flow in pipe that the transition to slug flow is based on the following relationship:

$$\frac{A_L}{h_L.A} \geq 0.5 \qquad (5.4)$$

where A_L = area of liquid flow (m^2)

A_G = area of gas flow (m^2)

A = pipe cross sectional area (m^2)

h_L = liquid hold-up = 0.7 [137].

It is recommended by Dukler and Taitel [137] that this relationship also holds for vertical downflow. Therefore, the transition point to slug flow occurs when:

$$\frac{A_L}{A} \geq 0.35 \qquad (5.5)$$

It is necessary, then, to find the ratio of the flow areas available to each phase.

Dukler and Taitel [137], recommend performing a momentum balance, followed by a procedure whereby the component parts are made dimensionless.

The momentum balance obtained from Figure 5.2 is:

$$-\tau_L(S_L/A_L)+\tau_i S_i(1/A_L + 1/A_G)+(\rho_L-\rho_G)g = 0 \qquad (5.6)$$

where τ_L = shear stress of liquid on wall (N/m^2)

τ_i = shear stress at liquid/gas interface (N/m^2)

S_i = perimeter length of interface (m)

S_L = perimeter of liquid on wall (m)

ρ_L = liquid density (kg/m^3)

ρ_G = gas density (kg/m^3)

g = acceleration due to gravity = 9.81 (m/sec^2)

The shear stresses can be evaluated using the average velocities of the phases (u_L and u_G respectively).

$$\tau_L = f_L \frac{\rho_L u_L^2}{2} \tag{5.7}$$

$$\tau_i = f_i \frac{\rho_G (u_G - u_i)^2}{2} \tag{5.8}$$

where the friction factors are calculated respectively from:

$$f_L = c_L (D_L u_L / v_L)^{-n} \tag{5.9}$$

$$f_i = c_G (D_G u_G / v_G)^{-m} \tag{5.10}$$

where

c_G, c_L = constants = 0.046 (both phases in turbulent flow)
= 16 (both phases in laminar flow)

D_L = liquid hydraulic diameter = $4A_L/S_L$ (m)

D_G = gas hydraulic diameter = $4A_G/(S_i)$ (m)

n,m = exponents = 0.2 (both phases in turbulent flow)
= 1.0 (both phases in laminar flow)

v = kinematic viscosity (m^2/sec)

subscript

i = value of parameter at liquid-gas interface

The turbulent and laminar flows are based on the Reynolds Number at the respective hydraulic diameter [137].

At flowrates which approach those near a flow regime transition point, the gas velocity (u_G) is much greater than the interface velocity (u_i) [137]. This results in a simplification of the interface shear stress relationship:

$$\tau_i = f_i \rho_G \frac{u_G^2}{2} \tag{5.11}$$

It is now useful to convert the previous equations to a dimensionless form. The nomenclature for this change is to convert all variables into an *italic form*.

Substitution yields,

$$X^2[(u_L D_L)^{-n} u_L^2 (S_L/A_L)] - (u_G D_G)^{-m} u_G^2 S_i (1/A_L + 1/A_G) - 4Y = 0 \tag{5.12}$$

where

$$X^2 = \frac{(4c_L/D)(u_{LS}D/\nu_L)^{-n}\rho_L(u_{LS})^2/2}{(4c_G/D)(u_{GS}D/\nu_G)^{-m}\rho_G(u_{GS})^2/2} = \frac{|(dP/dx)_{LS}|}{|(dP/dx)_{GS}|} \tag{5.13}$$

$$Y = \frac{(\rho_L - \rho_G)g}{(4c_G/D)(u_{GS}D/\nu_G)^{-m}\rho_G(u_{GS})^2/2} = \frac{(\rho_L - \rho_G)g}{|(dP/dx)_{GS}|} \tag{5.14}$$

where

$$A_L = \pi[h/D - (h/D)^2]$$

$$A_G = \pi(0.5 - h/D)^2$$

$$S_L = \pi$$

$$S_i = \pi(1 - 2h/D)$$

$$u_L = A/A_L$$

$u_G = A/A_G$

$D_L = 4A_L/S_L$

$D_G = 4A_G/(S_i)$

X = Lockhart-Martinelli Parameter [138].

Y = dimensionless inclination parameter [137].

x = downstream co-ordinate

P = pressure (Pa)

It is now necessary to calculate values of X and Y which yield the values of the gas and liquid superficial velocities (u_{GS} and u_{LS}) which gives h/D=0.097, which in turn gives A_L/A=0.35 [137].

Dukler and Taitel [137] found relatively good agreement for their transition model in 2.5 and 5.1 cm diameter tubes. In this thesis the diameter of the draft tube is 7.6 cm (0.076m), and the diameter of the mixing tube is 5.4 cm (0.054m).

There are difficulties in accurately predicting the transition point, but models such as that presented above give a reasonable starting point. It is possible that data is relatively specific to a certain sized column(or specific range of sizes), and scaling up may prove premature.

These sentiments were borne out in the work by Roustan et al [130]. In this work the pressure gradients and void fractions were modelled successfully in the bubble flow regime up to the transition point between slug and bubble flow, and beyond to the slug flow regime. However agreement about where the transition point was could not be determined. Roustan et al [130] also compared their results to their own critical review of the available literature.

Unfortunately their work was restricted to a 5.3cm diameter column, and their work, by their own admission, is not widely applicable.

Hewitt [136.] defines the phenomenon of slug flow as that situation which occurs when the diameter of the bubble and that of the tube approach each other. In bubble flow the bubbles are much smaller and flow in a continuous liquid phase without as much interaction and coalescence.

It is beyond this work to fully examine all of the flow regimes in two-phase flow. For further information the reader is directed to works such as Dukler and Taitel [137.] and by Roustan et al [130.], in which the former in particular contains extensive reference lists.

5.2 MASS TRANSFER AND TWO-PHASE DOWNFLOW

Much of the work in two-phase downflow mass transfer is performed in U-Tube or jet-loop reactors [129,130,132,133, 134,143,146.] , and to a certain extent in plunging jet reactors [133,135.]. Some work has also been done in the area of downflow bubble columns [140.], and in staged downflow bubble reactors [76.].

The major problem with most of this work is that it is generally specific, and not generally transferable to this area of work due to the high gas liquid ratios. For example:

TABLE 5.3 JET DOWNFLOW LIQUID VOLUMETRIC MASS TRANSFER COEFFICIENT CORRELATIONS

Column Type	Conditional Physical Range	k_La	Ref.
Venturi	$Q_G/Q_L < 1$ u_{LST}=0.95m/sec	$0.965(Q_G/Q_L)^{1.91}$	131
Ejector	$1.3 < Q_G/Q_L < 3$	$3.1e^{-4}(Re_n^2)dV_{ej}^{-.66}$	134
Jet Loop	Q_G <0.7 l/sec		143

where

u_{LST} = superficial throat liquid velocity (m/sec)

V_{ej} = volume of ejector (m^3)

d = diameter of ejector (m)

Re_n = Reynolds Number of liquid phase in nozzle

Both works [131,134] suggested that the mass transfer performance of the contactor increased up until the jet or annular flow regime was reached. After this point the results from the first two works [131,134] appear to diverge. Briens et al. [131] suggest a marked decrease in mass transfer coefficient for long annular flow through the contactor. Dirix and van der Wiele [134] suggest that there appears to be a plateau in jet flow, although they obtained a large scatter of results which they put down to random pulses in the two phase flow in the ejector.

In the work by Velan and Ramanujam [143]. it was found that an increase in gas and liquid rate, as well as nozzle diameter produced an increase in volumetric mass transfer coefficient. They also found that the optimum draft tube to column diameter ratio is 0.44 (This does not apply in the jet pump contactor at this stage, as there is no column). They [143]. also discussed the advantage of using a downflow jet rather than a co-current upflow jet due to the enhanced residence time of the gas phase due to flowing against the buoyancy forces.

5.3 HOLD-UP

As the gas velocity is greater, and the fact the volume of the gas will change with changing line pressure, this will mean that the volumetric fraction of liquid will vary along the length of the pipe. There are various methods of determining the liquid hold-up in pipes. Many studies have been concerned with counter-current flow, and several empirical relationships have been determined, such as those by Akita and Yoshida [38].(see section 4.1).

There are many ways of measuring the hold-up in a column. Perhaps the easiest method is to have two quick-acting valves in the column a certain length apart. The column flow is allowed to reach equilibrium, then the two valves are shut quickly to isolate a gas-liquid mixture between them. It is then a simple matter to measure the gas and liquid volumes respectively, in that isolated section. The fractional amount of liquid to the total enclosed volume will give the liquid hold-up [36]. The method used during this thesis is expounded in section 9.6. Further information on other techniques can be found in Coulson et al [36]. and Hewitt [136].

A study of the gas/liquid holdups in loop venturi reactors was done by Cramers et al. [129]. in which the effect of gas density on the hold-up and gas entrainment was examined.

However the thrust of the paper was the determination of the effect of gas density on hold-up within the main holding vessel of the loop, rather than in the diffuser, ejector, or draft tube. Their [129]. result for the holding vessel is as follows:

$$h_G = 7.7 * u_{GS} * (\rho_G/\rho_L)^{0.11} \qquad (+/- 10\%) \qquad (5.15)$$

where

$0.02 < u_{GS} < 0.1 m/sec$

$0.18 < \rho_G < 6.18 kg/m^3$

$\rho_L = 1000 kg/m^3$

6.0 BACTERIAL DISINFECTION

It was generally accepted that the disinfection, or inactivation, of viruses was similar to that of a first order decay process, if the biocidal or stressing agent remained in contact. This was first suggested in 1908 by H.Chick [67]. However, since that time laboratory studies have shown that this is not strictly true. In fact there are four basic inactivation rates which are reproduced in figure 6.1:

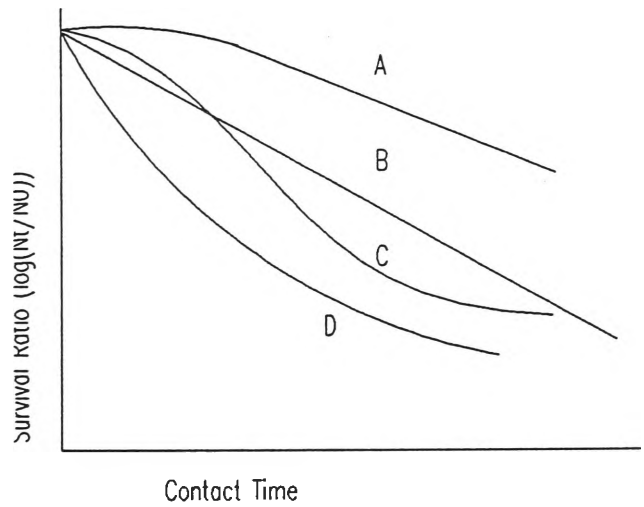

FIGURE 6.1 BACTERIAL SURVIVAL CURVES [64,68].

These survival curves, which were summarised by Moats [68], show the change in the rate of inactivation of the virus. It can be seen (figure 6.1) that the rate of disinfection of the virus tends to taper off (Curves C and D). Curve A, however, shows the typical effect of the biocide having multiple disinfection targets. Curve B shows the traditional first order disinfection process.

The curves C and D are known as biphasic curves. These types of curves are typical of bacterial populations which have a proportion of the population which is resistant to the stressing agent [64,69]. As can be seen from the curves in Figure 6.1, the rate of disinfection starts off at an initially high rate, followed by a decrease and levelling off in the rate as time increases.

This type of biphasic behaviour has been observed in a number of viruses, including the disinfection of poliovirus and Escherichia coli (E.coli), with ozone, under laboratory conditions [70,64].

With most of the disinfection systems in current use the rate of kill is usually 90 to 99.9% of the bacteria within a very short (less than 90 seconds) exposure time [64]. However, it is still important to realise that there may be a recalcitrant surviving fraction in the system. This fraction may still be a viable virus despite the treatment times and doses being theoretically sufficient [64]. This is particularly true in the case of Legionella Pneumophila(L.pneumophila). In this case viable fractions have been found in potable water treated with free chlorine with residual concentrations ranging between 0.2 to 2.0 mg/l [71,72,64]. This is despite laboratory experiments suggesting that chlorine doses of 1.25 mg/l should completely inactivate Legionella organisms [64,73].

This inactivation resistance is dependent on the type of inactivating agent used [64]. It is important to assess the extent of the viral resistance to the ozone treatment in addition to the initial inactivation rate. This is particularly true in the case of L.pneumophila as it is so virulent. It has been suggested by Berg et.al [64] that population fractions as small as 10^{-4} or 10^{-6} may still pose a health threat to humans.

Typically the growth of bacteria in the laboratory is done in either a batch or continuous culture. The method of continuous culture can be performed in a chemostat. In work by Berg et.al [64], it was found that the growth in the chemostat continuous culture with nutrient limited growth, yielded populations that were similar to the survival characteristics of those populations found in the environment. It seemed from their work that the recalcitrant populations were greater in these types of environments.

The suggestion of their work is that design procedures based on batch grown cultures may yield quite different results to that of sub-optimum nutrient growth in a chemostat. This may mean that the design information yielded in the laboratory may be incorrect in predicting the surviving fraction above the 99% inactivation level.

Berg et.al [64] also found that the simulation of natural environmental conditions in the chemostat may also be applicable to many different bacteria due to the fact that L.pneumophila and E.coli behaved in a very similar manner under the experimental conditions.

For the same extent of disinfection the use of ozone provides a much quicker rate of kill at a much lower concentration that for chlorine or iodine [70]. In fact this rapid disinfection

rate to 99% disinfection makes it very difficult to asses the kinetics for this region. In experiments by Katzenelson et.al [70] on Poliovirus I, Coliphage T_2 and E.coli, it was found that 99% disinfection was occurring in less than 10 seconds. Consequently they found that it was not possible to obtain to obtain the classic first order decay curve. For the substance previously mentioned it was found that the ozone dose only needed to be 0.2ppm. Above this dose the rate of activation did not appear to change.

In the work by Kazenelson et.al [70] it was found that the inactivation curve was a two stage process similar to that expounded in curves C and D above (Figure 6.1). Their explanation was to suggest that virus resistance was occurring, and was probably due in part to the clumping together of the viruses. The change in the state of effectiveness of the ozone was discounted due to the observation that a second dose of poliovirus added to the system after 56 seconds produced exactly the same rate shaped curve [70].

As the initial disinfection characteristic for 99% kill is so fast [70], this will mean additional modifications will need to be taken into account for mass transfer modelling. This is because originally the model was developed for slow reaction regimes where there is no mass transfer enhancement due to reactions at the interface (see section 3.4).

6.1 BACTERIAL DISINFECTION REQUIREMENTS

There are several criteria that can be used to provide a measure of the disinfection level required. One of these methods is the "CT" value. This value is defined as the product of the effective contact time between the primary disinfection agent (such as Ozone, Chlorine and Chlorine Dioxide) in minutes and the residual concentration of that species in mg/l (milligrams per litre). This "CT" value yields a number with the units of (mg.min)/l. These "CT" values are a function of the water composition matrix, and are particularly dependent on the type of disinfectant, the pH and temperature.

The Giardia Lamblia cysts are the most difficult to destroy, and so The US EPA (United States Environmental Protection Authority) has designated that the "CT" value which corresponds to 99.9% inactivation of these cysts probably will have been sufficient to have

brought the concentrations of other bacteria or micro-organisms down to appropriate levels [114]. This includes Legionella.

It is extremely important that the effective residence time(RT) of the water in the reactor system be determined. It is quite possible that the reactor in question is behaving in a non-ideal manner. For instance in most simulations, or models of reactors, particularly counter-current bubble columns, the flow regime is considered to be ideal plug flow. This is not always the case. In a study done by Nieminski [114] it was shown that it is certainly possible to obtain residence time which is only 50% of the theoretical value. The case in the jet pump is much worse (see section 9.2.1).

This type of result highlights the need for effective tracer studies of the reactors in question. There are numerous works which discuss non-ideality and tracer examination, including Levenspiel [74].(See Chapter 7), and an article on "CT" Disinfection Requirements by Nieminski [114].

However, the most important parameter is the dose response of the wastewater. It has been found [115] that although in laboratory studies of water with a zero ozone demand the contact time was important, this effect was less noticeable in secondary effluents.

There are a number of empirical models which are used to give information on dose response of ozone on secondary effluent. The form of the models is often [115]:

$$\log N/N_0 = b_0 + b_1 x1 + b_2 + e \qquad (6.1)$$

where

N = surviving concentration of bacteria

N_0 = initial concentration of bacteria

b_N = (N=0,1,2...) = model parameters for dependent variables(x_N)

x_N = terms relating to BOD_5, COD or transferred ozone dose

e = constant error

Finch and Smith [115] suggest that there is a large danger in using these type of empirical models due to the very specific nature of any constants determined.

A crucial piece of data that can be used to determine the CT value and disinfection efficiency is the average concentration of the disinfection agent in the reactor. This number may be significantly different than the residual concentration of the agent at the reactor exit.

Lev and Regli [118] formulated a number of guidelines to estimate the characteristic ozone concentration to be used for CT criteria. However, they stressed that site specific modelling still is extremely important, and where possible should be done. Their [118] study involved four major types of ozone contactors, their ozone concentration profiles, and corresponding characteristic concentration C. These being:

(i) Rigorously Mixed Systems:

$$C = C_{out}$$

(ii) Cocurrent contactors:

$$C = C_{out} \text{ or more conservatively } C = (C_{out}+C_{in})/2$$

(iii) Counter-current contactors:

$$C = C_{out}/S$$

(iv) Reactive flow segments

$$C = C_{out}$$

where

C = Characteristic Concentration (mg/L)

C_{out} = contactor outlet concentration (mg/L)

S = safety factor 2 or 3 (dimensionless)

C_{in} = contactor inlet ozone concentration (mg/L)

It again must be stressed that these C values are estimates and pilot studies are still the best design option.

Their [118.] studies produced ozone concentration profiles based on mathematical modelling. The results of this mathematical modelling of concentration profiles for co- and counter-current columns is presented in figure 6.2:

FIGURE 6.2 CONCENTRATION PROFILES FOR OZONE IN CO-CURRENT AND COUNTER-CURRENT COLUMNS [118.].

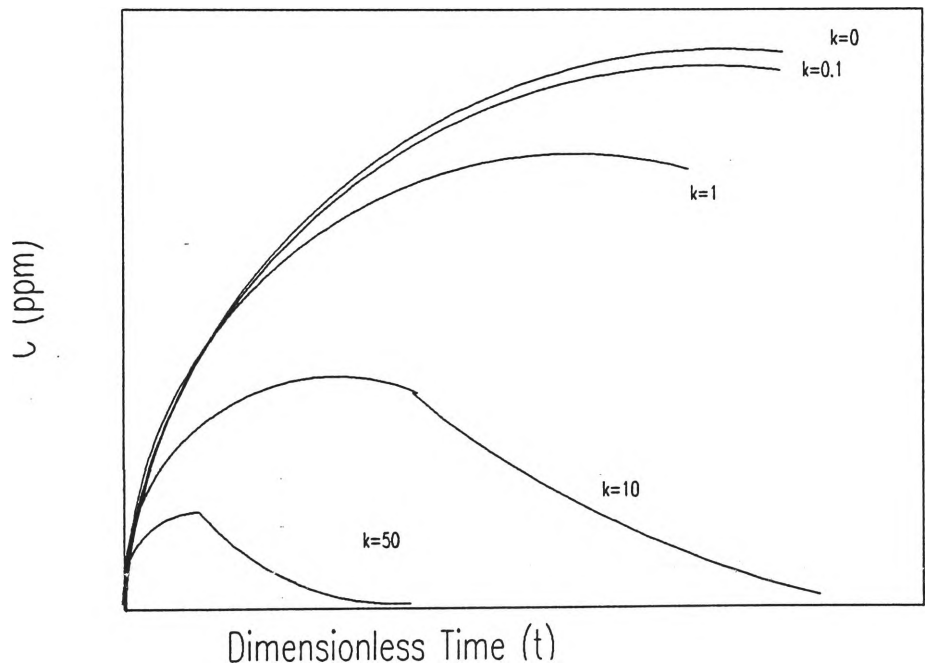

FIGURE 6.3 GAS-LIQUID CONCENTRATION PROFILES OF COCURRENT OZONE DISINFECTION CONTACTORS [118].

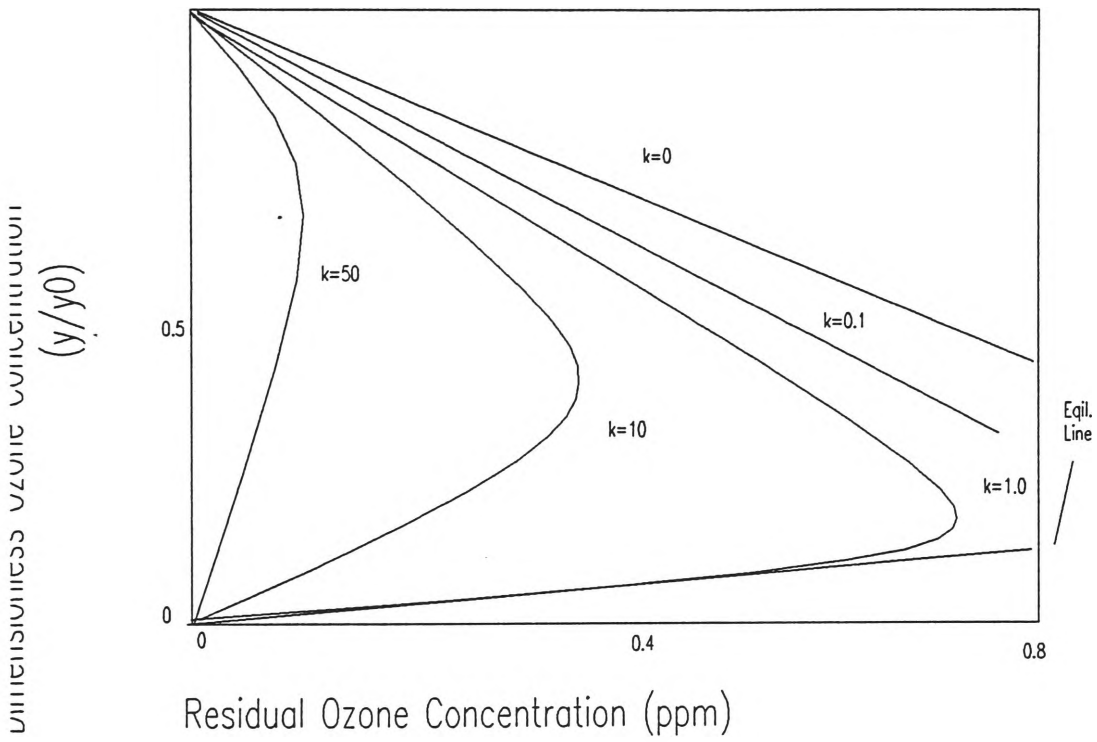

The constants in the Figures 6.2 and 6.3 are:

k_1 = ozone decomposition rate constant = $k'+k_2'R$

R = ozone demand concentration (kg O_3/kg Water)

k_La = volumetric liquid mass transfer coefficient (min^{-1})

k = k_1/k_La

y = gas phase ozone concentration (kg O_3/kg $_{gas}$)

y_0 = outlet ozone gas phase concentration (kg O_3/kg $_{gas}$)

As can be seen from figure 6.3 the dissolved ozone concentration is a monotonic decreasing function of time, and therefore reactor height. As the ozone in the gas phase tends to decrease, the driving force for mass transfer will decrease, and therefore the concentration of ozone in the liquid phase will tend to be controlled by the decomposition term ($-k_1.C$). All of the curves produced in figures 6.2 and 6.3 are for linear kinetics. Two major cases are presented [118].:

1. $k<<1$. This means that the mass transfer term is dominant, and the decomposition reaction kinetics are essentially negligible.

2. $k>>1$. This means that the decomposition kinetics are dominant. However this is still within the usually held assumption that k_La is not dependent on ozone concentration. That is, the interfacial ozone concentration will be much higher than in the bulk of the liquid phase.

For discussions of jet pump concentration profiles, see Chapter 9.

7.0 NON IDEAL REACTOR BEHAVIOUR

As has been mentioned before (section 4.4.1), the ideality of some reactor configurations is open to question. The danger is that modelling of reactor phenomena in a purely mathematical way without considering the non-ideal performance of the reactor may lead to severe underdesign.

Initial studies in this thesis were based on ideal plug flow occurring through out the entire length of the reaction vessel. Levenspiel [74.] defines plug flow as:

'the flow of fluid through the reactor is orderly with no element of fluid overtaking or mixing with any other element ahead or behind.'[74.].

This definition does present some difficulties in the case of the jet pump, because of the high gas velocities relative to the liquid velocities, there is likely to be liquid overtaking due to entrainment.

He [74.] then goes along to point out that there may be some lateral movements of the fluid element. Of course it then follows that all residence times for all of the fluid elements are identical.

This situation is very difficult to achieve in practical application. There arises in reaction vessels some or all of the following non-ideal flow situations:

- Regions of stagnation.

- Channelling of the fluid(s).

- Severe by-passing or short-circuiting.

These situations are reproduced in figure 7.1.

FIGURE 7.1 NON-IDEAL FLOW PATTERNS [74].

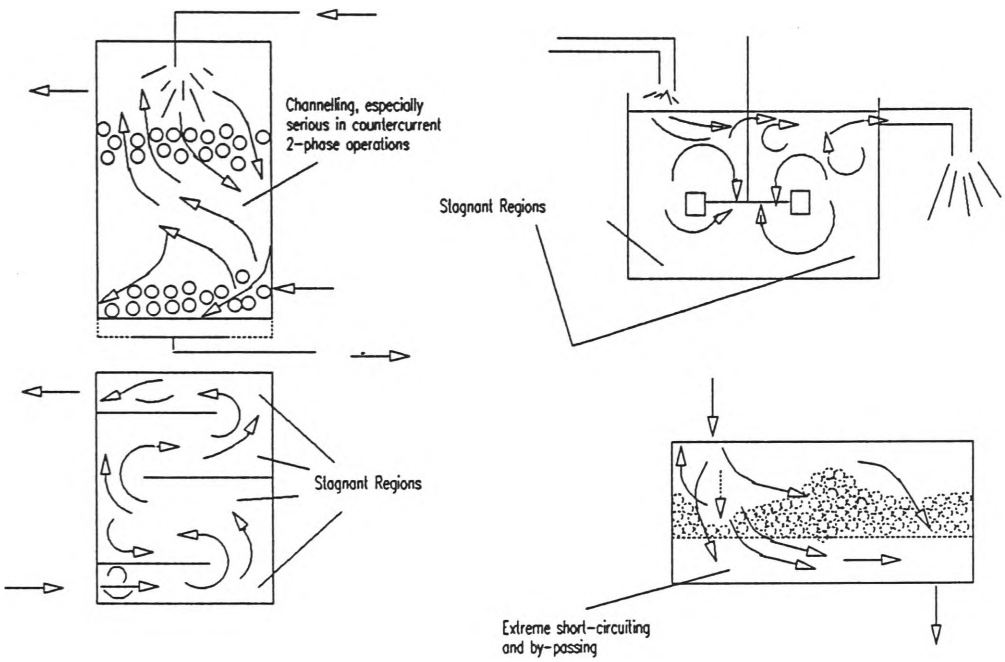

7.1 RESIDENCE TIME DISTRIBUTION

Some measure, of the non-ideality of the reactor needs to be determined to allow more accurate modelling to occur. However, the danger in scale-up from pilot size to commercial size reactors may also present non-ideal flow patterns if all parameters are not carefully evaluated.

Seeing as though the residence time of all fluid elements in a reactor are not necessarily identical, as advocated by the ideal plug flow model, then a distribution of the real residence times should be studied. The exit age distribution is more usually known as the residence time distribution (RTD). If this RTD is defined in such a way that the area under the curve is one (1), then:

$$E = \text{area under RTD curve} = {}_0\int^{\infty} E\, dt = 1 \qquad (7.1)$$

This measurement of RTD can be done in two ways, first by a pulse injection of a tracer, or second, by step injection of a tracer. These two situations are shown in figure 7.2 :

FIGURE 7.2 INJECTION OF A TRACER FOR RTD STUDIES

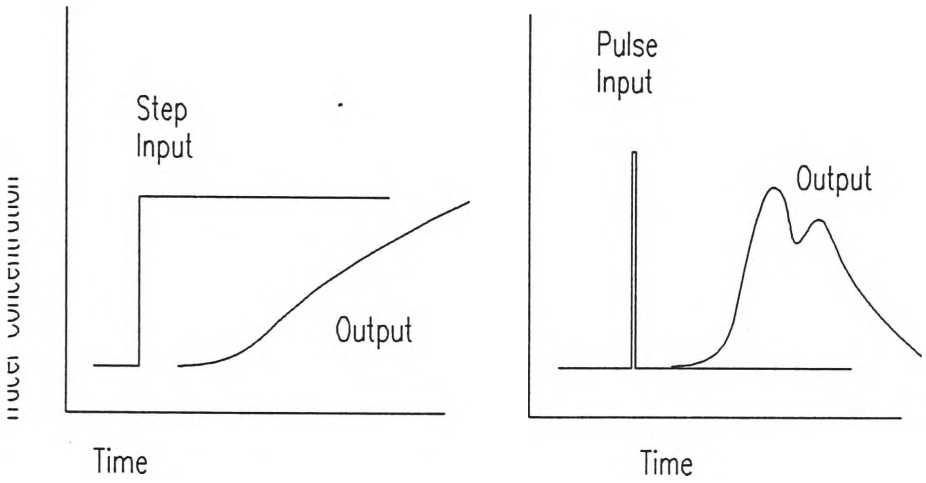

7.1.1 PULSE INJECTION OF A TRACER

The usual method of pulse tracer injection is to rapidly inject an inert material which does not interfere with the reacting species or the vessel. It should also be physically and chemically similar to reacting species.

The outlet concentration of this tracer is then measured against time to produce the concentration curve (or C-curve). The area under this curve (between 0 and infinity) multiplied by the flowrate should equal the amount of tracer injected.

The residence time distribution (RTD, or E) curve is usually represented as a fraction of material that has spent a certain time in the reactor. This E value is determined from:

$$E = \frac{C(t)}{\int_0^{\infty} C(t)\,dt} \qquad (7.2)$$

$$= \frac{C(t)}{\text{Area under C-curve}}$$

where

C(t) = concentration of tracer at time t

The exit age distribution curve may take on several shapes, and these are presented in figure 7.3:

FIGURE 7.3 SOME RTD FUNCTIONS

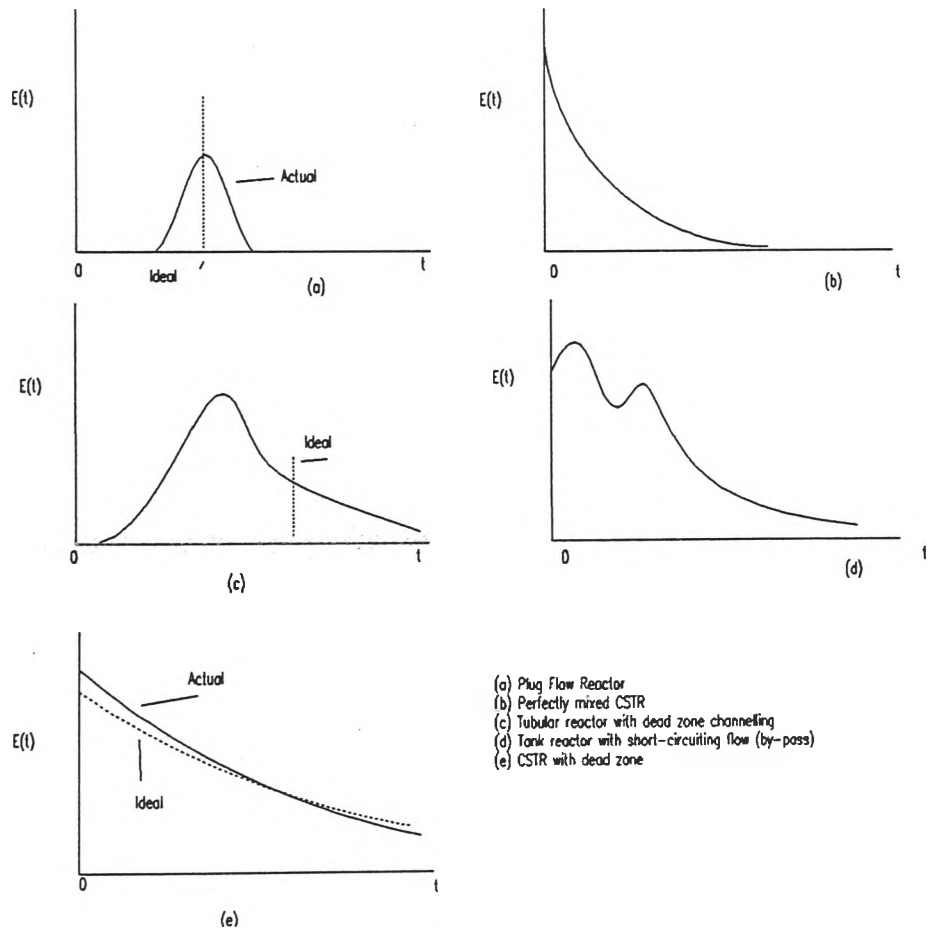

If the E function is integrated with respect to t from 0 to t_1 then this represents the fraction of material that spends less than t_1 in the reactor.

FIGURE 7.3A PROPERTIES OF THE E CURVE FOR VARIOUS FLOWS

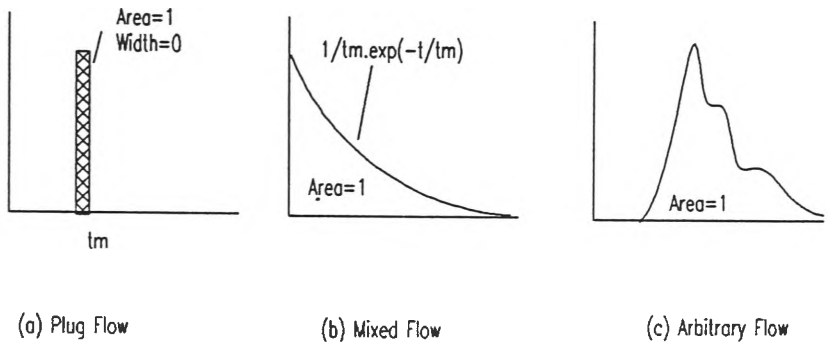

Another function can be defined, and this is known as the F-curve, or the cumulative RTD function.

FIGURE 7.4 F-CURVE: CUMULATIVE DISTRIBUTION FUNCTION

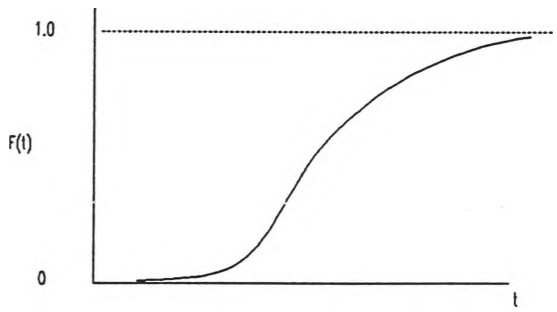

The F-curve is defined as:

$$F = \int_0^{\infty} E\, dt \qquad (7.3)$$

= material fraction in reactor for less than time t

Further information on the F-Curve is contained in the following section 7.1.2.

The residence time distribution can be related to the reactor mean residence time (t_m), or hydraulic residence time (HRT).

$$t_m = \frac{V}{Q} \tag{7.4}$$

where

V = volume of reactor (m^3)

Q = Effluent flow (m^3/sec)

This is related to E by the following relationship [74].:

$$t_m = {}_0\int^{\infty} tE\, dt \tag{7.5}$$

Note that all of the above relationships only apply for closed vessels. This means that the velocity profile of the fluid is the same along the length of the reactor.

This mean residence time is known as the first moment of the RTD function. There are three moments:

1. First Moment

Mean residence time(t_m)

2. Second Moment

Variance

$$\sigma^2 = {}_0\int^{\infty} (t - t_m)^2 E(t)\, dt \tag{7.6}$$

This gives some sort of indication of the spread of the RTD.

3. Third Moment

Skewness

$$S^3 = {}_0\int^{\infty} (t-t_m)^3 E(t)\, dt \qquad (7.7)$$

The skewness gives an indication of the symmetry of the RTD curve.

It is often more convenient to reduce the tracing data to an even more dimensionless function. This can be done by introducing a theta (θ) function, where:

$$\theta = \frac{t}{t_m} \quad \text{and} \quad d(\theta) = \frac{dt}{t_m} \qquad (7.8)$$

All subsequent functions and curves can then be related to the θ function.

i.e.

$$(\theta)E_\theta = t.E \qquad (7.9)$$

$$E_\theta = t_m.E \qquad (7.10)$$

The function theta represents is the normalised RTD function. In a physical sense θ represents the number of reactor volumes which pass through the reactor in time, t. This normalisation allows reactors of different sizes to be directly compared in terms of their RTD.

Once the RTD data has been examined, the correction for a real system can then be added to the model. Amongst such models are the dispersion model, the tanks in series model and the reactor exchange model. These models are discussed in more length in Levenspiel [74].

7.1.2 STEP INJECTION OF A TRACER

The step injection of a tracer is similar in approach to that used for pulse injection. The major difference between the two approaches is that the step change continually injects the tracer. The resulting F-curve should have the shape as depicted in figure 7.4 in the previous section (7.1.1). This curve is also known as the cumulative distribution function.

To calculate the mean residence time (t_m) for a given species in the reactor it is necessary to calculate the area above the F-Curve. This area for various flow regime types is demonstrated in Figure 7.5:

FIGURE 7.5 PROPERTIES OF THE F-CURVE[74].

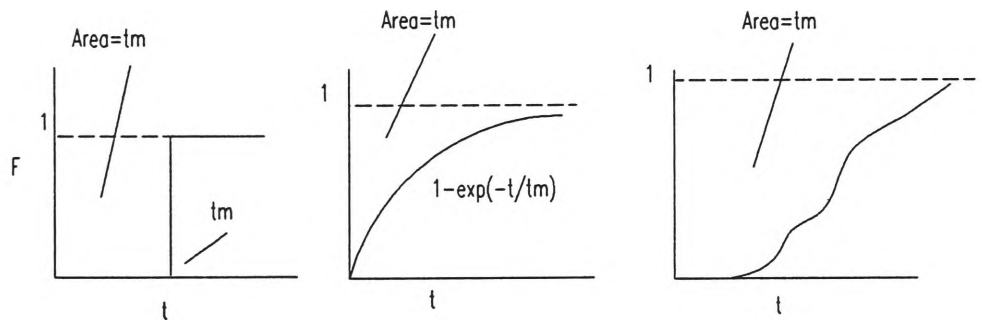

(a) Plug Flow (b) Mixed Flow (c) Arbitrary Flow

where

t_m = mean residence time (τ)

It is possible to convert between the F and E-Curves. From the previous section the following was defined [74].:

$$F = {}_0\int^{\infty} E\, dt \qquad (7.11)$$

it follows then,

$$E = \frac{dF}{dt} \qquad (7.12)$$

Therefore, the E-Curve can be also defined as the slope of the F-Curve at any point t. This definition allows mathematical tools developed for the E-Curve to be used for studies on the F-Curve (see Section 7.1.1).

7.2 RESIDENCE TIME DISTRIBUTION STUDIES OF U-TUBE GAS-LIQUID CONTACTORS

There have been several studies which examine the use of a U-Tube gas-liquid contactor [113,119,120,121]. these contactors are a co-current operation. The initial stage of the contactor is in fact the same as that for a jet-pump. As can be seen in figure 7.6 the water is injected into the top of the column, the corresponding negative pressure induced causes the gas to flow with the carrier liquid.

FIGURE 7.6 U-TUBE GAS LIQUID CONTACTOR [113].

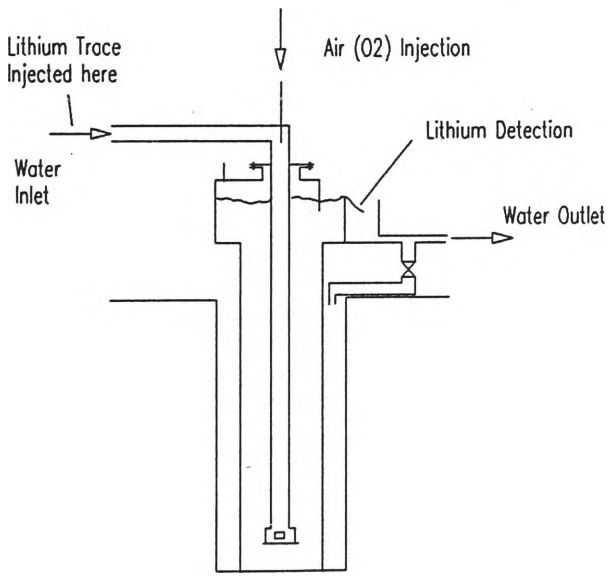

Studies on residence time distributions in these columns have been undertaken [113,121]., and these studies show a near perfect plug flow regime. This is shown by the near perfect 'pulse-like' peaks shown after lithium tracer injection. These results are shown in figure 7.7 [113,121].

FIGURE 7.7 U-TUBE TRACER RESULTS [113,121].

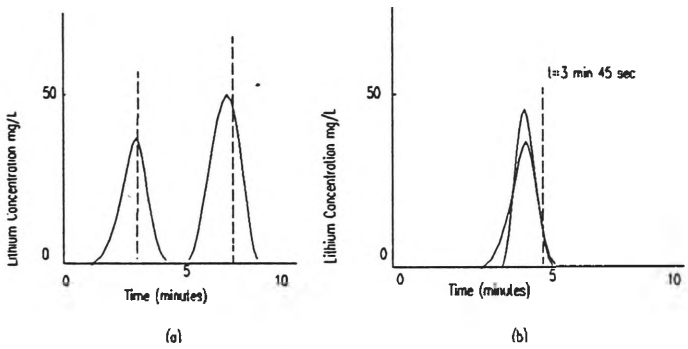

The study by Dauthuille et al [121]. shows that the plug flow is maintained for different water flow rates and for different gas-liquid ratios. In figure 7.7(a). it can be seen that as the liquid flow is doubled the residence time halves (gas free), and still the actual residence time nearly matches the theoretical residence time. In figure 7.7(b) the gas-liquid ratio is altered from 0.6 to 17% without the altering the residence time from the theoretical 3 minutes 45 seconds. The shorter, broader curve represents the lower gas-liquid ratio.

However, the u-tube reactor has a difference to the jet pump in one important respect. It has a back-pressure due to the tube having an upward as well as a downward leg. This may mean higher mass transfer than in a jet pump (or bubble column) for a corresponding set of flow conditions because of the enhanced pressure at the base of the column. This will improve the solubility behaviour of the gas. In addition the residence time for a given column length is going to be in the order of twice that for single pass columns due to the u-tube nature of the contactor.

7.3 HYDRAULIC RESIDENCE TIME AND WATER LOADING RATE

An important parameter in the column design is the amount of time that the water actually spends in the column. This is often known as the hydraulic residence time (HRT). This is usually defined as:

$$HRT = \frac{l}{u_{LS}} = \frac{V}{Q} \tag{7.13}$$

and,

$$u_{LS} = \frac{Q}{A} \tag{7.14}$$

where

u_{LS} = superficial liquid velocity (m/sec)

l = length of column (m)

A = cross sectional area available to liquid flow (m^2)
= A_L

Q = water flowrate (m^3/sec) = Q_L

V = volume of column (m^3) = A*l

Note that the use of the u and A terms are not their standard nomenclature. This is because the voidage of the column needs to be taken into account.

Another useful term used to describe the liquid flow through the column is the water loading rate (WLR). This term defines the water flow in terms of mass flow per unit cross section:

$$WLR = \frac{Q_m}{A} \tag{7.15}$$

where

Q_m = mass flow of water (kg/sec)

The HRT and the WLR are found without the gas flow.

7.4 GAS RESIDENCE TIME (GRT)

It is useful in this study to define another residence time. This is the gas residence time (GRT). This is analogous to the hydraulic residence time (HRT) described in section 7.3. The only major difference is that in general an assumption of constant density needs to be made. This is because of gas compressibility. However, in general, due to the free-flowing nature of the jet-pump system this should not present a significant error. The GRT can be defined:

$$GRT = \frac{l}{u_{GS}} = \frac{V}{Q} \tag{7.16}$$

and,

$$u_{GS} = \frac{Q}{A} \tag{7.17}$$

where

u_{GS} = superficial velocity (m/sec)

l = length of column (m)

A = cross sectional area available to gas flow (m^2) = A_G

Q = gas flowrate (m^3/sec) = Q_G

V = volume of column (m^3) = A*l

Again note that the use of the u and A terms are not their standard nomenclature. This is because the voidage of the column needs to be taken into account.

8.0 MODELLING OF OZONE TREATMENT

As discussed in the section on mass transfer with chemical reaction (section 3.4), there are several important reaction regimes that need to be considered when modelling the treatment behaviour. The reaction regimes range from very fast reactions, through intermediate, slow and infinitely slow reactions. However, these labels are also of a relative nature. It has been suggested [44] that typically the mass transfer and reaction regime for O_3-waste water systems is slow. This means that there is usually an O_3 concentration within the bulk of the water phase. This means that the mass transfer is not usually being enhanced by very rapid reactions taking place at or very near to the interface between the phases. This leads to the basic formulation of the model. If the slow reaction regime follows, then the mass transfer model takes in two stages. The first stage is the diffusion of the ozone gas across from the gaseous state to be absorbed in a physical manner into the waste water. The second stage of the process is the reaction of the ozone in this aqueous state. The ozone reaction can take on two major pathways. The direct action of ozone on reacting species in the water, or the degradation of the ozone. The reaction pathway chosen will highly depend on the kinetics of the reaction in question.

8.1 DEVELOPMENT OF THE MATHEMATICAL MODEL

8.1.1 STAGE 1

The models used for all experiments were developed using standard FORTRAN 77. The need to use differential equations then required the addition of Runge-Kutta 4th order numerical solution techniques. The most basic model consisted of a framework developed by Yuteri and Gurol[44,75]. Their model was for use in describing the contaminant removal characteristics of a counter-current liquid-gas contactor. The initial model developed in this study used similar parameters for modelling as did the Yuteri and Gurol [44,75] studies. This

was done to check the new model against the literature modelling. Consequently similar trend data was extracted from the new model, although several problems in the literature [44,75]. were found, and these are more fully expounded in Section 8.1.1.1.

The choice of this model was made due to its general nature. It presents the treatment characteristics in such a way that the change of contaminant or other system data can be easily handled. The model reduces the complex ozone-water and ozone-contaminant reactions and kinetics down to a simplified describer. This is known as the rate of aqueous ozone consumption (r). This rate can be represented by a simple first order expression[43,44].:

Performing a mass balance on the amount of ozone absorbed by the system(N_{O3}) yields:

N_{O3} = (O_3 leaving the system in the liquid phase) +

(O_3 Consumed by reactions)

$$N_{O3} = Q_L[O_3] + (O_3 \text{ Consumption}) \quad (8.1)$$

where

Q_L = liquid flowrate (l/s)

Now, the rate of ozone consumption is described by:

$$O_3 \text{ Consumption} = V_L\Sigma(k_i[S_i])[O_3]) + V_L k_d[O_3] \quad (8.2)$$

where

k_d = rate constant for ozone decomposition reactions (sec^{-1})

V_L = volume of liquid in reactor (l)

$[S_i]$ = concentration of organic compound i (mol/l)

k_i = rate constant for species i (l/mol.sec)

Now,

$$\text{let } w = \Sigma(k_i[S_i]) + k_d \tag{8.3}$$

then,

$$O_3 \text{ consumption} = V_L.w.[O_3] \tag{8.4}$$

and, on the basis of specific volume:

$$r = w.[O_3] \tag{8.5}$$

where

$[O_3]$ = liquid phase ozone concentration (mol/L)

w = reaction rate constant (sec^{-1})

= specific ozone utilisation rate (sec^{-1})

r = rate of ozone utilisation (mol/l.sec)

As can be seen in the definition of the w parameter, it is a function of the concentration of the species in the solution matrix. It is thus obvious that the value of w will change during exposure to ozone, as the concentration of the pollutants decrease. Therefore the rate of ozone decomposition will also change due to this change in composition. However, in this

investigation the w term is assumed to be constant. This is assumed because the concentration value of any target compound is assumed very small, so that $\Sigma(k_i[S_i]) << k_d$.

The next stage is to describe the rate of ozone transfer to the reaction system in terms of mass transfer coefficients. The rate for a given control volume can be described by the following:

$$N_{O3} = K_L a([O_3^*]-[O_3]) \qquad (8.6)$$

where

N_{O3} = rate of Ozone Mass Transfer (mol/l.sec)

$K_L a$ = volumetric mass transfer coefficient (sec^{-1})

$[O_3^*]$ = Ozone concentration at the gas-liquid interface (mol/l)

$[O_3]$ = Liquid phase ozone concentration (mol/l)

The determination of the gas-liquid phase concentration of ozone can be found from the equilibrium relationship of Henry's Law (see section 3.2).

The rate of ozone transfer can be affected by a number of parameters such as the concentration and type of species in the liquid phase, as well as other parameters such as pH (see section 2.2.1). In general the ozone reaction system follows the pattern of a slow reaction system (see section 3.4.2). This means that there are two distinct phases in the ozone mass transfer and disinfection system. The first phase is the transfer of the ozone from the gas phase to the liquid phase (physical absorption), followed by the reaction of ozone. These reactions form two main paths. The first is the reaction of ozone with the target organic species, and the second is the decomposition of the ozone (See sections 2.2.1 and 2.2.2). This slow regime does not always hold. A prime example is in biological systems, where the initial disinfection rate is often too rapid to be measured (section 6.0).

Due to the relatively slow nature of many of the ozone reactions this means that there tends to be a reasonable concentration of ozone in the liquid phase. This also means that the reactions do not give a reaction enhancement to the ozone mass transfer.

However the reaction system itself does affect the volumetric mass transfer coefficient. This means then that the mass transfer and reaction regimes cannot be completely separated. The use of empirical data for estimation of mass transfer coefficient, such as that of Akita and Yoshida [38]. (see section 4.1), may find limited application in many cases.

The model examined here is able to predict the volumetric mass transfer coefficient for a system. Comparison can then be made with the published empirical models.

As discussed previously (section 2.2.1) there are several mechanisms which contribute to the disinfection of organics in liquid systems. The organic components can be physically stripped from the waste stream by the gas or another liquid phase, the contaminant can be oxidised directly by ozone, or the decomposition products of ozone can disinfect as well.

In a sense it is difficult to tell which process is occurring, particularly in the case of direct and indirect oxidation. The two types of oxidation can be lumped into one parameter known as the overall oxidation rate constant (k_T). An overall rate expression can then be formed [43].:

$$r_i = k_T.[S_i].[O_3] \qquad (8.7)$$

where r_i = total rate of oxidation (mol/l.sec)

k_T = total oxidation rate constant (l/mol.sec)

$[S_i]$ = organic contaminant 'i' concentration (mol/l)

$[O_3]$ = ozone liquid phase concentration (mol/l)

For further information on k_T values see section 8.1.1.1.

Again it must be noted that particular Henry's Law constants (see section 3.2) for a system should be used with care as these constants are normally formulated for a clean system and not for a complex mixture.

8.1.1.1 COUNTER-CURRENT MODEL (STAGE 1)

For the basic first model a counter current model as shown in figure 8.1 was used:

FIGURE 8.1 COUNTER CURRENT COLUMN

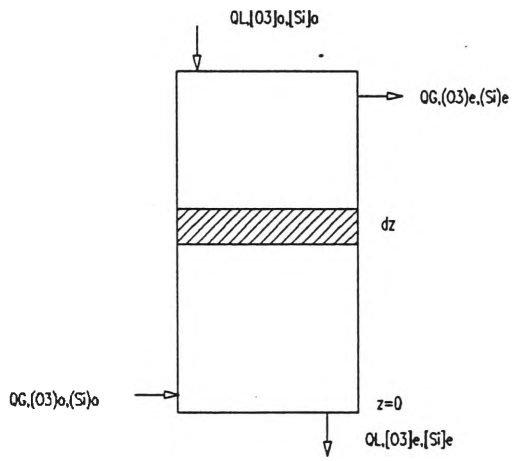

The assumptions for the model are that ideal plug flow is occurring, and that all reactions occur in the liquid phase.

Now, the steady-state balances for the equations are as follows:

Rate of change of [O3] over

the length of the column = $\frac{d[O_3]}{dz}$ = (mass transfer per unit length) - (rate of consumption of ozone per unit length)

i.e.,

$$\frac{d[O_3]}{dz} = \frac{k_L a([O_3^*]-[O_3])}{(Q_L/A)} - \frac{w[O_3]h_L}{(Q_L/A)}$$

$$\frac{(Q_L)}{(A)}\frac{d[O_3]}{dz} = k_L a([O_3^*]-[O_3]) - w[O_3]h_L \qquad (8.8)$$

Now,

Rate of change of O_3 concentration in the gas stream $= \frac{d(O_3)}{dz}$

= (rate of mass transfer per unit length)

i.e.,

$$\frac{d(O_3)}{dz} = \frac{k_L a([O_3^*]-[O_3])}{(Q_G/A)}$$

$$\frac{(Q_G)}{(A)} \quad \frac{d(O_3)}{dz} = k_L a([O_3^*]-[O_3]) \qquad (8.9)$$

Now,

Rate of change of the organic pollutant in the liquid phase = $\frac{d[S_i]}{dz}$

= (Rate of mass transfer of pollutant from the gas-liquid interface) - (rate of pollutant removal)

i.e.,

$$\frac{d[Si]}{dz} = \frac{(k_L a)_i([S_i^*]-[S_i])}{(Q_L/A)} - \frac{h_L k_T [O_3][S_i]}{(Q_L/A)} \qquad (8.10)$$

$$\frac{(Q_L)}{(A)} \quad \frac{d[Si]}{dz} = (k_L a)_i([S_i^*]-[S_i]) - h_L k_T [O_3][S_i]$$

Now,

Rate of change of the pollutant in the gas phase = mass transfer rate

$$= \frac{d(S_i)}{dz}$$

i.e.,

$$\frac{d(S_i)}{dz} = \frac{(k_L a)_i([S_i^*]-[S_i])}{(Q_G/A)}$$

$$\frac{(Q_G)}{(A)} \quad \frac{d(S_i)}{dz} = (k_L a)_i([S_i^*]-[S_i]) \qquad (8.11)$$

These equations hold for constant flow patterns through the column. To solve these equations numerically requires initial conditions to be known. However at the bottom of the column (z=0) the final liquid-phase concentration of the contaminant or ozone is not known. This means that to solve the equations, several concentration values need to be chosen. Then the equations iterated until a convergence is found.

In a paper by Yurteri and Gurol [44], it was suggested that if a shift was made from the z-domain to the t-domain (time), then this would alleviate the need for iteration. The reasoning was that all inlet concentrations (i.e. at t=0) are known. However, although this is true, it does not mean that iteration is avoided.

As can be seen in Figure 8.1 the flows in counter-current flow oppose each other (by definition). The model equations developed (equations 8.8 to 8.11) are interdependent, and so at each interval along the column the equations need to be solvable. Working from either t=0 to t=HRT or from z=0 to z=L (column length), still requires a knowledge of either the gas or liquid concentration profile. This cannot be done in the counter-current case without performing an initial guess and iteration procedure.

However the logic of Yurteri and Gurol [44] was followed through to see if similar results could be obtained. Near exact results of this incorrect procedure were obtained.

The second logical problem initially associated with the model was that the concentration gradient terms for the gas composition profile were those for co-current, rather than counter-current flow. That is:

$$\left(\frac{Q_G}{A}\right)\frac{d(O_3)}{dz} = k_L a([O_3]-[O_3^*]) \qquad (8.12)$$

instead of the correct (for counter-current flow):

$$\left(\frac{Q_G}{A}\right)\frac{d(O_3)}{dz} = k_L a([O_3^*]-[O_3])$$

and,

$$\left(\frac{Q_G}{A}\right)\frac{d(S_i)}{dz} = (k_L a)_i([S_i]-[S_i^*]) \qquad (8.13)$$

instead of the correct (for counter-current flow):

$$\left(\frac{Q_G}{A}\right) \frac{d(S_i)}{dz} = (k_L a)_i([S_i^*]-[S_i])$$

It must be pointed out, however, that if the authors had intended the gas flowrate term (Q_G) to be negative then their original equations would be correct.

The error becomes particularly noticeable when co-current studies are undertaken. When the model equations are altered for use in co-current simulation (see section 8.1.1.2) then the model starts to behave in a counter-current way. In reality then, the model developed by Yurteri and Gurol [44]. is actually a co-current rather than the counter-current model it is purported to be.

A third alteration to the literature [44]. model that was made was the removal of the $[O_3^*]$ term. This term is still used in this thesis, however, it may be slightly misleading when trying to solve the equations. It is defined as the ozone concentration at the liquid-gas interface:

$$[O_3^*] = \frac{(O_3)}{H} \qquad (8.14)$$

This means that, for example, in the equation below:

$$\left(\frac{Q_G}{A}\right) \frac{d(O_3)}{dz} = k_L a([O_3^*]-[O_3])$$

The right hand side of the equation is also function of (O_3). This is not immediately obvious from first observation. Changing the form of the equation to:

$$\left(\frac{Q_G}{A}\right) \frac{d(O_3)}{dz} = k_L a((O_3)/H-[O_3]) \qquad (8.15)$$

prevents any confusion. This does make a slight difference in numerical integration techniques, particularly the Runge-Kutta 4th order method used in this thesis. Note that all four modelling equations were changed to this form, as:

$$[S_i^*] = \frac{(S_i)}{H_i} \qquad (8.16)$$

In a later article [75], which tests the model against experimental data, the above three changes are made without explanation. Their previous misleading article is referenced as a source. The work in this last article [75] showed that the new counter-current model described the experimental observations very well.

Following in the next section is the procedure for changing the length domain (z) to the time domain (t).

8.1.1.1.1 TIME DOMAIN MODEL

Changing the model from the domain of length to the domain of time may present some advantages in some situations. The largest of these is that the time spent in the column can be measured and a true picture of flow regime and flow pattern is indirectly incorporated into the model.

For the initial solution model of the equations an empty bed column was chosen. The characteristics of the column are then:

$$t = \frac{V_{EB}}{Q_L} = \frac{\text{volume of empty bed}}{\text{Liquid flow rate}} \qquad (8.17)$$

$$= \frac{\text{Area} * \text{height}}{Q_L} \qquad (8.18)$$

$$dt = \frac{A\,dz}{Q_L} \qquad (8.19)$$

therefore,

$$dz = \frac{Q_L\,dt}{A} \qquad (8.20)$$

This approach is slightly simplistic, as the actual length to time conversion should not be based on the cross-sectional area of the column, but rather on the cross-sectional area available to each phase. The equation modelling should be based on the actual gas and liquid velocities(u_G and u_L), rather than the superficial velocity (u_{LS}) based on total cross section being available for liquid flow. The 'real' residence times are used in all modelling in this thesis.

Now changing all of the equations to the time domain (t) yields:

$$\frac{d[O_3]}{dt} = k_L a([O_3^*]-[O_3]) - w[O_3]h_L \tag{8.21}$$

$$\frac{d(O_3)}{dt} = k_L a([O_3^*]-[O_3])\frac{Q_L}{Q_G} \tag{8.22}$$

$$\frac{d[S_i]}{dt} = (k_L a)_i([S_i^*]-[S_i]) - h_L k_T[O_3][S_i] \tag{8.23}$$

$$\frac{d(S_i)}{dt} = (k_L a)_i([S_i^*]-[S_i])\frac{Q_L}{Q_G} \tag{8.24}$$

Now the initial values for the above equations usually are as follows:

@ t=0:

$[S_i]$ = known

$(S_i) = 0$

(O_3) = known

$[O_3] = 0$

Now from Henry's Law (see section 3.2):

$$[O_3^*] = \frac{(O_3)}{H} \tag{8.25}$$

$$[S_i^*] = \frac{(S_i)}{H_i} \tag{8.26}$$

The estimation of the value of the volumetric mass transfer coefficient for the organic species, $(k_La)_i$, was $0.6*k_La$. This is due to two studies. The first by Matter-Muller[59] and the second by Gurol and Singer[60].This value was also used in two studies by Gurol[43,44]. Matter-Muller[59] found that for oxygen and chlorinated hydrocarbon systems that the ratio of k_La to $(k_La)_i$ was 0.5, whilst Gurol and Singer[60] found that the ratio of $(k_La)_{O3}$ to $(k_La)_{O2}$ was 0.83.

As described previously, the model parameters chosen are the same as those in the Yuteri and Gurol[44] study. This includes the time increment used in the Runge-Kutta solution technique (increment = 0.25 seconds, over a total hydraulic residence time of 300 seconds). These values are shown in Table 8.1:

TABLE 8.1 BASE VALUES FOR MODEL (STAGE 1)

Parameter	Base Value
w	$0.05\ s^{-1}$
k_La	$0.03\ s^{-1}$
Q_G/Q_L	3
$(O_3)_o$	$0.135*10^{-3}$ mol/l
h_L	0.83
k_T	1000 l/(mol.s)
H_i	0.42
HRT	300 s

One additional feature was added to the model solving algorithm. This was added due to the likelihood of much smaller residence times than the 300 seconds used as a standard for the

basic model [44]. It was decided that for HRT times of less than 10 seconds that 100 points would be used to estimate the size of the increment .

As for the Yurteri and Gurol [44] study, four main chemical groups were used to examine the effects of changing various operational parameters of the column. These groups were as follows:

Group 1 Compounds:

These compounds represent highly reactive but low volatility compounds such as the aromatic compounds of phenol and naphthalene.

$H_i = 0.02$

$k_T = 1000$ l/(mol.s)

Group 2 Compounds:

These compounds represent compounds with high volatility and low reactivity such as trichloroethylene.

$H_i = 0.42$

$k_T = 10$ l/(mol.s)

Group 3 Compounds:

This group represents those compounds with high volatility and moderate reactivity such as o-xylene.

$H_i = 0.42$

$k_T = 100$ l/(mol.s)

Group 4 Compounds:

This group represents those compounds with high reactivity and low volatility such as 1,2,4-trimethylbenzene.

$H_i = 0.24$

$k_T = 500$ l/(mol.s)

The importance of the volatility of a compound cannot be overlooked in a disinfection or treatment system. This is because the compound being treated may simply be stripped out of the liquid phase by the ozone carrying stream. This process may or may not be desirable. However to neglect stripping may give a false impression of actual ozone disinfection performance.

8.1.1.2 CO-CURRENT MODEL (STAGE 1)

A similar procedure to that used for the counter-current model was used to develop the co-current model. Figure 8.2 shows a schematic of the co-current contactor used:

FIGURE 8.2 CO-CURRENT MODEL

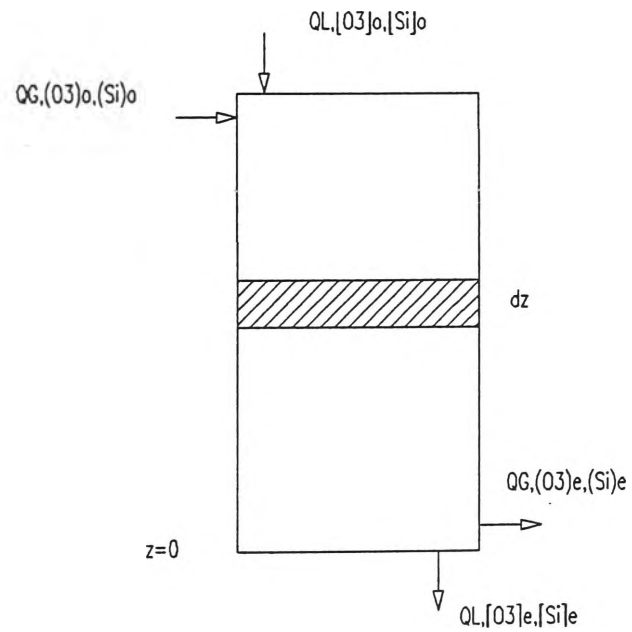

Two of the model equations (liquid phase) are identical to those of the counter-current model, and the two gas-phase describers for co-current flow are as follows:

Now,

Rate of change of O_3 concentration in the gas stream $= \frac{d(O_3)}{dz}$

= (rate of change of mass transfer per unit length)

i.e.,

$$\frac{d(O_3)}{dz} = \frac{k_L a([O_3^*]-[O_3])}{(-Q_G/A)}$$

$$\frac{(-Q_G)}{(A)}\frac{d(O_3)}{dz} = k_L a([O_3^*]-[O_3]) \qquad (8.27)$$

Note that the only change to the equation from that of the counter-current model is the change of the sign of the gas flowrate, since its flow is reversed. This, then, leads to the new equation for co-current flow in the time domain:

$$\frac{d(O_3)}{dt} = -k_L a([O_3^*]-[O_3])\frac{Q_L}{Q_G}$$

that is:

$$\frac{d(O_3)}{dt} = k_L a([O_3]-[O_3^*])\frac{Q_L}{Q_G}$$

or,

$$\frac{d(O_3)}{dt} = k_L a([O_3]-(O_3)/H)\frac{Q_L}{Q_G} \qquad (8.28)$$

In the equation below, that which describes the change of the target pollutant's concentration in the gas phase, there is also a Q_G term. Therefore, the stripping equation becomes:

$$\frac{d(S_i)}{dt} = (k_L a)_i([S_i^*]-[S_i])\frac{Q_L}{-Q_G}$$

or,

$$\frac{d(S_i)}{dt} = (k_L a)_i([S_i]-(S_i)/H_i)\frac{Q_L}{Q_G} \qquad (8.29)$$

The difference the reversal of direction of the gas flow makes on most of the actual equations is indirect. This manifests itself as changes in most of the physical parameters such as mass transfer co-efficients.

8.1.1.3 JET PUMP MODELLING

The aim of the mass transfer modelling in this thesis is to provide a mass transfer model which is able to be confirmed by experimentation. Much research has gone into mathematical modelling of counter-current bubble column contactors. However, the work on co-current downflow systems is limited. In particular the jet-pump system is poorly understood from an ozone mass transfer and reaction point of view. The partial aim of this thesis is to examine to what extent mathematical models developed for bubble columns can be used to describe the mass transfer in a jet pump system.

Initially it was decided that the use of the co-current model for bubble columns be tried. No changes to the mechanism of the model were made in the first instance. In a way the model presented in the previous sections may be more accurate than for bubble columns. The reason for this is that in a jet flow or annular flow regime (see Chapter 5.0 on two phase flow) there is less likelihood of liquid phase backmixing due to the high liquid film velocities. This means that near perfect plug flow will occur, which is essential for full model validity. Work

done by Briens et al. [131.] and by Dirix and van der Wiele [134.] tends to bear this assumption out. Shown in Figure 8.3 is the experimental set-up of the jet-pump contactor.

It is also suggested that in these jet-type reactors the liquid will tend to form a layer on the diffuser wall and the gas will flow through the centre, possibly carrying some entrained liquid [134.](see Chapter 5.0 on two-phase flow).

FIGURE 8.3 SCHEMATIC LAYOUT OF JET PUMP CONTACTOR SYSTEM

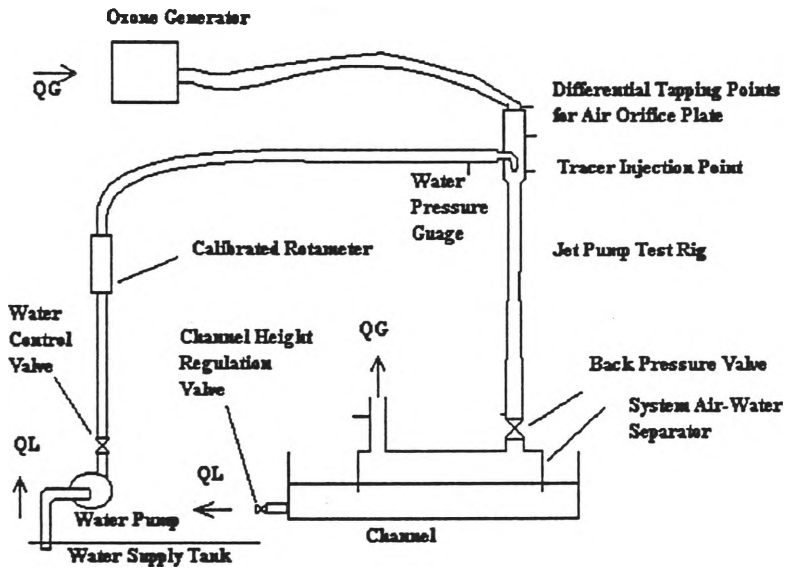

The jet pump modelling was initially performed in the time domain, and so certain assumptions were required to be made.

These assumptions are described in the following equations:

$$HRT = \frac{L}{u_L} \qquad (8.30)$$

where HRT = Hydraulic Residence Time (seconds)

L = Length of Column (Metres)

u_L = Liquid Velocity (ms^{-1})

but,

$$Q_L = u_L.A$$

i.e. $u_L = Q_L/A$ (8.31)

where Q_L = liquid flowrate (m^3/sec) (in this case)

A = Cross-sectional Area of Column (m^2)

However, actual residence time is longer due to the air-water separator at the base of the jet-pump column (see Figure 8.4). The ozone is therefore in contact with the water for extra time as it passes though this final stage. This separator is likely to produce end effects which are different to those in the main part of the column.

Following is a schematic of the air water separator.

FIGURE 8.4 SCHEMATIC OF AIR-WATER SEPARATOR

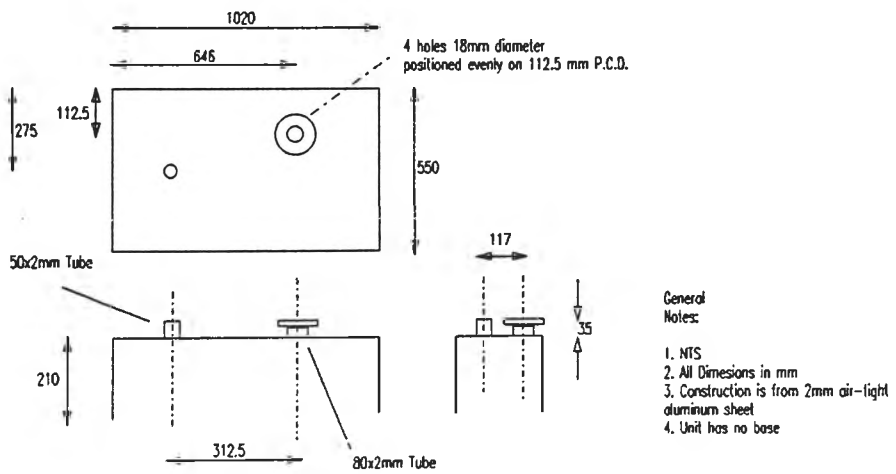

Note that all column data is available in Appendix

A_{sep} = separator cross-sectional area

= 1.020*0.550 = 0.561 m^2

L_{sep} = length of separator

= 0.210 m

therefore,

HRT_{sep} = HRT of separator (seconds)

$$= \frac{L_{sep} * A_{sep}}{Q_L} \quad (8.32)$$

L_M = length of mixing chamber (m) = 0.45m

L_D = length of diffuser (m) = 0.145m

D_{MC} = diameter of mixing chamber (m) = 0.054m

L_{BPV} = length of back pressure valve section (m) = 0.15m

therefore,

$$L = L_M + L_D + L_{BPV} \quad (8.33)$$

and,

$$HRT_{total} = HRT + HRT_{sep} \quad (8.34)$$

8.1.2 STAGE 2 DEVELOPMENT

Using the model of Yuteri and Gurol[44], as a basis, also presented the same drawbacks that were evident in their model. The most major of these is the lack of dependence between

the operational parameters. In this model the operational parameters more or less stand alone. The reality is that this would not be the case in a real system. The next stage of the model's development was therefore to examine which parameters should be tied together.

The first two parameters which are likely to have some interdependence are the volumetric mass transfer coefficient and the liquid or gas hold-ups.

To modify the model to handle the variations in gas hold-up it is necessary, at this stage, to manipulate the following empirical relationships (see section 4.1):

$$\frac{h_G}{(1 - h_G)^4} = 0.20(N_{Bo})^{1/8}(N_{Ga})^{1/12}(N_{Fr})^{1.0} \qquad (8.35)$$

$$= 0.20(N_{Bo})^{1/8}(N_{Ga})^{1/12}(U_G/[gD]^{0.5})^{1.0}$$

$$k_La = 0.6D_L^{0.5}(\mu)_L^{-0.12}(\sigma/\rho_L)^{-0.62}D^{0.17}g^{0.93}h_G^{1.1} \qquad (8.36)$$

Note that the equation presented above for the gas hold-up is the non-electrolyte version (see section 4.1). It also must be pointed out that as discussed in section 4.1 this k_La vs h_G relationship may not hold due to the size of the current jet pump column.

Now for bubble columns(BC),

$$h_L + h_G = 1 \qquad (8.37)$$

for packed bed columns(PC),

$$h_L + h_G = (1-\theta) \qquad (8.38)$$

where

h_L = liquid hold-up

h_G = gas hold-up

θ = packing fraction for a packed bed

$$= \frac{V_p}{V_{EB}} = \frac{\text{volume of packing}}{\text{volume of empty bed}} \quad (8.39)$$

and,

BC: $$V_{EB} = V_L + V_G \quad (8.40)$$

PC: $$V_{PC} = V_{EB}(1-\theta) \quad (8.41)$$

where

V_L = volume of liquid (m^3)

V_G = volume of gas(m^3)

Note that initially the jet pump contactor is treated as an empty column, and so the bubble column (BC) relationships apply.

From the column formulae and from the correlations of Akita and Yoshida[38], it may be possible to tie the volumetric mass transfer coefficients and gas/liquid hold-ups together for a given column specification a form similar to:

$$k_La = (\text{constant}).h_G^{1.1} \quad (8.42)$$

The value of the constant expression is not important in this application because the expression is only being used to show how k_La and h_G move relative to each other. As discussed in section 4.1, the correlation of Akita and Yoshida[38], is useful in determining the volumetric mass transfer coefficient (k_La) for ozone absorption from the reactor geometry

and reactor operating conditions. However, in a complex reaction matrix such as that of ozone disinfection, the various empirical relationships should be used with great caution. The reason is that the ozone system is very sensitive to many parameters. This is particularly true in the case of the chemical composition of the water. The main species in water which may highly affect the matrix are carboxylic acids, alcohols, phenols and surfactants[43,61]. The pH is also a very important factor, ranging from a low, relatively steady dissociation constant of k_d=0.27l/(mol.s) below pH=4 to a rate dependent value of $k_d=k_o[OH^-]^{0.55}$ at values pH>4 [45].(see section 2.2.1).

It is of value to examine the deviation of this model's predictions of k_La vs h_G from those of various empirical models (see Chapter 9). This new empirical correlation and data will act as a design aid for the physical design of the contacting column.

It is crucial that the full model parameters are available on the output of the model's solution. This is due to the fact the ozone reaction system is extremely sensitive to these parameters. For this reason the model can only be used for the exact system it is modelling. This means the kinetic data and geometric data are particular only to an exact case. The kinetic data, in particular must be obtained from the exact wastewater to be treated, and in a similar column. The model will have no validity if the kinetic data is obtained using clean water under semi-batch conditions, if the real system is to be 'dirty' water under counter-current continuous flow conditions.

Another difficulty which will arise in the predictive capability of any model development is the actual amount of dissociation of the ozone. It is assumed in all model development that the mass balance is simply:

Ozone in Entering Gas = Ozone in Exiting Gas + Ozone Mass Transfer to Liquid Phase (8.42)

However, there may be a certain level of ozone disintegration which is not catered for in any of the three above terms. This ozone disintegration will probably arise due to many factors and these could include disintegration due to energy transfer changes occurring through any

style of gas nozzle. There could also be disintegration due to the gas and liquid mixing system. It is reported in the literature that intense mixing of ozone in a reactor with the aid of a mechanical stirrer will lead to rapid disintegration of ozone. The suggestion of Schechter [99], in the case of mechanical stirring, is to avoid the stirring speed reaching 80 rpm (revolutions per minute). An analogous situation would be present in nozzle injection, column packing and liquid/gas distribution systems. The extent of the disintegration of ozone across the orifice plate was determined(see Chapter 9). However, the extent of disintegration in the chaotic mixing in the throat or diffuser is unknown.

8.1.3 STAGE 3 MODEL DEVELOPMENT

The third stage of the model's development was to examine more closely the two-phase nature of the system (see Chapter 5 Two Phase Flow). It is important to the applicability of the model that the flow regime is known. This will affect how appropriate the model's behaviour is. Visual examination of the flow regime in the jet pump (through the perspex section in the mixing tube), and the fact that the gas-liquid (Q_G/Q_L) ratios are high, suggests that the flow is annular, possibly with entrained liquid in the gas core. It is therefore important from a modelling point of view to confirm that this is the case.

It was decided to use the model of Dukler and Taitel [137] to determine the point of transition from annular flow. The description of this model appears in Chapter 5 on Two Phase flow.

There are two stages where the modelling of the flow regime is used. The first is to determine for a given column a transition profile, and the second is to determine for a given liquid and gas flowrate, the actual, rather than the superficial velocities for each phase. This actual data could then be compared to the measured residence time distribution (RTD) data. This comparison will then provide a guide to the applicability of the Dukler and Taitel [137] relationships.

8.1.3.1 SOLUTION OF TRANSITION POINT

Model equations are contained in Chapter 5.

The model was designed for use with ambient conditions and the air/water system as the default setting. Provision was made to change any of the physical data to suit. The physical data conditions were obtained from Holman [139].

The transition points for a user supplied column and materials were determined by manipulating the gas superficial velocity (u_{GS}). Once this value is known the Y parameter may be determined:

$$Y = \frac{(\rho_L-\rho_G)g}{(4c_G/D)(u_{GS}D/v_G)^{-m}\rho_G(u_{GS})^2/2} \tag{8.43}$$

In the first iteration of the model the Reynolds Number, and hence the flow regime of both phases, are based on the actual velocity (u_G) and hydraulic diameter (D_G) of the gas phase. The transition from laminar to turbulent flow regime was taken as a Reynolds Number of 2000.

Once Y is known then it can be substituted into the governing flow equation in its dimensionless form:

$$X^2[(u_LD_L)^{-n}u_L^2(S_L/A_L)]-(u_GD_G)^{-m}u_G^2S_i(1/A_L+1/A_G)-4Y=0 \tag{8.44}$$

All of the dimensionless variables (shown in *italics*) are functions of the film thickness divided by the pipe diameter (h/D). As discussed in section 5.1 the h/D ratio for transition is assumed to be 0.097. This means that X^2 is thus the only unknown. Once this has been calculated the appropriate liquid phase superficial velocity can be calculated from:

$$X^2=\frac{(4c_L/D)(u_{LS}D/v_L)^{-n}\rho_L(u_{LS})^2/2}{(4c_G/D)(u_{GS}D/v_G)^{-m}\rho_G(u_{GS})^2/2} \tag{8.45}$$

Once the liquid phase superficial velocity is known the actual liquid Reynolds Number (R_{eL}) is then calculated from the actual velocity (u_L) and hydraulic diameter (D_L) of the liquid phase. A check is then performed to make sure that the correct flow regime was chosen. If it is not correct then the model is iterated until agreement is made.

8.1.3.2 MODEL SOLUTION OF ACTUAL PHASE VELOCITY

A similar technique to that described in the previous section is employed to find actual rather than superficial velocities for user supplied flowrates. Full model equations are available in section 5.1.

In this case since superficial velocities of both phases are known, both the X^2 and Y parameters can be evaluated:

$$Y = \frac{(\rho_L-\rho_G)g}{(4c_G/D)(u_{GS}D/v_G)^{-m}\rho_G(u_{GS})^2/2} \tag{8.46}$$

$$X^2=\frac{(4c_L/D)(u_{LS}D/v_L)^{-n}\rho_L(u_{LS})^2/2}{(4c_G/D)(u_{GS}D/v_G)^{-m}\rho_G(u_{GS})^2/2} \tag{8.47}$$

As is the previous section an assumption has to be made in the first iteration as to the turbulent nature of each phase. This is individually determined using superficial velocities to evaluate the phase Reynolds Numbers (R_{eL} and R_{eG}).

Once X^2 and Y are known the governing equation needs to be solved. It must be noted that all of the dimensionless parameters (shown in *italic*) are functions of the h/D ratio. The following equation needs to be solved for this ratio.

$$X^2[(u_LD_L)^{-n}u_L^2(S_L/A_L)]-(u_GD_G)^{-m}u_G^2S_i(1/A_L+1/A_G)-4Y=0 \tag{8.48}$$

The solution of this equation requires an iteration technique. There are several numerical solving techniques that could be used. The decision was made to use the secant

method. This was done because some other methods, Newton's Method in particular, require the derivative of the equation be evaluated. This would be a complex technique in this case. A discussion of the Secant Method appears in appendix A 1.2.2.

After iteration to find the correct value of the film thickness to diameter ratio (h/D), the actual phase velocities can be determined. As a final check the phase Reynolds Numbers are checked to see if the correct regime was chosen for the iteration procedure. If the regime is wrong for either phase, the iteration procedure is repeated until the correct phase flow regime is determined.

An additional piece of information which may prove useful is the test to determine whether or not the flow regime is in annular or annular mist flow. This will have a bearing on the actual residence time distribution and the liquid volumetric mass transfer coefficient.

The suggested criteria for this transition is [142.]:

$$R_{eg}R_{el}^{0.301} = 1.199*10^{-6} \qquad (8.49)$$

The Reynolds numbers are the actual numbers based on real velocity and on hydraulic diameters.

It has also been pointed out that there are some concerns about using the Martinelli correlation (X^2) as it was originally developed for separate flow [142.].

9.0 EXPERIMENT AND RESULTS

(Note: This chapter only presents results and initial brief comments. A full discussion of the results follows in **Chapter 10**)

9.1 RESULTS OF CO-CURRENT MATHEMATICAL MODELLING

Figures 9.1 to 9.5A show the outputs of the model. The various parameters were altered one at a time and the remaining parameters were left at their base values (see Table 8.1). The trend of the data and the order of magnitude of the data compares favourably to the published model [44]. Within the bounds of the scaling of the literature data, this model compares quite satisfactorily. However, the concerns on the model voiced in chapter 8 still apply. The results described below are actually for a co-current bubble column, rather than the Yurteri and Gurol [44] results which they incorrectly suggest are for a counter-current bubble column.

FIGURE 9.1 % REMOVAL EFFICIENCY AS A FUNCTION OF K_T AND H_I (CO-CURRENT)

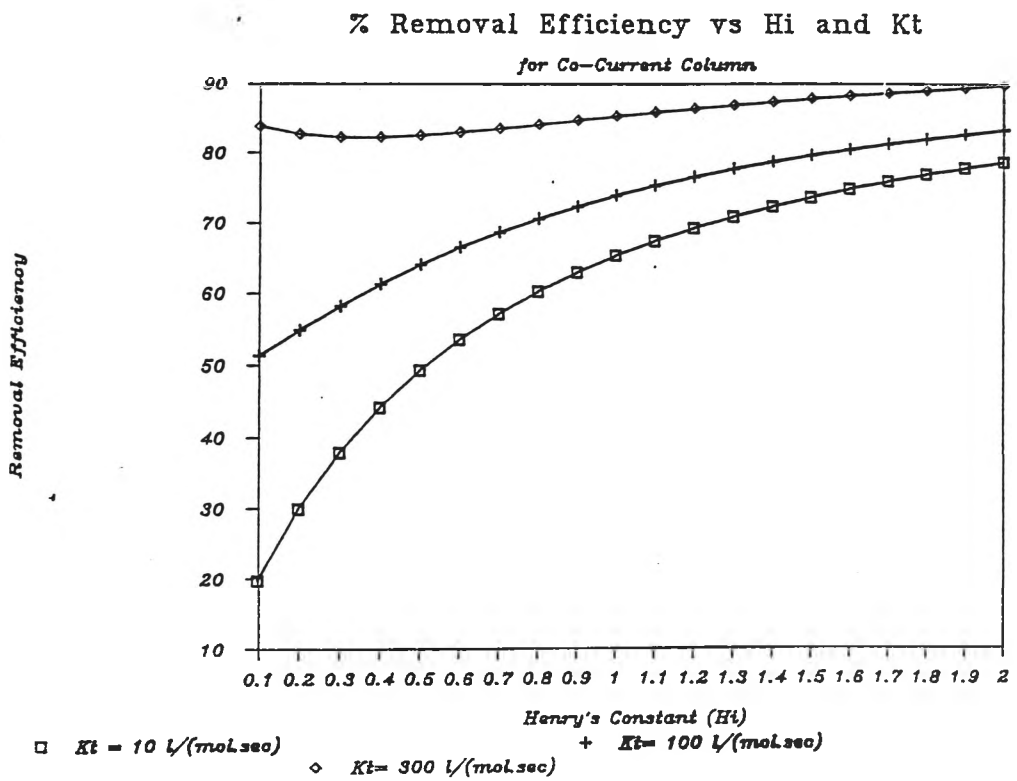

FIGURE 9.2 % REMOVAL EFFICIENCY VS GAS-LIQUID RATIO (CO-CURRENT)

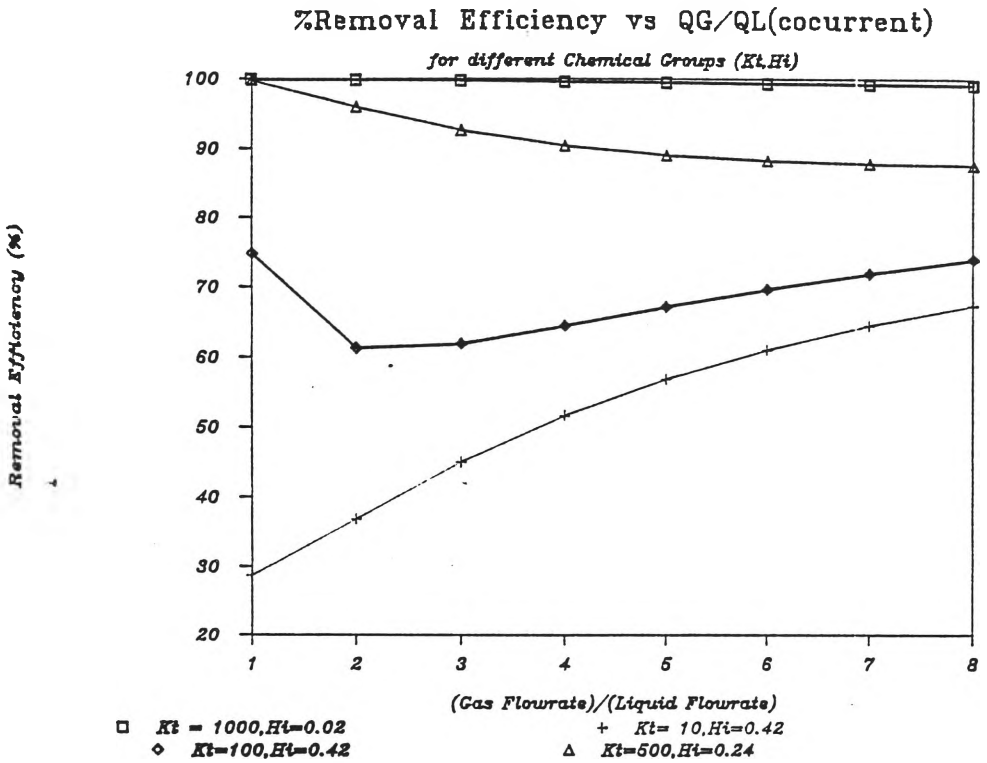

FIGURE 9.3 % REMOVAL EFFICIENCY VS VOLUMETRIC MASS TRANSFER COEFFICIENT (CO-CURRENT)

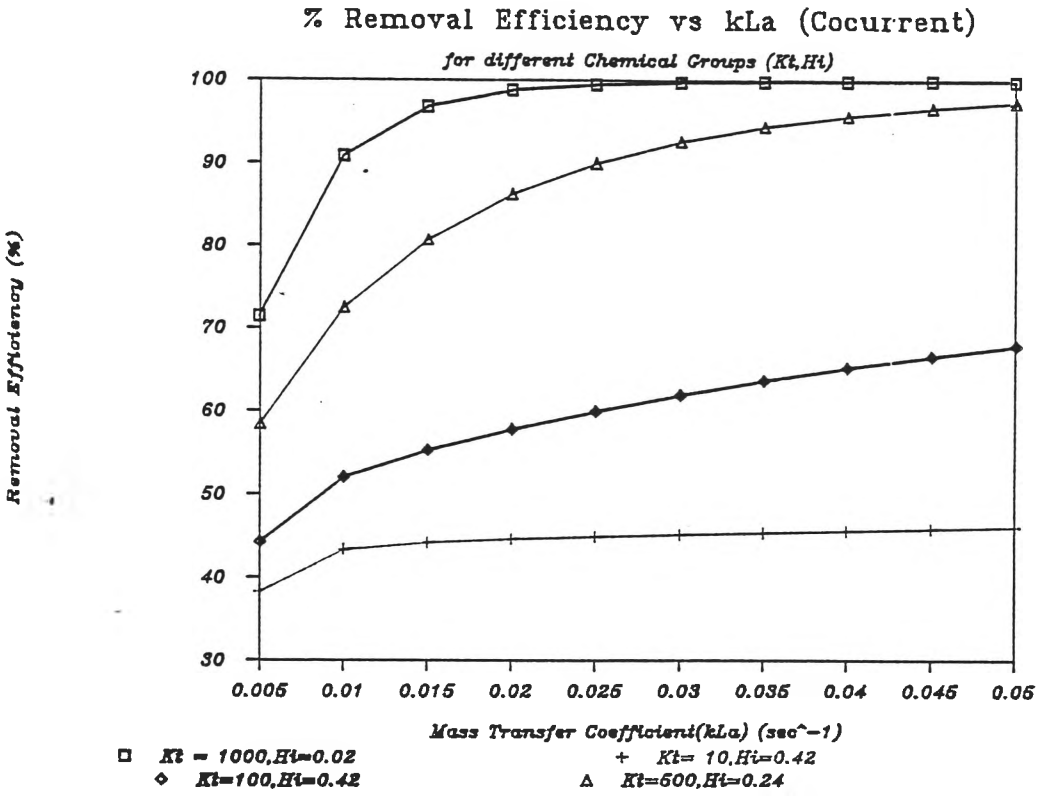

FIGURE 9.4 % REMOVAL EFFICIENCY VS SPECIFIC OZONE UTILISATION (CO-CURRENT)

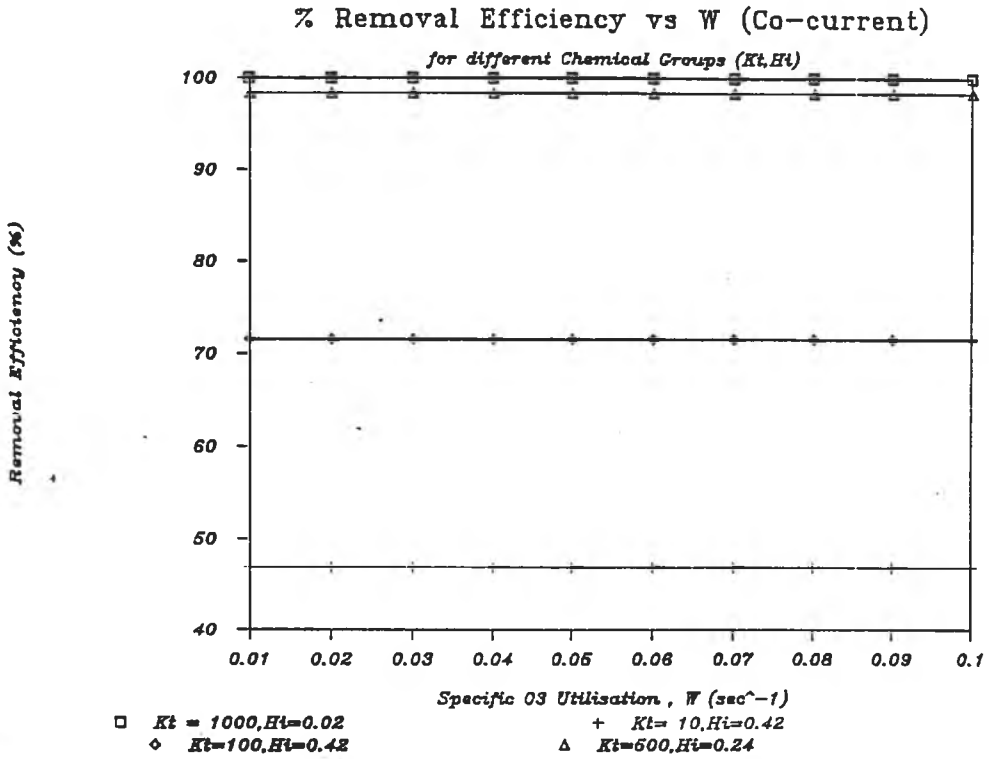

FIGURE 9.5 % REMOVAL EFFICIENCY VS LIQUID HOLD-UP (CO-CURRENT)

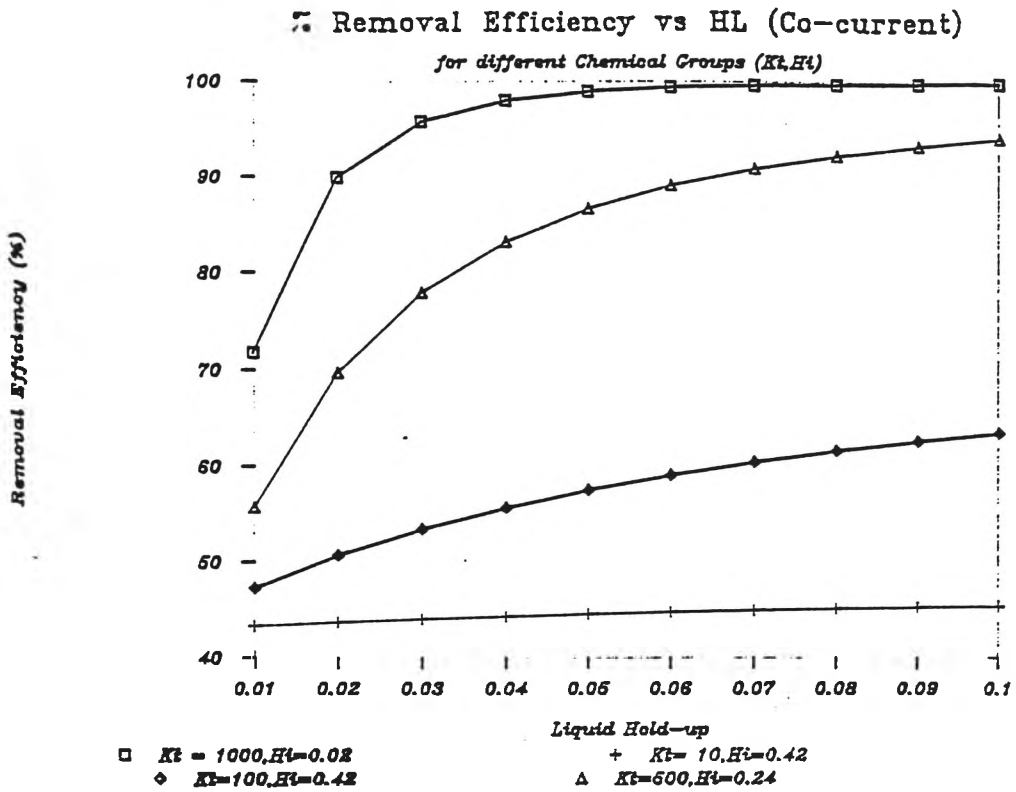

FIGURE 9.5A % REMOVAL VS INITIAL OZONE GAS CONCENTRATION

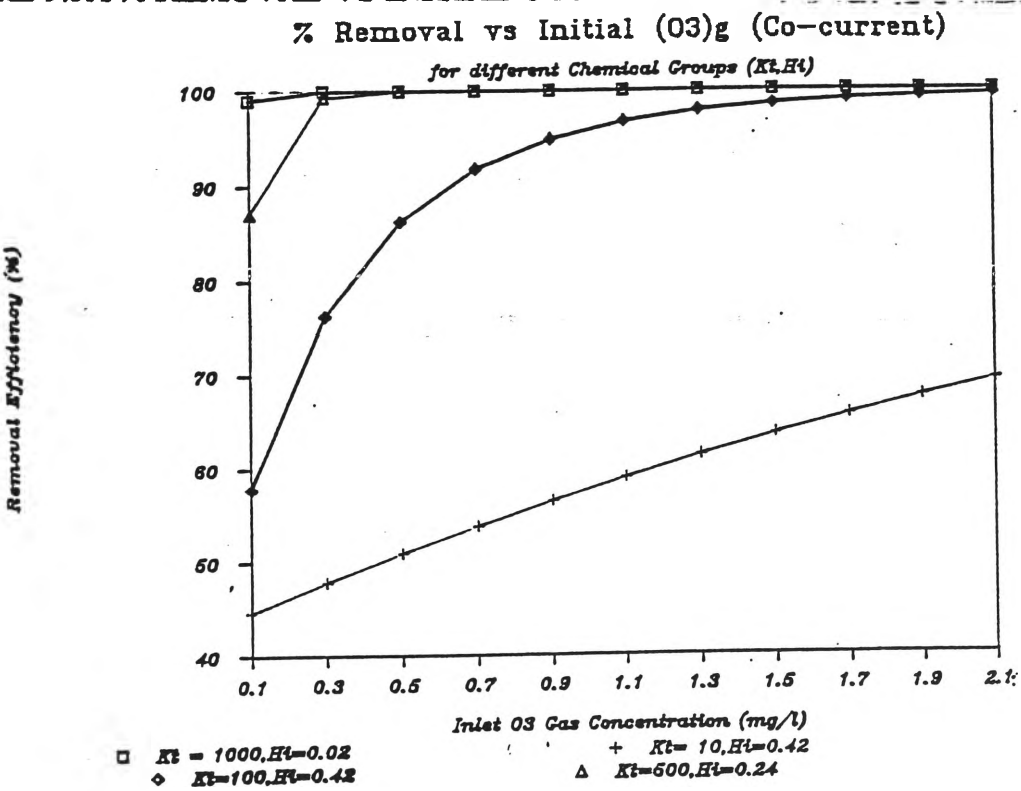

Some of the trends observed in the above data may be slightly exaggerated one way or another due to some interdependence between some of the parameters.

From a design point of view some of the combinations modelled above may be completely unobtainable in 'real life'. For example changing the gas to liquid rate ratio whilst maintaining the same volumetric mass transfer coefficient and hydraulic residence time may involve altering the geometry and packing of the column. This is also particularly true in the case of co-current contactors, where the co-current nature of the system limits the reactor combinations a great deal.

9.2 RESIDENCE TIME DISTRIBUTION STUDIES ON THE JET PUMP

9.2.1 GAS PHASE RTD

As described in chapter 7 it is imperative that the ideality of the reactor is examined to determine to what extent plug flow is occurring. This is particularly important in this case, as the mathematical modelling is based on plug flow. If the situation is such that plug flow is not occurring then this non-ideality must be examined and corrected for.

The second major piece of information that the RTD studies on the gas phase will determine is how well the predictive nature of two-phase flow models perform. These models (see chapter 5) try to predict the actual residence time in the column.

The actual contact time was examined by causing a step change in the ozone concentration in the feed gas. This step change was administered by turning off the ozone generator and monitoring the outlet ozone concentration. The method does present a problem, because the reaction and mass transfer component is being used as the tracer. The decision to do this was based on ease of detection, as the column is already set up to detect ozone. However, the accuracy of this method is really only at its best at high gas volumetric flowrates. This is because the difference between inlet and outlet ozone gas concentrations is of the order of 2ppm in 24ppm (say). This represents an 8.3% variation in concentration due

to mass transfer. Due to the likelihood of plug flow of the gas phase through the column it was decided for this investigation that any error present due to this mass transfer effect could be neglected.

In the case of the jet pump it is necessary to perform several different stages to examine the residence time distribution (RTD) of the system, including some difficult residence time manipulations. The need for a more complex approach than usual was due to the different and slow responses of the system and analysis equipment to step changes (see chapter 7 and appendix 2.0).

These stages are as follows:

- Time taken from the ozone generator to the actual mixing point of the ozone-air mixture with the liquid phase (water).
- The time from exit point to the detection point.
- The time taken for detection.
- The time taken in the portable air-water separator (if appropriate).

9.2.1.1 ENTRY END OF THE JET PUMP

The ozone-air feed gas is generated by passing air through an ozone generator. From the ozone generator the gas passes through a plastic feed hose until it reaches the top of the jet pump. From there it enters the aluminium suction chamber through an orifice (the air flow measuring device), and from there to the mixing point where it combines with the liquid phase. The actual contact time between the liquid and gas phases needs to be determined.

The entry end time correction is calculated by measuring the lengths and diameters of the various types of feed pipework, and then determining theoretically how long this should take. This is then compared with the actual time taken using an ozone detector at the mixing point. See Figures 9.6A and B.

FIGURE 9.6 ENTRY END RESIDENCE TIME CORRECTION FROM EXPERIMENT

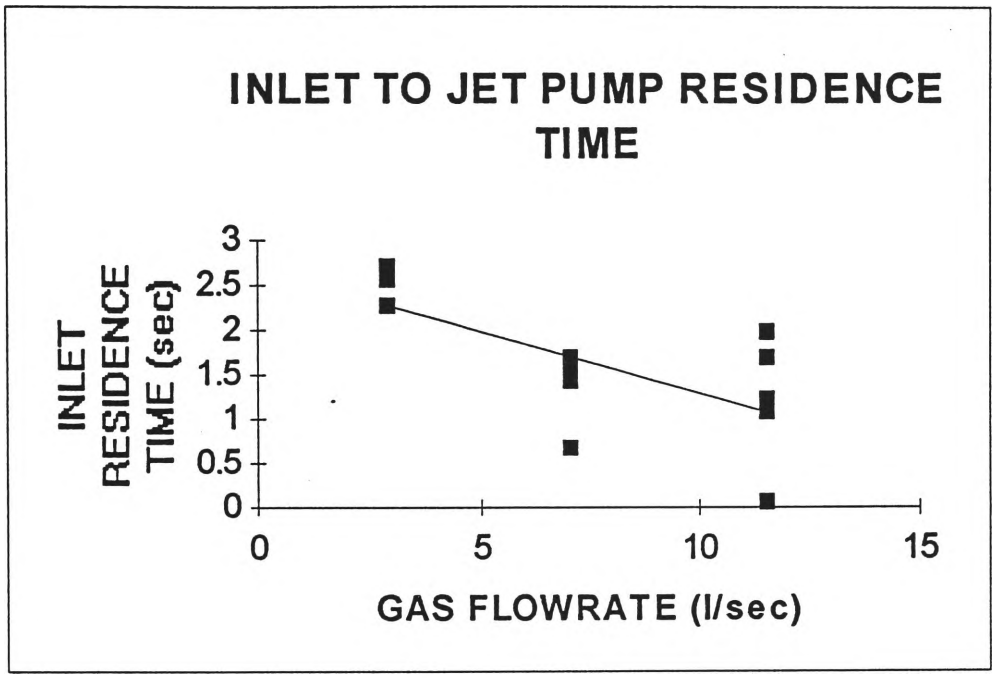

The line in figure 9.6 is the regression prediction of the data. The linear result of this prediction is:

$$GRT_{inlet} = -0.14Q_G + 2.68 \qquad (9.1)$$

where

GRT_{inlet} = experimental gas residence time for inlet to jet pump (seconds)

Q_G = gas volumetric flowrate (l/sec)

Figure 9.6 showing the residence time in the inlet line for the gas phase at the entry end of the jet-pump actually requires two different measurements. The first is a step change in the ozone concentration at the ozone generator, and the second is a step change in the ozone concentration at the sample point. The reason for this is that the sample curve can be

subtracted from the generator curve (via laplace transform and control theory-see appendix 2.0), and therefore the actual RTD profile can be found.

For the calculated entry-end residence time correction:

let

Q_G = gas volumetric flowrate (m^3/sec)

and,

$$Q_G = u_G.A \tag{9.2}$$

and,

$$u_G = l/t \tag{9.3}$$

where

l = length of pipe (m)

t = length of time in pipe (seconds)

u_G = velocity of gas (m/sec)

A = cross sectional area of pipe (m^2)

therefore,

$$t = l/(Q_G/A) \tag{9.4}$$

The major assumption in this calculation is that the air-gas mixture is near atmospheric pressure and is not undergoing any significant changes in its density.

The following physical data were obtained from the jet pump:

Length of plastic air inlet

hose to top of jet pump = l_t = 2455mm

Inside Diameter of Plastic inlet hose = d_t = 31mm (0.031m)

Length of Suction chamber from inlet hose to tapping point in jet pump = l_s = 210 mm

Inside Diameter of Suction Chamber = d_s = 76mm (0.076m)

for example:

if Q_G = 10 l/sec = 0.01 m^3/sec

then,

$$t = l_t/(Q_G/A_t) + l_s/(Q_G/A_s) \qquad (9.5)$$

= 0.466 seconds

FIGURE 9.6A COMPARISON OF ENTRY END RESIDENCE TIMES

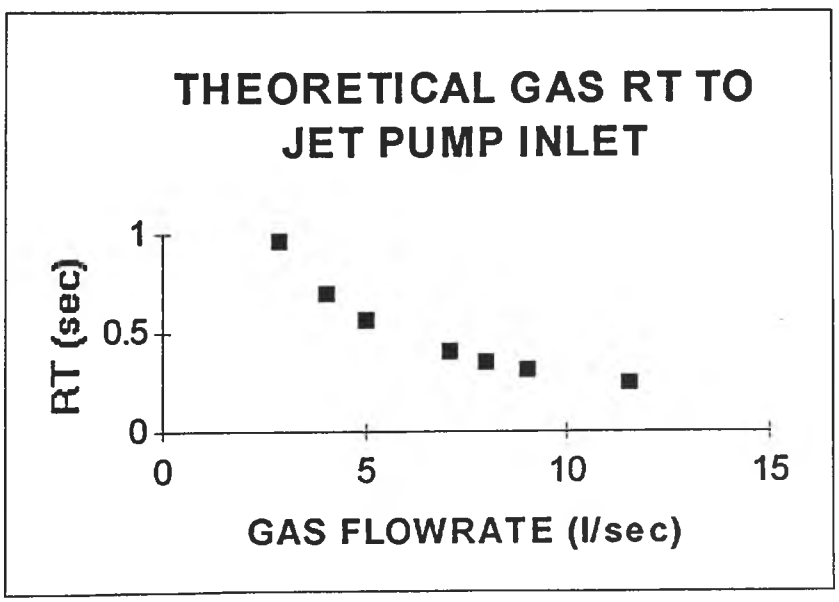

FIGURE 9.6B COMPARISON OF ENTRY END RESIDENCE TIMES

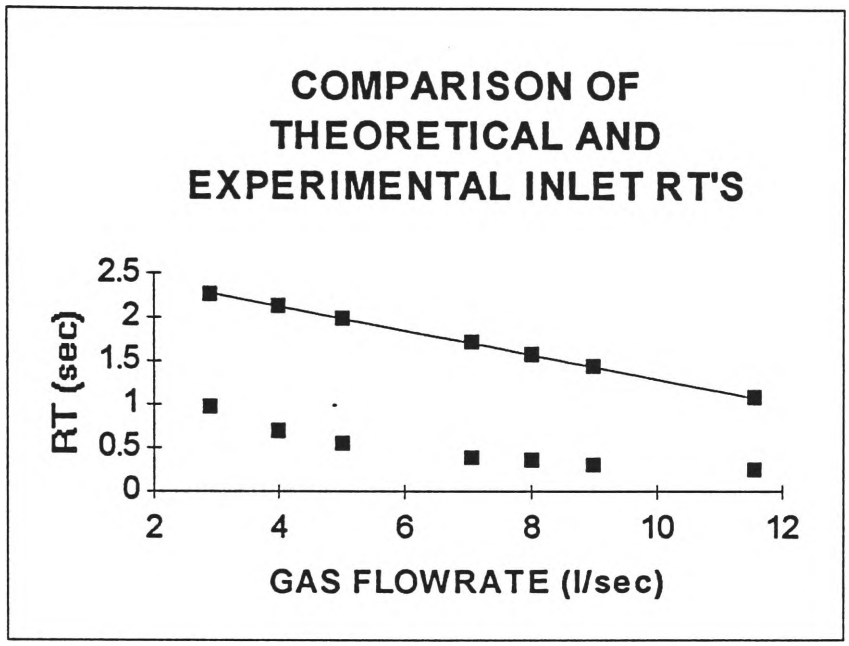

As can be seen from the previous two figures, there is a large difference between the theoretical entrance residence time for the gas phase. The theoretical is predicting a much smaller residence time.

9.2.1.2 OZONE DETECTOR RESIDENCE TIME CORRECTION

The ozone detector also has a time lag built in. This is due to the nature of the detection system. This is shown in Figure 9.7:

FIGURE 9.7 OZONE DETECTOR SET-UP

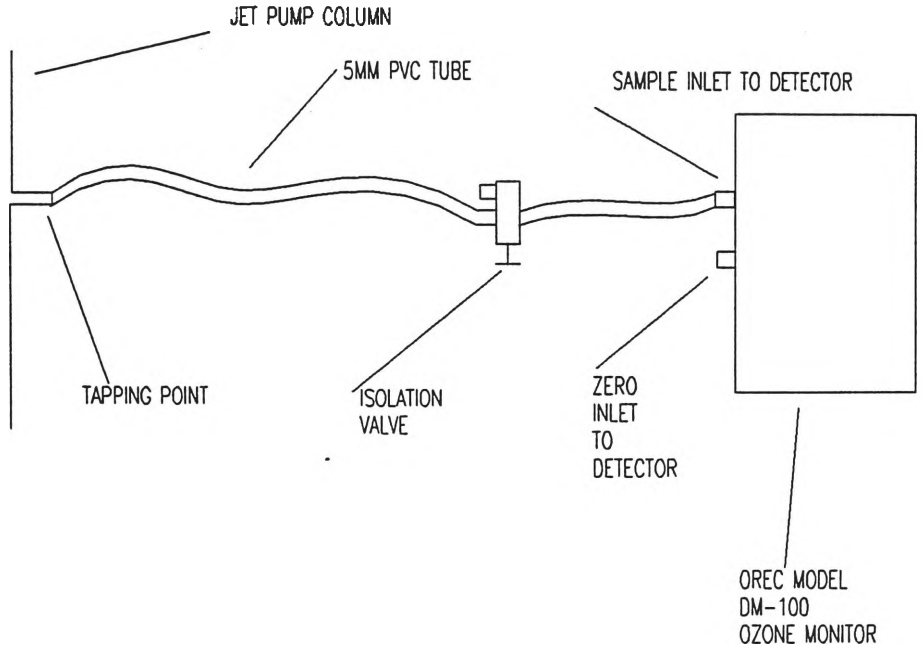

The detector (OREC Model DM-100 Ozone Monitor) works by the sample pump inside the detector drawing air at 1.5 l/min through the sample tubing. At the end of each minute a solenoid valve inside the detector switches and air is drawn through the sample zero inlet tube (see figure 9.7). This gas passes over a catalytic bed where any ozone that may be present is oxidised. This gives an on-line zero. This also causes problems as the most continuous on-line sampling that can occur is 1 minute. Whilst the zeroing is occurring the output reads the last value of ozone concentration measured.

The gas is drawn through the detector through tubing to a ultra-violet (UV) lamp. Then the light is absorbed and this absorbance is detected. This law is known as the Beer Law [150].:

$$I = I_W \exp(-LCX(273)(P)/(T.760)) \qquad (9.6)$$

where

I = light intensity with ozone

I_W = light intensity without ozone

C = ozone concentration (ppm)

X = absorption coefficient for ozone at 254 nm

T = sample temperature (K)

P = sample pressure (mmHG)

The method for determining the residence time in the ozone detector was to remove the detector feed line from the ozone containing air stream and record the corresponding ozone decay profile. This profile gives an indication of the time from the detection point to the recording point. This study was done for various initial ozone concentrations. The resulting experiments revealed that the RTD for the detector at the jet pump inlet is independent of initial concentration. Figure 9.8 below shows an example of the resulting curve, further raw curves appear in Appendix 4.0.

FIGURE 9.8 OZONE DETECTOR RTD (INTLET)

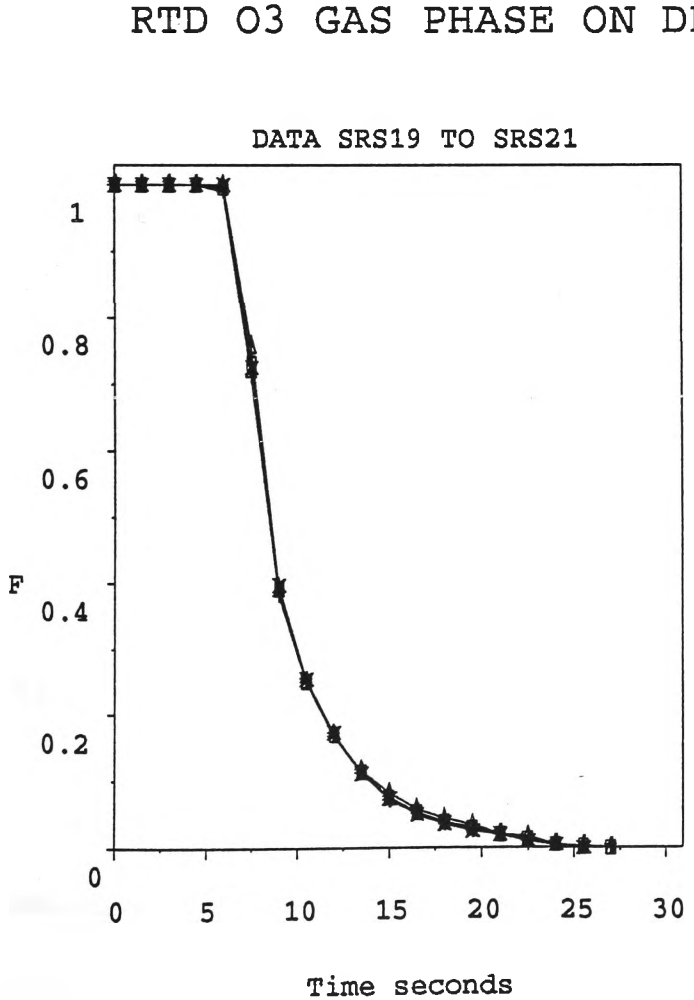

9.2.1.3 PORTABLE AIR-WATER SEPARATOR CORRECTION FACTOR

Full details of this unit appear in section 9.3. The methodology used is identical to that used for other corrective factors. The supply tube to the separator is disconnected from the jet pump system and the corresponding step-response for a number of cases is recorded. A selection of the results of this study appear in Figure 9.9.

FIGURE 9.9 PORTABLE AIR-WATER SEPARATOR RTD CURVE.

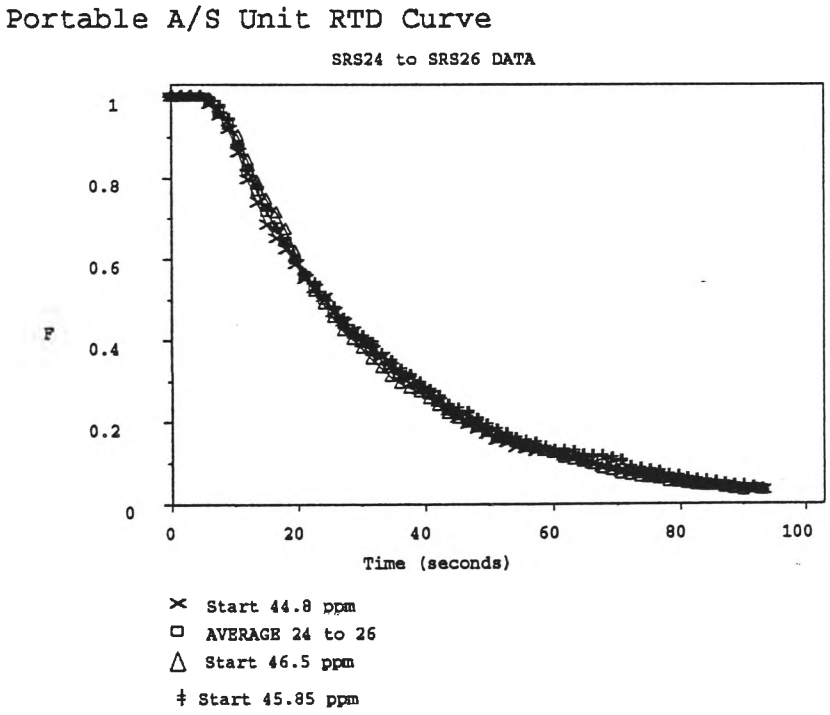

9.2.1.4 CORRECTED GAS PHASE JET PUMP RTD

The results of RTD studies on the jet pump revealed that a step change in the ozone concentration produces an exponential type of outlet curve. This is indicative of mixed flow.

However this is mainly due to the detection system response. Full graphical data appears in Appendix 4.0.

Figure 9.10 shows the residence time for the base of the jet pump column. This shows the time taken for the gas phase to reach the back pressure control valve. This value has been corrected for the residence time of the portable air-water separator (PAWS) and the ozone monitor. This is done by subtracting the values of each residence time. For example:

Residence time of jet pump + PAWS = 11.25 seconds

Residence time of PAWS = 5.15 seconds

therefore,

Residence time (including inlet residence time) = 11.25-5.15 = 6.1 seconds

FIGURE 9.10 BASE OF JET PUMP RESIDENCE TIME

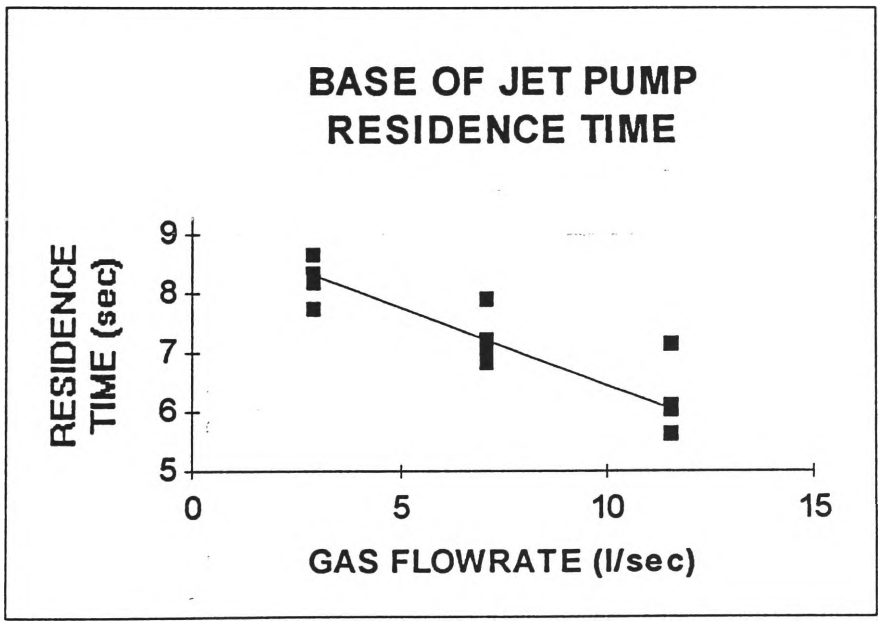

The fully corrected gas phase residence time is calculated by subtracting the inlet residence time from the base residence time. It is also necessary to subtract an additional inlet

factor. This is because the tapping point for inlet residence time is upstream of the gas-liquid mixing point. This is corrected for in a similar way to the theoretical study for inlet residence time. That is if the length of suction duct to the mixing point is (L) 0.51m and the diameter is 76mm(d), and the area (A) is 0.004536 m^2, then the time taken (t), for a given gas flow (Q_G) is $t = 0.51*A/Q_G$.

The following figure (9.10A) shows the fully corrected gas phase residence time from the mixing point with the liquid phase to the base of the column.

FIGURE 9.10A FULLY CORRECTED GAS PHASE RESIDENCE TIME THROUGH JET PUMP CONTACTOR

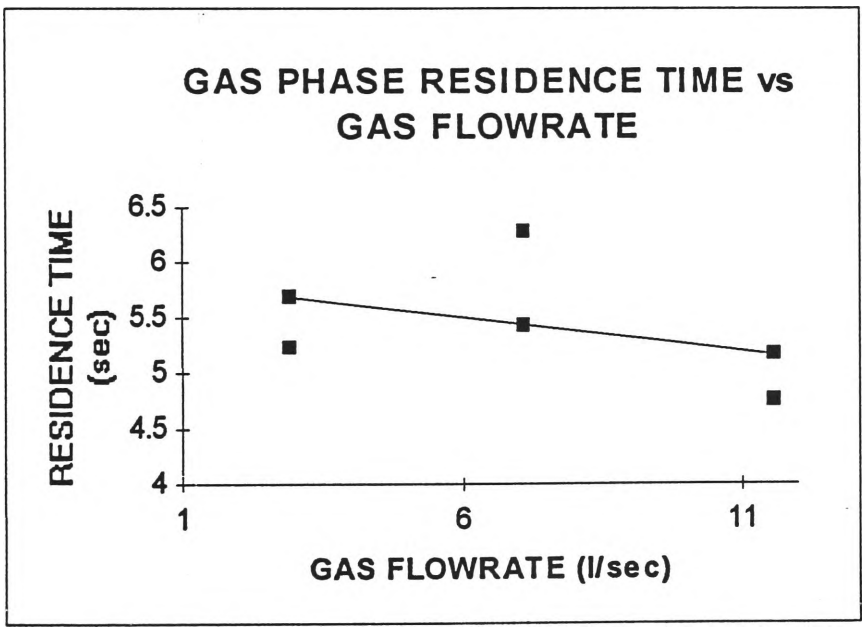

Figure 9.10A also shows the regression prediction for the column residence time. This regression model is as follows:

$$GRT = -0.06Q_G + 5.86 \qquad (9.7)$$

9.2.2 LIQUID PHASE RESIDENCE TIME DISTRIBUTION STUDIES

9.2.2.1 HYDRAULIC RESIDENCE TIME

The results of the hydraulic residence time are shown in figure 9.11.

FIGURE 9.11 LIQUID PHASE (HYDRAULIC) RESIDENCE TIME

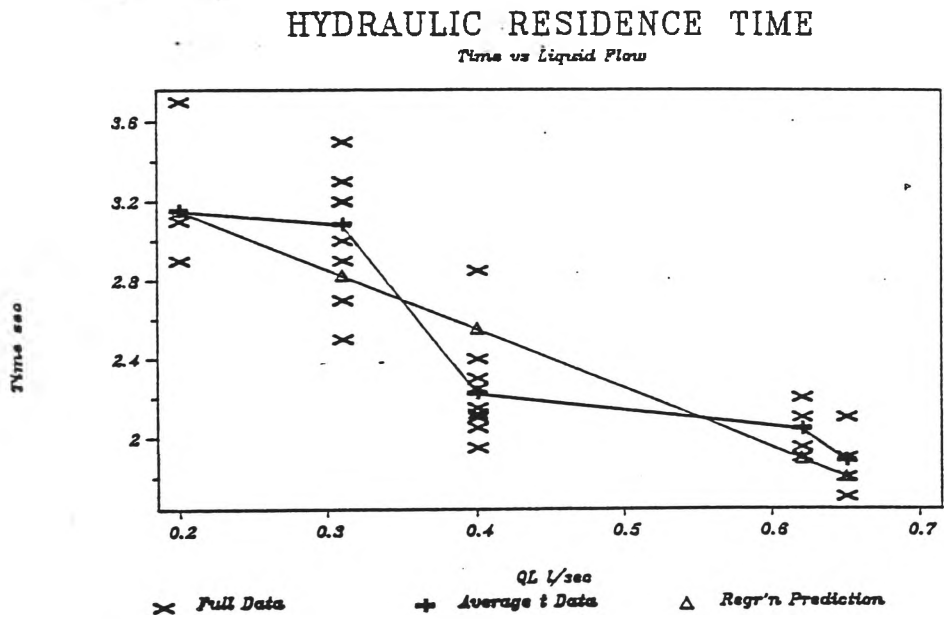

The graph in figure 9.11 shows three pieces of information. The actual experimentally determined residence times, the averages of this data and the regression fit of the data.

The linear fit of the residence time data is as follows:

$$HRT = -3.01*Q_L + 3.75 \qquad (9.8)$$

A study was also made of the hydraulic residence time with the gas flow off. The gas flow was stopped by removing the inlet hose to the jet pump, and stoppering the end with an adjustable clamp. The results of this study are shown in figure 9.12.

FIGURE 9.12 HYDRAULIC RESIDENCE TIME WITH NO GAS FLOW

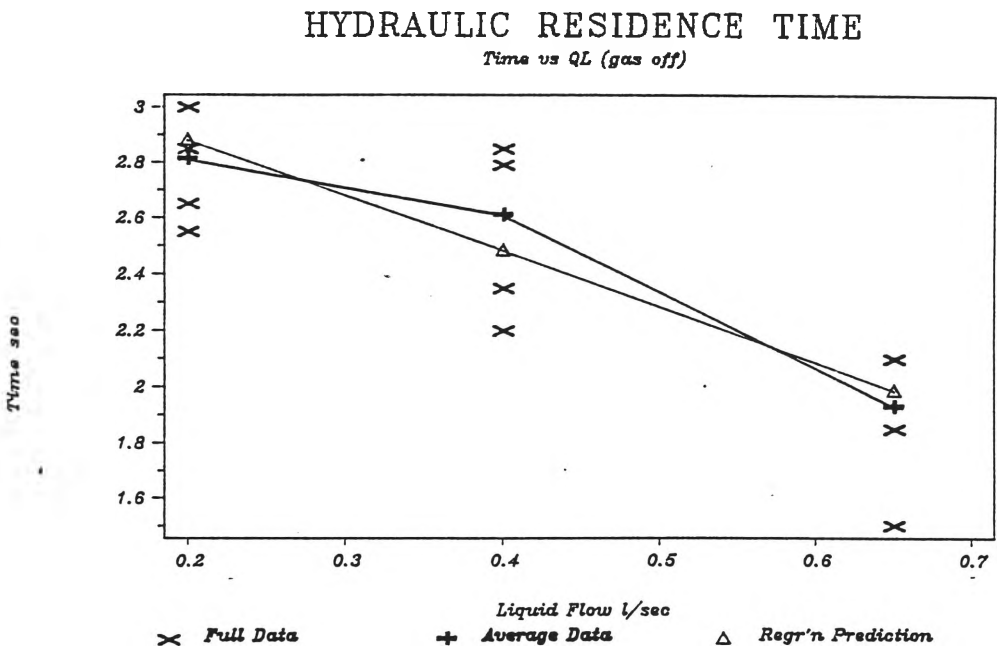

The linear regression fit for this data shows:

$$HRT(Q_G=0) = -1.99Q_L + 3.28 \qquad (9.9)$$

The following figure (9.12A) shows the difference between column residence times with and without gas flows. Data series 1 represents relationship with gas flow on. As can be seen there is not a large difference between the two cases. From obervation of the mixing section, it was no possible to tell from the flow pattern whether the gas was flowing or not.

FIGURE 9.12A COMPARISON BETWEEN HYDRAULIC RESIDENCE TIME WITH AND WITHOUT GAS FLOW

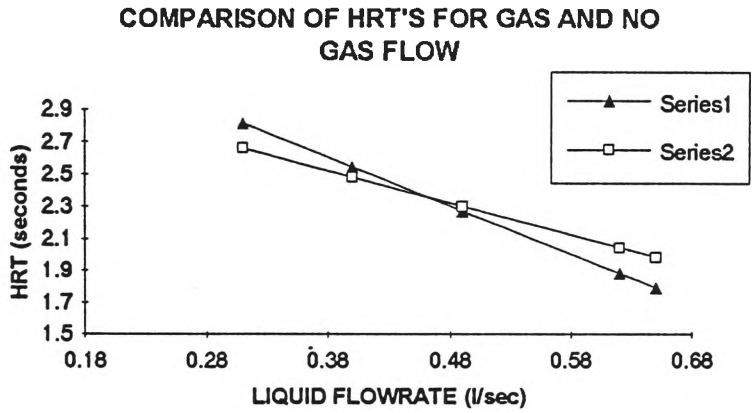

The hydraulic residence time was also determined at a point about half way down the jet pump column to examine the changes in residence time and hence velocity. This second injection point allows the predicted velocities calculated from the top injection point to be compared with those predicted from the lower point. This "mid-point" injection was carried out with the gas flow off.

The middle injection point is 1.18m from the column base.

The HRT in the column with and without the gas flow (Figure 9.12A) is not very different (only 5-10% different at upper and lower liquid rates). The HRT's are the same at approximately 0.45 l/sec. It would have been reasonable to expect a larger difference due to the high gas to liquid volumetric ratios in the jet pump column. From visual observation and from HRT data it appears that the liquid flow pattern is independent of gas flow despite a gas volumetric flowrate of 19 times that of the liquid rate.

FIGURE 9.13 "MID-POINT" HYDRAULIC RESIDENCE TIME

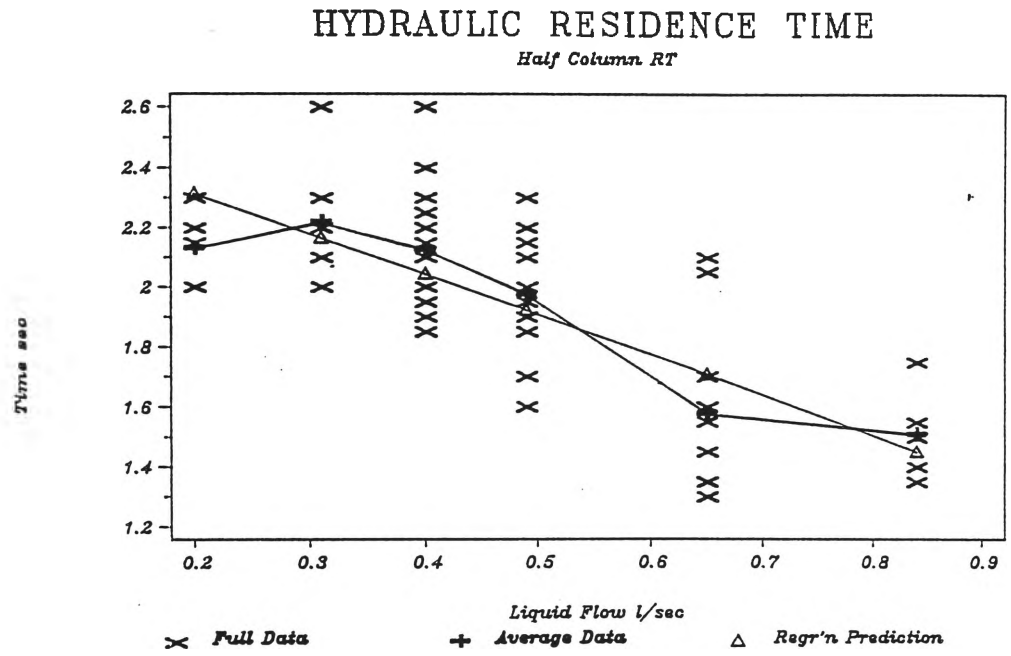

The linear regression fit for the "mid-point" hydraulic residence time is:

$$HRT(mid, Q_G=0) = -1.35*Q_L + 2.58 \qquad (9.10)$$

The calculated velocities for the liquid phase in the draft tube, based on the residence time studies (for mid-point flow) are presented in figure 9.14.

FIGURE 9.14 DRAFT TUBE VELOCITY WITH NO GAS FLOW

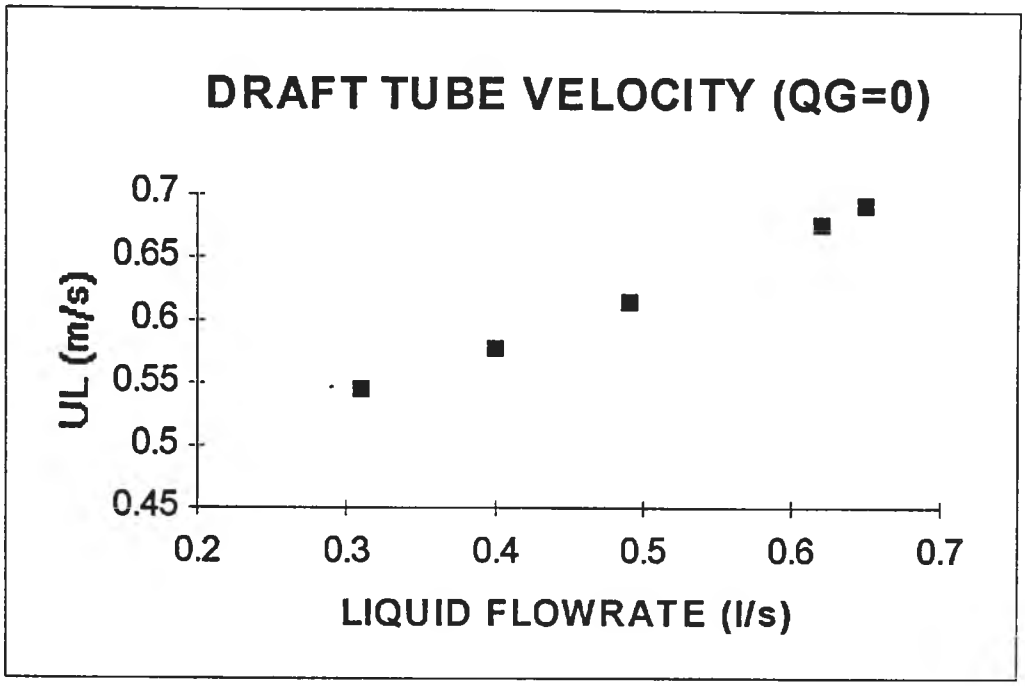

9.3 HOLD-UP STUDIES

There are many studies into hold-up in bubble contactors [38,148,97,131], and in fact there are many different correlations. However, many of these correlations are difficult to apply to the jet-pump system [134]. Initially, the method for determining liquid hold-up (h_L) values used in this study is the same as that used on the confirmation study of an ozone model by Yurteri and Gurol [75]. That is:

$$h_L = \frac{t_m}{HRT} \tag{9.11}$$

and,

$$h_G = \frac{t_m}{GRT} \tag{9.12}$$

where

t_m = mean residence time (seconds)

This method will be compared by a theoretical study to determine the predictive nature of the theoretical evaluation.

The liquid hold-up in the jet pump (and in any similar system) actually is a measure of the voidage of the column with respect to percentage of path available for liquid flow. One would expect that the path available through the column for liquid flow will be reduced in direct proportion to the gas flow (amongst other variables see section 4.1 and 5.3). There will be a difference in behaviour in the jet pump when compared to conventional counter-current systems, due to the co-current liquid-gas flow and the suction driving nature of the liquid stream, as well as the different flow regime.

In these jet-pump trials the liquid hold-up for a given nozzle and column type was determined by obtaining RTD and HRT data for a range of flowrates, and there-by finding the h_L as a function of water flowrate (Q_L).

9.3.1 CALCULATION OF LIQUID HOLD-UP FROM GAS FLOW DATA

In the first instance the liquid hold-up was actually calculated from the gas-hold-up. The gas residence time (GRT) was believed initially to be an easier property to measure due to the simplicity of ozone measurement with the on-line analysis equipment (Section 9.2.1.2). The relationship between h_L and h_G is as follows (see also section 8.1.2)[44]. for an unpacked column:

$$h_G + h_L = 1.0 \quad [44]. \tag{9.13}$$

where

h_G = gas hold-up

h_L = liquid hold-up

This study had to be abandoned because the experimental residence time appeared to be more than the theoretical, on the inlet corrector factor. The results of the full gas phase study are also open to question (see figure 9.10A).

9.3.2 LIQUID HOLD-UP FROM LIQUID PHASE STUDIES

Due to the unforeseen difficulties of RTD studies in the gas phase (see section 9.2.1/Appendix 4.0), it was felt that a more accurate, and therefore more useful study could be carried out by examining the liquid phase. One of the important criteria in the choice of a tracer for RTD studies is that the tracer is easily detected in the reactor effluent. It is also useful if the analysis of the tracer can be done on-line with a minimum of trouble. For the liquid phase RTD studies it was decided, therefore, that conductivity or pH measurements would provide the best solution.

The liquid phase residence time distribution (RTD) studies were carried out with the ozone generator off. This did not effect the gas phase flowrate or behaviour in the column.

The first difficulty to arise was the problem of how to obtain the effluent sample. This occurred because the jet-pump had no large sampling points. The second problem was that the addition of any sampling system should not add any extra response to the reactor response. This was the major problem in the gas phase studies (section 9.2). Therefore, it was decided to measure the effluent pH using a discrete sampling approach. The discrete response could then be used to estimate the continuous response.

The tracer injection was carried out by injection of strong sulfuric acid solution via a syringe into a point at the top of the reactor where the gas and liquid streams begin to mix. The discrete sampling involved the removal of a gas/liquid mixture from the final sampling point at the base of the reactor. The gas/liquid mixture was removed via a syringe. The contents of the syringe were then tested for pH.

This syringe sampling system had to be abandoned because the system was too inaccurate. This arose because the syringe removal system took up to 4 seconds per sample. This was due to the need for careful insertion of the syringe into the sample withdrawal point

in the jet pump column, and the slow speed at which the plunger had to be withdrawn. The syringe plunger had to be withdrawn slowly because of the large amount of air in the jet pump column. Quick sample withdrawal resulted in a syringe full of air, rather than an air/water mixture.

It was then decided to alter the jet pump column. This was done by inserting a 40mm (nominal internal diameter) pipe at 90^{o} to the jet pump at the base of the column. This pipe contained a socket suitable for the introduction of a conductivity probe, and a globe valve to throttle the flow to a desired level. The conductivity probe was then connected to a pen recorder. This system allowed continuous sampling of conductivity. This sampling system is shown in figure 9.16.

FIGURE 9.16 CONDUCTIVITY SAMPLING SYSTEM

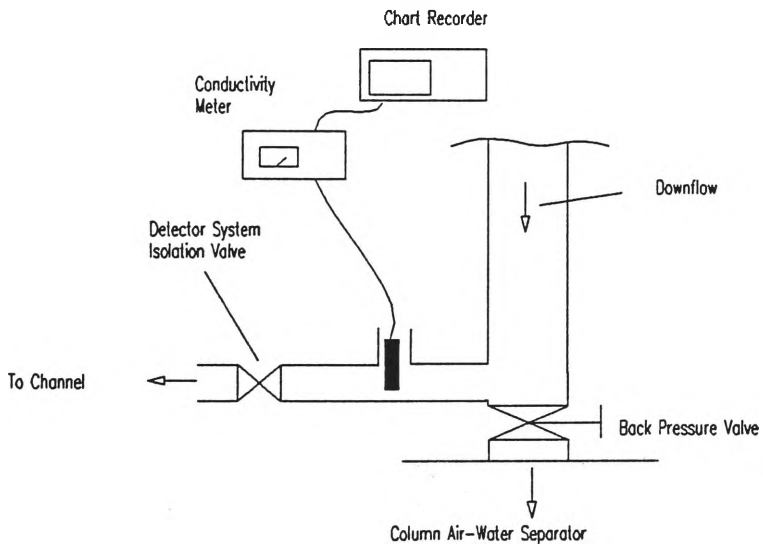

During operation of the injection and sampling system it was decided to use approximately 25% (by volume) sulfuric acid. This amount of acid could be modified further. The second change made from experience, was to only use about half a syringe of diluted acid (10mL). The reason for this was when a full syringe of acid was used it was difficult to obtain a pulse response due to the amount of time necessary to inject the acid. It was also found that with a larger injection there was a tendency to slow down during the injection. The result of

this was a double peak on the output response of the column, which was the fault of the injection, rather than the non-ideality of the column. The shorter and faster injection method led to a sharper and clear peak in the output response.

The next major thing that was noticed in the output response of the column was a slight tail which is characteristic of mixed flow.

Shown in figure 9.17 is a plot of the liquid hold-up calculated from flowrates as a function of liquid flowrate.

FIGURE 9.17 LIQUID HOLD-UP VS LIQUID FLOWRATE

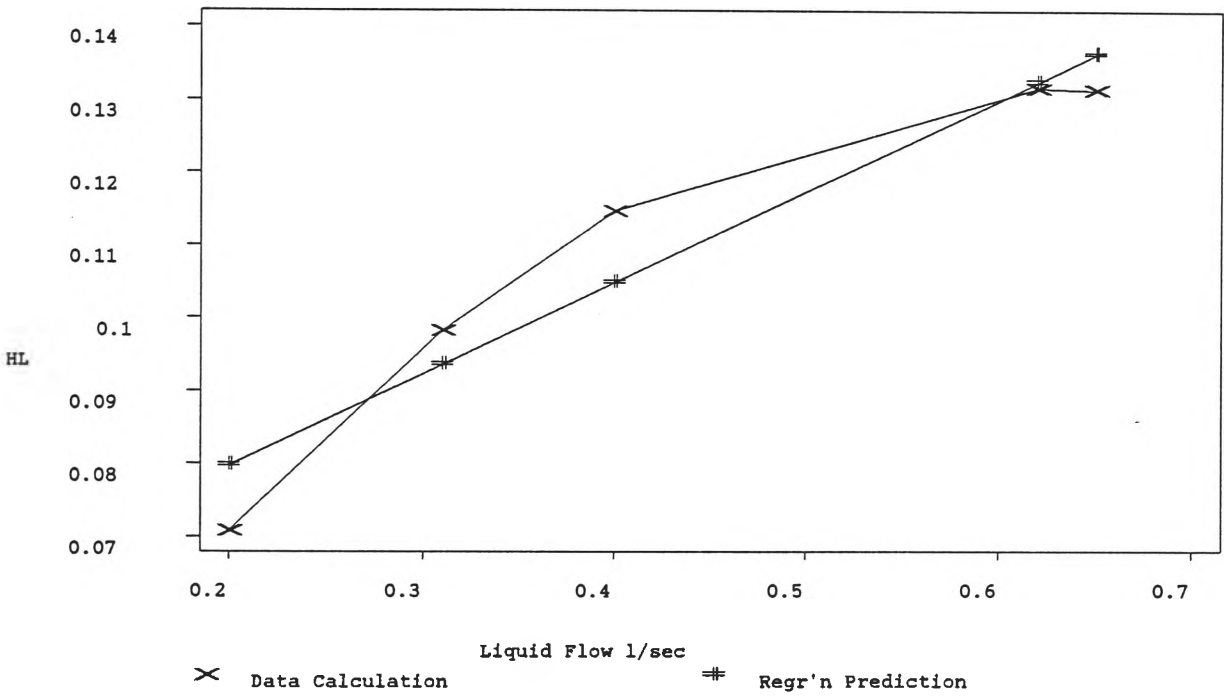

Further hold-up studies were performed on the jet-pump contactor. There were a further two methods of determining the hold-up for the liquid phase.

The first is known as the residence time method. This method involved performing experiments to find the actual liquid phase residence time . From this residence time the actual phase velocity could be calculated from:

$$u_L = \frac{Q_L}{A_L} \quad (9.14)$$

The corresponding area available for the gas flow must therefore be:

$$A_G = A - A_L \quad (9.15)$$

where

A = Total cross-sectional area of the column (m^2)

The ratio of the liquid phase area (A_L) to the total area (A) gives the liquid hold-up(h_L). The hold-up is a measure of the ratio of one phase to the other (see Chapter 5)

The second method of determination of the liquid hold-up is to measure the ratio of the volumetric liquid flowrate to the total of the gas and the liquid flowrates:

$$h_L = \frac{Q_L}{(Q_L + Q_G)} \quad (9.16)$$

The least squares linear regression prediction for this method is:

$$h_L = 0.13 * Q_L + 0.055 \quad (9.17)$$

The corresponding relationship between the two different methods is shown in figure 9.18.

FIGURE 9.18 COMPARISON BETWEEN TIME & FLOW METHODS FOR LIQUID HOLD-UP

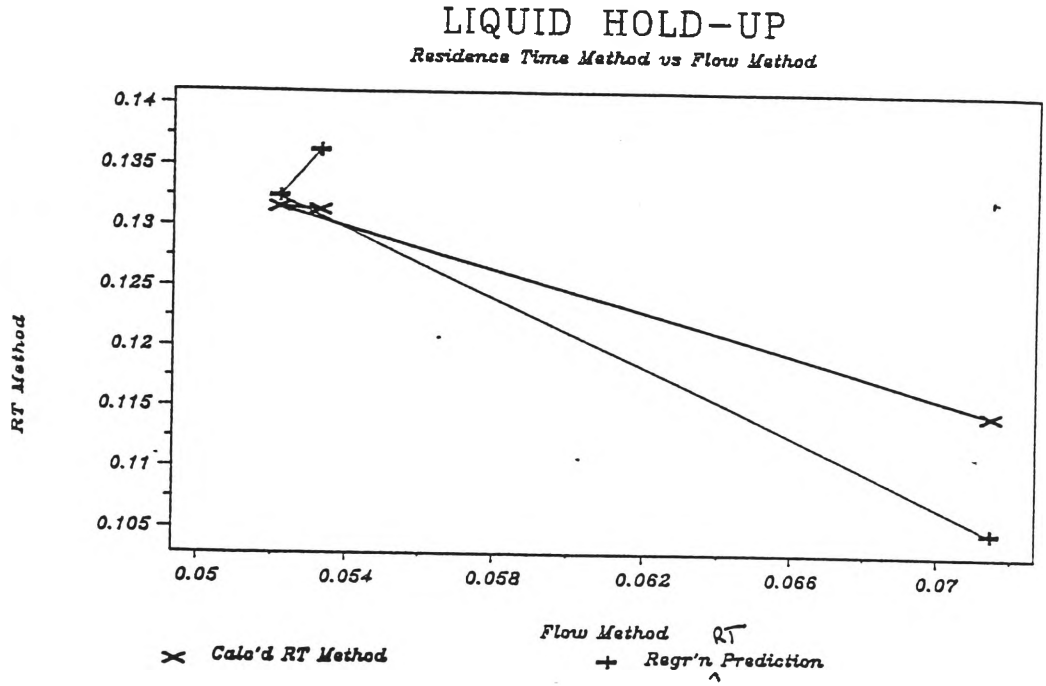

As can be seen there is a large difference between the two methods. The methods start to converge at higher liquid volumetric rates.

Two different linear regression results are shown below. These are for two versions of the residence time method. The first is for actual data, and the second (regression vs regression) is for the regression fit of the data.

These two model fits are as follows:

$$h_L(RT) = -0.90*h_L(calc) + 0.18 \quad (9.18)$$

$$h_L(RT) = -1.56*h_L(regr'n) + 0.22 \quad (9.19)$$

The determination of the gas hold-up was from the liquid hold-up data. This was simply performed by:

$$h_G = 1.0 - h_L \qquad (9.20)$$

This relationship holds true for an empty column. The gas hold-up is shown in figure 9.19 as a function of gas volumetric rate. This gas hold-up is calculated from data for the residence time method.

FIGURE 9.19 GAS HOLD-UP vs GAS VOLUMETRIC FLOWRATE

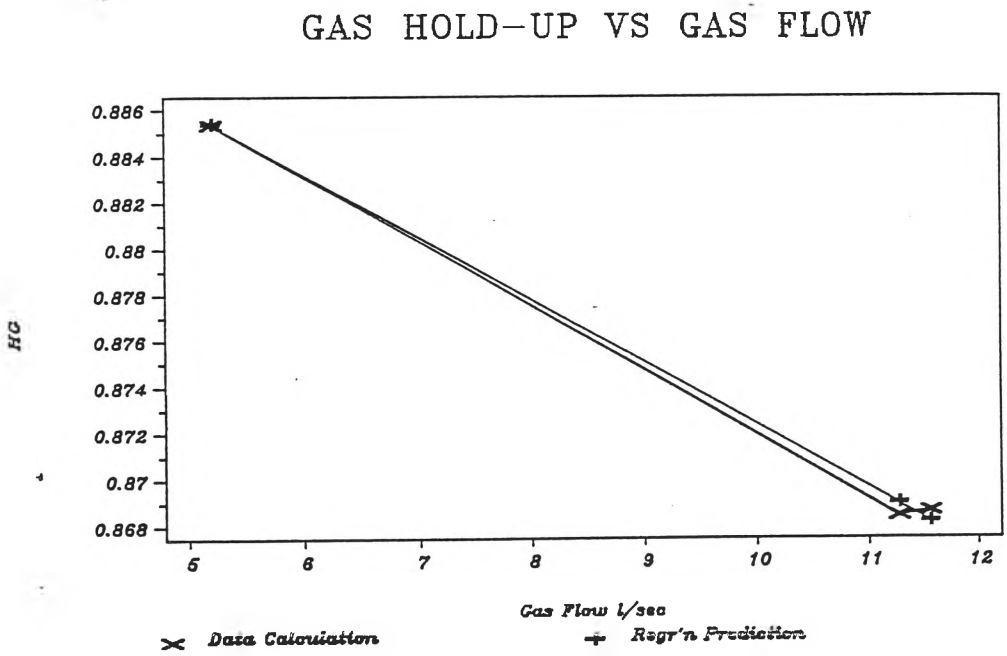

The linear fit of this data is:

$$h_G = -0.003 * Q_G + 0.90 \qquad (9.21)$$

9.4 GAS-PHASE CONCENTRATION PROFILE STUDIES

The model developed for the study of ozone mass transfer, also has a facility to give the gas or liquid phase concentration at any point in the column for either ozone or the contaminant. This is a useful feature to examine exactly how much mass transfer is occurring and where. It is also of great importance in evaluating the CT Disinfection Requirements (Chapter 6), because the mean value of ozone concentration is an important design parameter.

To evaluate and optimise this model function it is necessary to determine the field values and compare them with the model predictions. To do this it is necessary to have a number of test locations (see Figure 9.20), and a portable air-water separator (Figure 9.21).

FIGURE 9.20 JET PUMP TAPPING POINTS

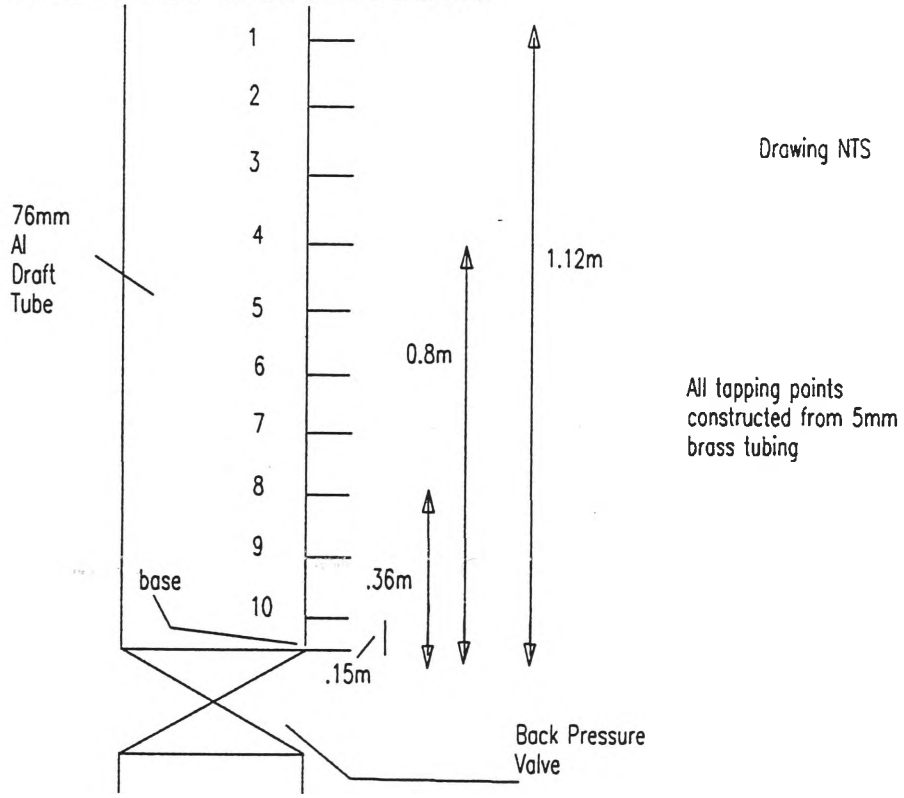

FIGURE 9.21 PORTABLE AIR-WATER SEPARATOR

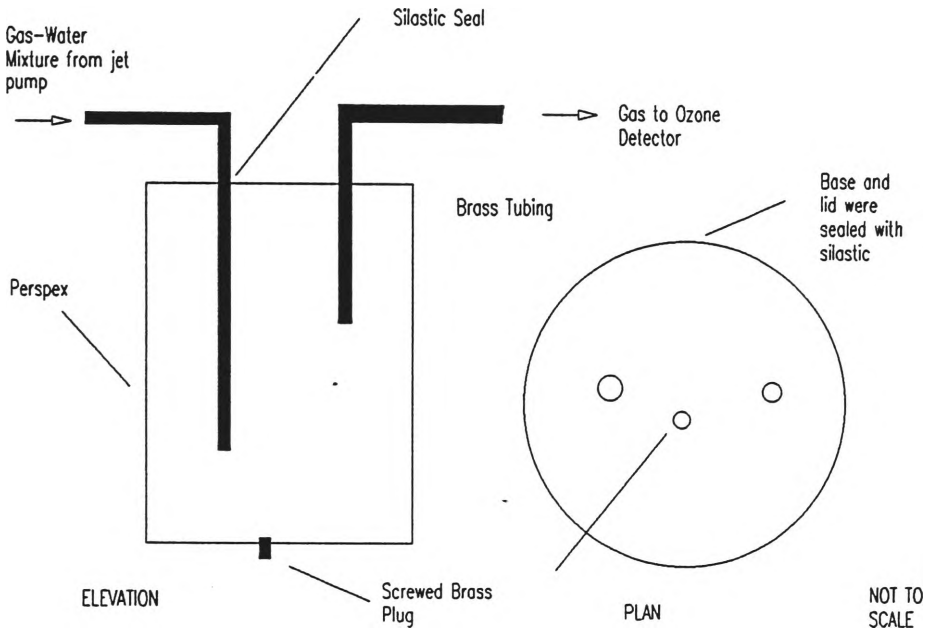

The tapping points are only used one at a time, and are stoppered when not in use.

The portable air-water separator is necessary as the gas concentration profile is being determined from an air-gas mixture. The separator works by drawing the air-water mixture along a tube into a large chamber where there is a 180^{o} change of direction. This causes the liquid to settle and the gas phase to continue along to the ozone detector. The liquid was periodically drained from the separator.

It was necessary to allow time correction factors for this separator because it was also used in the study of residence time distribution (RTD) . This portable separator also has the same problem of mixed flow as that of the jet pump air-water separator. The first assumption in this study is that the correction for this mixed flow with time lag can be made.

The second major assumption used in the design and evaluation of the ozone profile study was that the mass transfer occurring during the air-water separation, in the portable unit, was very small. This was achieved by minimising the amount of contact time between the two phases. This was done by keeping the entry tube to the air water separator as short as

possible. This would also allow quicker separation of the two phases. The second attempt at time lag and mixing limitation was to not have an overly large portable unit.

However, in practice, the unit that was used was in fact too large. This became evident in the difficulty in obtaining a steady-state reading. The method for obtaining steady state readings was to allow the portable air-water separator to become nearly full of water. This level was determined by allowing the water level to rise to a certain point which was marked on the separator unit. This point was found by trial and error. At this point and beyond, the fluctuation in readings of ozone concentration were more damped. The penalty of running the portable unit near to full was the limited measurement time available before the water level became too high.

To attempt to solve these problems the diameter of the portable air-water separator was reduced by nearly half, and a valve arrangement was installed near the base to allow easier water removal than the plug arrangement (see figure 9.22).

It was believed that it was unlikely that plug flow was occurring in the air-water separator. The reason for this was that the change from the jet-pump mixing chamber to the air-water separator involved a large change in velocity. This change in velocity occurred because of the two-phase flow entering a large rectangular space, as well as the flow coming into contact with a large flat surface of water. The carrying energy of the water would then be unable to counteract the buoyancy force of the gas. The gas would then flow backwards and out of the exhaust at the top of the separator. This would result in a certain level of mixed flow.

For this reason the portable air-water separator was used to study the RTD distribution of the column and to examine ozone samples before the column air-water separator. In the final results it was decided to use the outlet concentrations from the exit of the column air-water separator because to obtain a steady value of outlet concentration several factors needed to be taken into account. These factors centred around the air-water separation capacity and behaviour of the portable unit. The major problem with the portable unit was the determination of the steady state value of the ozone concentration. This was due to the fact that the portable unit had to wait until the concentration of ozone in the unit equalled the

concentration inside the column. This required several minutes each time a change was made. To achieve this steady-state value it was necessary to wait until the unit was near full of water. In fact the level of the inlet pipe to the unit was below the water level of the portable separator. This of course results in mass transfer. The portable unit then behaves like a semi-batch contactor. Not only was there mass transfer in the portable unit, but there was also mass transfer occurring in the inlet pipework to the portable unit. This was kept to a minimum by having the inlet hose reduced to less than 10 cm in length.

Based on these factors it was decided for mass transfer study purposes, that the concentration of the ozone exiting the column air-water separation unit may in fact be more representative of the exit column concentration than the gas exiting the portable air-water separation unit. The column separator appeared to behave with less air-water turbulent contacting than did the portable unit. Although at this stage the actual difference in behaviour is not able to be determined due to the fluctuating nature of the flow.

FIGURE 9.22 PORTABLE AIR-WATER SEPARATION UNIT

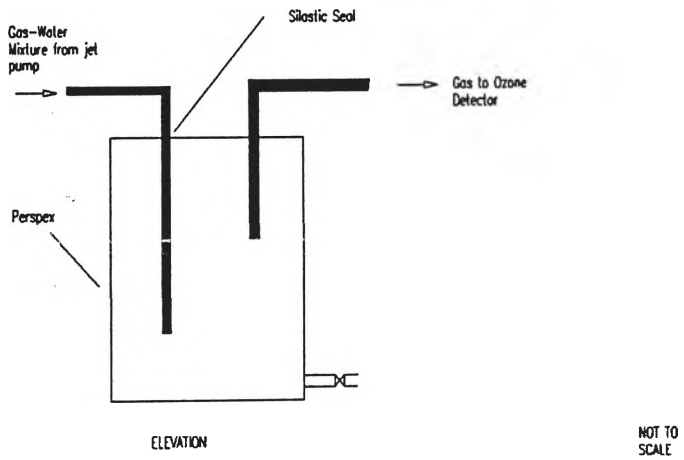

FIGURE 9.23 MODEL PREDICTION OF GAS PHASE CONCENTRATION PROFILE

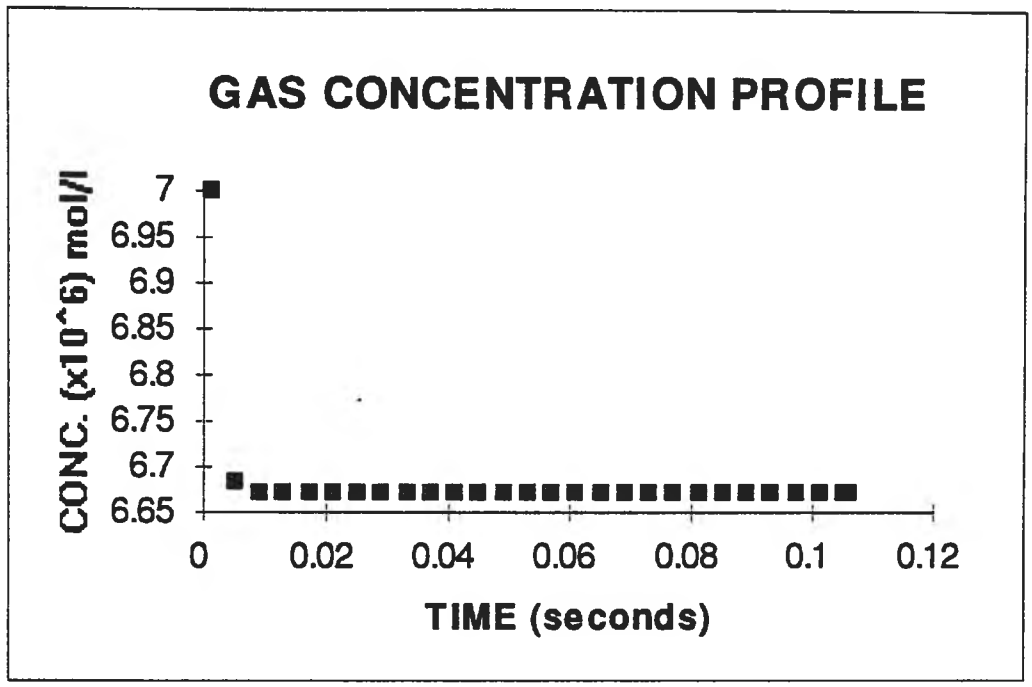

Note that there is no change in concentration after 0.01 seconds. It is unknown at this stage why this should be. There have been no reliable physical data obtained from the column, due to very large problems with the portable air-water separator.

9.5 GAS TO LIQUID RATIOS

The gas to liquid ratio is important in the model equations. It gives an insight into the effects of varying the flowrate of one phase with respect to the other. The gas liquid ratio was determined by varying the liquid flow rate and recording both it and the corresponding gas volumetric flowrate. The measurement of the liquid phase volumetric flowrate (Q_L) was determined by recording the rotameter value and using the calibration chart produced by Rowley [151]. This chart is reproduced overleaf.

FIGURE 9.24 CALIBRATION CHART FOR GEC-ELLIOT METRIC SERIES 2000 SIZE 47X ROTAMETER [151].

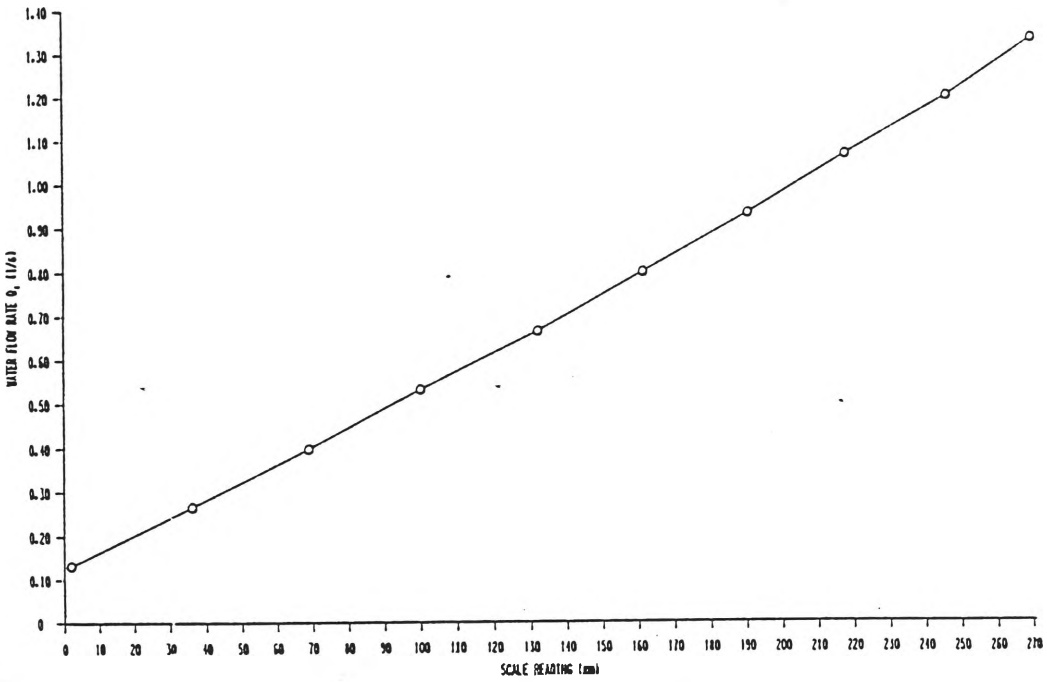

CALIBRATION CURVE FOR GEC-ELLIOT METRIC SERIES 2000 SIZE 47X ROTAMETER.

The gas phase volumetric flow (Q_G) was determined by measuring the pressure difference across the orifice plate in the jet pump suction line. This pressure difference was determined using a magnahelic pressure guage. This presented some problems due to needle fluctuation on the guage leading to errors of +/-2 Pa. These differential pressure readings were then evaluated using a calibration curve obtained from work by Rowley [51]. This curve is shown in figure 9.25.

FIGURE 9.25 AIR FLOW RATE CALIBRATION CURVE [151].

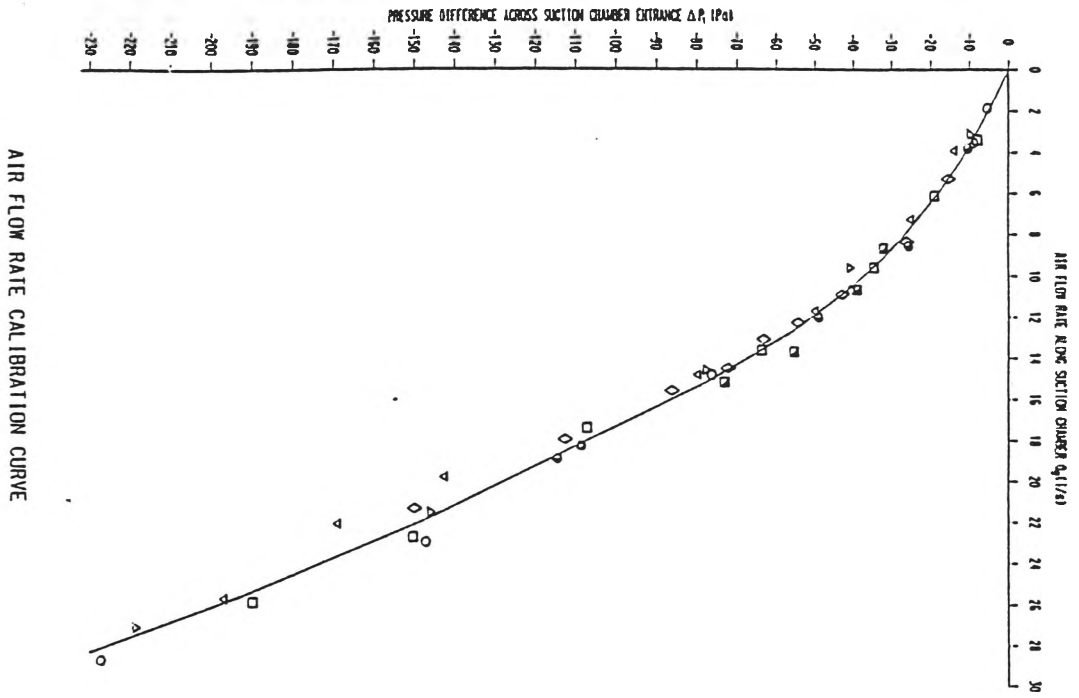

The gas volumetric flowrate for a given liquid volumetric flowrate is presented in figure 9.26. This was determined via use of the two curves presented in figures 9.24 and 9.25. For a given liquid rate the gas rate was determined.

FIGURE 9.26 LIQUID VOLUMETRIC FLOWRATE vs GAS VOLUMETRIC FLOWRATE

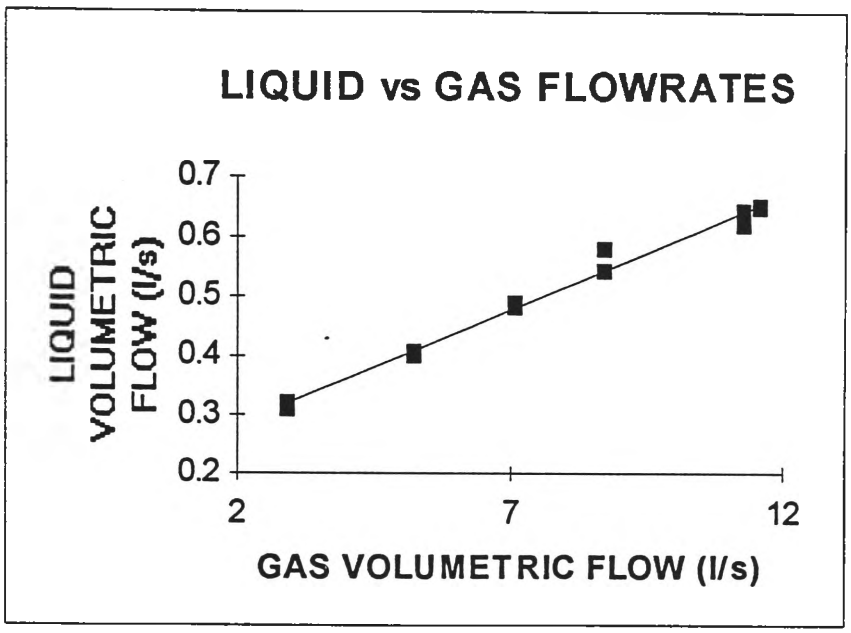

As can be seen the variation in liquid volumetric flow produces a linear response in the gas flowrate.

A least squares regression analysis on the Q_L vs Q_G data produced the following linear relationship:

$$Q_L = 0.04\, Q_G + 0.21 \qquad (9.22)$$

9.6 SUPERFICIAL PHASE VELOCITIES

The phase volumetric flowrates (Q_L and Q_G) were converted to the corresponding superficial velocities (u_{LS},u_{GS})via the following relationship:

$$u_{LS} = \frac{Q_L}{A} \qquad u_{GS} = \frac{Q_G}{A} \qquad (9.23)$$

where

A = cross-sectional area of jet pump column (m^2)

$= \pi*(d/2)^2$

d = column diameter = 76mm

$= (3.14159*(0.076/2)^2 = 0.00454\ m^2$

The resulting relationship between liquid and gas superficial velocities is shown in figure 9.27.

FIGURE 9.24 LIQUID SUPERFICIAL VELOCITY vs GAS SUPERFICIAL VELOCITY (for 76mm column)

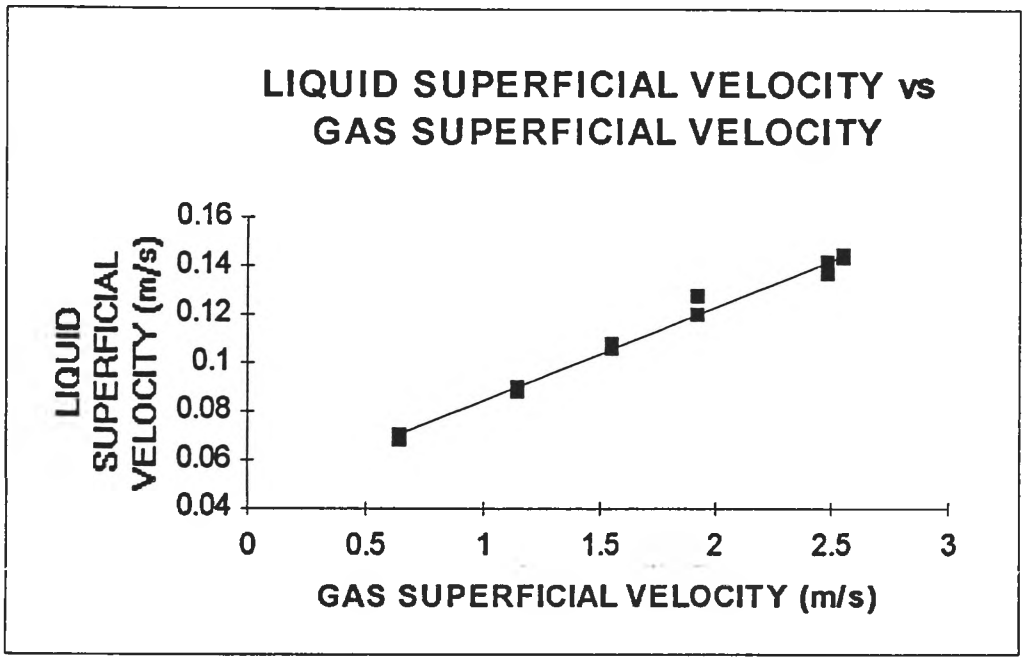

The least squares linear regression prediction is:

$$u_{LS} = 0.039u_{GS} + 0.0458 \qquad (9.24)$$

FIGURE 9.27A LIQUID SUPERFICIAL VELOCITY vs GAS SUPERFICIAL VELOCITY (for 54 mm column)

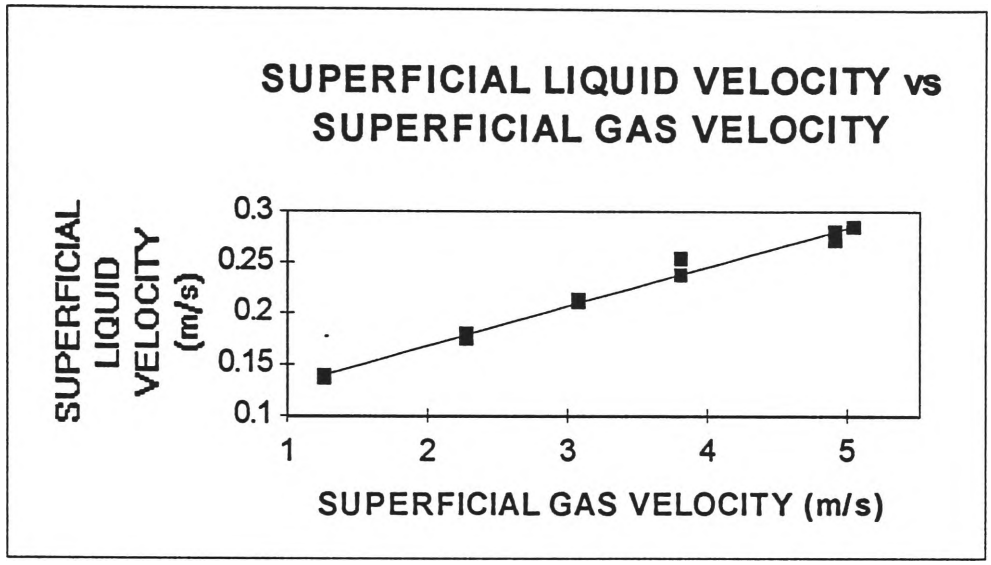

$$u_{LS} = 0.039u_{GS} + 0.091 \qquad (9.24)$$

9.7 MASS TRANSFER COEFFICIENT

The volumetric mass transfer coefficient (k_La) for the liquid phase was calculated using the hold-up, gas-liquid ratios and hydraulic residence times experimentally determined from the jet-pump contactor. These values were then substituted into the mathematical model to allow for prediction of k_La. The only other constant required in the mathematical model is the specific ozone utilisation rate (w). This was estimated to be 3 hr^{-1} from data from Yurteri and Gurol [42]. This value was not experimentally measured in this thesis.

On this basis the predicted volumetric mass transfer coefficient relationship for the jet-pump contactor is as follows:

FIGURE 9.28 MASS TRANSFER COEFFICIENT vs LIQUID VOLUMETRIC RATE

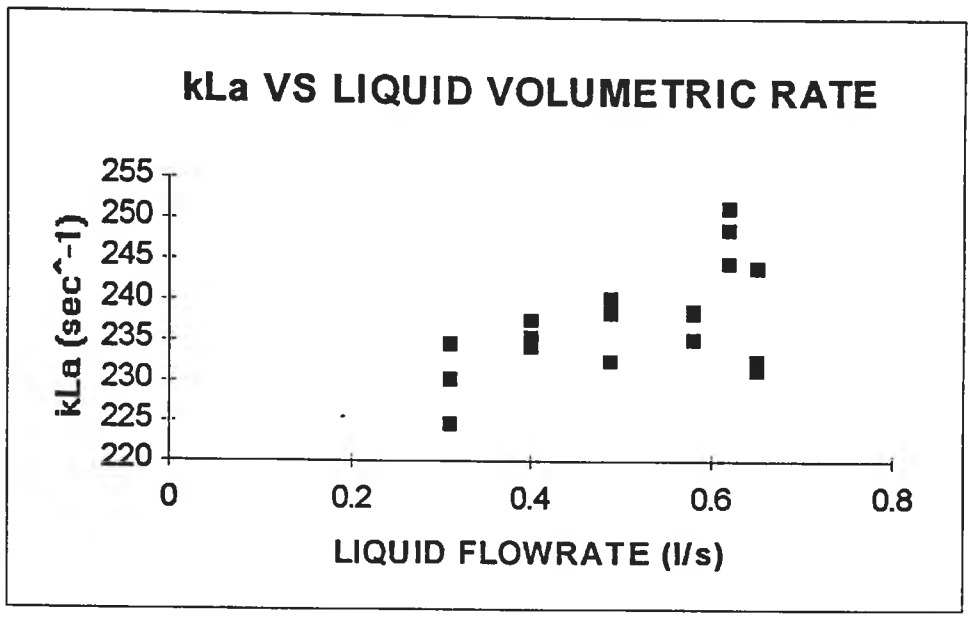

FIGURE 9.28B MASS TRANSFER COEFFICIENT vs GAS VOLUMETRIC RATE

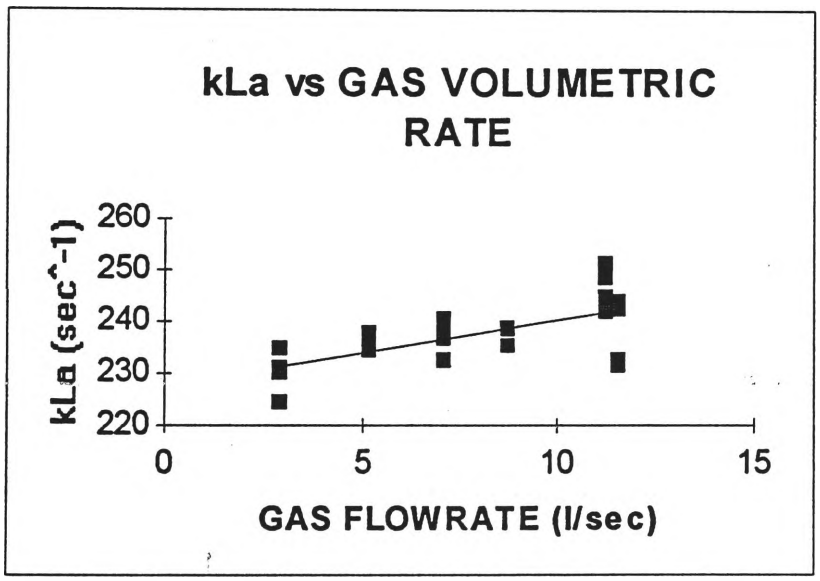

The line in figure 9.28B represnets the linear regression fit. The model is:

$$k_L a = 1.27Q_G + 227.57 \qquad (9.25)$$

It is also possible that the mass transfer coefficient is a function of the gas/liquid ratio. This relationship is presented in the following two figures, the second of which presents a different scale.

FIGURE 9.29 VOLUMETRIC MASS TRANSFER COEFFICIENT vs GAS/LIQUID VOLUMETRIC FLOW RATIO

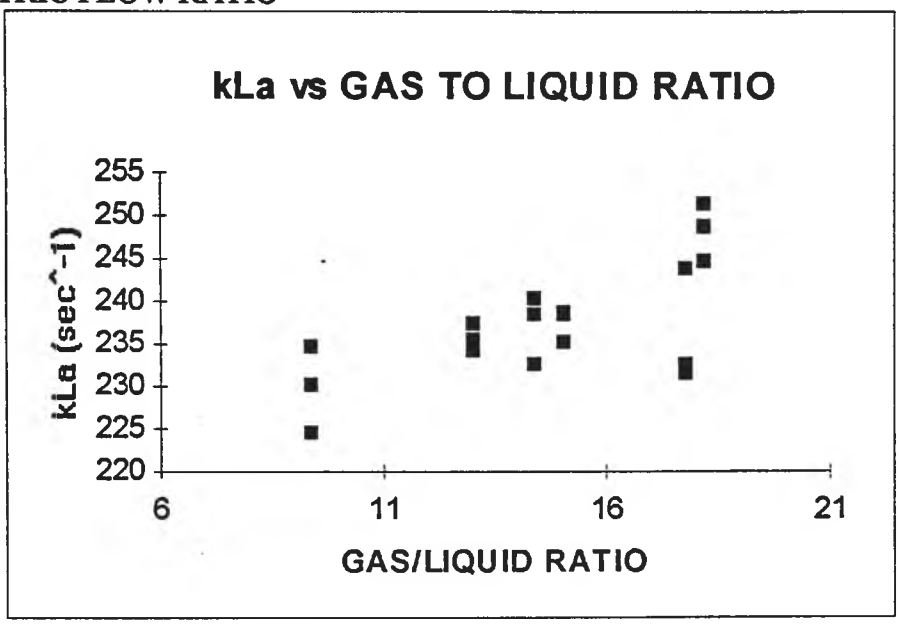

FIGURE 9.30 VOLUMETRIC MASS TRANSFER COEFFICIENT vs GAS/LIQUID VOLUMETRIC FLOW RATIO

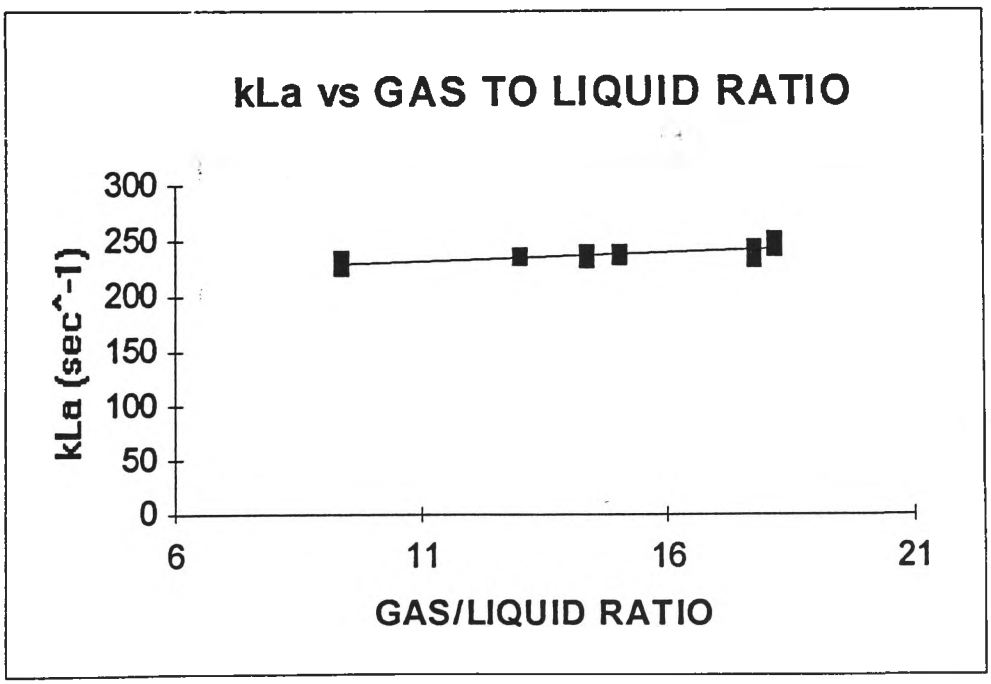

The corresponding regression fit for volumetric mass transfer coefficient vs gas/liquid ratio is:

$$k_La = 1.44*(Q_G/Q_L) + 216.37 \quad (9.26)$$

This linear fit is shown as the line in figure 9.30

It can be seen that the dependence of k_La on gas/liquid ratio is not strong, and in fact the relationship is near independent.

9.8 LIQUID PHASE OUTLET OZONE CONCENTRATION

Studies of computer simulation of the jet-pump system yielded the following outlet liquid phase ozone concentrations as a function of liquid flowrate. (Figure 9.31)

FIGURE 9.31 OUTLET LIQUID PHASE OZONE CONCENTRATION VS LIQUID VOLUMETRIC FLOWRATE

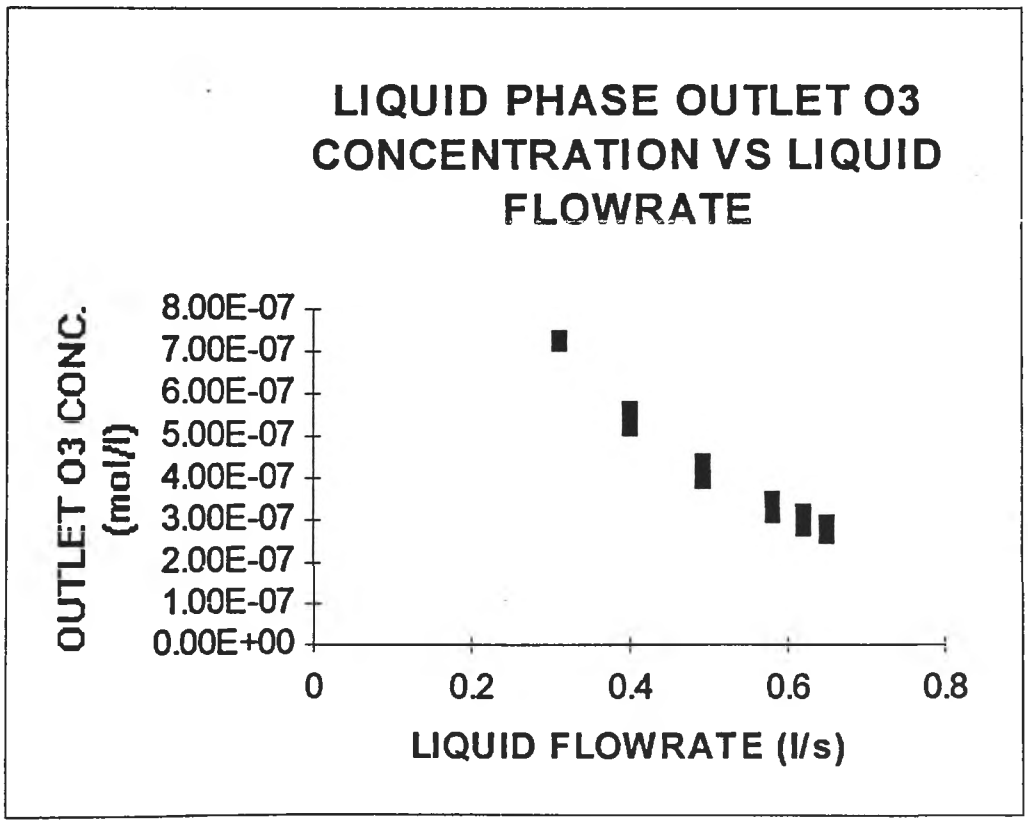

9.9 GAS PHASE OZONE CONCENTRATION

Inlet studies of the gas phase with the ozone monitor produced the following relationship of inlet gas phase ozone concentration as a function of gas volumetric flowrate (Figure 9.32).

FIGURE 9.32 INLET GAS PHASE OZONE CONCENTRATION VS GAS VOLUMETRIC FLOWRATE

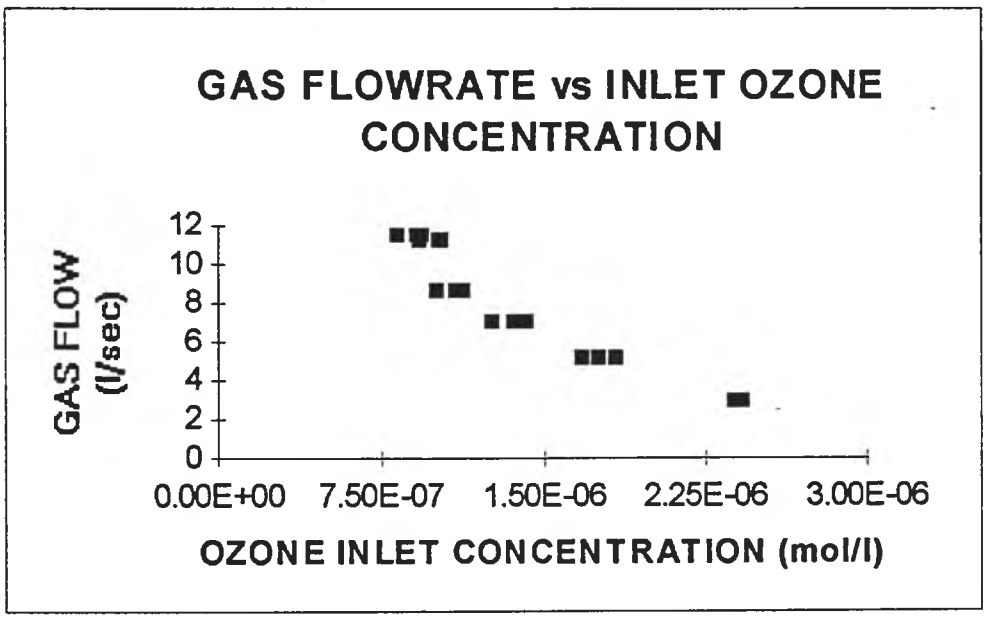

9.10 CT DISINFECTION DETERMINATION

From the model simulation the ozone liquid phase outlet concentration was obtained (see Figure 9.31). These values were then converted to mg/l. These outlet concentrations were then modified by the criteria for co-current contactors suggested by Lev and Regli [118]. (see also section 6.1). That is:

$$C = (c_{out} + c_{in})/2 \quad (9.27)$$

This "C" values obtained was then multiplied by the appropriate regression fitted residence time (T) for that flowrate. The results of these calculations are presented in Figure 9.33A. The unmodified CT curve appears in figure 9.33. The CT value for the unmodified curve is double that of the modified curve.

FIGURE 9.33 "CT" VALUES VS GAS/LIQUID VOLUMETRIC FLOW RATIO

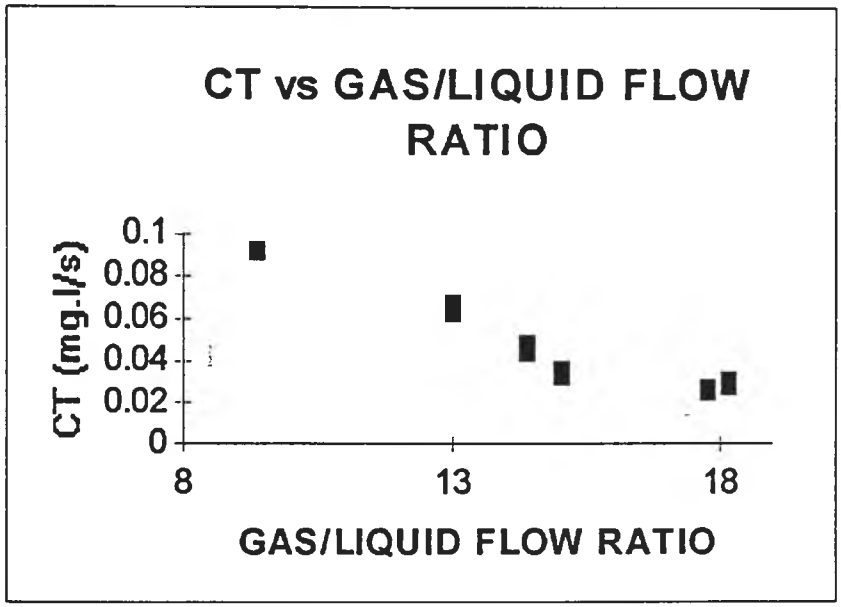

The linear regression fit for the unmodified CT data is as follows:

$$CT = -7.45x10^{-3}(Q_G/Q_L) + 0.16 \quad (9.28)$$

FIGURE 9.33A MODIFIED CT DISINFECTION RELATIONSHIP

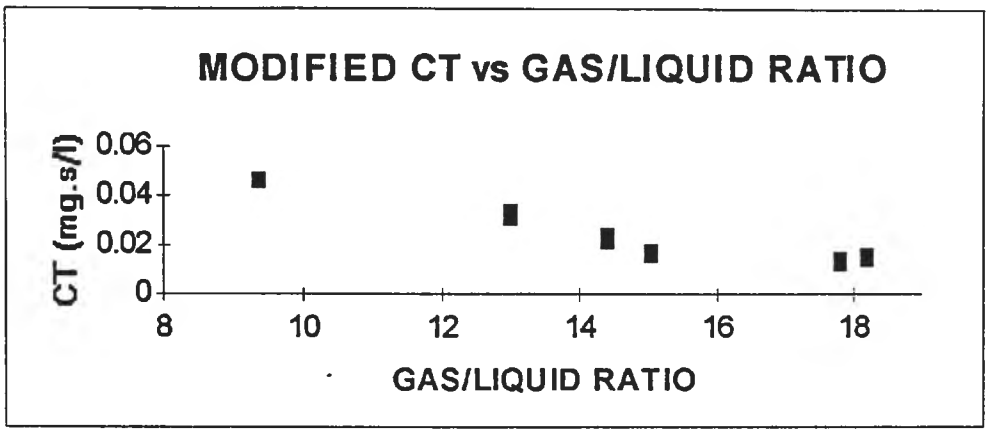

The linear regression fit for the modified CT data is as follows:

$$CT = -3.73x10^{-3}(Q_G/Q_L) + 0.079 \qquad (9.28A)$$

9.11 TWO PHASE FLOW MODELLING

9.11.1 TRANSITION FROM ANNULAR FLOW

The three figures (Figures 9.34 to 9.36) presented in this section are based on the mathematical model predictions proposed in section 8.1.3.1. The idea is to find the transition velocity at which the flow will tend toward slug flow from annular flow. Three column sizes are presented. The first is a 51 mm column (figure 9.34). This is presented because in the original literature source [137]., this column size was tested against a real system. This column is included as a test of the current model agreeing with the Dukler and Taitel [137]. original model. The other two figures (9.35 and 9.36) are shown as transitions in the mixing and draft tubes respectively.

FIGURE 9.34 TRANSITION POINT FOR ANNULAR FLOW (d=51 mm)

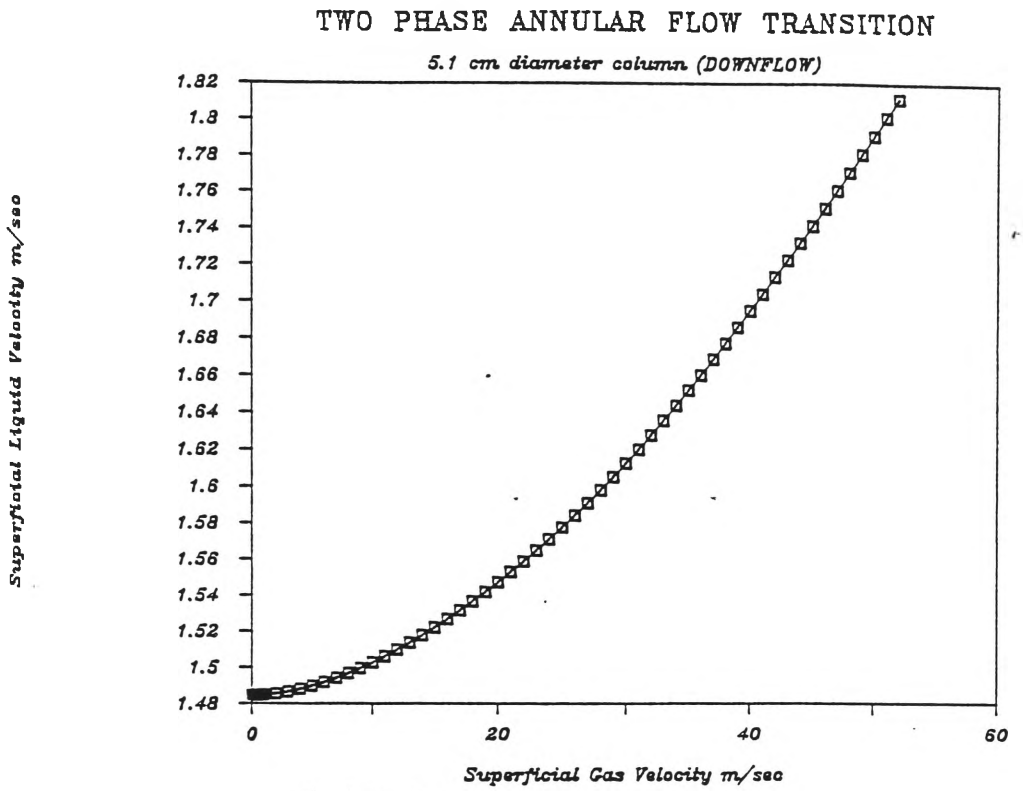

FIGURE 9.35 TRANSITION POINT FOR ANNULAR FLOW (d=54 mm)

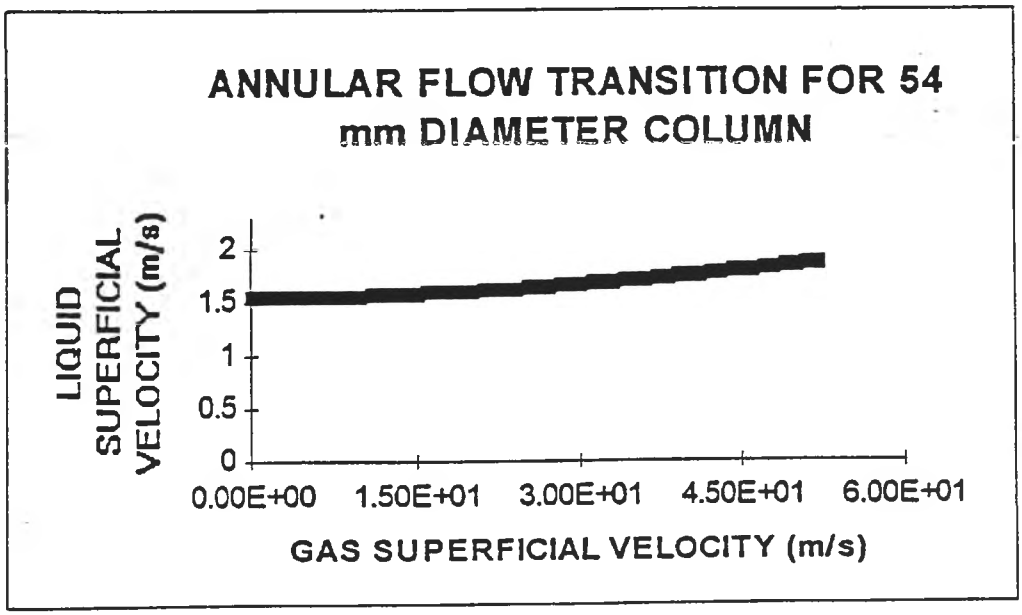

FIGURE 9.36 TRANSITION POINT FOR ANNULAR FLOW (d=76 mm)

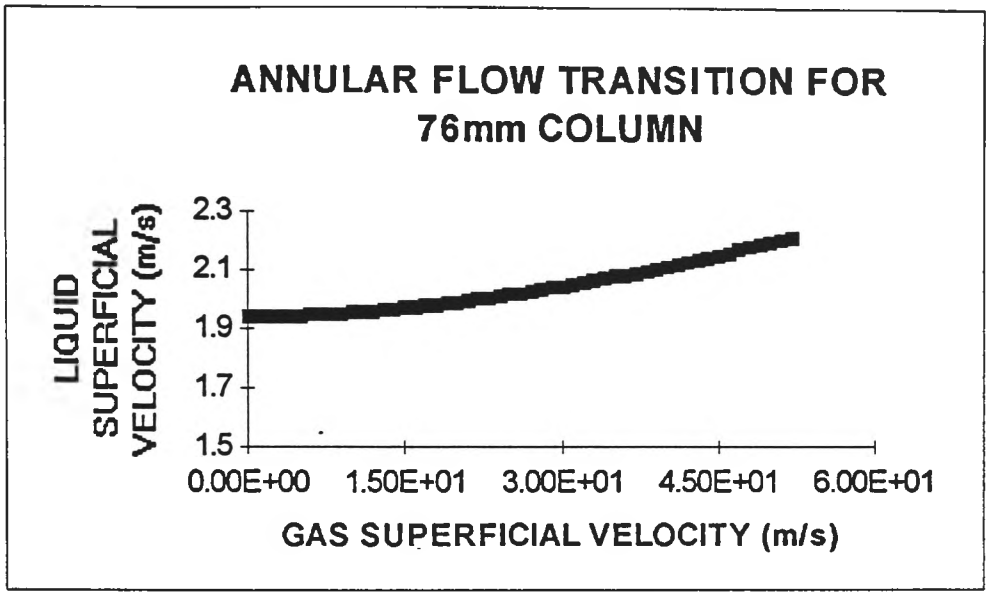

9.11.2 VELOCITY PREDICTIONS

In figures 9.37(A to C) and figures 9.38(A toC) are presented the major results of the two phase downflow model simulation. This model is that presented in section 8.1.3.2. Also presented are the corresponding liquid film thicknesses as a function of liquid rates for each column size. The reason for the 54 mm and the 76 mm column predictions is that the perspex mixing tube in the column is of diameter 54 mm and the aluminium draft tube is of diameter 76 mm.

FIGURE 9.37A LIQUID PHASE VELOCITY PREDICTION (d=76 mm)

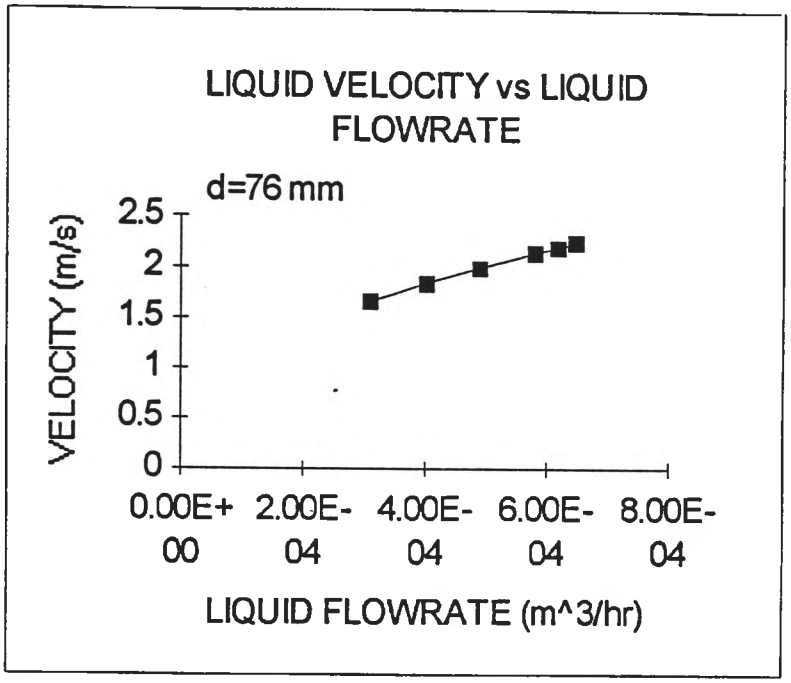

As can be seen the velocity behaves in a near linear fashion with respect to liquid flowrate in the annular flow regime. The regression fit of this data is:

$$u_L = 1462.7Q_L + 1.01 \qquad (9.29)$$

FIGURE 9.37B GAS PHASE VELOCITY PREDICTION (d=76 mm)

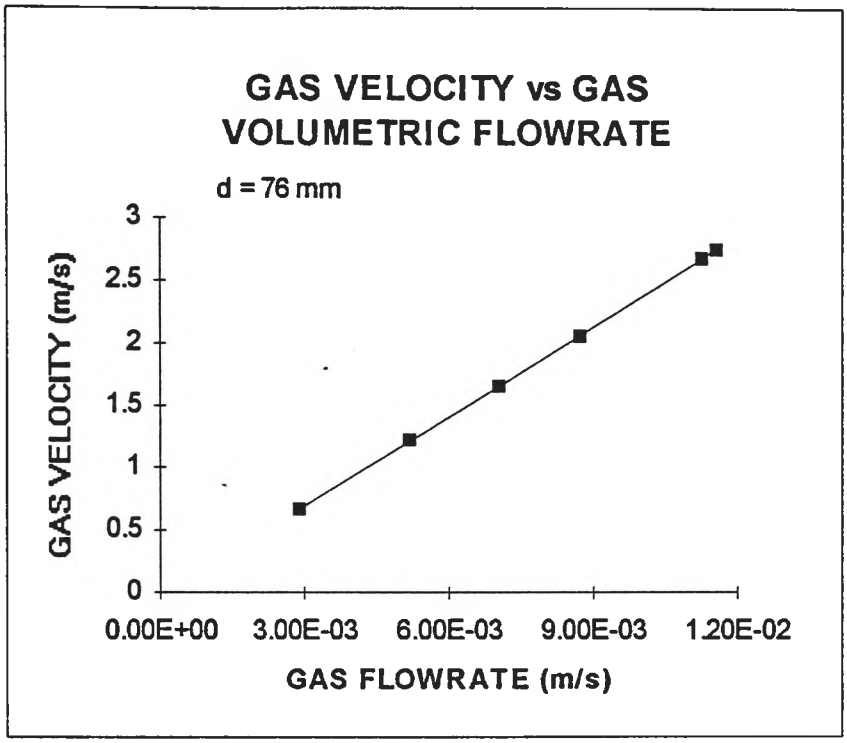

Gas velocity also varies near linearly with gas flowrate. The linear model fit of this data is:

$$u_G = 240.15Q_G - 0.03 \qquad (9.30)$$

FIGURE 9.37C LIQUID FILM THICKNESS FOR 76 mm COLUMN

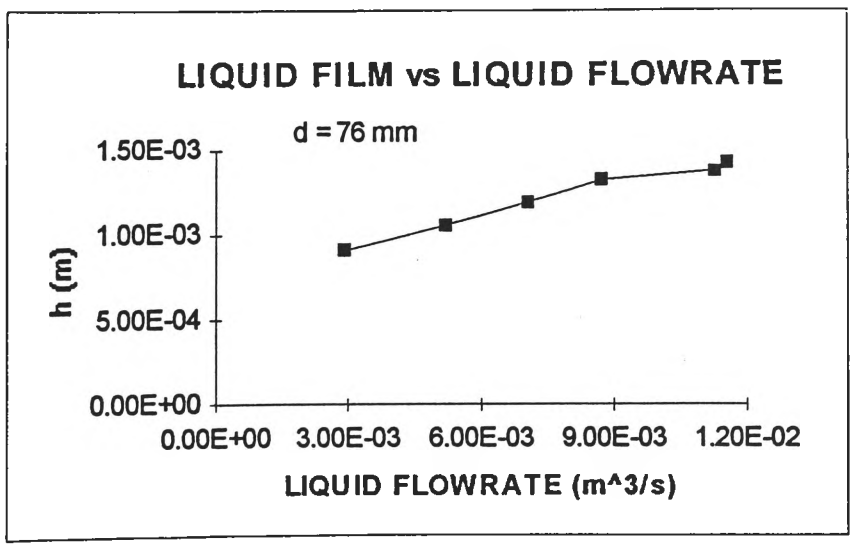

The h/d ratio for transition into slug flow is 0.097 (see section 8.3.1.2). This means that for a given column diameter of 0.076m (76 mm) that the film thickness is $7.37*10^{-3}$ m. As can be seen from figure 7.37C this column's film behaviour is some 5 times smaller, even at the maximum liquid throughput.

FIGURE 9.38A LIQUID PHASE VELOCITY PREDICTION (d=54 mm)

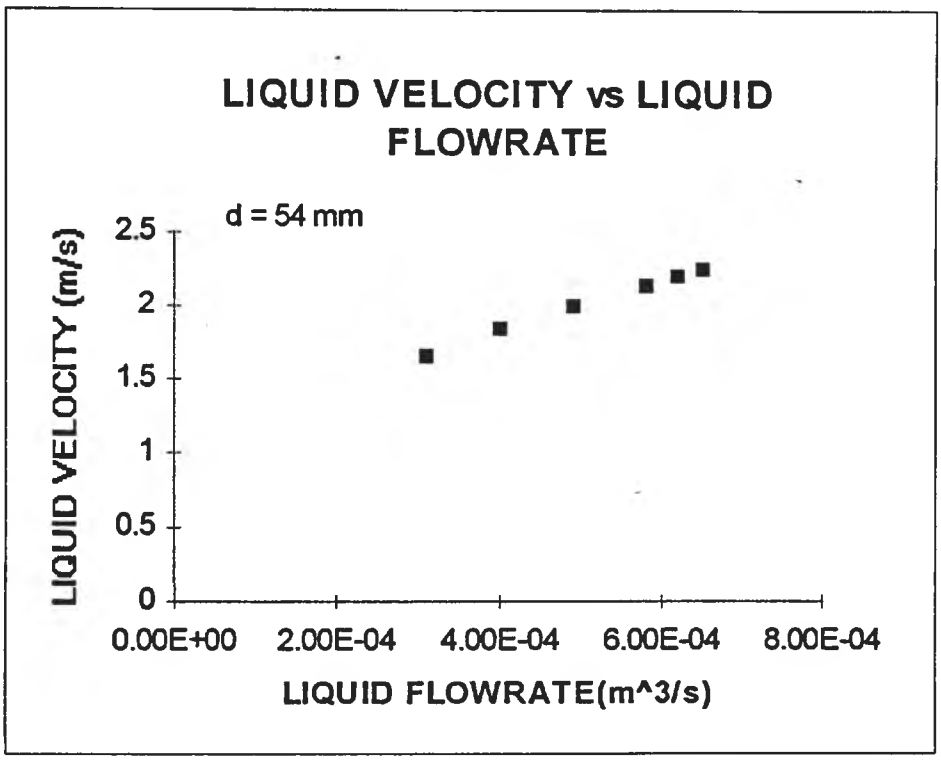

Again a near linear dependence of real phase velocity with liquid volumetric rate is evidenced in figure 9.38A. The linear regression model fit of this data is:

$$u_L = 1689.6Q_L + 1.16 \qquad (9.31)$$

FIGURE 9.38B GAS PHASE VELOCITY PREDICTION (d=54 mm)

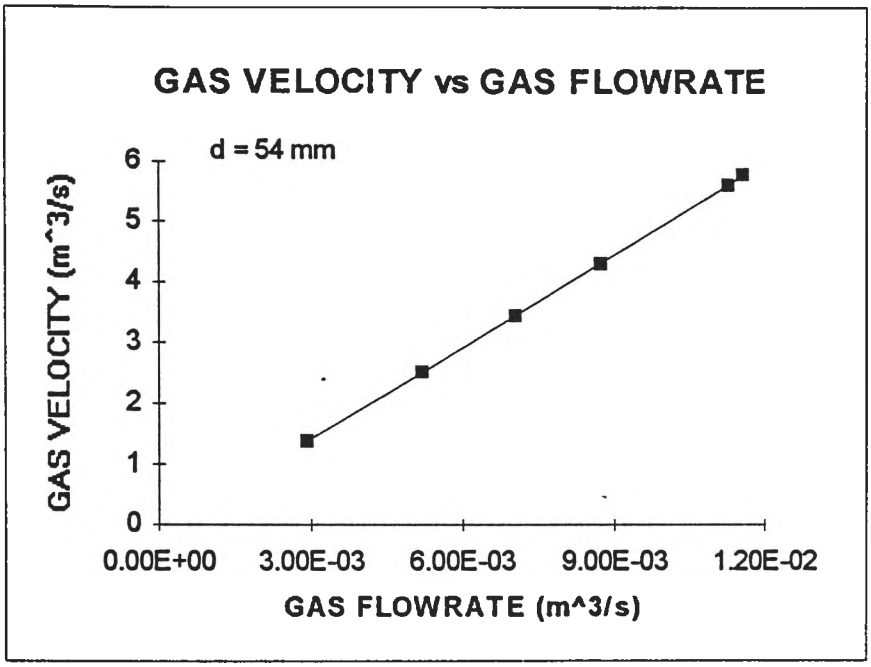

The linear regression model fit of the relationship between velocity and flowrate for the gas phase is:

$$u_G = 508.63Q_G - 0.12 \qquad (9.32)$$

FIGURE 9.38C LIQUID FILM THICKNESS FOR 54 mm COLUMN

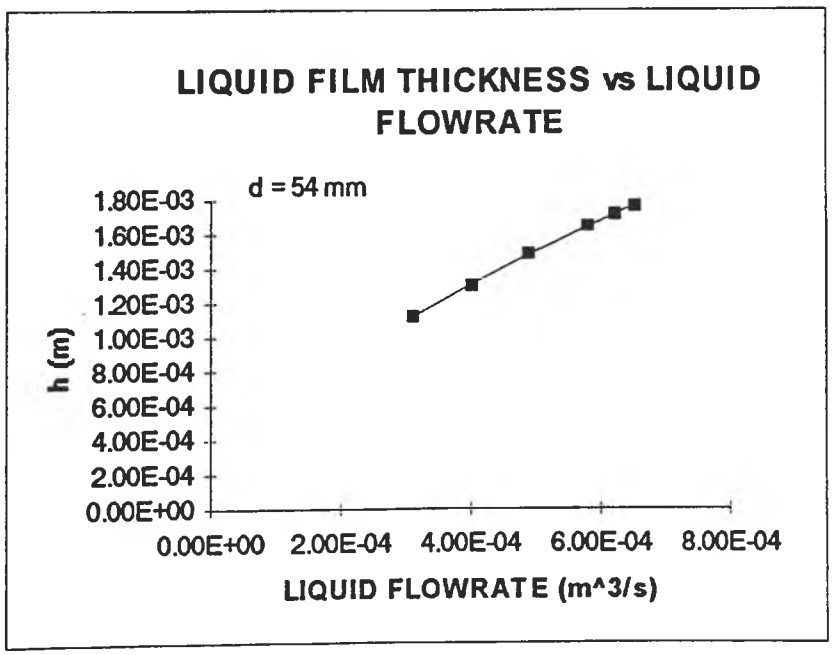

For a column of 54 mm the film thickness required for transition is given by h/d=0.097 (see section 8.1.3.2). This means the flow with transfer to slug flow at a film thickness of $5.2*10^{-3}$ m. The maximum film thickness reached here is some 3 times thinner than this at its maximum value.

Presented in Figure 9.39 (A to D) is the result of comparing the residence time determined from the liquid phase tracer experiments to the residence time predicted from the mathematical two-phase downflow model.

This experiment was done by using the velocity obtained from the model and via the following relationship:

$$t = L/u \tag{9.33}$$

where

t = residence time of a phase (seconds)

u = phase velocity as predicted by model (m/s)

L = length of particular jet pump column (m)

The dimensions of the particular jet pump column sections are as follows:

COLUMN SECTION	DIAMETER (m)	LENGTH (m)
Mixing Tube	0.054	0.449
Diffuser	0.054 to 0.076	0.145
Draft Tube	0.076	1.315

It can be seen that the diffuser has a range of diameters. This is because it is a conical diverging pipe section. The velocity in this section was taken as the average of the velocities of the phases at 0.054 and 0.076 m respectively.

FIGURE 9.39A PREDICTED RESIDENCE TIME FOR LIQUID PHASE FROM TWO-PHASE FLOW MODEL

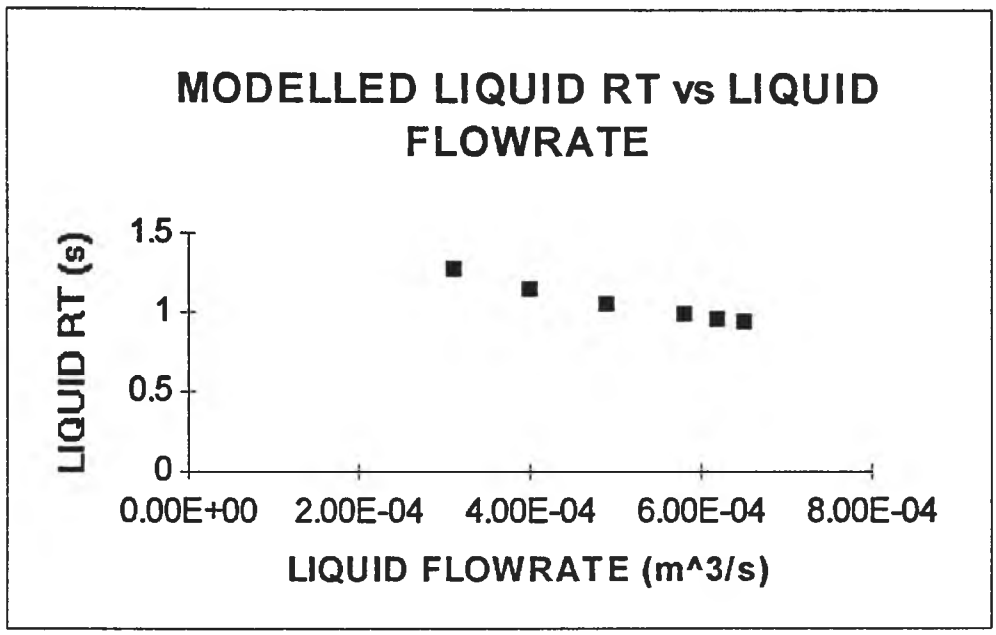

As can be seen in the following figure (9.39B) the two-phase flow model appears to predict a much lower residence time that was measured via acid tracer. This effect is less pronounced at the lower liquid flowrates. The line represents the tracer measurements for the same liquid volumetric flowrate.

FIGURE 9.39B ACTUAL RESIDENCE TIME vs MODEL PREDICTED RESIDENCE TIME FOR LIQUID PHASE

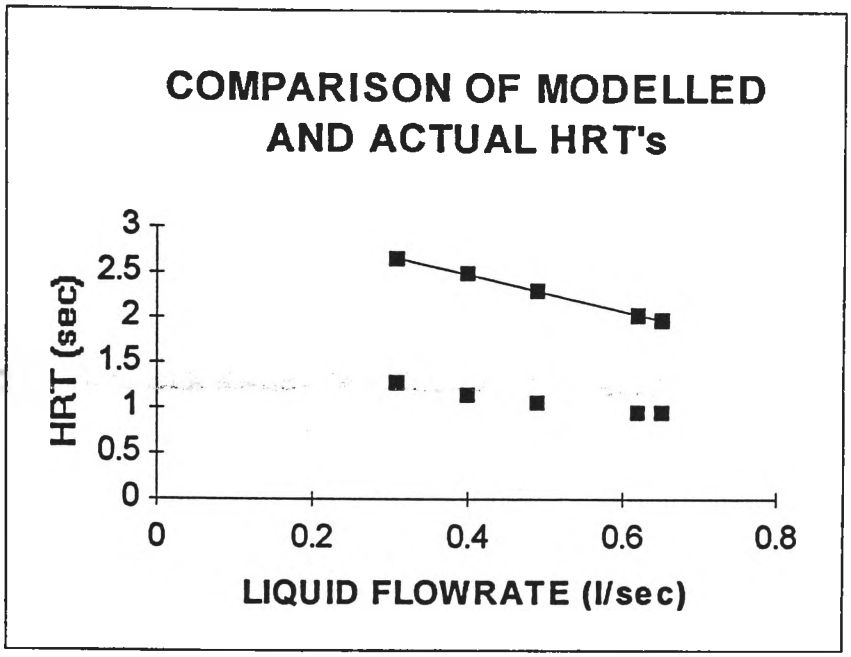

FIGURE 9.39C PREDICTED RESIDENCE TIME FOR GAS PHASE FROM TWO-PHASE FLOW MODEL

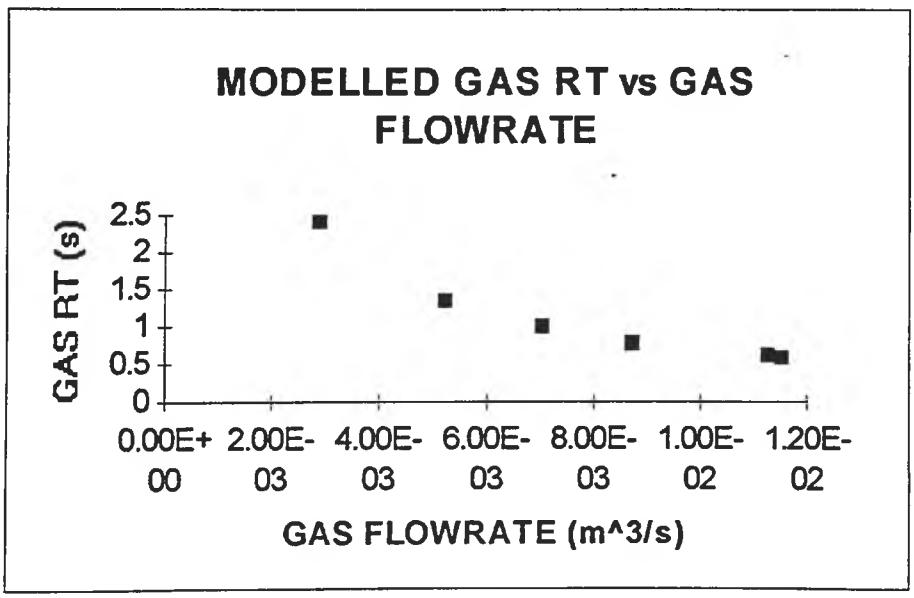

The 2-phase model predicted gas phase residence times (data series 2) are then compared to the data produced from the step response studies (data series 1). The result appears in figure 9.39D.

FIGURE 9.39D COMPARISON OF MODEL PREDICTED vs EXPERIMENTAL GAS PHASE RESIDENCE TIME

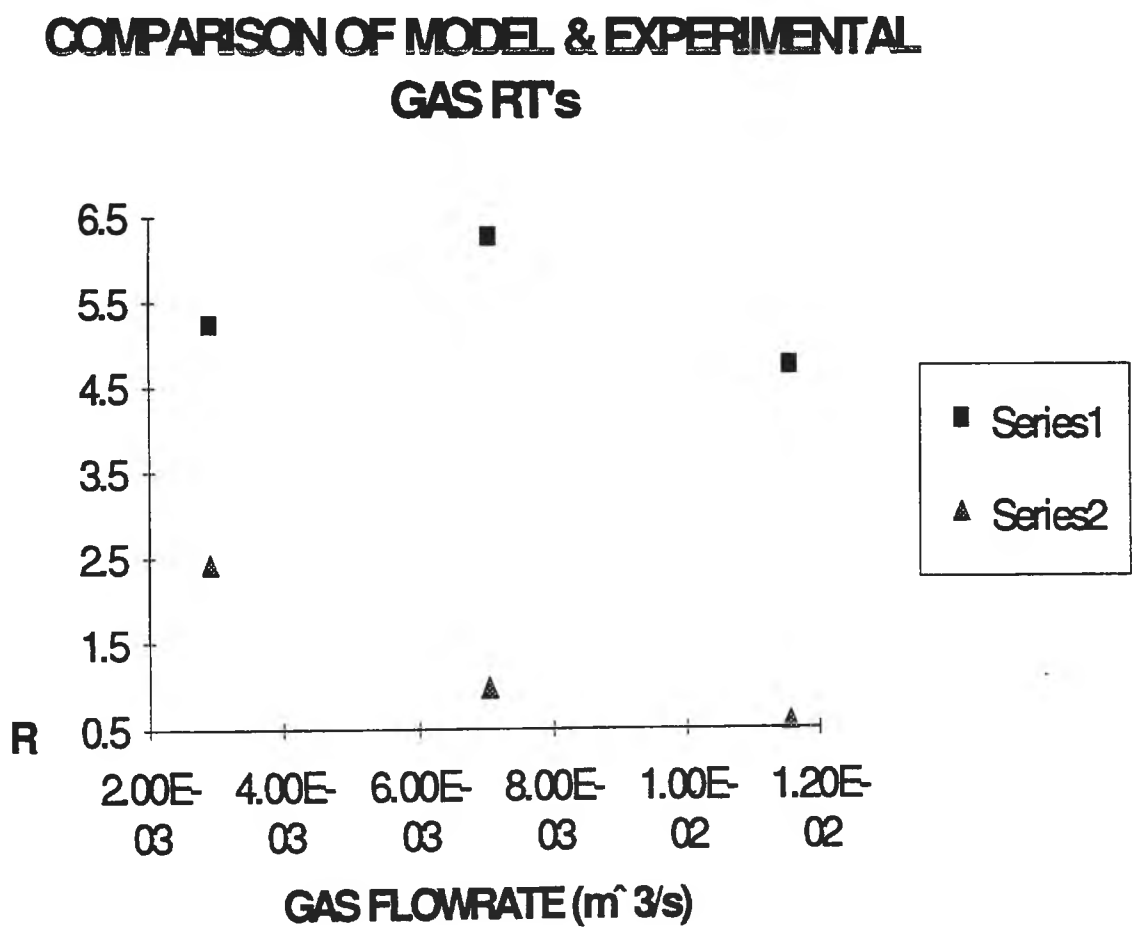

9.12 LITERATURE VOLUMETRIC LIQUID MASS TRANSFER COEFFICIENT

FIGURE 9.40 $k_L a$ PREDICTION BY BRIENS ET AL [131].

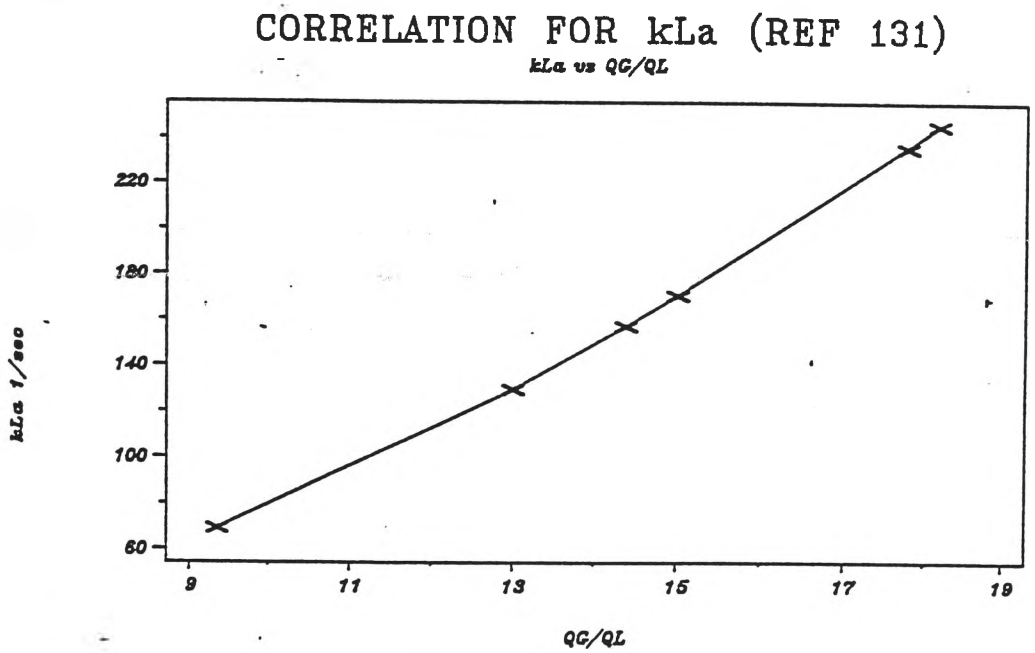

FIGURE 9.41 $k_L a$ PREDICTION BY SENO ET AL [147].

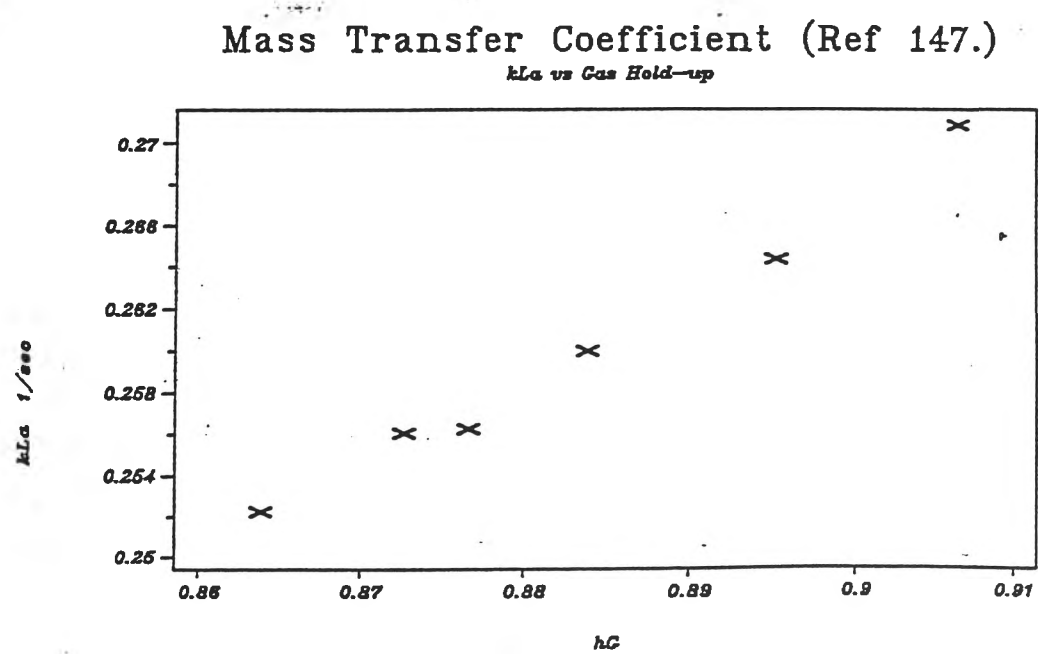

FIGURE 9.42 $k_L a$ PREDICTION BY SENO ET AL [147].

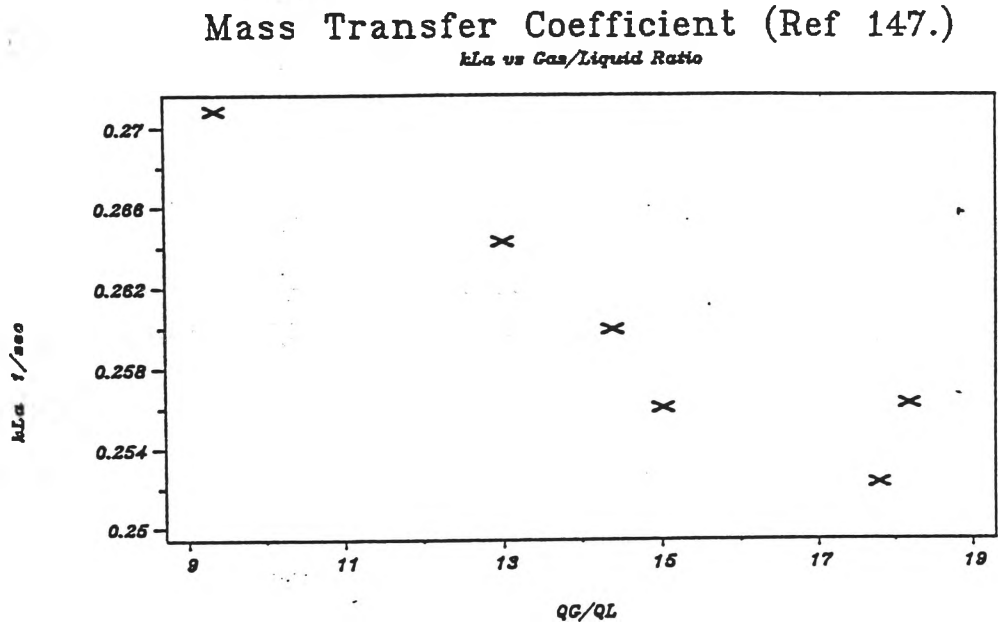

FIGURE 9.43 $k_L a$ PREDICTION BY AKITA AND YOSHIDA [38].

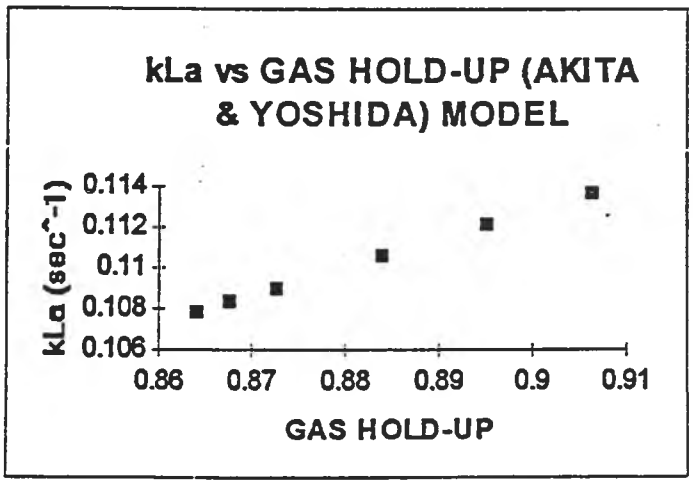

9.13 DISSOCIATION OF OZONE GAS ACROSS JET PUMP ORIFICE PLATE

Experiments were carried out to examine the possible effect of ozone loss across the orifice plate in the inlet line to the jet pump. The point was to examine the difference to see if the ozone gas was likely to be affected by pressure changes. The results appear in figure 9.44. The line represents the upstream ozone concentration. As can be seen the difference is minimal.

FIGURE 9.44 DISSOCIATION OF OZONE GAS ACROSS JET PUMP ORIFICE PLATE

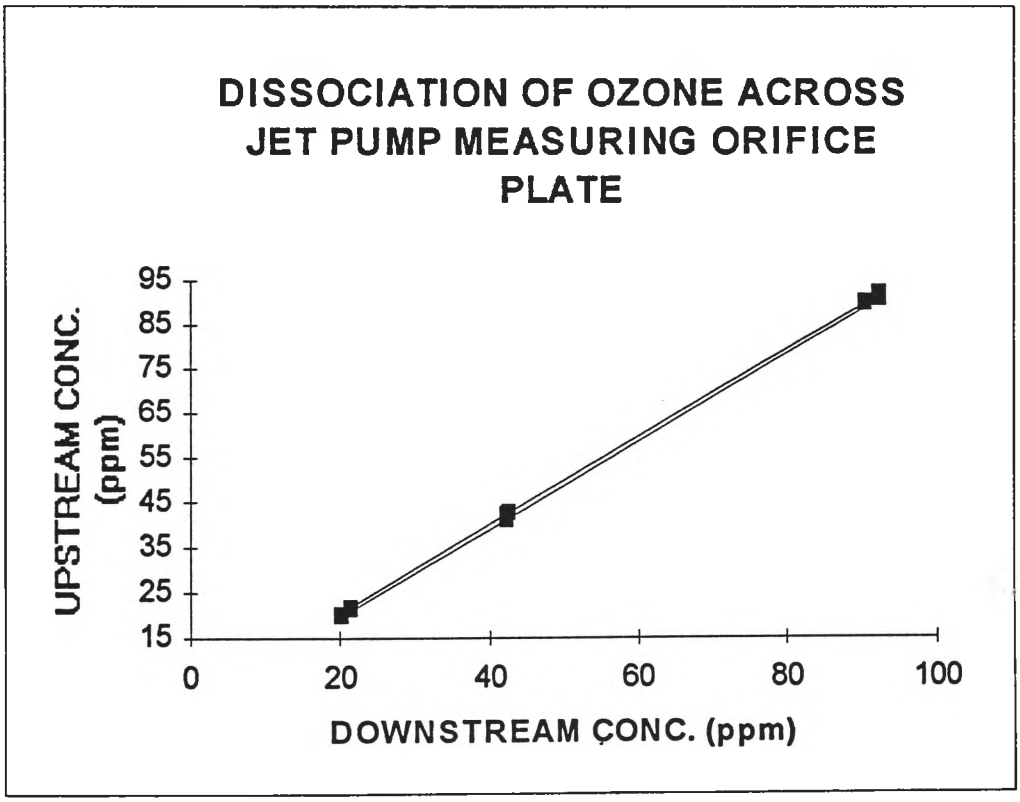

An average sample of the data points is:

□

EXAMINATION OF OZONE DATA

COMPARISON OF DIFFERENCES BETWEEN DATA OBTAINED ACROSS THE ORIFICE PLATE, AS COMPARED TO DATA OBTAINED ACROSS THE JET PUMP COLUMN

ALL CONCENTRATIONS ARE FOR GAS PHASE

ACROSS JET PUMP:

O3 INLET ppm	O3 OUTLET ppm	DIFFERENCE ppm	% CHANGE
19.8	18.2	1.6	8.080808
22	19.3	2.7	12.27273
24	21.6	2.4	10
30.2	27.2	3	9.933775
40.4	35.8	4.6	11.38614
58	50	8	13.7931
83	69.6	13.4	16.14458
22.3	20	2.3	10.3139
24.3	21.8	2.5	10.28807
26.3	23.5	2.8	10.64639
32.6	29	3.6	11.04294
42.1	37.4	4.7	11.1639
58	49.4	8.6	14.82759
89	74.7	14.3	16.06742
21.9	20.1	1.8	8.219178
24.6	21.8	2.8	11.38211

9.14 OZONE MASS BALANCE

Following is data from model simulation. The data is manipulated to check for mass balance consistancy.

MASS BALANCE TESTS ON JET PUMP MODEL

QG L/SEC	(O3)i MOL/L	(O3)o MOL/L	MASS TRANS'D MOL/SEC	QL L/SEC	MODEL O3 LIQ'D MOL/L	MAX O3 LIQ'D MOL/L	% MAX
11.56	8.23E-07	7.57E-07	7.69E-07	0.65	2.65E-07	1.18E-06	22.36458
11.56	9.27E-07	8.32E-07	1.11E-06	0.65	2.91E-07	1.7E-06	17.09542
11.56	9.11E-07	8.36E-07	8.65E-07	0.65	2.92E-07	1.33E-06	21.95573
11.27	9.15E-07	8.03E-07	1.27E-06	0.62	2.81E-07	2.04E-06	13.7499
11.27	1.01E-06	9.07E-07	1.17E-06	0.62	3.17E-07	1.88E-06	16.856
11.27	1.02E-06	9.07E-07	1.31E-06	0.62	3.17E-07	2.12E-06	14.97254
8.71	9.98E-07	8.98E-07	8.69E-07	0.58	3.14E-07	1.5E-06	20.95521
8.71	1.09E-06	9.77E-07	1.01E-06	0.58	3.42E-07	1.75E-06	19.53733
8.71	1.13E-06	1.01E-06	1.05E-06	0.58	3.52E-07	1.81E-06	19.42875
7.05	1.26E-06	1.13E-06	8.8E-07	0.49	3.95E-07	1.8E-06	22.02561
7.05	1.36E-06	1.21E-06	1.06E-06	0.49	4.22E-07	2.15E-06	19.5766
7.05	1.41E-06	1.25E-06	1.14E-06	0.49	4.38E-07	2.33E-06	18.75396
5.2	1.68E-06	1.49E-06	9.95E-07	0.4	5.21E-07	2.49E-06	20.93088
5.2	1.75E-06	1.56E-06	1.02E-06	0.4	5.44E-07	2.54E-06	21.40776
5.2	1.83E-06	1.61E-06	1.12E-06	0.4	5.64E-07	2.81E-06	20.07258
2.9	2.41E-06	2.08E-06	9.65E-07	0.31	7.27E-07	3.11E-06	23.35852
2.9	2.41E-06	2.05E-06	1.04E-06	0.31	7.18E-07	3.35E-06	21.47108
2.9	2.38E-06	2.08E-06	8.8E-07	0.31	7.27E-07	2.84E-06	25.59813

FIGURE 9.45 % OZONE RETENTION vs LIQUID VOLUMETRIC RATE

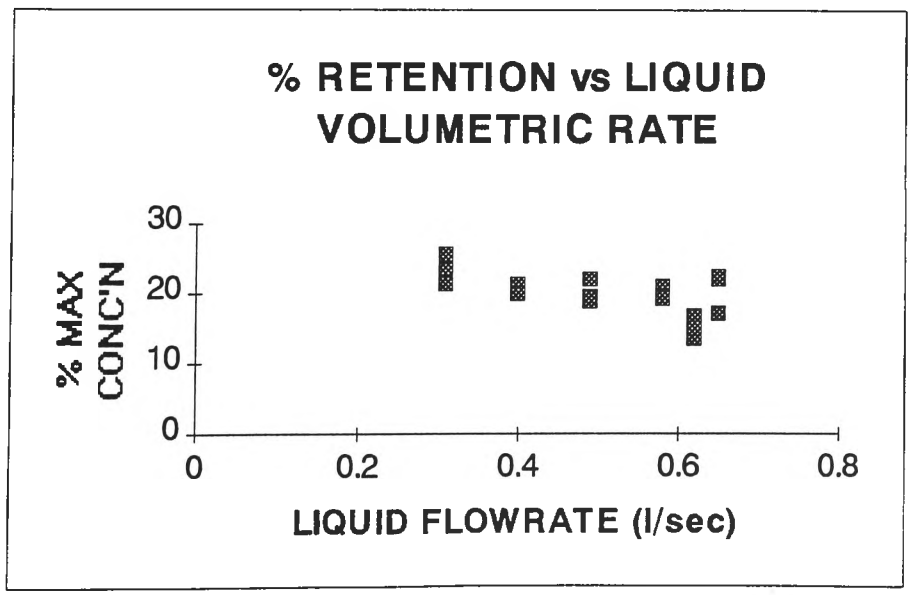

10.0 DISCUSSION

10.1 FLOW RATIOS

In the jet pump very high gas to liquid ratios were obtained. The variation of gas rate with liquid rate was linear over the range studied. This near linear relationship of gas entrained by a liquid flowing through a nozzle was also observed by Cramers et al [129]. Their study was for liquid flows of 1 to 7 m^3/hr compared to this study having a maximum flow of 2.34 m^3/hr.

The gas to liquid volumetric flow ratios (Q_G/Q_L) are much higher than those observed in the literature (see Table 5.3). The Cramers et al [129] study only produced ratios of 3.4. This ratio is less than half the lowest ratio study here. The maximum gas to liquid volumetric flow ratio in this study was 19.

It was also made apparent that even the absolute values of velocity and of loading for a given column area were higher than those in literature. This made a comparison of the flow effects and regime behaviour difficult to compare.

In the case of flow measurement the determination of the liquid flowrate was a simple matter. The flow produced by the pump was steady and the rotameter value held constant. The same situation could not be said for the gas phase. The determination of flow was made by the reading of the differential pressure across an orifice plate in the suction line of the jet pump. This pressure was determined by use of a magnahelic differential guage (0 to 75 Pa). This value could be correlated to a volumetric flowrate based on a previous calibration study [151] (see figures 9.24 and 9.25). The problem with this type of measurement was the random pulsating action of the two phase flow developed in the throat of the jet pump. Due to the sensitivity of measurement being undertaken with the magnahelic this also resulted in fluctuations in the value of differential pressure recorded. Values of variation ranged typically from ± 2Pa to ±5Pa as a worst case. This variation was evident on a 0-75 Pa magnahelic pressure guage. The pulsating action was evident from the observation of the flow through the perspex mixing chamber at the top of the column.

A major feature of the jet pump is its capacity to produce these extremely high gas to liquid ratios. The hope was that these ratios would present a boost in mass transfer performance. The ratios did present a very high volumetric mass transfer coefficient. However, over the range of rates the mass transfer coefficient did not improve (see section 10.4).

10.2 HYDRAULIC RESIDENCE TIME

The hydraulic residence time is a very important parameter in ozone water treatment systems. This is because of the definition of the 'CT' disinfection requirement (see chapter 6). It is therefore important to determine the correct residence time.

In this thesis the residence time was measured by use of an acid tracer (see section 9.3.2). This was chosen due to the ease of measurement of the acid concentration via use of a conductivity meter. The major difficulty, in measurement, which arose was due to the column design. The final design in this thesis for measurement location was a 40 mm ID pipe running perpendicular from the base of the column with a 12 mm socket for the insertion of the conductivity meter probe. Although this method proved able to measure the conductivity with ease there are large doubts as to the validity of the information. The trouble with the current design is that the back pressure valve at the base of the column needs to be throttled or closed to divert the column liquid flow past the meter's probe. The result of this is that the residence time distribution curves begin to tail out, in a characteristic display of mixed flow. This is shown schematically in figure 10.1.

FIGURE 10.1 RESIDENCE TIME DISTRIBUTION CURVE FOR MIXED FLOW

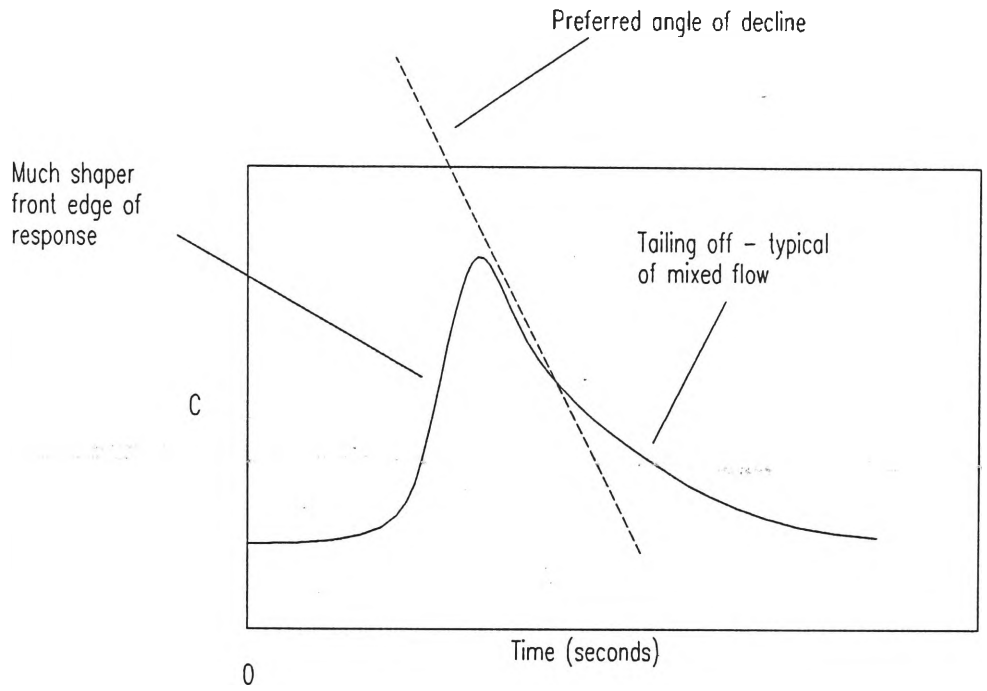

It is entirely possible that this mixing is a backmixed effect caused by the need for the flow to negotiate a 90° bend through a pipeline size change from 76 to 40 mm prior to detection. The liquid/gas flow is travelling quite fast vertically, and then hits the partially shut back pressure valve. This may cause the flow to 'bounce', and therefore become partially backmixed at that point. In fact it may be possible that there is a liquid level which accumulates or locally floods at the base of the jet pump draft tube just above the valve. Although with the entire draft tube section of the column is constructed from aluminium tubing, this flooding is impossible to prove. If it is occurring then this will have two effects. The first effect is that it makes the residence time distribution of the column appear in mixed flow. The second effect is that the residence time will appear longer than it actually is. This longer residence time is caused by the longer axial distance that the liquid particle must travel. This also has implications for two phase flow modelling, which are discussed in a later section.

Plug flow is the type of flow that is assumed to be occurring in the column. Both phases are flowing quickly in a co-current manner downwards. The possibility of liquid phase

backmixing is unlikely (except for flow interruptions) due to the velocity and direction of the gas phase. In countercurrent columns it is possible for the liquid phase to be pumped back up the column due to high velocity up flowing gas. This is not the case in cocurrent downflow. However, the opposite case is more likely, that of the liquid phase being pumped downward by the much higher gas velocity. In fact it is extremely likely that the liquid phase is entrained to a certain extent within the gas phase. This means that essentially it is possible that the liquid flow is violating the definition of plug flow according to [74]. (see Chapter 7). The extent of entrainment cannot be quantified at this point. Although the residence time curves do have a fairly sharp leading edge.

As can be seen in figure 9.11 there is a fair distribution of residence times around the average and regression fitted lines. A linear fit, may also not be the ideal fit to this data, due to the spread of the points. There is a much wider spread at the lower liquid rates (Q_L<0.4 l/sec). During column operation this was the point where pulsating flow patterns were very much in evidence in the perspex mixing section. Although the liquid feed to the column did not pulse. The spread, however, appears to be over an approximate range of ±13 to 26% , for example, at Q_L=0.3 l/sec. In summary, then, for the range studies the linear fit appears reasonably satisfactory. However, the behaviour of extrapolated data is unknown. This leads to the conclusion that a much larger series and range of data points are required.

In figures 9.11 and 9.12A hydraulic residence times with no gas flow are presented . These measurements were studied and compared because of the observation that there seemed little difference between observed flow patterns in the mixing tube. This is also a test for annular flow. According to models proposed by Dukler and Taitel [137]. there should be annular flow occurring at very low gas rates with the types of liquid downflow rate in this column (see sections 5.1.1 and 9.11.1).

As can be seen from the results of this study, there is no large difference in behaviour between the two states. The gas-on regression model has a 51% greater slope, although this is tempered by the gas-off model being shifted higher up the axis. This leads to there only being a 7-8 % difference in hydraulic residence times at the extremes of volumetric liquid flow examined.

The data presented does also show that the two-phase downflow model is predicting in "the right ball-park" for annular flow at low gas velocity (see section 10.8).

The velocity of the liquid phase in the draft tube was examined by injection of a tracer 1.18 m from the base of the draft tube. This was done to isolate the "real" velocity in this section. This was done without gas flow. The reason for this is that it does not appear to make any difference whether the gas is on or not. The velocity findings will be discussed later in this chapter in two-phase flow modelling (section 10.8).

10.3 RESIDENCE TIME DISTRIBUTION GAS PHASE

An intensive study was made in the early stages of the jet pump investigation in an attempt to quantify the gas phase residence time. As has been discussed before, this study was done with the view of examining the flow regime and ideality of the flow. It was thought that given the ozone detector, and access to chart recording of the system response to a step change in ozone concentration, that a relatively accurate picture of the gas phase behaviour would result. From the velocity and flow regime observed visually in the perspex section of the column it was very likely that the gas was flowing in an annular flow manner. The gas phase is also likely to be carrying entrained droplets.

In appendix 4.0 the residence time distribution results appear in graphical format. For each study there are several graphs. The first is the normalised data, this produces the F curve. This is done by dividing every part per million (ppm) concentration figure by the initial concentration. This produces a function which decays from 1 to 0. As described in appendix 2.0 it was decided to use laplace transform manipulation to try and remove the detector and/or portable air-water separator response from the jet pump system response. This was done by formulating a model of the total response along the lines of:

$$y = e^{at} \qquad (10.1)$$

The results of this modelling is presented along with each data set. The model is more satisfactory in some cases than others. The model is only fitted at the point where the curve begins to decay from 1. The initial time (t=0) for these exponential model fits is thus arbitrarily placed. It really begins at the end of the F=1 section of the response being modelled. The full description of this methodology can be found in appendix 2.0.

The resulting response of the form:

$$y_S(t) = 1 - (1-(a/b))e^{-bt} + (a/b) \qquad (10.2)$$

is plotted and presented for each data set. The assumption made is that the curve represents the step part of the jet pump curve. This is shown in figure 10.2.

FIGURE 10.2 IDEAL OUTPUT RESPONSE CURVE

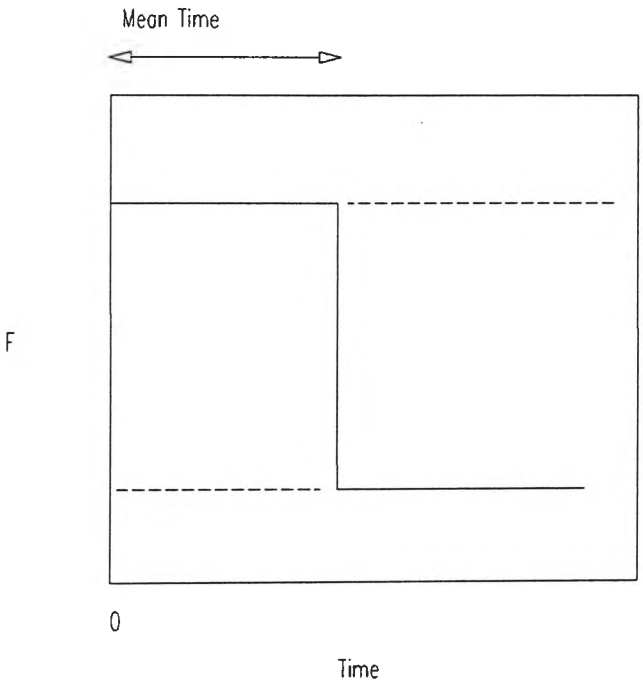

This would suggest that the residence time of the jet pump is actually the time at the tangent to the curve where the decay from F=1 begins. This methodology was followed for both the inlet to the jet pump residence time correction factor, and the outlet of the jet pump. The outlet to the jet pump was taken as being a tapping point just above the back pressure

valve (section 8.3). A further correction factor had to be added in. This was to account for the time taken from the tapping point to the actual mixing point.

The values of the a and b constants were often fairly similar and these values are evident in appendix 4.0.

The first difficulty that arose was that the entrance, or inlet, correction factors were significantly different to that from theoretical flowrate and area studies (see figure 9.6B). This is only single phase flow. The assumption that plug flow was occurring here may be flawed. If plug flow occurred, then the two residence time values would be equal. This first part of the gas phase residence time was thought to provide a useful idea of how the methodology was going to behave.

The results obtained were less than satisfactory. The assumption that switching off the ozone generator (a 4 cell UV style) would produce a step may be flawed. This is because of two main factors. The first is that the exit to the four cells is a larger conical shaped aluminium pipe which feeds into the jet pump gas inlet hose. Due to its reducing conical shape it is likely that there is a backmixed effect occurring. The second is that turning off the power may not result in a zero production of ozone. This is because the UV tubes are still emitting radiation and therefore still causing ozone to be produced. The nett effect of these two effects is not quantifiable at this stage.

There is an approximate 2 to 3 fold difference between the theoretical and actual residence times, with the theoretical being smaller. This may also be put down to the very large change in diameter going from the plastic inlet hose (31 mm) to the aluminium suction chamber (76 mm). The change in diameter is around 2.5 times. The change in cross-sectional area is around 6 times. This may create a swirling effect and thereby mixed flow in a similar way that this would be occurring in the jet pump air-water separator. This mixed flow may significantly change the mean residence time.

The other major piece of information gained from the large difference in residence times is that the laplace transform model is likely to be flawed. However, the balance of the results were still studied via this method, to see what overall effect would be produced.

As evidenced in figure 9.6 there is a large spread of data for the inlet correction factor. A three or four fold difference is evident at Q_G=7.05 l/sec, for example. This is partly the fault of operator error. To achieve the required correction factors, a step change had to be introduced. To do this, the power to the ozone generator had to be switched off at exactly the same time as the chart recorder was started to record the corresponding response.

The second physical reason for variation in residence time is the fluctuating nature of the gas flow. In the theoretical study the gas flowrate assumed is an average value that should be occurring at that liquid rate. The gas flow was not measured at each residence time determination. The reason for this is that the flow tends to fluctuate around a particular value. However, it is possible that this value itself is flawed due to the response and accuracy of the magnahelic differential pressure guage used to determine the drop across the gas measuring orifice plate. The calibration of the magnahelic was not checked independently.

It also must be noted, that the slopes of the theoretical and experimental residence times are not parallel (figure 9.6B). The theoretical study also is more exponential in behaviour (figure 9.6A) than the experimental study.

Figures 9.8 and 9.9 show that the system appears to be showing a type of mixed response 74.

The portable-air water separator presented the largest physical problem in the gas phase residence time study. The reason for this is more fully covered in section 9.4. Several designs were tried with only limited success.

The final result of the study was the fully corrected residence time for the gas phase presented in figure 9.10A. The first major problem which is evident is that the trend appears incorrect. The averaged data points for Q_G=7.05 l/sec present a residence time greater than for a Q_G=2.9 l/sec. The residence time is some 15% higher for the higher flowrate. This does not make sense. It would be only possible if the liquid film became much thinner, thereby allowing a wider cross-section for gas flow and therefore leading to a longer residence time. This does not happen in this case, as the liquid rate increases with the gas rate, and in any case the gas residence time (GRT) at Q_G=11.56 l/sec is lower.

The value, then, of the experimental GRT study is somewhat questionable. The assumptions made and the theoretical results from the laplace transform model may need further enhancement, or a different approach altogether. A number of recommendations are presented in chapter 11.

10.4 VOLUMETRIC MASS TRANSFER COEFFICIENT

The determination of the volumetric mass transfer coefficient (k_La) in units of sec^{-1} was via the use of the mathematical model developed for this thesis (see Chapter 8). The specific interfacial area (a, m^2/m^3) was not experimentally determined, and so the k_La term has been determined in this lumped variable form only. As can be seen from the determination of k_La from the use of real data on the mathematical model, very high values of k_La were obtained. The second important feature of the k_La data is the near independence of k_La on physical parameters such as flow and flow ratios for the range studied.

The determination of the k_La term was by using a manual iteration of the mathematical model. This was done by using the experimentally determined value of the outlet gas phase ozone concentration ($(O_3)_O$). The k_La value in the model was then altered until the model predicted value of $(O_3)_O$ matched the actual value.

The results in the literature disagree on the behaviour of k_La in jet (annular) flow regimes (see section 9.12). The literature discussion is presented in section 5.2. The most striking feature of the results obtained is the magnitude of the mass transfer coefficient. This magnitude, in the order of 240 sec^{-1}, is often in the order of 10^2 greater than in literature studies. This is particularly the case when comparing traditional countercurrent bubble columns (see below). Extrapolation of some models such as that presented by Briens et al 131. :

$$k_La = 0.965(Q_G/Q_L)^{1.91} \qquad (10.3)$$

does produce a number in the same order of magnitude as this study. For example, a gas-liquid ratio of 17 produces a k_La of 216.15 sec^{-1}. However, their [131] study only examined gas to liquid ratios up to 0.7, and in any case they suggested that k_La should fall off at these higher rates. Their [131] model shows a strong dependency on Q_G/Q_L, whereas this current study and studies of others suggest that this dependency on Q_G/Q_L disappears once the flow regime enters jet flow [131,132]. This lack of dependence has been verified in this work.

Examination of the model proposed by Dirix and van der Wiele [134] has shown some similarities in some of the mathematical modelling. However, they examine the k_La value from the point of view of the liquid phase behaviour. They measured the dissolved gas concentration (oxygen in their case) at the inlet and outlet and applied the following model [134] (modified for ozone):

$$[O_3]_o = [O_3]_i(Q_L/(Q_GH) + e^{-kLa\tau}) \qquad (10.4)$$

where

τ = liquid phase residence time (seconds)

This model is the solution form of the following two equations [134]:

$$Q_L\, d[O_3] = k_La([O_3^*]-[O_3])\, dV \qquad (10.5)$$

and

$$Q_L([O_3]_i-[O_3]) = Q_G\,(O_3) = Q_G\,H\,[O_3^*] \qquad (10.6)$$

where

dV = volume unit

These equations are the same form as the equations used in the mathematical model developed in this thesis (see chapter 8). The major difference is the lack of the term used to describe the ozone demand ($w.h_L.[O_3]$). The same technique as presented in this thesis was used by Dirix and van der Wiele [134.] to convert the equations to the time domain. It can be seen from the above equations (eqns 10.4 to 10.6) that plug flow is assumed to be occurring, as well as the lack of resistance to mass transfer in the gas phase. It is also necessary to disregard the Q_L/Q_GH term in most of the integration due to its relatively small size. The magnitude of this term is smaller with oxygen, as its Henry's Law constant (H) is 33 [134.], whilst it is 2.98 for ozone. However, this is to some extent balanced out in this work due to the much larger gas to liquid volumetric flow ratios (9 to 19). The ratios used by Dirix and van der Wiele [134.] are $1.3<Q_G/Q_L<3$.

An attempt was also made to quantify how well models developed for counter-current bubble columns could be extrapolated to co-current downflow liquid jet columns. The model of Akita and Yoshida [38.] was tested, and the results appear in figure 9.43. As can be seen the model is near linear over the range studied, however the extremely low magnitude of their k_La, 0.107 to 0.114 sec^{-1}, does not agree with the 240 sec^{-1} magnitudes found by the model developed in this thesis. It must also be pointed out that there a good chance the Akita and Yoshida [38.] would not predict the mass transfer coefficient, due to the large difference in application in this study. The other major factor, which has been previously mentioned, is that the column diameter is too small. They [38.] suggest that their model does not predict properly below diameters of 0.152 m. This column ranged from 0.054 m to 0.076 m.

The mass transfer coefficient performance of the jet pump did not really alter across the range of study. In fact a doubling of the Q_G/Q_L ratio did not present much enhancement. So from the mass transfer coefficient point of view it does not matter which area of operation the column works in. The mass transfer and disinfection performance, together with the most energy efficient point to operate the column may be a more realistic starting point for column design.

10.5 HOLD-UP STUDIES

The hold-up studies were originally to be carried out using the gas-phase as the predictive model. This approach had to be abandoned due to the difficulties in gas phase studies (see section 10.3). This meant that studies were performed on the basis of measurements made in the liquid phase. The resulting linear regression fit for the gas-liquid flow ratio produced a reasonable fit. However, it may be that the curve is more of a log or exponential style of fit.

The difference between the two methods converge at a higher liquid volumetric rate. The difference becomes approximately 60% at the lower rates. The residence time method was used in all modelling calculations. The gas to liquid volumetric ratio may present a more simplistic view of the "real" situation. However, the residence time method does rely on there being an accurate picture of residence time. This is open to some question, as has been previously discussed.

The method of residence times also does present an averaged hold-up in its present form. This is because the column was assumed to be all 76 mm diameter. This is not strictly true as the column is 1.315 m of draft tube, the balance of the 1.98 m column length being made up of a 54 mm mixing tube and a 54 to 76 mm conical diverging diffuser. The assumption was made that the hold-up would remain constant throughout. This is probably not the case.

The important outcome of the hold-up study in its present form is the extremely low liquid hold-up (around 0.1). This is in comparison to the liquid hold-ups in typical bubble column studies [147] of around 0.8 to 0.99. In some jet studies, liquid hold-up (h_L) ranges from 0.99 to 0.6 [129], 0.95 to 0.75 [132], and 0.6 to 0.85 [131].

10.6 GAS PHASE CONCENTRATION PROFILE STUDIES

The gas phase concentration profile study presents a useful tool to guage what is happening in the column. The reason for this study is that the mass transfer rate is controlled by the concentration gradient. For this reason the gradient is required to be known. This gradient is related in this thesis via the two film model. In this model the ozone concentration

in the film is related by Henry's Law. This equilibrium relationship helps dictate the rate of mass transfer.

The other major reason to study this area is due to the uncertainty of the stability of the ozone under this type of contacting. It may be that the ozone profile assumed by this model bares no resemblance to the actual ozone concentration profile.

There were many problems with the portable air-water separator in this experiment and no stable concentration profiles were obtained. It is of great importance that the true gas phase concentration profile is found. The presents a challenge to produce a more efficient and reliable portable air-water separator

The model predicted profile is presented in figure 9.23.

10.7 CT DISINFECTION DETERMINATION

As was discussed in chapter 6 the CT disinfection requirement is very important to insure that the full level of disinfection has occurred. Figure 9.33 presents a CT vs Q_G/Q_L for the full range of the jet-pump studied. The study suggests that as the flow ratio moves from 9 to 18 the CT changes from 0.093 to 0.025 mgO_3.min/l. That is, for a doubling of the flow ratio a 3.7 times decreasing effect on CT results. The shape of the curve produced suggests that in fact it may be possible that as the higher ratios (Q_G/Q_L=17 to 18) are approached, the decrease in CT begins to level off. There is not enough data beyond this point to confirm this.

The major problem with the jet pump column highlighted by this particular study, is the size of the CT value. It is very small. This is due to two factors, both the residence time and ozone residual are small. Separating the CT terms the ozone residual ranges from 0.013 to 0.035 mg/l, whilst the residence time varies from 1.99 to 2.66 seconds. This C term is the actual term and not the corrected term suggested by Lev and Regli [118]. If this criteria is followed then the picture for the characteristic concentration C is worse; ranging from $6.5x10^{-3}$ to 0.0175 mg/l. This is shown in figure 9.33A.

The exact CT disinfection requirement for legionella is not available at this stage. Although, from Katzenelson et.al [70], it can be seen that 99% kill rates for ozone acting on E.coli is occurring in 30 seconds with an ozone residual of 0.04 mg/l. This puts the CT at about 1.2 mg.s/l. Even the best modified figure of approximately 0.045 mg.s/l is some 27 times smaller. The 99.9 % kill rate occurs in about 50 seconds leading to CT = 2 mg.s/l, some 44.4 times greater than the best CT available in the jet pump contactor (0.045 mg.s/l).

From this study it can be seen that the jet pump is unlikely to be appropriate for the disinfection of cooling tower waters for legionella control. This is primarily due to the problem of a very low CT value for the column. A high mass transfer coefficient and high liquid rates and efficiencies are not important if the primary goal cannot be achieved. The challenge is to increase this CT value and thereby increase the microbial disinfection efficiency of the contactor. A number of recommendations are presented in chapter 11.

10.8 TWO PHASE DOWNFLOW MODELLING

The two-phase downflow modelling met with mixed success. The reason for this is the lack of reliable results, and the physical constraints of the current column set-up.

The major physical problems with the column stem from the fact that most of the column is constructed from aluminium tubing. This makes it impossible to accurately determine what is going on for the entire length of the column. This is particularly true at the base of the column. The reason for the base suspicion is from the hydraulic residence time studies suggesting a mixed flow somewhere in the column. The two-phase flow model assumes steady-state downflow without any obstructions. This data then is compared to velocities and residence times predicted from the tracer data. This hydraulic residence time tracer data is slightly questionable.

The physical constraints also included the fact that it was not possible to easily force the column to deviate from annular flow. Therefore the annular flow regime transition point is at this stage not proven. Although studies have confirmed one aspect of the annular flow transition, that it does not transfer to annular flow at a negligible gas rate. The transitions

theoretically appear at approximately u_{LS} = 1.5 m/s in 54 mm tubes and u_{LS} = 2 m/s in 76 mm tubes. This corresponds to liquid flowrates of 3.4 l/sec and 9.1 l/sec respectively. Considering the maximum flowrate studied is 0.65 l/sec, the transition from annular flow is not likely.

Film thicknesses and gas and liquid velocities vs gas and liquid rates tended to produce near linear relationships. This makes for good modelling.

In figure 9.39B the liquid residence time from the model and the tracer measurements was examined. As can be seen the tracer is predicting approximately double the residence time predicted by the two-phase flow model. This also means that velocities are double those suggested from tracer data. If the velocities are higher then the path available for liquid flow must be less and therefore the liquid hold-up calculated from the two-phase flow model would also be in the order of half. This is because the theoretical flow area must be half to produce double the velocity for the same flowrate. Further more accurate liquid phase residence time studies are required over a wider range of values before the actual validity of the model can be determined. If there is flooding and backmixing occurring at the base of the column then significantly higher liquid residence times can result. This may explain the deviation between actual and modelled data.

As similar story is evident in the gas phase studies summarised in figure 9.39D. From this data it can be seen that the two-phase downflow model presents a much lower gas residence time than does the experimental model. In fact the 2-phase model ranges from half the experimental model at Q_G = 2.9 l/s, to 1/10th that of the experimental model at Q_G = 11.56 l/s.

It is believed that the experimental gas flow model is extremely flawed, for reasons discussed in section 10.3. However, it is not easily determined how accurate a picture of gas flow and velocity profile is presented by the 2-phase downflow model. This cannot be determined until a more accurate experimental picture of true gas residence time is found.

10.9 BUBBLE COLUMN MODELLING RELATIONSHIPS

In figures 9.1 to 9.5A are presented a series of graphs illustrating co-current model behaviour at physical values more appropriate to bubble columns. This data is applicable to studies suggested in section 8.1.1.1.1.

Figure 9.1 shows that the removal efficiency improves with increasing reactivity of the chemical species for a given volatility. It must be noted that the removal efficiency is nearly independent of volatility at k_T=300 l/(mol.sec).

The model also shows that the removal efficiency does not improve once gas-liquid volumetric rates increase too high. In figure 9.2 it can be seen that rates have more or less levelled off at Q_G/Q_L=7. It is interesting to note that for high reactivity and low volatility compounds, the efficiency appears to drop at the higher rates (k_T = 500 l/(mol.sec), H_i=0.24).

Figure 9.3 shows that compounds of high reactivity do improve their removal efficiency at increased values of k_La. Although this tends to level off above $k_La = 0.03\ sec^{-1}$. Low reactivity compounds are not as influenced by the volumetric mass transfer coefficient. In fact for group 1 compounds, there is no removal efficiency benefit above $k_La = 0.01\ sec^{-1}$.

Figure 9.4 suggests that the removal efficiency is independent of specific ozone utilisation (w). The higher reactivity compounds have a higher removal efficiency than do the lower ones. However, this is not dependent on the w of that wastewater.

A very interesting result is presented in figure 9.5. This shows that as the liquid hold-up is increased ,then the removal efficiency increases. This effect is more enhanced for the higher reactivity compounds. It is particularly interesting to note that the optimum liquid hold-up is around 0.09 to 0.1. This is exactly the region studied in the jet pump contactor.

The initial ozone gas concentration has an impact on the removal efficiency. This is shown in figure 9.5A. However, for the mid to high reactivity compounds the efficiency does not improve much beyond the $(O_3)i$ = 1.3 mg/l figure. However, for very unreactive compounds the removal efficiency is still only 60% at 1.3 mg/l. The rate for these types of

compounds (high volatility, low reactivity) linearly increases at nearly 10% removal improvement for every 1 mg/l increase in concentration in the feed gas.

It is of little value to examine the model from this point of view in much more detail, as these results are difficult to compare to real values, and in particular to the jet pump. This is because the jet pump operates in a much different flow regime, and under a much different set of conditions.

10.10 MASS BALANCE RELATIONSHIPS

It was decided that due to the very high mass transfer coefficient ($k_L a$) values obtained, that an examination of the overall mass balance would be a useful check on broad validity of results. This study is shown in section 9.14.

It can be seen that the overall mechanics of the model are correct. This is evidenced by less ozone mass appearing in the liquid phase, than was transferred from the gas phase. This is expected due to reactions. From conservation of mass it can be seen that more mass cannot appear in the liquid side. At this stage the exact contribution of the reactions have not been confirmed. This means that errors in the model may still be possible However, the mathematics of the model appear to be predicting a reasonable figure at the very least.

An interesting feature of the study is that the liquid phase ozone residual is only about 20 % of that which could be possible given no dissociation or other oxidation reactions. This study is presented in figure 9.45. It is therefore obvious that reactions and dissociations are of critical importance in this kind of mass transfer, as they make up some 80 % of the phenomena. Again, what is of interest is the flat profile with respect to liquid flowrate.

11.0 CONCLUSION

The aim of this study originally was to develop a mathematical model for ozone transfer into water. The reason for this was to allow for parameter estimation and optimisation to facilitate design of ozone-water contactors. This model was to be then applied to the study of a particular contactor, the jet pump.

The preceding aim has not been completely achieved, however, the original study has been modified and broadened due to findings in the literature. Further controlling factors were also brought to light. Initial literature investigation showed that a good broad study of literature was required, and to this end 151 sources were examined. This study consists of both general gas-liquid mass transfer, and specific ozone-water and gas-water mass transfer studies in downflow over the last 10 years. This size and type of study was warranted due to the relatively small amount of work available on high gas-liquid flow ratio mass transfer. From the sources reviewed, it was not possible to find similar transfer phenomena to that occurring in the jet pump. This was surprising. The literature review highlighted that there were often orders of magnitude difference in gas-liquid ratios, concentrations, or reactor geometry.

The other major result to come out of literature reviews was the small amount of study undertaken on two phase cocurrent downflow. This area requires further investigation, and a more extensive review of literature. Examination of published models in this work was confined mainly to annular flow phenomena, and transition studies in particular. It became obvious from jet pump observation, and mass transfer coefficients that the plug flow and bubble column models may have limited accuracy in annular flow regimes, and the results obtained may be simplistic.

The literature review is very important to this work and to the initial mass transfer model and two phase downflow model developed. The review provides information and literature sources essential to further work on these models. Data, models, results and sources in the literature presented here also provide good information for further, more experimental, work in this field.

The mathematical model was developed by closely examining the literature, and deciding on a model which provides ease of manipulation of physical and chemical parameters. It was decided to use a basic bubble column lumped parameter model, due to the large amount of work in this area. The model developed here provides a platform for a further, more sophisticated model. The lumping together of reaction rate constants, in particular, is very useful as it simplifies some of the terms. The reactions appear very important and simulation studies suggest that they may contribute some 80% of the mass transfer phenomena.

An examination of mass balance over the entire jet pump via use of the mathematical model has revealed that the model developed in this work predicts liquid phase results with the correct order of magnitude. The model usefully describes the overall gas phase ozone behaviour. It is premature to suggest that the accuracy of the liquid phase concentration is high. This does present a limitation of the current model. However, given that the final application of the model is likely to be in the area of microbiol control in water, the literature review and model simulation has revealed that the liquid phase ozone concentrations and residence times are in the order of 27 to 44 times too small for this application. The mathematical model developed is at least sufficient to show that the jet pump performance is an order of magnitude away from efficient disinfection at best.

Several parameters such as liquid hold-up, residence times and gas phase concentrations were required in this study. To this end limited experimental work was conducted to provide realistic data for model testing. The experimental work revealed large deficiencies in the equipment. This led to questionable results in some areas, and provided for a large number of recommendations. The experimental work revealed the need for accurate ozone detection in both liquid and gas phases.

Transient gas phase studies were very difficult to perform, and poor success in mathematical modelling of gas phase residence times was achieved. Further investigation is essential in this area if accurate predictions are to occur.

Experimental liquid phase ozone studies are essential to allow for model validation. This was not possible due to a lack of equipment. A reliable on-line system capable of transient studies would be preferred, although accurate batch studies would suffice.

The experimentation has shown that it is essential that a good review of ozone instrumental analysis is required. Further literature study on reactor tracer techniques, particularly gas phase, is also required.

Reconstruction of the jet pump system completely from perspex would also allow more accurate information on two phase flow phenomena.

This study provides a general framework to build on for future development of the jet pump for ozone water treatment. What has been highlighted from this study is that the mass transfer coefficient is very high, although to what exact extent is still open to question due to the definition of mass transfer coefficient and lack of liquid phase studies. The mass transfer coefficient in this study was independent of hydraulic operational parameters, such as flowrate, across the range studied.

Gas phase residence time (GRT) studies and models were found to be lacking in accuracy, and there was some question about the liquid residence times. These factors leave two-phase flow modelling predictions unproved. It also may be that the two phase models are unsuitable for this application, as they were originally developed for flow regime transition studies only.

A rethink will have to occur on the design of the jet pump for microbiol disinfection due to the low residence times and characteristic concentrations obtained. A way will have to be found to increase one or both of these factors to a suitable level.

A large volume of work still needs to be carried out before this model can be used as a final design aid for scale-up to industrial scale applications. The reason for this is that the liquid phase has not been completely studied, particularly the outlet residual concentration. For this reason, although useful as a starting point, the model validity cannot be fully tested.

However, a large number of references and recommendations are provided by this thesis as a good guide for future work.

12.0 RECOMMENDATIONS

12.1 FAST REACTIONS

As mentioned in Chapter 6 the reaction rate is extremely fast for microbiol disinfection. This may mean mass transfer enhancement for a brief period of time during the contacting. This type of enhancement may need to be incorporated into the model. However, it is also possible that due to the other reactions and interactions of chemical species in the effluent stream, that no enhancement is occurring to any observable level.

Sources such as Levenspiel [74.], and Mehta et.al [46.] present good starting points for further study in this area. In particular Mehta et.al [46.] presents a very comprehensive study on mass transfer, selectivity and also reaction enhancement based on two-film models.

It is also important to obtain good rate constant and Henry's Law data on the microbes to be examined. This will allow for better assessment of how the reactions should be accounted for. As discussed in the chapter 8 formulation of the model, there was an assumption made that the mass transfer was broken down into discrete stages. This is less likely to occur with microbiol disinfection due to the higher rates [70.].

12.2 COLUMN DESIGN AND LIQUID REDISTRIBUTION

The top part of the jet pump column has a clear perspex section. This allows the flow to be viewed easily. In future column development the entire column should be manufactured of a clear material to allow the operation to be viewed over the entire column length. However, in this column it is evident that the liquid flow tends to 'stick' to the column walls. This obviously has a large impact on the mass transfer efficiency. This is because if a water droplet has one side against the column wall then this surface is not available for mass transfer. This probably reduces mass transfer to this droplet by at least 50%. This figure may even be higher, depending upon the thickness of the layer flowing down the wall. Packed towers also tend to

have a problem of the liquid phase channelling down the wall. A method of solving this problem is to redistribute the liquid away from the wall.

The liquid migrates to the walls for a number of reasons and these include liquid and gas rates, nozzle and mixing chamber design, and the degree of column tilt from the vertical. In small columns (diameter less than 0.6 m), it is suggested that a 'wall wiper'[127] style of liquid redistributor is employed. It is important that the design of the redistributor is such that it does not cause large pressure drops in the gas flow and cause local flooding. This is particularly important in the jet pump, as it is very prone to flooding.

It is very difficult with the current back pressure valve style to throttle the flow to obtain a certain liquid level in the base of the column draft tube. A 10-20^{o} movement of the valve may cause the column to completely flood. The valve at the column base is a gate valve, and has very poor turndown. Its tendency is to go from full flow to near no flow. A globe valve or other similar valve is required for studies involving throttling of flow at the column base. The column draft tube is made from aluminium, which makes the onset of flooding near impossible to detect.

The spacing of the redistributors in the column varies according to the packing arrangement used, and in the case of the jet pump where the column is empty, a trial and error approach will need to be adopted. As an initial estimate a 'wall wiper'[127] distributor (shown in figure 12.1) should be placed at the base of the perspex section and approximately half way down the main aluminium part of the column. The second redistributor will require the addition of a set of flanges in the aluminium (or new perspex) part of the column. The decision to ensure that the liquid redistributor is flange mounted is to allow for easy removal should there be any problems. The second reason for easy removal is that the exact effect of one of two redistributors on residence time and mass transfer could be examined.

The size of the distributor will need to be assessed.

FIGURE 12.1 LIQUID REDISTRIBUTOR [127].

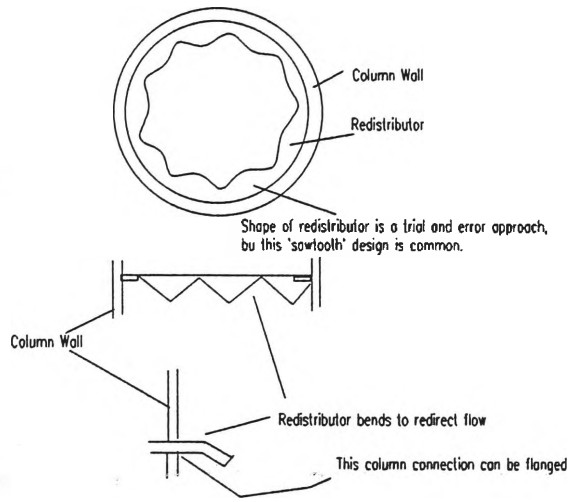

The addition of a redistribution system will also have the effect of increasing the residence time, which will also have an impact on the CT value of the column.

12.3 GAS FLOWRATE

It is important to note that the mass transfer efficiency increases as the inlet ozone concentration increases. Therefore it is worthwhile examining the effect of model behaviour, and correspond liquid phase ozone residual for different inlet ozone concentrations that presented in this thesis. This can be done in two ways. First by altering nozzles to give a different gas-liquid flow range. Second to insert a manual valve in the gas inlet line. This valve should have a high turndown to allow a wide range of easily controlled flows to be examined. This will produce a different Q_L to Q_G relationship than that presented in this thesis.

The other point to be noted is that this will not dramatically affect the Q_L vs hydraulic residence time relationship. This is because when the gas flow was throttled to zero, only a small change in liquid flowrate vs residence time behaviour was noted.

12.4 GAS PHASE RESIDENCE TIME STUDIES

Large problems with the gas residence time study were evident in this thesis. The were discussed in chapters 9 and 10. The major problem was the extreme difficulty in obtaining measurements with the equipment available. All of the equipment had its own separate no linear response. Each subsequent measurement involved a compounding of the exponential-type responses previous to it. No reliable and accurate way of removing these responses was found.

The first problem is the portable air-water separator. This produces a liquid free air for the ozone detector. This is essential for concentration determination, even if not used for gas phase residence time determination. A more efficient separator needs to be designed. The reason for this is that the current two models are a failure. The larger model (figure 9.21) can take up to 20 minutes or half an hour of manipulation to reach a steady-state value. This is because of its size, and the constant need to disconnect the unit from the ozone contactor to remove the base plug and let the water out. Letting the water out of the separator actually draws in fresh air, thereby reducing the value of ozone determined. This then has to reach steady-state again. It is possible that the liquid level is too high again. The other major problem with this unit is that the gas-water mixture is undergoing mass transfer during separation. This is because the air-water mixture is drawn along 5 mm ID PVC tubing and then into the unit. Once in the unit the inlet line is often under the water level, allowing a bubbling mass transfer to occur.

The smaller unit (figure 9.22) did not solve the problem. The valve arrangement still required removal of the unit from the column, and subsequent air ingress.

In summary a new portable air-water separator is essential for more accurate O_3 detection in the two-phase flow.

The second problem is that of using the reaction system as a tracer. It would be probably of more valve to determine how tracer studies are done in two phase flow. Works such as Hewitt [136]. should provide a useful starting point. It is likely that something such as a radioisotope be used. If this is the case then a negligible detection response would result.

Another major improvement in tracer studies in the gas phase should be to inject the tracer at the exact gas-liquid mix point. This would allow a true profile to be studied and alleviate the need for correction factors. These correction factors complicate the system, and lead to further inaccuracy.

Once a better picture of gas phase residence time is obtained, then a better understanding of the two phase flow modelling can be found. At this stage the model in this thesis is neither proven or disproved.

12.5 LIQUID ENTRAINMENT BY GAS PHASE

As gas phase behaviour is more accurately modelled, it is important to consider to what extent the gas phase entrains droplets of liquid within it. This is important as the gas phase behaviour will then alter slightly the hydraulic residence time. This also has a mass transfer benefit which needs to be accounted for. An initial starting point for annular-mist flow is presented by Hsu and Graham [142].

12.6 LIQUID PHASE RESIDENCE TIMES

The major problem with the liquid phase studies is the need for the column flow pattern to be altered slightly to allow for a side stream flow to be analysed for conductivity changes after the addition of an acid tracer. This could be improved by repositioning the conductivity probe into the main column. If a socket were placed in the main column just allowing for the tip of the conductivity probe to intrude past the column inside wall, then no alteration in column behaviour need occur.

This improved detection system would allow a more accurate hydraulic residence time (HRT) to be determined. This allows for more accurate mass transfer modelling, and to allow for a more realistic evaluation of the co-current two-phase downflow model.

The use of a conductivity meter as a detector of the acid tracer assumes that the response of the meter to a change in pH is fast enough. This was not investigated in this study, however it is worthwhile for future study. The conductivity meter output may need a correction factor, or a different liquid tracer response system may need to be installed.

It is also important to increase the HRT. This is due to the CT disinfection requirements not being met. A common way of doing this is to attach a shorter draft tube than the 1.35 m in this thesis, and to direct the gas-liquid flow into a bubble column, or u-tube type of column. This jet loop and u-tube reactor is common and is examined in a number of sources 129,130,132,133,134,143,146,135.

12.7 MATHEMATICAL MODELLING

Two mathematical model programs were presented in this thesis. The first was the mass transfer model, and the second was the cocurrent two-phase down flow model.

Improvements that can be made to these two models, without altering the methodology, includes:

- streamlining of the code.

- more user friendly operator interface.

- better file input/output handling.

- improvement of numerical solving techniques. For example the mass transfer model requires manual iteration to obtain a result. A number of different techniques were tried without success. This includes the method of Newton and regula falsi [122].

- It also may be possible to obtain useful results for mass transfer modelling that do not involve differential equations. Packages such as Mathematica do allow for simultaneous

solving of differential equations. Initial solving studies for simplified columns provided encouraging results. These studies were performed via use of mathematica. The result of this study is presented in appendix 1.0. The result is a very complex expression.

- simplification of two phase flow model equations, to allow for symbolic solving rather than the iterated solving technique used in the computer model. A brief study was done on this, and results appear in appendix 1.0. A less than satisfactory result was obtained.

12.8 LIQUID PHASE CONCENTRATION

To fully evaluate the mathematical model it is necessary to examine a full liquid phase ozone concentration profile. This was not done in this study. It is necessary to experimentally determine the liquid phase ozone so as the mass transfer behaviour of the model can be evaluated to determine the real C in the CT term, and to find out to what extent the ozone is transferring to the liquid phase, rather than being dissociated in the gas phase, or reacting with the organic or microbe constituent before entering the bulk. There are a number of ways of examining the concentration, and an on-line method rather than a titration method would be preferred. In the study by Katzenelson [70]. conductivity of the liquid phase was related to ozone concentration.

REFERENCES

1. Bourbigot, M.M
"Ozone Disinfection in Drinking Water"
Journal NEWWA, March 1989 pp1-9

2. Echols, J.T. and Mayne, S.T.
"Cooling Tower Management using Ozone instead of Multichemicals"
ASHRAE Journal, June 1990 pp34-38

3. Coin, L., Gomella, C. and Hannoun, C
"Inactivation par l'ozone du virus de la poliomyelite present dans les eaux."
La Presse Medicale, 37, September 1964, pp1880-1884

4. NSW Department of Industrial Relations and Employment
"The Management of Microbial Hazards of Air Conditioning and Warm Water Systems"
Occupational Health and Safety Bulletin No:081188/13
December 1988

5. Edwards, H.E
"Ozone-An Alternative Method of Treating Cooling Tower Water"
Journal of the Cooling Tower Institute, Vol.8,No.2 Summer 1987

6. Lorch, W. (editor)
Stucki, S. (Author, editor of chapter 15)
Handbook of Water Purification, 2nd edition, 513-529

7. Razumovskii, S.D. and Zaikov, G.E.
Ozone and its Reactions with Organic Compounds
Elsevier, Netherlands, 1984

8. Battino, R. (Editor)
'Oxygen and Ozone'
IUPAC Solubility Data Series Vol.7
Permagon Press, 1987

9. Sotello, J.L, Beltran, F.J, Benitez, F.J., Beltran-Heredia, J.
'Henry's Law Constant for the Ozone-Water System'
Water Resources, Vol. 23 No.10 1989, pp1239-1246
Permagon Press 1989

10. Kawamura F.
'Investigation of Ozone. The solubility of Ozone in water and in Dilute Sulfuric Acid'
J.Chem.Soc.Jap, 53, 1932, pp783-787

11. Briner, E. and Perrottet, H.
'Determination of the Solubilities of Ozone in water and in Aqueous solution of Sodium Chloride. Calculation of the solubilities of atmospheric ozone in waters.'
Helv. chim.Acta, 22, 1939, pp397-404

12. Rawson, A.E.
'Ozonization.II.Solubility of Ozone in Water'
Wat.Wat.Engng, 57, 1953, pp102-111

13. Stumm, W.
'Ozone as a disinfectant for water and sewage'
J.Boston Soc.civ.Engng, 45, 1958, pp68-79

14. Mailfert, M.
International Critical Tables, 1st edition Vol. III
McGraw-Hill, 1970, New York

15. Li, K.Y
'Kinetic and Mass Transfer Studies of ozone-phenol reactions in liquid-liquid and gas-liquid systems'
Ph.D Dissertation, 1977, Mississippi State Uni, Miss (USA)

16. Kirk-Othmer (editors)
Nebel, C. (author) 'Ozone'
Kirk-Othmer:Encyclopaedia of Chemical Technology
3rd edition, Vol.16, Wiley-New York, 1981

17. Roth, J.A. and Sullivan, D.E.
'Solubility of Ozone in Water'
Ind.Engng.Chem.Fundam., 20, 1981, pp 137-140

18. Caprio, V., Insola, A., Lingola, P.G., Volpicelli, G.
'A new Attempt for the Evaluation of the Absorption constant of Ozone in Water.'
Chem.Engng.Sci., 37, 1982, pp122-124

19. Morris, J.C.
'The Aqueous Solubility of Ozone-A review'
Ozone News, 16, 1988, pp14-16

20. Hines, A.L and Maddox, R.N
Mass Transfer - Fundamentals and Applications
Prentice-Hall, New Jersey(USA), 1985

21. Wright, P.C.
Removal of Organics from Bayer Liquors using Ozone
BE Thesis, University of NSW (Sydney, Aust), 1991

22. Bird, R.B., Stewart, W.E. and Lightfoot, E.N.
Transport Phenomena
John Wiley & Sons, Singapore, 1960

23. Sherwood, T.K., Pigford, R.L. and Wilke, C.R.
Mass Transfer
McGraw-Hill, New York, 1975

24. Gilliland, E.R.
Ind.Eng.Chem., 26, 681, 1934

25. Fuller, E.N., Schettler, P.D. and Giddings, J.C.
Ind.Eng.Chem., 58, 19, 1966

26. Marrero, T.R. and Mason. E.A.
J.Phys.Chem.Ref.Data., 1, 3, 1972

27. Frenkel, J.
Kinetic Theory of Liquids
Clarendon Press, Oxford (UK), 1946

28. Wilke, C.R. and Chang, P.
AIChemE J., 1, 264, 1955

29. Sitaraman, R., Ibrahim, S.H. and Kuloor, N.R.
J.Chem.Eng.Data., 8, 198, 1963

30. Vignes, A.
Ind.Eng.Chem.Fundam., 5, 189, 1966

31. Leffler, J. and Cullinan, H.T.
Ind.Eng.Chem.Fundam., 9, 84, 1970

32. Nernst, W.
Z.Phys.Chem., 2, 613, 1888

33. Robinson, R.A. and Stokes, R.H.
Electrolyte Solutions, 2nd ed
Academic Press, McGraw-Hill, New York, 1977

34. Perry, R.H. and Green, D. (editors)
Perry's Chemical Engineers' Handbook, 6th edition
McGraw-Hill, Singapore, 1987

35. Smith, J.M. and Van Ness, H.C.
Introduction to Chemical Engineering Thermodynamics
McGraw-Hill, Singapore, 1987

36. Coulson, J.M., Richardson, J.F., Backhurst, J.R., Harker, J.H.
Chemical Engineering Volume 1, 3rd edition (SI Units)
Permagon Press, Great Britain, 1988

37. Boddeus, K.S
A Study of the Phenomena Associated with the Mass Transfer of Ozone to Cooling Tower Waters
ME Thesis, University of Wollongong, 1991

38. Akita, K. and Yoshida, F.
'Gas Hold-up and Volumetric Mass Transfer Coefficient in Bubble Columns'
Ind.Eng.Chem.Process Des.Develop., Vol. 12, No.1, 1973

39. Akita, K. and Yoshida, F.
A.I.Ch.J., Vol.11, No.9, 1965

40. Fair, J.R., Lambright, A.J. and Anderson, J.W.

Ind.Eng.Chem.Process Des.Develop., 1, 33, 1962

41. Echols, J.T. and Mayne, S.T.
'Cooling Tower Water Clean-up by Ozone'
Chemical Engineering, May 1990, 163-167

42. Yuteri, C. and Gurol, M.D.
'Specific Ozone Utilisation in Waste Waters: The Effects of Background Organic Matter, pH and Carbonate Species'
Ozone Sci.,Eng, Vol. 10, 1987, pp 277-290

43. Gurol, M.D.
Factors Controlling the Removal of Organic Pollutants in Ozone Reactors'
Jour.AWWA, 77, 55, 1985

44. Yurteri, C. and Gurol, M.D.
'Removal of Dissolved Organic Contaminants by Ozonation'
Environmental Progress, Vol.6, No.4, 1987, 240-245

45. Gurol, M.D. and Singer, P.C.
'Kinetics of Ozone Decomposition:A Dynamic Approach'
Environ.Sci.Technol., Vol.16, No.7, 1982, 377-383

46. Mehta, Y.M., George, C.E. and Kuo, C.H.
'Mass Transfer and Selectivity of Ozone Reactions'
The Canadian Journal of Chemical Engineering, Vol.67, February 1989, 118-126

47. Whitman, W.G.
'The Two-film Theory of Absorption'
Chem. and Met.Eng., 29, 147, 1923

48. Higbie, R.
'The Rate of Absorption of Pure Gas into a Still Liquid During Short Periods of Exposure.'
Trans.Am.Inst.Chem.Eng., 31, 365, 1935

49. Danckwerts, P.V.
'Significance of liquid film coefficients in gas absorption.'
Ind.Eng.Chem., 43, 1460, 1951

50. Harriott, P.
'A Random Eddy Modification of the Penetration Theory.'
Chem.Eng.Sci., 17, 149, 1962

51. Toor, H.L. and Marchello, J.M.
'Film-penetration model for Mass and Heat Transfer.'
A.I.Ch.E. Jl., Vol. 4, 1958, p 97

52. Stich, F.A. and Bhattacharyya, D.
'Ozonolysis of Organic Compounds in a Two-Phase Fluorocarbon-Water System'
Environmental Progress, Vol.6, No.4, Nov 1987

53. Klien,E., McKelvey and Weber, B.G.

'The Simultaneous Measurement of Distribution Coefficients and Hydrolysis Rates'
J.Chem.Phys., 62, 286-288, March 1958

54. Kuo, C.H. and Huang, C.J.
'Liquid Phase Mass Transfer with Complex Chemical Reaction'
AIChemE Journal, 16, No.3, 493-496, May 1970

55. Merchuk, J.C. and Farino, I.H.
'Simultaneous Diffusion and Chemical Reaction in Two Phase Systems.'
Chem.Eng.Sci., 31, 645-650, 1976

56. Sharma, M.M and Mhaskar, R.D.
'Extraction with Reaction in Both Phases.'
Chem.Eng.Sci., 30, 811-818, 1975

57. Glynn, W.K.
'Two-Phase Oxidation of Toxic Organic Compound.'
M.S.Thesis, Univ of Kentucky (Lexington KY), USA, 1984

58. Hoigne, J. and Bader, H.
'Rate Constants of Reactions of Ozone with Organic and Inorganic Compounds in Water'
Water.Res., Vol.11, 1983, 173

59. Matter-Muller, C. et.al
'Transfer of Volatile Substances from Water to the Atmosphere'
Water Res., 15:1271, 1981

60. Gurol, M.D. and Singer, P.C.
'Dynamics of the Ozonation of Phenol-Mathematical Simulation'
Water Res.,17:1173, 1983

61. Gurol, M.D. and Nekouinaini, S.
'Effects of Organic Substances on Mass Transfer in Bubble Aeration'
Jour. WPCF, 57:3:235, 1985

62. Shah, Stiegel, Sharma
J.Am.Inst.Chem.Eng., 24, 1978, 369

63. Sherwood, Pigford and Wilke
Mass Transfer
McGraw-Hill, New York (USA), 1975, p615

64. Berg, J.D., Hoff, J.C., Roberts, P.V. and Matin, A.
'Resistance of Bacterial Subpopulations to Disinfection by Chlorine Dioxide'
Journal AWWA, September 1988, pp115-119

65. Yuteri, C., Ryan, D.F., Callow, J.J. and Gurol, M.D.
'The Effect of Chemical Composition on Henry's Law Constant'
Journal WPCF, Vol. 59, No.11, 950-956

66. Lincoff, A.H. and Gossett, J.M.

'The Determination of Henry's Law Constant for Volatile Organics by Equilibrium Partitioning in Closed Systems.'
International Symposium on Gas Transfer at Water Surfaces , Cornell University, Ithaca, N.Y., 1983

67. Chick. H.
'An Investigation into the Laws of Disinfection.'
Jour.Hygiene, 8, 92, 1908

68. Moats, W.A.
'Kinetics of Thermal Death of Bacteria'
Jour. Bacteriol., 105:165, 1971

69. Gard, S.
'Chemical Inactivation of Viruses'
Ciba Foundation Symposium on Nature of Viruses, 1957

70. Katzenelson,E., Kletter, B. and Shuval, H.I.
'Inactivation Kinetics of Viruses and Bacteria in Water by Use of Ozone'
Jour. AWWA., 66:12:725, December 1974

71. Tilson, D.L. and Siedler, R.T.
'Legionella Incidence and Density in Potable Drinking Water Supplies'
Appl.Envir.Microbiol., 45:337, 1983

72. Plouffe, J.F.
'Relationship Between Colonisation of Hospital Buildings with L.pneumophila and Hot Water Temperatures'
Appl.Envir.Microbiol., 46:769, 1983

73. Wang, W.L.L.
'Growth, Survival and Resistance of Legionnaires' Disease Bacterium.'
Annals Internal Med., 90:614, 1979

74. Levenspiel, O.
Chemical Reaction Engineering
2nd Edition, John Wiley & Sons, Singapore, 1972

75. Yurteri,C. and Gurol, M.D.
'Ozonation of Trace Organic Compounds: Model Predictions versus Experimental Data'
Ozone Sci.,Eng, Vol.12 No.3., 1990, 217-229

76. Munter, R., Kamenev, S. and Sarv, L.
'Design and Modelling of a Staged Downflow Bubble Reactor.'
Ozone Sci.,Eng., Vol.12 No.4., 1990, 437-455

77. Schneider, K.R., Steslow, F.S., Sierra, F.S., Rodrick, G.E. and Noss, C.I.
'Ozone Disinfection of Vibrio vulnificus in Artificial Seawater.'
Ozone Sci.,Eng., Vol.12 No.4., 1990, 423-435

78. Merz, E. and Gaia, F.
'Comparison of Economics of Various Ozone Generation Systems.'

Ozone Sci.,Eng., Vol.12 No.4., 1990, 401-419

79. Sotelo, J.L., Beltran, F.J., Encinar, J.M. and Gonzalez, M.
'Application of Gas Absorption Theories to o-Cresol Ozonation in Water.'
Ozone Sci.,Eng., Vol.12 No.4., 1990, 341-353

80. Nilmani, M., Maxwell, T.T., Robertson, D.G.C. and Spalding, D.B.
'Prediction of Initial Motion of a Gas Bubble in Liquids.'
Appl.Math.Modelling, Vol.5 Feb.1981, 24-28

81. Whitlow, J.E. and Roth, J.A.
'Heterogeneous Ozonation Kinetics of Pollutants in Wastewater.'
Environ. Prog., Vol.7 No.1., Feb 1988, 52-57

82. Betterton, E.A. and Hoffmann, M.R.
'Henry's Law Constants of Some Environmentally Important Aldehydes.'
Environ.Sci.Technol., Vol.22 No.12., 1988, 1415-1418

83. Sehested, K., Hanne, C., Holcman, J., Fischer, C.H. , Hart, E.J.
'The Primary Reaction in the Decomposition of Ozone in Acidic Aqueous Solutions.'
Environ.Sci.Technol., Vol.25, No.9, 1991

84. Weiss, J.
Trans.Faraday Soc, Vol. 31, 1935, pp 668-681

85. Sotelo, J.L., Beltran, F.J., Benitez, F.J., Beltran-Heredia
J.Ind.Eng.Chem.Res., Vol.26, 1987, 39-43

86. Forchheimer, O.L., Taube, H.
J.Am.Chem.Soc., Vol.76, 1954, 2099-2103

87. Benson, S.W. and Axeworthy, A.E.
J.Chem.Phys, Vol.26, 1957, pp1718-1726

88. Norrish, R.G.W., Wayne, R.P.
Proc.R.Soc.London, A 1965, 288, 361-373

89. Sehested, K., Holcman, J., Hart, E.J.
J.Phys.Chem., Vol.88, 1984, 4144-4147

90. Bielski, B.H.
J.Photochem.Photobiol., Vol.28, 1978, 645-649

91. Sehested, K., Holcman, J.
J.Phys.Chem., Vol.87, 1983, 1951-1954

92. Sehsted, K., Holcman, J., Bjergbakke, E., Hart, E.J.
J.Phys.Chem., Vol.88, 1984, 269-273

93. Sehested, K., Lang Rasmussen, O., Fricke, H.
J.Phys.Chem., Vol.72, 1968, 626-631

94. Asher, W.E., Pankow, J.F.
'Prediction of Gas/Water Mass Transfer Coefficients by a Surface Renewal Model'
Environ.Sci.Technol., Vol.25, No.7, 1991, 1294-1300

95. Shetty, S.A., Kantak, M.V. and Kelkar, B.G.
'Gas-Phase Backmixing in Bubble-Column Reactors.'
AIChE Journal, Vol.38 No.7, July 1992, 1013-1026

96. Leva, Max
'Reconsider Packed-Tower Correlations.'
Chem.Eng.Prog., January 1992, 65-72

97. Abraham, M. and Sawant, S.B.
'Hydrodynamics and Mass Transfer Characteristics of Packed Bubble Columns.'
The Chemical Engineering Journal, Vol.43, 1990, 95-105

98. Kawase, Y. and Tokunaga, M.
'Characteristic Mixing Length in Bubble Columns.'
The Canadian Journal of Chemical Engineering, Vol.69, Oct 1991, 1228-1231

99. Schechter, H.
'Spectrophotometric Method for Determination of Ozone in Aqueous Solutions.'
Wtr.Res., &:729, 1973

100. Xenos, Dennis John
'Further Investigation on the Design of a Venturi Suction System and Contact Chamber for Ozone Injection into Cooling Tower Water.'
BE Thesis, University of Wollongong, 1991

101. Soh, Wee-King, Montagner, G.John and Rowley, S.D.
'A Jet Ejector System for the Transfer of Ozone into Water.'
Transport Phenomena in Heat and Mass Transfer, J.A. Reizes (Editor), Elsevier Science Publishers, 1992

102. Zhu, Qingshi, Liu, Cunli and Xu, Zhengyu
'A Study of Contacting Systems in Water and Wastewater Disinfection by Ozone. 2. Mathematical Models of the Ozone Disinfection Process with a Static Mixer.'
Ozone Sci.,Eng., Vol. 11, 1989, pp189-207

103. Rakness, K.L., Renner, R.C., Hegg, B.A. and Hill, A.G.
'Practical Design Model for Calculating Bubble Diffuser Contactor Ozone Transfer Efficiency.'
Ozone Sci.,Eng., Vol. 10, 1988, pp173-214

104. Yurteri, C. and Gurol, M.D.
'Ozone Consumption in Natural Waters: Effects of Background Organic Matter, pH and Carbonate Species.'
Ozone Sci.,Eng., Vol. 10, 1988, pp 277-290

105. Wickramanayake, G.B. and Sproul, O.J.
'Ozone Concentration and Temperature Effects on Disinfection Kinetics.'
Ozone Sci.,Eng., Vol. 10, 1989, pp123-135

106. Stankovic, Ivan
'Comparison of Ozone and Oxygen Mass Transfer in a Laboratory and Pilot Plant Operation.'
Ozone Sci.,Eng., Vol. 10, 1988, pp 321-338

107. Zhu, Qingshi, Liu, Cunli and Xu, Zhengyu
'A Study of Contacting Systems in Water and Wastewater Disinfection by Ozone. 1.Mechanism of Ozone Transfer and Inactivation Related to the Contacting Method Selection.'
Ozone Sci.,Eng., Vol. 11, 1989, pp 169-188

108. Kaiga, N., Seki, T. and Iyasu, K.
'Ozone Treatment in Cooling Water Systems.'
Ozone Sci.,Eng., Vol. 11, 1989, pp 325-338

109. Grasso, Domenic
'Ozonation of Drinking Water: A Design Methodology. I.Background and Design Rationale.'
Ozone Sci.,Eng., Vol. 9, 1987, pp 109-124

110. Grasso, Domenic
'Ozonation of Drinking Water: A Design Methodology. II.Mass Transfer and Contacting.'
Ozone Sci.,Eng., Vol. 9, 1987, pp 125-140

111. Wellauer, R. and Oldani, M.
'Cooling Water Treatment with Ozone.'
Ozone Sci.,Eng., Vol. 12 No.3, 1990, pp 243-253

112. Quederni, A., Mora, J.C. and Bes, R.S.
'Ozone Absorption in Water: Mass Transfer and Solubility.'
Ozone Sci.,Eng., Vol. 9 No.1, 1987, pp 1-12

113. Richard, Yves.R.
'Improvement of Ozone Oxidation and Disinfection Design.'
Ozone Sci.,Eng., Vol. 8 No.3, 1986, pp 261-273

114. Nieminski, Eva.E.
'Ozone Contactor Hydraulic Considerations in Meeting "CT" Disinfection Requirements.'
Ozone Sci.,Eng., Vol. 12 No.2, 1990, pp 133-143

115. Finch, Gordon R. and Smith, Daniel W.
'Evaluation of Empirical Process Design Relationships for Ozone Disinfection of Water and Wastewater.'
Ozone Sci.,Eng., Vol. 12 No.2, 1990, pp 157-175

116. Xu, Fuchun and Lui, Cunli
'Mass Balance Analysis of Ozone in a Conventional Bubble Column.'
Ozone Sci.,Eng., Vol. 12 No.3, 1990, pp 269-279

117. Zhu, Qingshi, Liu, Cunli and Xu, Zhengyu

'A Study of Contacting Systems in Water and Wastewater Disinfection by Ozone. 1. Mechanism of Ozone Transfer and Inactivation Related to the Contacting Method Selection.'
Ozone Sci.,Eng., Vol. 11, 1989, pp169-188

118. Lev, O. and Regli, S.
'Evaluation of Ozone Disinfection Systems: Characteristic Concentration C.'
J.Envir.Engrg., Vol. 118 No.4, July-Aug 1992, pp477-494

119. Brodard, E., Roustan, M. and Mallevaille, J.
'A New Method to Dissolve Ozone into Water: Deep U-Tube.'
Proc. 6th Ozone World Congress, Intl.Ozone Assoc., 1983, pp 27-29

120. Brodard, E., Duguet, J.P., Mallevaille, J. and Roustan, M.
'Le Tube en U, un nouveau reacteur de desinfection des eaux par l'ozone.'
L'Eau, l'Industrie, les Nuisances, 91, 1985, pp20-24

121. Dauthuille, P., Druesne, M. and Richard, Y.
'Tracage au lithium du tube en U d'Aubergenville.'
Document interne Degremont, 1985

122. Kreyszig, E.
Advanced Engineering Mathematics, 6th Edition
John Wiley & Sons, USA, 1988

123. Singer, Phillip C.
'Critical Elements of Process Design for Ozonation systems.'
Proc. of the 1991 AWWA Annual Conf., Philadelphia (USA), June 23-27, 1991

124. Jensen, J.N. and Coulibaly, T.
'Ozone Demand of Raw Drinking Water.'
Proc. of the 1991 AWWA Annual Conf., Philadelphia, June 23-27, 1991

125. Danckwerts, P.V.
Gas-Liquid Reactions
McGraw-Hill, New York, 1970

126. Mecklenburgh, J.C. and Hartland, S.
The Theory of Backmixing (The Design of Continuous Flow Chemical Plant with Backmixing).
John Wiley and Sons, London, 1975

127. Coulson, J.M., Richardson, J.F. and Sinnott, R.K.
Chemical Engineering Volume 6 - Design (in SI Units)
Permagon Press, Great Britain, 1986

128. Azzopardi, B.J.
'Liquid Distribution in Venturi Scrubbers: The Importance of Liquid Films on the Channel Walls'
Chem.Eng.Sci., Vol.48 No.15, 1993, pp 2808-2813

129. Cramers, P.H.M.R., van Dierendonck, L.L. and Beenackers, A.A.C.M.
'Influence of the Gas Density on the Gas Entrainment Rate and Gas Hold-Up in Loop-Venturi Reactors.'

Chem.Eng.Sci., Vol.47 No.9-11, 1992, pp 2251-2256

130. Roustan, M., Line, A. and Wable, O.
'Modelling of Vertical Downward Gas-Liquid Flow for the Design of a New Contactor.'
Chem.Eng.Sci., Vol.47 No.13/14, 1992, pp3681-3688

131. Briens, C.L., Huynh, L.X., Large, J.F., Catros, A., Bernard, J.R. and Bergougnou, M.A.
'Hydrodynamics and Gas-Liquid Mass Transfer in a Downward Venturi-Bubble Column Combination.'
Chem.Eng.Sci., Vol.47 No.13/14, 1992, pp3549-3556

132. Cramers. P.H.M.R., Beenackers, A.A.C.M. and van Dierendonck, L.L.
'Hydrodynamics and Mass Transfer Characteristics of a Loop-Venturi Reactor with a Downflow Liquid Ejector.'
Chem.Eng.Sci., Vol.47 No.13/14, 1992, pp3557-3564

133. Evans, G.M., Jameson, G.J. and Atkinson, B.W.
'Prediction of the Bubble Size Generated by a Plunging Liquid Jet Bubble Column.'
Chem.Eng.Sci., Vol.47. No.13/14, 1992, pp3265-3272

134. Dirix, C.A.M.C. and van der Wiele, K.
'Mass Transfer in Jet Loop Reactors.'
Chem.Eng.Sci., Vol.45 No.8, 1990, pp2333-2340

135. Zhu, Z.M., Hannon, J. and Green, A.
'Use of High Intensity Gas-Liquid Mixers as Reactors.'
Chem.Eng.Sci., Vol.47 No.9-11, 1992, pp2847-2852

136. Hewitt, G.F.
Measurement of Two-Phase Flow Parameters.
Academic Press Inc. (London), 1978

137. Dukler, A.E. and Taitel, Y.
'Flow Pattern Transitions in Gas-Liquid Systems: Measurement and Modelling.'
Chapter 1 in Multiphase Science and Technology -Volume 2
Hewitt, G.F., Delhaye, J.M. and Zuber, N.(editors)
Hemisphere Publishing Corporation (USA), 1986

138. Lockhart, R.W. and Martinelli R.C.
'Proposed Correlation of Data for Isothermal Two-Phase Flow in Pipes.'
Chem.Eng.Prog., Vol. 45, 1949

139. Holman, J.P.
Heat Transfer (SI Metric Edition)
McGraw-Hill, Singapore, 1989

140. Herbrechtsmier, P., Schafer, H. and Steiner, R.
'Oxygen and Ozone Absorption in Downflow Bubble Columns.'
Ozone Sci.,Eng., Vol.9, 1987, pp217-232

141. Stephanopoulos, G.

Chemical Process Control - An Introduction to Theory and Practice.
Prentice-Hall(USA), 1984

142. Hsu, Yih and Graham, Robert W.
Transport in Boiling and Two-Phase Systems
Hemisphere Publishing (USA), 1976

143. Velan, M. and Ramanujam, T.K.
'Gas-liquid Mass Transfer in a Down Flow Jet Loop Reactor.'
Chem.Eng.Sci., Vol.47 No.9-11, 1992, pp 2871-2876

144. Rice, R.G.
'Applications of Ozone in Soft Drink Bottling Plants.'
Rice International Consulting Enterprises, Maryland USA, 1987

145. Nagel, O. , Hegner, B. and Kurten, H.
'Criteria for the Choice and Design of Gas/Liquid Reactors.'
Chemie Ingenieur Technik, 1978, pp934-944

146. Dutta, N.N. and Raghavan, K.V.
'Mass Transfer and Hydrodynamic Characteristics of Loop Venturi Reactors with Downflow Liquid Jet Ejector.'
The Chem.Eng.J., Vol.36, 1987, pp 111-121

147. Seno, Tadachika , Uchida, Shigeo and Tsuyutani, Shinji
'Mass Transfer in Countercurrent and Cocurrent Bubble Columns.'
Chem.Eng.Technol., Vol.13, 1990, pp 113-118

148. Gharat, S.D. and Joshi, J.B.
'Transport Phenomena in Bubble Column Reactors I: Flow Pattern.'
The Chem.Eng.J., Vol.48, 1992, pp141-151

149. Hewitt, G.F. and Govan, A.H.
'Multiphase Flow Systems.'
Imperial College of Science, Technology and Medicine: Department of Chemical Engineering and Chemical Technology-Research Review 1989-1991
Miter Press Ltd., London, January 1992

150. Calibration Manual for OREC Model DM-100 Ozone Monitor
Ozone Research and Equipment Corporation
Phoenix, Arizona (USA)

151. Rowley, S.D.
'The Design of a Venturi Suction System and Contact Chamber for Ozone Injection into Cooling Tower Water.'
BE Thesis, University of Wollongong, Februrary 1990

APPENDIX 1.0

A1.1 GRAPHICAL TECHNIQUES

A1.1.1 SIMPSON'S RULE

In Residence Time Distribution (RTD) Studies one of the important methods for evaluating data on mean residence times was finding the area under curves. This was achieved using Simpson's Rule. This rule is much more accurate than other area calculations such as the Rectangular Rule and the Trapezoidal Rule. This is because the former is based on constant approximations of area and the later is based on linear approximations of area, whilst Simpson's Rule is based on quadratic approximations of area.

The algorithm used was based on that of Kreyszig [122]. This algorithm is as follows:

Compute area under curve between:

$x = a$ and $x = b$ for equidistant values of x

i.e.

$$x_0 = a,\ x_1 = x_0+h,\ x_2 = x_0+2h \ldots\ x_{2n} = x_0 + 2nh = b$$

and

$$f_0 = f(x_0) = f(a),\ f_1 = f(x_1),\ \ldots,\ f_{2n} = f(x_{2n}) = f(b)$$

and so compute

$$s_0 = f_0 + f_{2n}$$

$$s_1 = f_1 + f_3 + \ldots + f_{2n-1}$$

$$s_2 = f_2 + f_4 + \ldots + f_{2n-2}$$

$$h = (b-a)/2n$$

$$\text{Area} = (h/3)(s_0 + 4s_1 + 2s_2)$$

A1.2 SOLUTION OF EQUATIONS BY ITERATION

A1.2.1 NEWTON'S METHOD OF SOLVING EQUATIONS OF f(x)=0.

A common method used to solve equations of this form is the Newton Method or the Newton-Raphson method. The Newton method is normally a quick method of solving equations. Its basis of converging on the solution is to approximate the curve by a series of tangents. The method is started by an initial estimate of the value of x ($x=x_0$)that will make $f(x)=0$. If the tangent of f(x) is projected to the $f(x)=0$ line this will give the value of x_1. This method is then repeated with x_1 supplying the point $f(x_1)$, and so on until the difference between the current and the previous root reaches a suitably small value. Therefore the 'real' root is found. This is shown diagramatically below:

FIGURE A1.1 NEWTON'S METHOD [122].

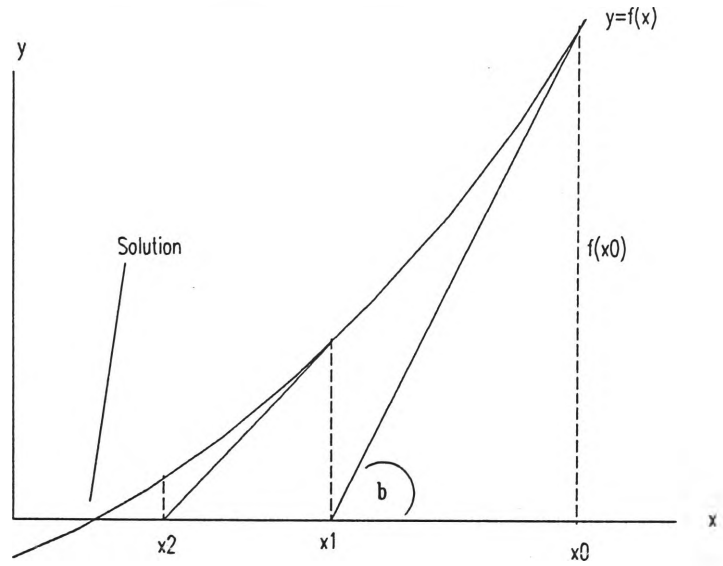

Kreyszig [122] states that this method assumes a continuous derivative along all of f(x), as this is necessary to find the solution. The slope or derivative at a point on f(x) is defined by:

$f'(x) = f(x_0)/(x_0-x_1)$ and so on.

The value of x_1 is then:

$$x_1 = x_0 - f(x_0)/f'(x_0)$$

and so in general [122].:

$$x_{n+1} = x_n - f(x_n)/f'(x_n)$$

A1.2.2 SECANT METHOD FOR SOLVING EQUATIONS

This method is similar to the Newton Method of solving equations of the form f(x)=0, except the derivative f'(x) is not evaluated. Instead a difference quotient is evaluated [122]. This quotient is similar to the derivative.

That is:

$$f'(x_n) = \frac{f(x_n)-f(x_{n-1})}{x_n - x_{n-1}}$$

This result gives the corresponding equation for determination of the root:

$$x_{n+1} = x_n - f(x_n)\ \frac{(x_n - x_{n-1})}{(f(x_n)-f(x_{n-1}))}$$

This result is shown in figure A1.2:

FIGURE A1.2 SECANT METHOD FOR EQUATION SOLVING [122].

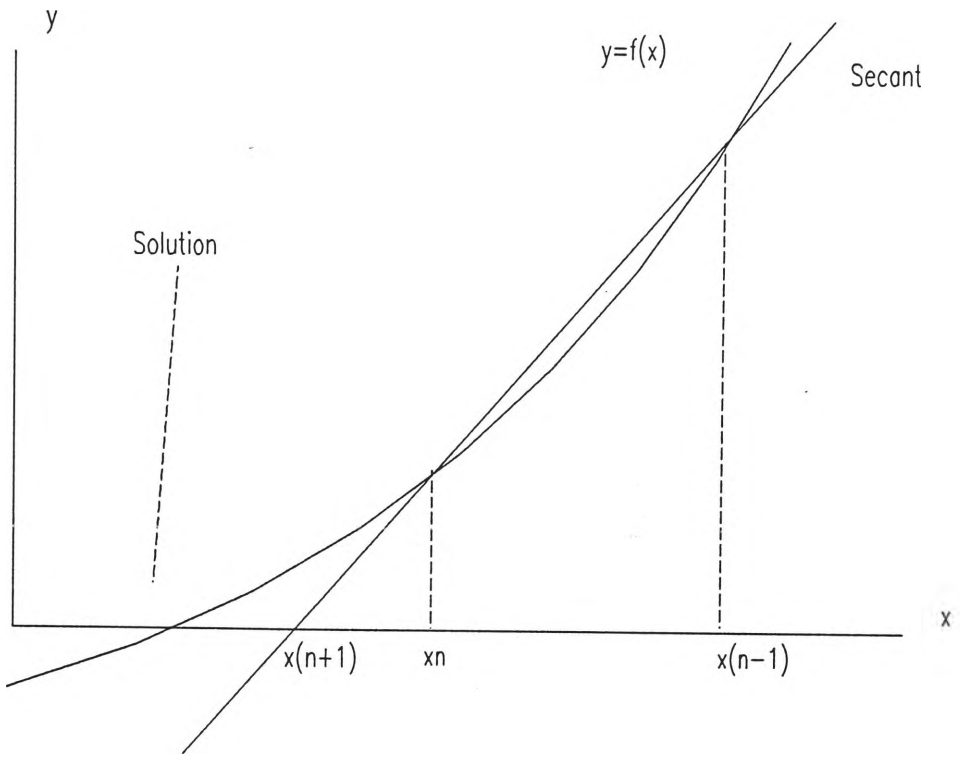

This method is used where the evaluation of the derivative of f(x) is difficult. Kreyszig [122.] suggests that this method "is still preferable when the work of computing a value of f'(x) is more than 1/2 times more the work of computing a value of f(x)". He [122.] also warns that this method may not be as accurate as the Newton method.

This method requires two initial estimates of x values to compute the third point.

A 1.3 TWO PHASE DOWNFLOW MODEL MANIPULATION

TWO PHASE FLOW MODELLING OF MODEL FOR CO-CURRENT DOWNFLOW (PROPOSED BY DUKLER & TAITEL)

Initial Parameters:

$A_L = \pi \cdot z \cdot (-1 + z)$ $A_L = \pi \cdot (z - z^2)$ $S_i = \pi \cdot (1 - 2 \cdot z)$

$A_G = \pi \cdot (0.5 - z)^2$ $S_L = \pi$

Now,

$z = \frac{h}{D}$ Where h= film thickness (m)
D= pipe diameter (m)

$U_L = \frac{A_L + A_G}{A_L}$ Substituting: $U_L = \frac{\left[\pi \cdot (z - z^2) + A_G\right]}{\left[\pi \cdot (z - z^2)\right]}$

$U_L = \frac{\left[\pi \cdot (z - z^2) + \pi \cdot (.5 - z)^2\right]}{\left[\pi \cdot (z - z^2)\right]}$

Simplifying:

$U_L = \frac{-1}{(4 \cdot (z \cdot (-1 + z)))}$

$U_G = \frac{A_L + A_G}{A_G}$ Substituting: $U_G = \frac{\left[-\pi \cdot z \cdot (-1 + z) + A_G\right]}{A_G}$

$U_G = \frac{\left[-\pi \cdot z \cdot (-1 + z) + \pi \cdot (.5 - z)^2\right]}{\left[\pi \cdot (.5 - z)^2\right]}$

Simplifying:

$U_G = \frac{1}{(-1. + 2. \cdot z)^2}$

Hydraulic Diameter Parameters:

$D_L = 4 \cdot \frac{A_L}{S_L}$ Substituting: $D_L = \left[\frac{4}{S_L} \cdot A_L = \frac{4}{S_L} \cdot \pi \cdot (z - z^2)\right]$

$D_L = \left(\frac{4}{\pi} \cdot A_L = 4 \cdot z - 4 \cdot z^2\right)$

$D_G = 4 \cdot \frac{A_G}{S_i}$ Substituting: $D_G = \left[\frac{4}{S_i} \cdot A_G = \frac{4}{S_i} \cdot \pi \cdot (.5 - z)^2\right]$

$D_G = \left[\frac{4}{(\pi \cdot (1 - 2 \cdot z))} \cdot A_G = \frac{4}{(1 - 2 \cdot z)} \cdot (.5 - z)^2\right]$

$D_G = \left[\frac{-4}{(\pi \cdot (-1 + 2 \cdot z))} \cdot A_G = 1. - 2. \cdot z\right]$

Substitute into correlation equation, and manipulate:

$$X^2\cdot\left[\left(U_L\cdot D_L\right)^{-1\cdot n}\cdot U_L^{\,2}\cdot\frac{S_L}{A_L}\right]-\left(U_G\cdot D_G\right)^{-1\cdot m}\cdot U_G^{\,2}\cdot S_i\cdot\left(\frac{1}{A_L}+\frac{1}{A_G}\right)-4\cdot Y=0$$

Note that effectively this equation is dimensionless. The X and Y parameters are functions of the column.

$$X^2\cdot\left(U_L\cdot D_L\right)^{(-n)}\cdot U_L^{\,2}\cdot\frac{S_L}{A_L}-\left[U_G\cdot(1.-2.\cdot z)\right]^{(-m)}\cdot U_G^{\,2}\cdot S_i\cdot\left(\frac{1}{A_L}+\frac{1}{A_G}\right)-4\cdot Y=0$$

$$\frac{1}{16}\cdot X^2\cdot\frac{\left[\frac{-1}{(4\cdot(z\cdot(-1+z)))}\cdot D_L\right]^{(-n)}\cdot S_L}{\left[z^2\cdot(-1+z)^2\right]\cdot A_L}-\left[U_G\cdot(1.-2.\cdot z)\right]^{(-m)}\cdot U_G^{\,2}\cdot S_i\cdot\left(\frac{1}{A_L}+\frac{1}{A_G}\right)-4\cdot Y=0$$

$$\frac{1}{16}\cdot X^2\cdot\frac{\left[\frac{-1}{(4\cdot(z\cdot(-1+z)))}\cdot D_L\right]^{(-n)}\cdot S_L}{\left[z^2\cdot(-1+z)^2\right]\cdot A_L}-\frac{\left[\frac{1}{(-1.+2.\cdot z)^2}\cdot(1.-2.\cdot z)\right]^{(-m)}}{(-1.+2.\cdot z)^4}\cdot S_i\cdot\left(\frac{1}{A_L}+\frac{1}{A_G}\right)-4\cdot Y=0$$

$$\left[\frac{-1}{16}\cdot X^2\cdot\frac{\left[\frac{-1}{(4\cdot(z\cdot(-1+z)))}\cdot D_L\right]^{(-n)}\cdot S_L}{\left[z^3\cdot(-1+z)^3\right]\cdot\pi}-Q\right]-4\cdot Y=0$$

Where $$Q=\frac{\left[\frac{1}{(-1.+2.\cdot z)^2}\cdot(1.-2.\cdot z)\right]^{(-m)}}{(-1.+2.\cdot z)^4}\cdot S_i\cdot\left[\frac{-1}{(\pi\cdot(z\cdot(-1+z)))}+\frac{1}{A_G}\right]$$

And

$$\frac{-1}{16}\cdot X^2\cdot\frac{\left[\frac{-1}{(4\cdot(z\cdot(-1+z)))}\cdot D_L\right]^{(-n)}\cdot S_L}{\left[z^3\cdot(-1+z)^3\right]\cdot\pi}-P-4\cdot Y=0$$

Where $$P=\frac{\left[\frac{1}{(-1.+2.\cdot z)^2}\cdot(1.-2.\cdot z)\right]^{(-m)}}{(-1.+2.\cdot z)^4}\cdot S_i\cdot\left[\frac{-1}{(\pi\cdot(z\cdot(-1+z)))}+\frac{1}{\left[\pi\cdot(.5-z)^2\right]}\right]$$

And

$$\frac{-1}{16}\cdot X^2\cdot\frac{\left[\frac{-1}{(4\cdot(z\cdot(-1+z)))}\cdot D_L\right]^{(-n)}\cdot S_L}{\left[z^3\cdot(-1+z)^3\right]\cdot\pi}-N-4\cdot Y=0$$

Where: $$N=\frac{\left[\frac{1}{(-1.+2.\cdot z)^2}\cdot(1.-2.\cdot z)\right]^{(-m)}}{(-1.+2.\cdot z)^4}\cdot\pi\cdot(1-2\cdot z)\cdot\left[\frac{-1}{(\pi\cdot(z\cdot(-1+z)))}+\frac{1}{\left[\pi\cdot(.5-z)^2\right]}\right]$$

$$\frac{-1}{16}\cdot X^2\cdot\frac{\left[\frac{-1}{(4\cdot(z\cdot(-1+z)))}\cdot D_L\right]^{(-n)}}{\left[z^3\cdot(-1+z)^3\right]}-M-4\cdot Y=0$$

Where

$$M=\frac{\left[\frac{1}{(-1.+2.\cdot z)^2}\cdot(1.-2.\cdot z)\right]^{(-m)}}{(-1.+2.\cdot z)^4}\cdot\pi\cdot(1-2\cdot z)\cdot\left[\frac{-1}{(\pi\cdot(z\cdot(-1+z)))}+\frac{1}{\left[\pi\cdot(.5-z)^2\right]}\right]$$

$$\frac{-1}{16}\cdot X^2\cdot\frac{\left[\frac{-1}{(4\cdot(z\cdot(-1+z)))}\cdot\left(4\cdot z-4\cdot z^2\right)\right]^{(-n)}}{\left[z^3\cdot(-1+z)^3\right]}-L-4\cdot Y=0$$

Where

$$L=\frac{\left[\frac{1}{(-1.+2.\cdot z)^2}\cdot(1.-2.\cdot z)\right]^{(-m)}}{(-1.+2.\cdot z)^4}\cdot\pi\cdot(1-2\cdot z)\cdot\left[\frac{-1}{(\pi\cdot(z\cdot(-1+z)))}+\frac{1}{\left[\pi\cdot(.5-z)^2\right]}\right]$$

As can be seen this equation ends up being extremely difficult to solve for z and so for the film thickness h. Therefore a numerical iterative solution to this equation is preferable.

A 1.4 OZONE MASS TRANSFER MODEL MANIPULATIONS

The following data is mathematical manipulation of the ozone mass transfer model equations developed in this thesis. It is presented as a guide of the complexitity of mathematical equation solving. The nomenclature is as that presented in chapter 8 and in computer modelling. (Output from MATHEMATICA package)

```
o3g'[t]==kLa (o3[t]-o3g[t]/H) (QLQG)
eqn1=%
o3'[t]==kLa (o3g[t]/H-o3[t])-w o3[t] hl
eqn2=%
```

$$o3g'[t] == kLa\ QLQG\left(o3[t] - \frac{o3g[t]}{H}\right)$$

$$o3g'[t] == kLa\ QLQG\left(o3[t] - \frac{o3g[t]}{H}\right)$$

$$o3'[t] == -(hl\ w\ o3[t]) + kLa\left(-o3[t] + \frac{o3g[t]}{H}\right)$$

$$o3'[t] == -(hl\ w\ o3[t]) + kLa\left(-o3[t] + \frac{o3g[t]}{H}\right)$$

The following line presents solving of gas and liquid ozone concentrations with respect to time. The solving is of simultaneous differential equations.

Initial liquid phase ozone concentration is zero.

```
DSolve[{eqn1,eqn2,o3[0]==0.0},{o3g[t],o3[t]},t]
```

Solution of gas phase concentration with respect to time.

```
{{o3g[t] ->

  (-(H kLa - kLa QLQG + H hl w -

          2    2          2             2       2
      Sqrt[H  kLa  + 2 H kLa  QLQG + kLa  QLQG  +

         2
      2 H  hl kLa w - 2 H hl kLa QLQG w +
```

$$2\ 2\ 2$$
$$H\ hl\ w\ ])\ /$$

$$(2\ \text{Power}[E,\ (t$$

$$(H\ kLa + kLa\ QLQG + H\ hl\ w +$$

$$2\quad 2\qquad 2$$
$$\text{Sqrt}[H\ kLa\ + 2\ H\ kLa\ QLQG +$$

$$2\qquad 2\qquad 2$$
$$kLa\ QLQG\ + 2\ H\ hl\ kLa\ w -$$

$$2\ 2\ 2$$
$$2\ H\ hl\ kLa\ QLQG\ w + H\ hl\ w\ ]))\ /$$

$$2\quad 2\qquad 2$$
$$(2\ H)]\ \text{Sqrt}[H\ kLa\ + 2\ H\ kLa\ QLQG +$$

$$2\qquad 2\qquad 2$$
$$kLa\ QLQG\ + 2\ H\ hl\ kLa\ w -$$

$$2\ 2\ 2$$
$$2\ H\ hl\ kLa\ QLQG\ w + H\ hl\ w\ ]) +$$

$$(\text{Power}[E,\ (t\ (-(H\ kLa) - kLa\ QLQG - H\ hl\ w +$$

$$2\quad 2\qquad 2$$
$$\text{Sqrt}[H\ kLa\ + 2\ H\ kLa\ QLQG +$$

$$2\qquad 2\qquad 2$$
$$kLa\ QLQG\ + 2\ H\ hl\ kLa\ w -$$

$$2\ 2\ 2$$
$$2\ H\ hl\ kLa\ QLQG\ w + H\ hl\ w\ ]))\ /$$

$$(2\ H)]\ (H\ kLa - kLa\ QLQG + H\ hl\ w +$$

$$2\quad 2\qquad 2$$
$$\text{Sqrt}[H\ kLa\ + 2\ H\ kLa\ QLQG +$$

$$2\qquad 2\qquad 2$$
$$kLa\ QLQG\ + 2\ H\ hl\ kLa\ w -$$

```
                                        2  2 2
      2 H hl kLa QLQG w + H  hl  w ])) /

           2    2            2                2        2
   (2 Sqrt[H  kLa  + 2 H kLa  QLQG + kLa  QLQG  +

       2
      2 H  hl kLa w - 2 H hl kLa QLQG w +

       2  2 2
      H  hl  w ])) C[1],

o3[t] ->

((-1 + Power[E, (t

           2    2           2
      Sqrt[H  kLa  + 2 H kLa  QLQG +

           2        2       2
       kLa  QLQG  + 2 H  hl kLa w -

                                  2  2 2
      2 H hl kLa QLQG w + H  hl  w ]) / H])

  kLa C[1]) /

 (Power[E, (t (H kLa + kLa QLQG + H hl w +

           2    2           2
      Sqrt[H  kLa  + 2 H kLa  QLQG +

           2        2       2
       kLa  QLQG  + 2 H  hl kLa w -

                                  2  2 2
      2 H hl kLa QLQG w + H  hl  w ])) / (2 H)

          2    2            2                2        2
   ] Sqrt[H  kLa  + 2 H kLa  QLQG + kLa  QLQG  +

      2                                      2  2 2
   2 H  hl kLa w - 2 H hl kLa QLQG w + H  hl  w ]

  )}}
```

APPENDIX 2.0

A2.1 RESPONSE STUDIES

In the analysis of gas-phase residence time distribution (RTD) it was found that there were several problems. This was due to the response time and mixed flow nature of both the portable air-water separator and the ozone concentration detector.

It was then decided to use a control theory analogy to describe the RTD study. Essentially what was done was to invoke a step response into each element of the system. The only unknown behaviour was the jet-pump gas phase residence time distribution (RTD).

A2.1.1 RESPONSE STUDY OF JET-PUMP AND O_3 ANALYSIS SYSTEM.

The system was broken down into a number of transfer functions which were analysed individually.

The analysis and manipulation of transfer functions is based on control theory which is expounded in numerous texts such as Stephanopoulos [141].

A2.1.1.1 STUDY OF INLET HOSE TO JET PUMP

To study the inlet hose to the jet pump a step response was inserted into the system by switching off the ozone supply. This causes the ozone level to fall from a steady-state value to zero. This should more or less occur in a step-like manner due to the plug flow which should be occurring in the feed pipe. However, the response at the detector was that of an exponentially decreasing function. The reason for this was that the detector

tended to mix the flow coming in, thereby producing a mixed response. The second problem of the ozone detector is the time taken from the column to the detection point, through 1.5m of 5mm NB plastic hose. This also has to be corrected for.

The response of the detector by itself was determined by removing the detector hose from the column (step change). The detector could then be examined by itself. The response was of the form:

$$y = e^{-at} \tag{A2.1}$$

Now taking the laplace transform yields:

$$y(s)_m = 1/(s+a) \tag{A2.2}$$

and from control theory:

$$y(s)_m = G(s)_m y(s) \tag{A2.3}$$

where

$y(s)_m$ =Laplace transform of detector response

$G(s)_m$ = Transfer function of detector system

$y(s)$ =Laplace transform of step input = -1/s

Similarly, this sort of analysis can be performed with the system + the detector:

$$y(s)_s = G(s)_m G(s)_s y(s) \tag{A2.4}$$

where

$y(s)_S$ = Laplace transform of system+detector response

= $1/(s+b)$

$G(s)_S$ = Transfer function of system+detector

$y(s)$ = Laplace transform of step input = $-1/s$

and

$$y_S(s) = y(s)G_S(s) \qquad \text{(A2.5)}$$

It is the response of $y_S(t)$ that is the RTD of the inlet hose to the system.

Manipulation yields:

$$y_S(s) = 1/(s+b) + a/(s(s+b)) \qquad \text{(A2.6)}$$

Taking the inverse Laplace Transform yields:

$$y_S(t) = (1-(a/b))e^{-bt} + (a/b) \qquad \text{(A2.7)}$$

The values of a and b can be obtained by regression analysis on the respective curve using the exponential power model.

APPENDIX 3.0 MATHEMATICAL MODEL CODES

A3.1 MASS TRANSFER MODEL

```
      PROGRAM model
c
c
c     Written by: PHILLIP WRIGHT 1992/1993
c     This program simulates an ozone mass transfer-disinfection system
c     by use of model equations and by use of numerical equation
c     solving techniques.
c
c
c
      REAL w,kla,qgql,o3g,hl,kt,hi,hrt,h,r,y,o3,p,q,f1,f2,f3,f4
      REAL t,s,klai,veb,phi,vp,trial,cc
      INTEGER i,j,type,exp,mode,n,m
      REAL ql,qg,a,l,v,ulsep,hrtsep,lm,ld,dmc,asep,bpv,lsep,ul,ug
      REAL fx,fdx
      REAL dodt,o3act,err,klaold,kerr1,kerr2,div,test
c
c
c     Input of Initial Data
c
c
c     o3=[o3*] ; q=[Si*] ; (Si)=s ; [O3]=y
c
c     Initial Model Default Data:
c     w = 0.05 ; kla = 0.03 ; qgql = 3. ; o3g = 0.135 ; hl = 0.83
c     kt = 1000. ; hi = 0.42 ; hrt = 300. ; h = 2.86 ; r = 0.6*kla
c
c
c     Open devices for import and export of data
c
c
      OPEN(2,FILE='c:\phil\model.in')
      OPEN(3,FILE='c:\phil\model1.out')
      OPEN(4,FILE='c:\phil\model2.out')
      OPEN(5,FILE='c:\phil\model3.out')
      OPEN(6,FILE='c:\phil\model4.out')
      OPEN(7,FILE='c:\phil\model5.out')
      OPEN(8,FILE='c:\phil\model6.out')
      OPEN(9,FILE='c:\phil\jet.in')
c
c
c     READ(2,*)w,kla,qlqg,o3g,hl,kt,hi,hrt,h,s,y,p
c
c     klai = (0.6*kla) ; o3=o3g/h ; q=s/hi ; t=0.0
c
```

```
c     ********************
c     TRANSFER TO INPUT DATA SUBROUTINE
c     ********************
c
        CALL input(type,veb,phi,vp,mode,cc,trial)
c
c
c
c     ********************
c     TRANSFER TO APPROPRIATE SUBROUTINE
c     ********************

        IF(trial.EQ.1)THEN
              WRITE(*,*)'*******************************'
              WRITE(*,*)' '
              WRITE(*,*)'Single Trial.'
              WRITE(*,*)' '
              WRITE(*,*)'*******************************'
              CALL strial(cc)
c
        ELSEIF(trial.EQ.3)THEN
              WRITE(*,*)'*******************************'
              WRITE(*,*)' '
              WRITE(*,*)'Mass Transfer Coefficient.'
              WRITE(*,*)' '
              WRITE(*,*)'*******************************'
              CALL mtc(cc,type)
c
c
c
        ELSE
              WRITE(*,*)'*******************************'
              WRITE(*,*)' '
              WRITE(*,*)'Experimental Trials.'
              WRITE(*,*)'Running Experiments 1 to 6.'
              WRITE(*,*)' '
              WRITE(*,*)'*******************************'
              CALL et
        ENDIF
c
c
c     Notify user that model calculations are complete
c
        WRITE(*,*)' '
        WRITE(*,*)'*******************************'
        WRITE(*,*)'Output to files = model(i).out'
        WRITE(*,*)'Calculations Complete'
        WRITE(*,*)'*******************************'
        WRITE(*,*)' '
```

```
c
c
      END



      SUBROUTINE input(type,veb,phi,vp,mode,cc,trial)
c
      REAL veb,phi,vp,trial,cc
      INTEGER type,mode,yn
c
      WRITE(*,*)' '
      WRITE(*,*)'*******************************'
      WRITE(*,*)'Ozone Contactor Simulation'
      WRITE(*,*)'*******************************'
      WRITE(*,*)' '
      WRITE(*,*)' '
      WRITE(*,*)'Contactor Type:'
      WRITE(*,*)' '
      WRITE(*,*)'1. Empty Bed Column'
      WRITE(*,*)'2. Packed Bed Column'
      WRITE(*,*)'3. Jet Pump (Venturi Suction System) Reactor'
      WRITE(*,*)' '
      READ(*,*)type
c
c
      IF(type.EQ.1)THEN
            WRITE(*,*)' '
            WRITE(*,*)'*******************************'
            WRITE(*,*)'Contactor Type: EMPTY BED COLUMN'
            WRITE(*,*)'*******************************'
            WRITE(*,*)' '
            WRITE(*,*)'Enter Volume of Bed(m^3):'
            READ(*,*)veb
c
c
      ELSEIF(type.EQ.2)THEN
            WRITE(*,*)' '
            WRITE(*,*)'*******************************'
            WRITE(*,*)'Contactor Type:PACKED BED COLUMN'
            WRITE(*,*)'*******************************'
            WRITE(*,*)' '
            WRITE(*,*)'Enter Packing Voidage Fraction:'
            READ(*,*)phi
            WRITE(*,*)'Enter Volume of Bed(m^3):'
            READ(*,*)veb
            veb=veb*(1.-phi)
            WRITE(*,*)'Actual Bed Volume(m^3):',veb
```

```
            vp=phi*veb
            WRITE(*,*)'Packing Volume(m^3):',vp
c
c
      ELSE
            WRITE(*,*)' '
            WRITE(*,*)'*****************************'
            WRITE(*,*)'Contactor Type:JET PUMP REACTOR'
            WRITE(*,*)'*****************************'
            WRITE(*,*)' '
c
c     Column type by definition is co-current(mode=2),
c     so therefore select this type and go to label 1000
c
      mode=2
c
      GOTO 1000
c
      ENDIF
c
c
c     ********************************************************
c
c     CHECK TO SEE IF CO/COUNTER-CURRENT OPERATION
C
C     ********************************************************
c
      WRITE(*,*)' '
      WRITE(*,*)'Enter Column Mode of Operation:'
      WRITE(*,*)' '
      WRITE(*,*)'1. Counter-current Operation'
      WRITE(*,*)'2. Co-current Operation'
c
      READ(*,*)mode
c
1000  IF(mode.EQ.1)then
            cc=1.
      ELSE
            cc=-1.
      ENDIF
c
c     Choose to run standard experiments or a particular case
c
      WRITE(*,*)' '
      WRITE(*,*)'Enter Selection for Experiment Type:'
      WRITE(*,*)' '
      WRITE(*,*)'1. Single Trial'
      WRITE(*,*)'2. Series of Experimental Trials'
      WRITE(*,*)'3. Find Mass Transfer Coefficient'
```

```
      WRITE(*,*)' '
      READ(*,*)trial
c
c     Check to See if Data is in Input File
c
      WRITE(*,*)' '
      WRITE(*,*)'*******************************'
      WRITE(*,*)'Do you wish to update Data input File? (1=yes/2=no)'
      READ(*,*)yn
      WRITE(*,*)'*******************************'
      WRITE(*,*)' '
c
      IF(yn.EQ.1)THEN
            CALL datain
      ELSE
            WRITE(*,*)'OK'
      ENDIF
c
c
      RETURN
      END


      SUBROUTINE datain
c
      REAL w,kla,qlqg,o3g,hl,kt,hi,hrt,h,s,y,p
c
c
      WRITE(*,*)' '
      WRITE(*,*)'*******************************'
      WRITE(*,*)'DATA ENTRY MODULE'
      WRITE(*,*)'*******************************'
      WRITE(*,*)' '
      WRITE(*,*)'Enter W:'
      READ(*,*)w
      WRITE(*,*)'Enter estimate of Mass Transfer Coefficient (kla):'
      READ(*,*)kla
      WRITE(*,*)'Enter Liquid/Gas Ratio:'
      READ(*,*)qlqg
      WRITE(*,*)'Enter Initial Ozone Gas Phase Conc. (O3):'
      READ(*,*)o3g
      WRITE(*,*)'Enter Liquid Hold-up (hl):'
      READ(*,*)hl
      WRITE(*,*)'Enter overall Rate Constant (kt):'
      READ(*,*)kt
      WRITE(*,*)'Enter Contaminant Henrys Law Constant (Hi):'
      READ(*,*)hi
      WRITE(*,*)'Enter Hydraulic Residence Time (HRT):'
      READ(*,*)hrt
```

```
      WRITE(*,*)'Enter Henrys Law Constant (H):'
      READ(*,*)h
      WRITE(*,*)'Enter Initial Contaminant Concentration [Si]:'
      READ(*,*)s
      WRITE(*,*)'Enter initial O3 conc in Liquid [O3]:'
      READ(*,*)y
      WRITE(*,*)'Enter initial contaminant conc in Liquid [Si]:'
      READ(*,*)p
      WRITE(*,*)' '
      WRITE(*,*)'Sending Data to Model.in'
      WRITE(*,*)'*****************************'
c
c     Write this altered information to File = Model.in
c
      WRITE(2,*)w,kla,qlqg,o3g,hl,kt,hi,hrt,h,s,y,p
c
      CLOSE(2)
c
      RETURN
      END




      SUBROUTINE strial(cc)
c
c     ************************************************************
c
c     SINGLE TRIAL
c
c     ************************************************************
c
      REAL w,kla,qgql,o3g,hl,kt,hi,hrt,h,r,y,o3,p,q,f1,f2,f3,f4
      REAL t,s,klai,veb,phi,vp,trial,cc
      INTEGER i,j,type,exp,mode,n,m
      REAL ql,qg,a,l,v,ulsep,hrtsep,lm,ld,dmc,asep,bpv,lsep,ul,ug
      REAL fx,fdx
      REAL dodt,o3act,err,klaold,kerr1,kerr2,div,test

c
c
      WRITE(*,*)' '
      WRITE(*,*)'*****************************'
      WRITE(*,*)'Data Should be Entered in the File'
      WRITE(*,*)'called MODEL.IN !!!'
      WRITE(*,*)' '
      WRITE(*,*)'Data outputs to MODEL1.OUT'
      WRITE(*,*)' '
```

```
      WRITE(*,*)'Now simulating single trial.....'
      WRITE(*,*)'*****************************'
      WRITE(*,*)' '
c
c
      OPEN(2,FILE='c:\phil\model.in')
      READ(2,*)w,kla,qlqg,o3g,hl,kt,hi,hrt,h,s,y,p
      CLOSE(2)
c
      klai = (0.6*kla)
      o3=o3g/h
      q=s/hi
      t=0.0
c
c
c
c     Write input data to model.out
c
      WRITE(3,*)'Input Data for Single Experiment'
      WRITE(3,*)'w=',w,'kla=',kla,'QL/QG=',qlqg
      WRITE(3,*)'(O3)=',o3g,'Hl=',hl,'Kt=',kt
      WRITE(3,*)'Hi=',hi,'HRT=',hrt,'H=',h
      WRITE(3,*)'(Si)=',s,'[O3]=',y,'[Si]=',p
c
c     Run experiment
c
      CALL rk4(w,kla,qlqg,o3g,hl,kt,hi,t,h,s,y,p,hrt,klai,o3,q,cc)
c
c     Send appropriate data to output file=model.out
c
      WRITE(3,*)'Output Data for Single Experiment'
      WRITE(3,*)'w=',w,'kla=',kla,'QL/QG=',qlqg
      WRITE(3,*)'(O3)=',o3g,'Hl=',hl,'Kt=',kt
      WRITE(3,*)'Hi=',hi,'HRT=',hrt,'H=',h
      WRITE(3,*)'(Si)=',s,'[O3]=',y,'[Si]=',p
      WRITE(3,*)'[O3*]=',o3,'[Si*]=',q
c
      RETURN
      END




      SUBROUTINE mtc(cc,type)
c
c     ******************************************************
c
c     ITERATE TO FIND MASS TRANSFER COEFFICIENT
```

```
c
c     ********************************************************
c
        REAL w,kla,qgql,o3g,hl,kt,hi,hrt,h,r,y,o3,p,q,f1,f2,f3,f4
        REAL t,s,klai,veb,phi,vp,trial,cc
        INTEGER i,j,type,exp,mode,n,m
        REAL ql,qg,a,l,v,ulsep,hrtsep,lm,ld,dmc,asep,bpv,lsep,ul,ug
        REAL fx,fdx
        REAL dodt,o3act,err,klaold,kerr1,kerr2,div,test

c
        WRITE(*,*)' '
        WRITE(*,*)'*******************************'
        WRITE(*,*)'ITERATION TO FIND MASS TRANSFER COEFFICIENT'
        WRITE(*,*)'*******************************'
        WRITE(*,*)' '
c
        OPEN(2,FILE='c:\phil\model.in')
        READ(2,*)w,kla,qlqg,o3g,hl,kt,hi,hrt,h,s,y,p
        CLOSE(2)
        klaold=kla
c
c     ************************
c     NOW PERFORM SIMULATION
C     ************************
c
c     Set Counter to 0
        n=0
c
c
c     ***************
c     JET PUMP
c     ***************
c
1002    IF(type.EQ.3)THEN
                WRITE(*,*)' '
                WRITE(*,*)'*******************************'
                WRITE(*,*)'       JET PUMP'
                WRITE(*,*)'Appropriate Data is read in from:'
                WRITE(*,*)'         JET.IN'
                WRITE(*,*)'*******************************'
                WRITE(*,*)' '
c
c     Read in Jet Pump Data
c
c     NOTE: Specific Ozone Utilisation, Henry's Law
c     Constant and similar data read in from model.in
c
        OPEN(2,FILE='c:\phil\model.in')
```

```
      READ(2,*)w,kla,qlqg,o3g,hl,kt,hi,hrt,h,s,y,p
      CLOSE(2)
c
c     Data is then updated to be Jet Pump Specific
c
      OPEN(9,FILE='c:\phil\jet.in')
      READ(9,*)o3act
      CLOSE(9)
c
c
      ELSE
c
c     ***************
c     BUBBLE COLUMN
c     ***************
c
            WRITE(*,*)' '
            WRITE(*,*)'*******************************'
            WRITE(*,*)'      BUBBLE COLUMN'
            WRITE(*,*)'Appropriate Data is read in from:'
            WRITE(*,*)'        MODEL.IN'
            WRITE(*,*)'*******************************'
            WRITE(*,*)' '
c
      OPEN(2,FILE='c:\phil\model.in')
      READ(2,*)w,kla,qlqg,o3g,hl,kt,hi,hrt,h,s,y,p
      CLOSE(2)

      ENDIF
c
      kla=klaold
      klai = (0.6*kla)
      o3=o3g/h
      q=s/hi
      t=0.0
c     Write input data to model.out
c
      WRITE(3,*)'Input Data for Mass Transfer Solution'
      WRITE(3,*)'w=',w,'kla=',kla,'QL/QG=',qlqg
      WRITE(3,*)'(O3)=',o3g,'Hl=',hl,'Kt=',kt
      WRITE(3,*)'Hi=',hi,'HRT=',hrt,'H=',h
      WRITE(3,*)'(Si)=',s,'[O3]=',y,'[Si]=',p
      WRITE(3,*)' '
c
      CALL rk4(w,kla,qlqg,o3g,hl,kt,hi,t,h,s,y,p,hrt,klai,o3,q,cc)
      WRITE(*,*)' '
      WRITE(*,*)'Iteration Number=',n
      WRITE(*,*)' '
      WRITE(*,*)'kla =',kla
```

```
      WRITE(*,*)'(O3) Model=',o3g
      WRITE(*,*)'(O3) Actual=',o3act
      err=abs(1.-o3g/o3act)
      WRITE(*,*)'Error in (O3)model =',err
c
      WRITE(*,*)' '
      WRITE(*,*)'Do You wish to adjust kla? 1=yes & 2=no'
      READ(*,*)test
      IF(test.EQ.1)THEN
            WRITE(*,*)'Enter new kla:'
            READ(*,*)klaold
            n=n+1
            GOTO 1002
      ELSE
            WRITE(*,*)'Send Data to Output file? 1=yes & 2=no'
            READ(*,*)test
            IF(test.EQ.1)THEN
                  GOTO 1003
            ELSE
                  WRITE(*,*)'Complete!'
                  STOP
            ENDIF
      ENDIF
c
c     Send appropriate data to output file=model.out
c
1003  WRITE(*,*)' '
      WRITE(*,*)'Simulation Complete.'
      WRITE(*,*)' '
      WRITE(3,*)'Output Data for Single Experiment'
      WRITE(3,*)'w=',w,'kla=',kla,'QL/QG=',qlqg
      WRITE(3,*)'(O3)=',o3g,'Hl=',hl,'Kt=',kt
      WRITE(3,*)'Hi=',hi,'HRT=',hrt,'H=',h
      WRITE(3,*)'(Si)=',s,'[O3]=',y,'[Si]=',p
      WRITE(3,*)'[O3*]=',o3,'[Si*]=',q
c
      RETURN
      END



      SUBROUTINE rk4(w,kla,qlqg,o3g,hl,kt,hi,t,h,s,y,p,hrt,klai,o3,q,cc)
c
c
c     Define variables
c
c
      REAL inc,k11,k12,k13,k14,k21,k22,k23,k24,k31,k32,k33,k34
```

```
      REAL k41,k42,k43,k44,f1,f2,f3,f4
      REAL kla,klai,kt
      INTEGER n,i
c
c
c     This subroutine performs the Runge-Kutta 4th order differential
c     equation solver.
c
c
c     Computes the result of an equation of the form:
c
c     y'=f(x,y) at equidistant points and with initial values:
c     y(x0)=y) at points:
c     x1=x0+h ; x2=x0+2h.....
c
c     f has a unique solution in the range [x0,xN]
c
      n=hrt/0.25
c
c     increment size = 0.25
      inc=0.25
c
c     Need to adjust increment size for very small HRT
c
      IF(hrt.LT.10)THEN
            n=hrt/.001
            inc=0.001
      ENDIF
c
c     R-K For function 1
c
c
      DO 10 i=0,(n-1)
      k11=inc*f1(kla,o3,hl,w,y)
      k12=inc*f1(kla,o3,hl,w,(y+0.5*k11))
      k13=inc*f1(kla,o3,hl,w,(y+0.5*k12))
      k14=inc*f1(kla,o3,hl,w,(y+k13))
c
c
c
c     R-K for function 2
c
      k21=inc*f2(kla,y,o3g,qlqg,cc,h)
      k22=inc*f2(kla,y,(o3g+0.5*k21),qlqg,cc,h)
      k23=inc*f2(kla,y,(o3g+0.5*k22),qlqg,cc,h)
      k24=inc*f2(kla,y,(o3g+k23),qlqg,cc,h)
c
c
c
```

```
c     R-K for function 3
c
        k31=inc*f3(klai,q,p,hl,kt,y)
        k32=inc*f3(klai,q,(p+0.5*k31),hl,kt,y)
        k33=inc*f3(klai,q,(p+0.5*k32),hl,kt,y)
        k34=inc*f3(klai,q,(p+k33),hl,kt,y)
c
c
c
c     R-K for function 4
c
c
        k41=inc*f4(kla,p,s,qlqg,h,cc)
        k42=inc*f4(kla,p,(s+0.5*k41),qlqg,h,cc)
        k43=inc*f4(kla,p,(s+0.5*k42),qlqg,h,cc)
        k44=inc*f4(kla,p,(s+k44),qlqg,h,cc)
c
c
c
c     Calculate new values of parameters
c
        t=t+inc
        y=y+((1./6.)*(k11+(2.*k12)+(2.*k13)+k14))
        o3g=o3g+((1./6.)*(k21+(2.*k22)+(2.*k23)+k24))
        p=p+((1./6.)*(k31+(2.*k32)+(2.*k33)+k34))
        s=s+((1./6.)*(k41+(2.*k42)+(2.*k43)+k44))
        o3=o3g/h
        q=s/hi
c
10    CONTINUE
c
c
        RETURN
        END




        FUNCTION f1(kla,o3,hl,w,y)
c
        REAL kla
c
c     Solves Equation:
c
c     d[O3]/dt = kLa{[O3*]-[O3]}-hL*w*[O3]
c
```

```
c     let y = [O3]
c     let o3 = [O3*]
c     let x = t
c
        f1 = kla*(o3-y)-(hl*w*y)
c
        RETURN
        END



        FUNCTION f2(kla,y,o3g,qlqg,cc,h)
c
        REAL kla
c
c     Solves equation:
c
c     d(O3)/dt = kla{[O3]-[O3*]}*(ql/qg)
c
c     let o3g = (O3)
c     let qlqg=ql/qg
c
        f2 = kla*((o3g/h)-y)*(qlqg)*(cc)
c
        RETURN
        END



        FUNCTION f3(klai,q,p,hl,kt,y)
        REAL klai,kt
c
c
c     Solves Equation:
c
c     d[Si]/dt = (kla)i*{[Si*]-[Si]}-hl*kt*[Si][O3]
c
c     let p = [Si]
c     let q = [Si*]
c     let klai = (kla)i
c
        f3 = klai*(q-p)-(hl*kt*p*y)
c
        RETURN
        END
```

```
      FUNCTION f4(klai,p,s,qlqg,h,cc)
c
      REAL klai
c
c     Solves Equation:
c
c     d(Si)/dt = (kla)i*{[Si]-[Si*]}(ql/qg)
c
c     let s = (Si)
c
      f4 = klai*((s/h)-p)*(qlqg)*cc
c
      RETURN
      END



      SUBROUTINE et
c
c     ************************************************************
c
c     EXPERIMENTAL TRIALS
c
c     ************************************************************
c
      REAL w,kla,qgql,o3g,hl,kt,hi,hrt,h,r,y,o3,p,q,f1,f2,f3,f4
      REAL t,s,klai,veb,phi,vp,trial,cc
      INTEGER i,j,type,exp,mode,n,m
      REAL ql,qg,a,l,v,ulsep,hrtsep,lm,ld,dmc,asep,bpv,lsep,ul,ug
      REAL fx,fdx
      REAL dodt,o3act,err,klaold,kerr1,kerr2,div,test
c
c     Solve Differential Equations
c
c
      DO 100 exp=1,6
c
      IF(exp.EQ.1)THEN
c
c     ********************************************************
c     Experiment 1
c     ********************************************************
c     % Removal vs kt and Hi
c
```

```
c
      WRITE(*,*)'Calculating Experiment 1'
      WRITE(*,*)'% Removal vs Various Kt and Hi Values.'
      WRITE(*,*)' '
      DO 20 j=1,3
c
c
      DO 10 i=1,20
      OPEN(2,FILE='c:\phil\model.in')
      READ(2,*)w,kla,qlqg,o3g,hl,kt,hi,hrt,h,s,y,p
      CLOSE(2)
      IF(j.EQ.1)THEN
            kt=10.0
      ELSE IF(j.EQ.2)THEN
            kt=100.0
      ELSE
            kt=300.0
      ENDIF
c
      hi=0.1*i
      klai = (0.6*kla)
      o3=o3g/h
      q=s/hi
      t=0.0
c
c
c
c     Write input data to model.out
c
      WRITE(3,*)'Input Data for Experiment 1 , iteration=',i
      WRITE(3,*)'w=',w,'kla=',kla,'QL/QG=',qlqg
      WRITE(3,*)'(O3)=',o3g,'Hl=',hl,'Kt=',kt
      WRITE(3,*)'Hi=',hi,'HRT=',hrt,'H=',h
      WRITE(3,*)'(Si)=',s,'[O3]=',y,'[Si]=',p
c
c     Run experiment
c
      WRITE(*,*)'i=',i,'j=',j
      CALL rk4(w,kla,qlqg,o3g,hl,kt,hi,t,h,s,y,p,hrt,klai,o3,q,cc)
c
c     Send appropriate data to output file=model.out
c
      WRITE(3,*)'Output Data for Experiment 1 , iteration=',i
      WRITE(3,*)'w=',w,'kla=',kla,'QL/QG=',qlqg
      WRITE(3,*)'(O3)=',o3g,'Hl=',hl,'Kt=',kt
      WRITE(3,*)'Hi=',hi,'HRT=',hrt,'H=',h
      WRITE(3,*)'(Si)=',s,'[O3]=',y,'[Si]=',p
      WRITE(3,*)'[O3*]=',o3,'[Si*]=',q
c
```

```
10    CONTINUE
20    CONTINUE
c
      ELSE IF(exp.EQ.2)THEN
c
c     ********************************************************
c     EXPERIMENT 2
c     ********************************************************
c
c     % Removal vs Gas/Liquid Ratio
c     at various Kt and Hi values
c
      WRITE(*,*)'Calculating Experiment 2'
      WRITE(*,*)'% Removal vs Gas/Liquid Ratio at Different'
      WRITE(*,*)'Kt and Hi Values.'
      WRITE(*,*)' '
      DO 15 j=1,4
      DO 11 i=1,8
      OPEN(2,FILE='c:\phil\model.in')
      READ(2,*)w,kla,qlqg,o3g,hl,kt,hi,hrt,h,s,y,p
      CLOSE(2)
      IF(j.EQ.1)THEN
            hi=0.02
            kt=1000.
      ELSE IF(j.EQ.2)THEN
            hi=0.42
            kt=10.
      ELSE IF(j.EQ.3)THEN
            hi=0.42
            kt=100.
      ELSE
            hi=0.24
            kt=500.
      ENDIF
c
      qlqg=(1.0/i)
      klai = (0.6*kla)
      o3=o3g/h
      q=s/hi
      t=0.0
c
c
c
c     Write input data to model.out
c
      WRITE(4,*)'Input Data for Experiment 2 , iteration=',i
      WRITE(4,*)'w=',w,'kla=',kla,'QL/QG=',qlqg
      WRITE(4,*)'(O3)=',o3g,'Hl=',hl,'Kt=',kt
      WRITE(4,*)'Hi=',hi,'HRT=',hrt,'H=',h
```

```
      WRITE(4,*)'(Si)=',s,'[O3]=',y,'[Si]=',p
c
c     Run experiment
c
      WRITE(*,*)'i=',i,'j=',j
      CALL rk4(w,kla,qlqg,o3g,hl,kt,hi,t,h,s,y,p,hrt,klai,o3,q,cc)
c
c     Send appropriate data to output file=model.out
c
      WRITE(4,*)'Output Data for Experiment 2 , iteration=',i
      WRITE(4,*)'w=',w,'kla=',kla,'QL/QG=',qlqg
      WRITE(4,*)'(O3)=',o3g,'Hl=',hl,'Kt=',kt
      WRITE(4,*)'Hi=',hi,'HRT=',hrt,'H=',h
      WRITE(4,*)'(Si)=',s,'[O3]=',y,'[Si]=',p
      WRITE(4,*)'[O3*]=',o3,'[Si*]=',q
c
11    CONTINUE
15    CONTINUE
c
      ELSE IF(exp.EQ.3)THEN
c
c     ************************************************************
c     EXPERIMENT 3
c     ************************************************************
c
c     %Removal vs ozone initial concentration
c     at various kt and hi values
c
      WRITE(*,*)'Calculating Experiment 3'
      WRITE(*,*)'% Removal vs Ozone Initial Concentration'
      WRITE(*,*)'at Various Kt and Hi Values.'
      WRITE(*,*)' '
      DO 16 j=1,4
      DO 12 i=1,21,2
      OPEN(2,FILE='c:\phil\model.in')
      READ(2,*)w,kla,qlqg,o3g,hl,kt,hi,hrt,h,s,y,p
      CLOSE(2)
      IF(j.EQ.1)THEN
            hi=0.02
            kt=1000.
      ELSE IF(j.EQ.2)THEN
            hi=0.42
            kt=10.
      ELSE IF(j.EQ.3)THEN
            hi=0.42
            kt=100.
      ELSE
            hi=0.24
            kt=500.
```

```
        ENDIF
c
        o3g=(i*0.1)/(1000.)
        klai = (0.6*kla)
        o3=o3g/h
        q=s/hi
        t=0.0
c
c
c
c     Write input data to model.out
c
        WRITE(5,*)'Input Data for Experiment 3 , iteration=',i
        WRITE(5,*)'w=',w,'kla=',kla,'QL/QG=',qlqg
        WRITE(5,*)'(O3)=',o3g,'Hl=',hl,'Kt=',kt
        WRITE(5,*)'Hi=',hi,'HRT=',hrt,'H=',h
        WRITE(5,*)'(Si)=',s,'[O3]=',y,'[Si]=',p
c
c     Run experiment
c
        WRITE(*,*)'i=',i,'j=',j
        CALL rk4(w,kla,qlqg,o3g,hl,kt,hi,t,h,s,y,p,hrt,klai,o3,q,cc)
c
c     Send appropriate data to output file=model.out
c
        WRITE(5,*)'Output Data for Experiment 3 , iteration=',i
        WRITE(5,*)'w=',w,'kla=',kla,'QL/QG=',qlqg
        WRITE(5,*)'(O3)=',o3g,'Hl=',hl,'Kt=',kt
        WRITE(5,*)'Hi=',hi,'HRT=',hrt,'H=',h
        WRITE(5,*)'(Si)=',s,'[O3]=',y,'[Si]=',p
        WRITE(5,*)'[O3*]=',o3,'[Si*]=',q
c
12    CONTINUE
16    CONTINUE
c
        ELSE IF(exp.EQ.4)THEN
c
c     ********************************************************
c     EXPERIMENT 4
c     ********************************************************
c
c     % Removal vs Mass Transfer Coefficient
c     at various kt and Hi values
c
        WRITE(*,*)'Calculating Experiment 4'
        WRITE(*,*)'% Removal vs Mass Transfer Coefficient at'
        WRITE(*,*)'Various Kt and Hi Values.'
        WRITE(*,*)' '
        DO 17 j=1,4
```

```
      DO 13 i=1,10
      OPEN(2,FILE='c:\phil\model.in')
      READ(2,*)w,kla,qlqg,o3g,hl,kt,hi,hrt,h,s,y,p
      CLOSE(2)
      IF(j.EQ.1)THEN
            hi=0.02
            kt=1000.
      ELSE IF(j.EQ.2)THEN
            hi=0.42
            kt=10.
      ELSE IF(j.EQ.3)THEN
            hi=0.42
            kt=100.
      ELSE
            hi=0.24
            kt=500.
      ENDIF
c
      kla=i*0.005
      klai = (0.6*kla)
      o3=o3g/h
      q=s/hi
      t=0.0
c
c
c
c     Write input data to model.out
c
      WRITE(6,*)'Input Data for Experiment 4 , iteration=',i
      WRITE(6,*)'w=',w,'kla=',kla,'QL/QG=',qlqg
      WRITE(6,*)'(O3)=',o3g,'Hl=',hl,'Kt=',kt
      WRITE(6,*)'Hi=',hi,'HRT=',hrt,'H=',h
      WRITE(6,*)'(Si)=',s,'[O3]=',y,'[Si]=',p
c
c     Run experiment
c
      WRITE(*,*)'i=',i,'j=',j
      CALL rk4(w,kla,qlqg,o3g,hl,kt,hi,t,h,s,y,p,hrt,klai,o3,q,cc)
c
c     Send appropriate data to output file=model.out
c
      WRITE(6,*)'Output Data for Experiment 4 , iteration=',i
      WRITE(6,*)'w=',w,'kla=',kla,'QL/QG=',qlqg
      WRITE(6,*)'(O3)=',o3g,'Hl=',hl,'Kt=',kt
      WRITE(6,*)'Hi=',hi,'HRT=',hrt,'H=',h
      WRITE(6,*)'(Si)=',s,'[O3]=',y,'[Si]=',p
      WRITE(6,*)'[O3*]=',o3,'[Si*]=',q
c
13    CONTINUE
```

```
17    CONTINUE
c
      ELSE IF(exp.EQ.5)THEN
c
c     ************************************************************
c     EXPERIMENT 5
c     ************************************************************
c
c     % Removal vs Specific Ozone Utilisation
c     at various kt and Hi values
c
      WRITE(*,*)'Calculating Experiment 5'
      WRITE(*,*)'% Removal vs Specific Ozone Utilisation at'
      WRITE(*,*)'Various Kt and Hi Values.'
      WRITE(*,*)' '
      DO 18 j=1,4
      DO 14 i=1,10
      OPEN(2,FILE='c:\phil\model.in')
      READ(2,*)w,kla,qlqg,o3g,hl,kt,hi,hrt,h,s,y,p
      CLOSE(2)
      IF(j.EQ.1)THEN
            hi=0.02
            kt=1000.
      ELSE IF(j.EQ.2)THEN
            hi=0.42
            kt=10.
      ELSE IF(j.EQ.3)THEN
            hi=0.42
            kt=100.
      ELSE
            hi=0.24
            kt=500.
      ENDIF
c
      w=(0.01*kla)
      klai = (0.6*kla)
      o3=o3g/h
      q=s/hi
      t=0.0
c
c
c
c     Write input data to model.out
c
      WRITE(7,*)'Input Data for Experiment 5 , iteration=',i
      WRITE(7,*)'w=',w,'kla=',kla,'QL/QG=',qlqg
      WRITE(7,*)'(O3)=',o3g,'Hl=',hl,'Kt=',kt
      WRITE(7,*)'Hi=',hi,'HRT=',hrt,'H=',h
      WRITE(7,*)'(Si)=',s,'[O3]=',y,'[Si]=',p
```

```
c
c     Run experiment
c
        WRITE(*,*)'i=',i,'j=',j
        CALL rk4(w,kla,qlqg,o3g,hl,kt,hi,t,h,s,y,p,hrt,klai,o3,q,cc)
c
c     Send appropriate data to output file=model.out
c
        WRITE(7,*)'Output Data for Experiment 5 , iteration=',i
        WRITE(7,*)'w=',w,'kla=',kla,'QL/QG=',qlqg
        WRITE(7,*)'(O3)=',o3g,'Hl=',hl,'Kt=',kt
        WRITE(7,*)'Hi=',hi,'HRT=',hrt,'H=',h
        WRITE(7,*)'(Si)=',s,'[O3]=',y,'[Si]=',p
        WRITE(7,*)'[O3*]=',o3,'[Si*]=',q
c
14    CONTINUE
18    CONTINUE
c
        ELSE
c
c     ********************************************************
c     EXPERIMENT 6
c     ********************************************************
c
c     % Removal vs Liquid Hold-up
c     at Various Kt and Hi values
c
        WRITE(*,*)'Calculating Experiment 6'
        WRITE(*,*)' % Removal vs Liquid Hold-up at Various'
        WRITE(*,*)'Kt and Hi Values.'
        WRITE(*,*)' '
        DO 19 j=1,4
        DO 21 i=1,10
        OPEN(2,FILE='c:\phil\model.in')
        READ(2,*)w,kla,qlqg,o3g,hl,kt,hi,hrt,h,s,y,p
        CLOSE(2)
        IF(j.EQ.1)THEN
                hi=0.02
                kt=1000.
        ELSE IF(j.EQ.2)THEN
                hi=0.42
                kt=10.
        ELSE IF(j.EQ.3)THEN
                hi=0.42
                kt=100.
        ELSE
                hi=0.24
                kt=500.
        ENDIF
```

```
c
      hl=(0.1*i)
      klai = (0.6*kla)
      o3=o3g/h
      q=s/hi
      t=0.0
c
c
c
c     Write input data to model.out
c
      WRITE(8,*)'Input Data for Experiment 6 , iteration=',i
      WRITE(8,*)'w=',w,'kla=',kla,'QL/QG=',qlqg
      WRITE(8,*)'(O3)=',o3g,'Hl=',hl,'Kt=',kt
      WRITE(8,*)'Hi=',hi,'HRT=',hrt,'H=',h
      WRITE(8,*)'(Si)=',s,'[O3]=',y,'[Si]=',p
c
c     Run experiment
c
      WRITE(*,*)'i=',i,'j=',j
      CALL rk4(w,kla,qlqg,o3g,hl,kt,hi,t,h,s,y,p,hrt,klai,o3,q,cc)
c
c     Send appropriate data to output file=model.out
c
      WRITE(8,*)'Output Data for Experiment 6 , iteration=',i
      WRITE(8,*)'w=',w,'kla=',kla,'QL/QG=',qlqg
      WRITE(8,*)'(O3)=',o3g,'Hl=',hl,'Kt=',kt
      WRITE(8,*)'Hi=',hi,'HRT=',hrt,'H=',h
      WRITE(8,*)'(Si)=',s,'[O3]=',y,'[Si]=',p
      WRITE(8,*)'[O3*]=',o3,'[Si*]=',q
c
21    CONTINUE
19    CONTINUE
c
      ENDIF
c
c
100   CONTINUE
c
      RETURN
      END
```

A3.2 TWO PHASE MODEL

```
      PROGRAM Vel
c
c     Written by: PHILLIP WRIGHT, 1993
c
c     This program determines various two-phase flow paramaters
c     which are used primarily in JET PUMP mass transfer
c     simulation studies.
c
c     This program will determine if the column selected will
c     operate in annualar or jet flow. This is important to the
c     applicability of the mass transfer model development.
c
c     This program will first determine where the transition
c     point for annular flow occurs for the specific column
c     being studied. This data is then sent to a file for later
c     study and evaluation.
c
c     The program also will determine actual velocities of both
c     the liquid and gas phases from user supplied superficial
c     velocities. This will allow the user to obtain information
c     on theoretical residence time of each phase.
c
c     ********************************************************
c     DECLARATION OF VARIABLES
c     ********************************************************
      REAL x,y,cl,cg,d,rhol,rhog,ugs,uls,vg,vl,n,m,h,z
      REAL al,ag,sl,si,ald,agd,sid,sld,dl,dg,dld,dgd
      REAL nul,nug,ul,ug,t,p,x1,y1,x2,y2,mx,bx
      REAL rel,reg,ql,qg,area,pi,ad,ldim,kdim
      INTEGER sys
c
c
c     ********************************************************
c     OPEN FILES
c     ********************************************************
      OPEN(UNIT=1,FILE='c:\phil\trans.out')
      OPEN(UNIT=2,FILE='c:\phil\vel.out')
c
c     ********************************************************
c     DETERMINE PHYSICAL PARAMATERS
c     ********************************************************
c
2     WRITE(*,*)' '
      WRITE(*,*)'CALCULATION OF TRANSITION FROM ANNULAR
FLOW.'
      WRITE(*,*)' '
      WRITE(*,*)'Physical data is for air-water system near ambient'
```

```
      WRITE(*,*)'conditions (Default 101.3 kPa(abs) and 20 Deg C).'
      WRITE(*,*)' '
      t=20
      p=101.3
      WRITE(*,*)'Leave as default system (1=YES/2=NO)?'
      READ(*,*)sys
      IF(sys.EQ.1)THEN
c
c     Calculate gas phase conditions from near default values
c
c     Density of Gas
c
c     yi=density in kg/m3 and xi=temp in deg C
c
1     y1=1.4128
      x1=250.-273.
      y2=1.1774
      x2=300.-273.
      mx=(y2-y1)/(x2-x1)
      bx=y1-(mx*x1)
c
      rhog=(mx*t)+bx
c
c     Calculate gas viscosity in kg/m.s
c
c     yi=viscosity in kg/m.s and xi=temp in deg C
c
      y1=1.599e-5
      x1=250.-273.
      y2=1.8462e-5
      x2=300.-273.
      mx=(y2-y1)/(x2-x1)
      bx=y1-(mx*x1)
c
      nug=(mx*t)+bx
c
c     Calculate Liquid-phase conditions from near default values
c
c     Density of Liquid
c
c     yi=density in kg/m3 and xi=temp in deg C
c
      y1=998.6
      x1=15.56
      y2=997.4
      x2=21.11
      mx=(y2-y1)/(x2-x1)
      bx=y1-(mx*x1)
c
```

```
      rhol=(mx*t)+bx
c
c     Calculate liquid viscosity in kg/m.s
c
c     yi=viscosity in kg/m.s and xi=temp in deg C
c
      y1=1.12e-3
      x1=15.56
      y2=9.8e-4
      x2=21.11
      mx=(y2-y1)/(x2-x1)
      bx=y1-(mx*x1)
c
      vl=(mx*t)+bx
c
c
      ELSE
            WRITE(*,*)'Change Temperature/Pressure (1=YES/2=NO)?'
            READ(*,*)sys
            IF(sys.EQ.1)THEN
            WRITE(*,*)'Enter new Pressure kPa(abs):'
            READ(*,*)p
            IF(p.EQ.101.3)THEN
            WRITE(*,*)'Enter new temperature (deg C):'
            READ(*,*)t
            IF(t.GT.27.)THEN
            WRITE(*,*)'Enter Liquid Density (kg/m3):'
            READ(*,*)rhol
            WRITE(*,*)'Enter Liquid viscosity (kg/m.sec):'
            READ(*,*)nul
            WRITE(*,*)'Enter Gas Density (kg/m3):'
            READ(*,*)rhog
            WRITE(*,*)'Enter Gas viscosity (kg/m.sec):'
            READ(*,*)nug
            ELSE
            GOTO 1
            ENDIF
            ENDIF
            ENDIF
            ENDIF
c
c     Calculate Kinematic Viscosities (vl&vg)
c
      vl=nul/rhol
      vg=nug/rhog
c
c     ************************************************
c     DETERMINATION OF TRANSITION FROM ANNULAR FLOW
c     ************************************************
c
```

```
c
c       For a given pipe size will determine the transition point
c       from annular flow for superficial gas velocities ranging
c       from 0.01 m/sec.
c
        pi=(22./7.)
        WRITE(*,*)'Enter the diameter of the duct (m):'
        READ(*,*)d
        area=pi*((d/2.)**2.)
c
        WRITE(1,*)'DETERMINATION OF TRANSITION FROM THE'
        WRITE(1,*)'ANNULAR FLOW REGIME.'
c
c       now z=h/d where h is width of liquid phase (m)
c       and for transition z=0.097.
c       Therfore film thickness (h) =
        z=0.097*d
        WRITE(*,*)'Film Thickness (h) =',z,' metres'
        WRITE(1,*)'Film Thickness (h) =',z,' metres'
c
c       Find film cross-sectional area (al)
        al=area-pi*((((d-2*h)/2.)**2.))
c
c       Area Available to Gas Flow
c
        ag=pi*((((d-2.*h)/2.)**2.))
c
c       Liquid Perimeter (sl)
        sl=((pi)*d)
c
c       Find Liquid Hydraulic Diameter (dl)
c
        dl=4.*al/sl
c
c       Gas Perimeter (si)=interface perimeter
c
        si=((pi)*(d-(2.*h)))
c
c       Find Gas hydraulic Diameter(Dg)
c
        dg=4*ag/si
c
c       Calculate Dimensionless Parameters
c
        CALL dim(ald,agd,sld,sid,ad,uld,ugd,dld,dgd,z,pi)
c
c       ************************************************
c       Now create data for transition
c       ************************************************
c
```

```
      ugs=0.01
      uls=0.0
c
      DO 10 i=0,60
c
      IF(i.LT.10)THEN
      ugs=uls+0.1
      ELSE
      ugs=ugs+1
      ENDIF
c
      qg=ugs*area
c
c     Now calculate actual gas velocity (ug).
c
      ug=qg/ag
c
c     Find actual Gasynolds Number (Rel)
c
      reg=rhog*ug*dg/nug
      IF(reg.LT.2000.)THEN
            cg=16.
            m=1.0
c     and assume that liquid phase is the same regime
            cl=cg
            n=m
      ELSE
            cg=0.046
            m=0.2
            n=m
            cl=cg
      ENDIF
c
c     Calculate two-phase Y parameter
c
11    a=(rhol-rhog)*9.81
      b=4.*cg/d
      c=(ugs*d/vg)**(-1.*m)
      e=rhog*(ugs**2)
c
      y=a/(b*c*e/2.)
c
c     Calculate value of X Parameter (actually X^2)
c
      f=4.*cl/d
      g=(d/vl)**(-1.*n)
      l=ldim(uld,dld,n,sld,ald)
      k=kdim(ugd,dgd,m,sid,ald,agd)
c
```

```
c       Solve for X^2
c
        x=(4.*y+k)/l
c
c       Calculate Liquid Superficial Velocity
c
        uls=(((a/y)*x)/(g*f*(rhol/2.)))**(-1.*(2.-n))
c
c       Now need to check flow regime assumption for Liquid
c
        ql=uls*area
c
        ul=ql/al
        rel=rhol*ul*dl/nul
c
        IF(rel.LT.2000.)THEN
c       flow regime is laminar - now check estimated regime
c
        IF(n.EQ.1.0)THEN
c       Assumption was OK therefore can output result
        ELSE
c       Assumption was wrong, therefore must iterate to check
                n=0.2
                cl=0.046
                GOTO 11
        ENDIF
c
        ELSE
c       flow regime is turbulent
        IF(n.EQ.0.2)THEN
c               assumption OK
        ELSE
                n=1.0
                cl=16
                GOTO 11
        ENDIF
        ENDIF
c
c       Output data to file=1 'trans.out'
c
        WRITE(1,*)'ugs=',ugs,'uls=',uls
c
c       Go on to next point.
c
10      CONTINUE
c
        CLOSE(UNIT=1)
c
c       ************************************************
```

```
c       DETERMINE ACTUAL VELOCITIES IN COLUMN
c       ****************************************************
c
c       The user supplies the gas flowrate, and the liquid flow.
c       The program converts this data to superficial velocity
c       data and then computes the actual gas and liquid velocities
c       through the column.
c
20      WRITE(*,*)' '
        WRITE(*,*)'CALCULATION OF ACTUAL GAS & LIQUID VELOCITIES.'
        WRITE(*,*)' '
        WRITE(*,*)'Enter Gas Flowrate (m3/sec):'
        READ(*,*)qg
        WRITE(*,*)' '
        WRITE(*,*)'Enter Liquid Velocity (m3/sec):'
        READ(*,*)ql
c
c       Now convert this data to superficial velocity
c
        ugs=qg/area
        uls=ql/area
c
        WRITE(*,*)' '
        WRITE(*,*)'Superficial Gas Velocity (Ugs)=',ugs,'m/sec'
        WRITE(*,*)' '
        WRITE(*,*)'Superficial Liquid Velocity (Uls)=',uls,'m/sec'
        WRITE(*,*)' '
        WRITE(*,*)'Column Area =',area,'m2'
        WRITE(*,*)' '
c
c
c       Now need to choose flow regimes (Laminar/Turbulent).
c       Will make this decision based on the superficial velocities
c       of the phases. This decision may need to be modified later.
c
        rel=rhol*uls*d/nul
        reg=rhog*ugs*d/nug
c
        IF(rel.LT.2000.)THEN
                n=1.0
                cl=16.
        ELSE
                n=0.2
                cl=0.046
        ENDIF
c
        IF(reg.LT.2000.)THEN
                m=1.0
                cg=16.
```

```
      ELSE
            m=0.2
            cg=0.046
      ENDIF
c
c     Use SECANT METHOD to solve X2 & Y parameter equation.
c     The reason for this method is due to difficulty of
c     performing differentiation on the describing equation.
c     The method is used to find z and hence h/d and this
c     gives the flow areas available to each phase, and so
c     the actual velocity.
c           Z must lie between 0 and 1. Two initial guesses
c     are required for z. Error handling ensures that correct
c     values of z are maintained.
c
110   zn=0.01
      zn1=0.02
c
      WRITE(*,*)' '
      WRITE(*,*)'Calculating z.....'
      DO 100 i=0,1000
c
c
c     Calculate Dimensionless Parameters
c
      CALL dim(ald,agd,sld,sid,ad,uld,ugd,dld,dgd,zn1,pi)
      l=ldim(uld,dld,n,sld,ald)
      k=kdim(ugd,dgd,m,sid,ald,agd)
c
      fn1=(x*l)-k-(4.*y)
c
      CALL dim(ald,agd,sld,sid,ad,uld,ugd,dld,dgd,zn,pi)
      l=ldim(uld,dld,n,sld,ald)
      k=kdim(ugd,dgd,m,sid,ald,agd)

      fn=(x*l)-k-(4.*y)
c
      zn2=zn1-fn1*((zn1-zn)/(fn1-fn))
c
c     Tolerance set at 0.0001
c
      tol=abs(zn2-zn1)
      IF(tol.LE.0.0001)THEN
            WRITE(*,*)'Converged to tolerance.'
            z=zn2
            GOTO 101
      ENDIF
      zn=zn1
      zn1=zn2
```

```
100   CONTINUE
c
      z=zn2
      WRITE(*,*)'Terminated before tolerance condition satisfied.'
      WRITE(*,*)'Actual Deviation=',tol
      WRITE(*,*)'z at this tolerance=',z
      WRITE(*,*)' '
c
101   WRITE(*,*)' '
      WRITE(*,*)'Checking initial regime assumptions.'
      h=d*z
      WRITE(*,*)'Film Thickness=',h,'metres.'
c
c     Liquid Area
c
      al=area-pi*((((d-2*h)/2.)**2.))
c
c     Area Available to Gas Flow
c
      ag=pi*((((d-2*h)/2.)**2.))
c
c     Liquid Perimeter (sl)
      sl=((pi)*d)
c
c     Find Liquid Hydraulic Diameter (dl)
c
      dl=4.*al/sl
c
c     Gas Perimeter (si)=interface perimeter
c
      si=((pi)*(d-(2*h)))
c
c     Find Gas hydraulic Diameter(Dg)
c
      dg=4*ag/si
c
      ul=ql/al
      ug=qg/ag
c
c     Calculate Real Reynolds Numbers
c
      rel=rhol*ul*dl/nul
      reg=rhog*ug*dg/nug
c
c
      IF(rel.LT.2000.)THEN
c     flow regime is laminar - now check estimated regime
c
      IF(n.EQ.1.0)THEN
```

```
c       Assumption was OK therefore can output result
        ELSE
c       Assumption was wrong, therefore must iterate to check
                n=0.2
                cl=0.046
                GOTO 110
        ENDIF
c
        ELSE
c       flow regime is turbulent
        IF(n.EQ.0.2)THEN
c               assumption OK
        ELSE
                n=1.0
                cl=16.
                GOTO 110
        ENDIF
        ENDIF
c
c       Output correct data
c
        WRITE(*,*)' '
        WRITE(*,*)'Calculations complete.'
        WRITE(*,*)' '
        WRITE(*,*)'Summary of Conditions:'
        WRITE(*,*)' '
        WRITE(*,*)'Gas Volumetric Flowrate=',qg,'m3/sec'
        WRITE(*,*)'Liquid Volumetric Flowrate=',ql,'m3/sec'
        WRITE(*,*)'Superficial Liquid Velocity=',uls,'m/sec'
        WRITE(*,*)'Superficial Gas Velocity=',ugs,'m/sec'
        WRITE(*,*)'Film Thickness=',h,'metres'
        WRITE(*,*)'Gas Velocity=',ug,'m/sec'
        WRITE(*,*)'Liquid Velocity=',ql,'m/sec'
c
c       Send data to file
c
        WRITE(2,*)' '
        WRITE(2,*)'Sending copy of data to "vel.out"'
        WRITE(2,*)'Summary of Conditions:'
        WRITE(2,*)' '
        WRITE(2,*)'Gas Volumetric Flowrate=',qg,'m3/sec'
        WRITE(2,*)'Liquid Volumetric Flowrate=',ql,'m3/sec'
        WRITE(2,*)'Superficial Liquid Velocity=',uls,'m/sec'
        WRITE(2,*)'Superficial Gas Velocity=',ugs,'m/sec'
        WRITE(2,*)'Film Thickness=',h,'metres'
        WRITE(2,*)'Gas Velocity=',ug,'m/sec'
        WRITE(2,*)'Liquid Velocity=',ql,'m/sec'
        WRITE(2,*)' '
c
```

```
c       Another calculation?
c
        WRITE(*,*)'Any further calculations ?(1=YES/2=NO)'
        READ(*,*)sys
        IF(sys.EQ.1)THEN
              GOTO 2
        ENDIF
c
        CLOSE(UNIT=2)
        STOP
        END



        SUBROUTINE dim(ald,agd,sld,sid,ad,uld,ugd,dld,dgd,z,pi)
c
c       Calculate Dimensionless Parameters
c
        ald=(pi)*(z-(z**2))
        agd=(pi)*((0.5-z)**2)
        sld=pi
        sid=pi*(1-2.*z)
        ad=ald+agd
        uld=ad/ald
        ugd=ad/agd
        dld=4.*ald/sld
        dgd=4.*agd/sid
c
        RETURN
        END



        FUNCTION kdim(ugd,dgd,m,sid,ald,agd)
c
        REAL ugd,dgd,m,sid,ald,agd,k,kdim
c
        k=((ugd*dgd)**(-1.*m))*(ugd**2)*sid*((1./ald)+(1./agd))
c
        kdim=k
c
        RETURN
        END



        FUNCTION ldim(uld,dld,n,sld,ald)
```

```
c
      REAL uld,dld,n,sld,ald,l,ldim
c
      l=((uld*dld)**(-1.*n))*(uld**2.)*sld/ald
c
      ldim=l
      RETURN
      END
```

□

APPENDIX 4.0 RAW DATA

Raw data, including full graphs, spreadsheets and regression data is available from the author, or from the Department of Mechanical Engineering at the University of Wollongong.